

**Investigation of the cellular location of
Multicopper Oxidase and its contribution to
copper tolerance and immune resistance in
*Staphylococcus aureus***

A thesis submitted for the degree of Doctor in Philosophy

by

Martin Sutton

2022

Moyne Institute of Preventive Medicine

Department of Microbiology

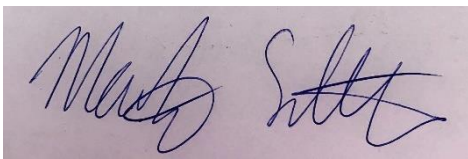
School of Genetics and Microbiology

Trinity College Dublin

Declaration

I declare that this thesis has not been submitted as an exercise for a degree at this or any other university and it is entirely my own work, except where it is duly acknowledged in the text.

I agree to deposit this thesis in the University's open access institutional repository or allow the library to do so on my behalf, subject to Irish Copyright Legislation and Trinity College Library conditions of use and acknowledgement.

A rectangular box containing a handwritten signature in blue ink. The signature appears to read "Martin Sutton".

Martin Sutton

Acknowledgements

To my supervisor Professor Joan Geoghegan, thank you a million times over. I was incredibly fortunate to have you as my mentor for my PhD studies. You are an amazing teacher, boss, and role model. You had unending patience for my unending questions, and somehow always found time to give for any issue big or small. Thank you.

To Professor Tim Foster, thank you for giving your time to review some of my thesis drafts. Your suggestions and wise insight were very much appreciated. To Professor Steve Smith in Saint James's, it's your fault I started this PhD! Thank you for nurturing me as a scientist at such a pivotal stage of my career and guiding me down this route.

Thaina, my wonderful ray of Brazilian sunshine, I am so grateful our paths crossed in October 2018. I will cherish our memories together in the Geoghegan lab forever. You are the bestest of friends, and will always be an inspiration to me. My fellow Staph fanatics in the Geoghegan lab, I am so grateful that I got to meet and work with all of you. Thank you to members past and present, Aisling, Sabrina, Chanelle, Mary and Dee in our TCD division, and Sara, Emma and Laura in our Birmingham division.

Brenda, Amy, Dani, German, Eoin, Roberto, Isa, Stefani, AJ, Zoe, Stephen, Fergal, Ali, Sally, Elaine, Namrata, Kevin, Sarah and the rest of the postgrad community in the Moyne, thank you for all of your wonderful friendships. Dr. Michael Beckett, thank you for every science conversation we've ever had, and for teaching me the life-long skill of home brew beer making! Stephen and Ronan, Jayne and Noreen, and the rest of the Moyne staff, thank you for making the Moyne a great place to work. Thank you to Richard Wubben and Dr. Nigel Stephenson for your collaboration performing qRT-PCR experiments with us. To all of my phlebotomy donors, thank you from the bottom of my heart for giving your arm for my needle, and blood for my research.

To my counsellor Chuck Rashleigh, thank you for keeping me sane this past year. To my second counsellor, Mick in TCD security, thank you for all of our chats the last few years. To my housemate Dr. Roddy Condon and furry companion Jack, thank you for your support and friendship the last few years, and for sharing your experience of academia with me. Let's make more beer!

Andrea, thank you for always being so encouraging and supportive of me throughout this process. You've given me more strength and joy than you can imagine.

Summary

Copper is an essential trace element required for many biological processes. However in high levels copper is highly toxic to cells. Bacteria have developed copper tolerance mechanisms to tightly control intracellular copper concentrations to permit growth, but prevent copper overload and toxicity. In recent years a growing body of evidence is demonstrating that bacterial copper tolerance genes contribute to pathogenicity and virulence during infection. Here, the contribution of the *Staphylococcus aureus* multicopper oxidase (Mco) to copper tolerance and resistance to immune cell killing was examined. Isogenic deletion mutants of *mco* and other copper tolerance genes were generated, and their contribution to copper tolerance was investigated. Mco contributed to copper tolerance in *S. aureus* in a variety of different growth conditions. The phenotype was successfully complemented by introducing the *mco* gene on to the chromosome under the transcriptional control of its native promoter. Fusion of Mco to a 3X-FLAG followed by western immunoblotting of subcellular *S. aureus* fractions permitted discovery that Mco is localised to the cytoplasmic membrane of *S. aureus*. The first 26 amino-acids of Mco contained a cleavable secretory signal peptide that delivered a reporter protein to the culture supernatant. This signal peptide was not recognised by the twin-arginine translocation system of *S. aureus*. This is the first reported Gram-positive multicopper oxidase not transported by the twin-arginine translocation system.

A link was found between the *S. aureus* cadmium resistance genes *cadA* and *cadC* and copper tolerance by analysis of growth of isogenic *cadAC* deletion mutants in copper supplemented media. Recent discoveries have shown that some bacterial copper tolerance genes improve intracellular survival within host phagocytes. The contribution of multiple copper tolerance genes in *S. aureus* to survival during infection was examined using an *ex vivo* model of human blood infection. No difference in survival in whole human blood or purified primary human neutrophils was reported for any of the *S. aureus* copper tolerance genes tested. This suggests that these genes do not contribute to survival of MRSA252 in the conditions tested here.

Biofilm formation is a major virulence mechanism employed by bacteria to colonise and cause persistent and life threatening infections. They pose a significant challenge to overcome as they are typically heavily resistant to treatment requiring longer hospital stays and higher-dose longer-term antimicrobial therapy. Novel anti-biofilm therapies are crucially required to improve patient outcomes and alleviate the pressure placed on healthcare facilities by biofilm-associated infections. This study investigates the effect of copper on *S. aureus* biofilm formation to explore if it exhibits anti-biofilm properties. An *in vitro* biofilm assay was employed to examine the effect of copper supplementation of biofilm growth media on the ability of *S. aureus* to form biofilm. The effect of copper on a panel of clinical *S. aureus* isolates from device-related and biofilm-associated infections from Irish hospitals was investigated. A diverse biofilm response to copper treatment was observed, where in many cases, copper significantly reduced biofilm formation of clinical isolates of *S. aureus*. However, in some conditions copper increased biofilm formation of clinical isolates of *S. aureus*. In one case, it was demonstrated that copper stimulated the production of a proteinaceous biofilm matrix in otherwise biofilm negative conditions. As a result, additional research is required to further understand the complex effect of copper on biofilm formation of *S. aureus* before copper-mediated anti-biofilm therapies can be considered in the clinic. However, this study suggests that there are many cases where copper can effectively reduce biofilm formation by biofilm associated clinical isolates of *S. aureus*, potentially reducing their burden in the healthcare environment.

Publications

Manuscript based on Chapter 3 of this thesis is in the journal submission process, preprint expected to be available on bioRxiv in December 2022.

Table of Contents

Declaration	i
Acknowledgements	ii
Summary	iii
Publications	v
Table of Contents	vi
List of Tables	xiii
List of Figures	xiv
Key to Abbreviations	xviii
Chapter 1 Introduction	1
1.1 The Biology of Staphylococci	2
1.1.1 Classification and Identification.....	2
1.1.2 Colonisation and Disease.....	2
1.1.3 Methicillin-resistant <i>Staphylococcus aureus</i>	3
1.1.4 Mobile Genetic Elements of <i>S. aureus</i>	4
1.2 <i>S. aureus</i> virulence factors.....	6
1.2.1 Chemotaxis inhibition by <i>S. aureus</i>	6
1.2.2 Opsonisation inhibition by <i>S. aureus</i>	6
1.2.3 Toxin mediated killing of neutrophils	7
1.2.4 Neutrophil disorders and increased susceptibility to <i>S. aureus</i> infection	9
1.3 Biofilm Formation by <i>Staphylococcus aureus</i>	10
1.4 Copper Biology	13
1.4.1 Copper homeostasis disorders in humans	14
1.4.2 The bactericidal properties of copper	15
1.4.3 Copper catalysed generation of hydroxyl radicals	15
1.4.4 Copper and mismetallation	15

1.4.5	Copper and disruption of iron sulphur clusters	16
1.4.6	Metallic copper proposed mechanisms of bactericidal activity ...	16
1.4.7	GSH and copper	17
1.4.8	Copper and the human immune system	18
1.4.9	Copper use by macrophages to enhance intracellular bacterial killing	19
1.5	Copper tolerance genes in <i>S. aureus</i>	20
1.6	Multicopper oxidases – a widely conserved family of proteins.....	24
1.7	Bacterial multicopper oxidases.....	25
1.7.1	<i>Escherichia coli</i> multicopper oxidase	25
1.7.2	<i>Salmonella enterica</i> serovar Typhimurium multicopper oxidase .	26
1.7.3	<i>Acinetobacter baumannii</i> multicopper oxidase	26
1.7.4	<i>Pseudomonas aeruginosa</i> multicopper oxidase	29
1.7.5	<i>Mycobacterium tuberculosis</i> multicopper oxidase.....	29
1.7.6	<i>Staphylococcus aureus</i> multicopper oxidase	29
1.7.7	<i>Listeria monocytogenes</i> multicopper oxidases.....	31
1.7.8	<i>Rhodococcus erythropolis</i> multicopper oxidase	31
1.7.9	<i>Rhodobacter capsulatis</i> multicopper oxidase.....	32
1.7.10	<i>Alphaproteobacteria</i> multicopper oxidase	32
1.7.11	<i>Desulvibrio</i> multicopper oxidase.....	32
1.7.12	<i>Pseudomonas syringae</i> pathovar <i>tomato</i> multicopper oxidase .	33
1.8	Protein translocation across bacterial membranes	33
1.9	Metals and Biofilm Formation in <i>Staphylococcus aureus</i>	39
1.10	Aims and objectives of this thesis.....	40
Chapter 2	Materials and Methods.....	41
2.1	Bacterial growth conditions	42
2.2	Plasmids and primers in this study	42

2.3	DNA manipulation.....	42
2.3.1	Isolation of genomic and plasmid DNA.....	42
2.3.2	Polymerase Chain Reaction (PCR).....	42
2.3.3	Colony PCR screening of <i>E. coli</i> and <i>S. aureus</i>	43
2.3.4	Agarose Gel Electrophoresis.....	43
2.4	Plasmid construction	43
2.4.1	Sequence and Ligase-independent Cloning.....	43
2.4.2	Generation of pRMC2::D3D4::NoSP	44
2.4.3	Generation of pRMC2::D3D4::Mco1-56	44
2.4.4	Generation of pRMC2::D3D4::Mco1-26	44
2.4.5	Generation of pRMC2::D3D4::Mco27-56	44
2.4.6	Generation of pRMC2::D3D4::Mco1-56 KQ and pRMC2::D3D4::Mco1-26 KQ	47
2.4.7	Generation of pCL55:UCMF	47
2.4.8	Generation of pCL55:UCMFΔMco2-53	48
2.4.9	Generation of pCL55:UCM.....	48
2.5	Strain construction by allelic exchange	48
2.5.1	Generation of MRSA252Δmco	48
2.5.2	Generation of LAC* <i>spa sbi</i> Δ <i>tatAC</i>	50
2.5.3	Generation of MRSA252 14 gene KO.....	50
2.5.4	Generation of MRSA252Δ <i>cadA</i> and MRSA252Δ <i>mco</i> Δ <i>cadA</i>	50
2.5.5	Generation of MRSA252Δ <i>cadAC</i> and MRSA252Δ <i>mco</i> Δ <i>cadAC</i>	51
2.6	Transformation	51
2.6.1	Preparation of chemical competent <i>E. coli</i>	51
2.6.2	Preparation of electrocompetent <i>S. aureus</i>	52
2.6.3	Transformation of <i>E. coli</i> by heat shock	52
2.6.4	Transformation of <i>S. aureus</i> by electroporation	52

2.6.5	Transformation of <i>S. aureus</i> with pCL55 plasmids	52
2.7	Fractionation of <i>S. aureus</i>	53
2.8	TCA Precipitation of Supernatant Proteins	54
2.9	SDS-PAGE and Western Blotting	54
2.10	Growth of <i>S. aureus</i> in subinhibitory concentrations of copper in TSB....	55
2.11	Growth of <i>S. aureus</i> in subinhibitory concentrations of copper in RPMI .	55
2.12	Growth of <i>S. aureus</i> on TSA supplemented with CuCl ₂	56
2.13	Macrophage survival assay	56
2.14	Whole blood survival assay	56
2.15	Bacterial growth in purified human plasma.....	57
2.16	Neutrophil isolation from whole human blood	57
2.17	Serum isolation from whole human blood	58
2.18	Neutrophil survival assay	58
2.19	Neutrophil activation for gene expression analysis.....	58
2.20	RNA extraction using Norgen Biotek corp RNA kit	59
2.21	Reverse transcription (cDNA synthesis).....	59
2.22	Quantitative RealTime-Polymerase Chain Reaction (qRT-PCR)	59
2.23	Microtitre plate biofilm assay	59
2.24	Minimum Inhibitory Concentration Assay	60
2.25	<i>in silico</i> data analysis and statistical tests.....	60
Chapter 3	Results Chapter 1 - Mco is a membrane localised protein in <i>S. aureus</i> that contributes to copper tolerance in aerobic conditions	62
3.1	Introduction	63
3.2	Similarities and differences between <i>S. aureus</i> Mco and <i>E. coli</i> CueO.....	65
3.3	Modelling the structure of Mco	68
3.4	Generation of pIMAY:: Δ mco by allelic exchange	70
3.5	Generation of MRSA252 Δ mco by allelic exchange with pIMAY:: Δ mco	72

3.6	Growth or haemolysis of MRSA252 Δ <i>mco</i>	76
3.7	Expression of Mco with an N-terminal 3X-FLAG tag in response to copper supplementation.....	78
3.7.1	Generation of pCL55::UCMF.....	78
3.7.2	Generation of pCL55::UCMF Δ Mco2-53.....	80
3.8	Mco is a membrane-located protein in <i>S. aureus</i>	82
3.9	Mco confers copper tolerance to MRSA252.....	86
3.10	Growth of <i>S. aureus</i> in copper supplemented anaerobic conditions.....	90
3.11	Growth of MRSA252 Δ <i>mco</i> in TSBd supplemented with copper.....	93
3.12	Growth of MRSA252 Δ <i>mco</i> in RPMI supplemented with copper.....	95
3.13	Generation of reporter protein expression constructs.....	98
3.14	Residues 1-56 of Mco contains a cleavable signal peptide that delivers a reporter protein to the supernatant.....	101
3.15	Generation of pRMC2::D3D4Mco1-26 and pRMC2::D3D4Mco27-56	104
3.16	Mco1-26 contains a cleavable secretory signal sequence.....	106
3.17	Mco residues 1-26 do not direct protein secretion through the TatAC pathway	108
3.18	Discussion.....	112
3.19	Results Chapter 1 Summary.....	117
Chapter 4	Results Chapter 2 - Investigation into novel genes involved in copper tolerance in <i>S. aureus</i>	118
4.1	Introduction.....	119
4.2	Whole genome sequence analysis of MRSA252 Δ <i>mco</i> clones.....	120
4.3	Gene deletion profile of MRSA252 14 gene KO.....	123
4.4	Mutagenesis leading to generation of MRSA252 14 gene KO.....	126
4.5	Analysis of the growth profile of MRSA252 14 gene KO in copper supplemented media.....	130
4.6	Generation of MRSA252 Δ <i>cadA</i> , MRSA252 Δ <i>cadAC</i> , MRSA252 Δ <i>mco</i> Δ <i>cadA</i> and MRSA252 Δ <i>mco</i> Δ <i>cadAC</i>	136

4.7	Investigation of the contribution of the <i>cadAC</i> operon to copper tolerance of MRSA252	138
4.8	Discussion.....	143
4.9	Results Chapter 2 Summary	149
Chapter 5	Results Chapter 3 - Investigating the role of copper tolerance genes in resisting killing by host immune cells	150
5.1	Introduction	151
5.2	Survival of copper sensitive <i>S. aureus</i> in murine macrophages.....	153
5.3	Survival of copper sensitive <i>S. aureus</i> in whole human blood.....	155
5.3.1	Survival of copper sensitive mutants of MRSA252; <i>cadA</i> , <i>cadAC</i> , <i>mco cadA</i> , <i>mco cadAC</i> and <i>copZ</i> , in whole human blood	157
5.3.2	Survival of <i>S. aureus</i> in whole human blood using different initial inocula	159
5.3.3	Whole blood survival of <i>S. aureus</i> grown in copper before incubation in blood and plasma.....	162
5.4	Expression of copper importing genes in primary human neutrophils ..	164
5.5	Survival of <i>S. aureus</i> when incubated with primary human neutrophils in RPMI	167
5.5.1	The survival of <i>S. aureus</i> when incubated with primary human neutrophils in Hanks Balanced Salt Solution.....	169
5.5.2	The survival of copper sensitive mutants of <i>S. aureus</i> in primary human neutrophils.....	171
5.6	Neutrophil survival of <i>S. aureus rexB</i>	173
5.7	Neutrophil survival of an <i>S. aureus</i> 14-2533T and 14-2533T pSCBU	173
5.8	Discussion.....	175
5.9	Results Chapter 3 Summary	182
Chapter 6	Results Chapter 4 - The effect of copper on biofilm formation of biofilm positive clinical isolates of <i>S. aureus</i>	183
6.1	Introduction	184
6.2	Results.....	186
6.2.1	The effect of copper on biofilm formation of MRSA252	186

6.2.2	The effect of copper on biofilm formation of ED83	189
6.2.3	The effect of copper on biofilm formation of a panel of isolates of <i>S. aureus</i> from cystic fibrosis patients	192
6.2.4	Effect of copper on biofilm formation by <i>S. aureus</i> isolates from device related infections.....	194
6.2.5	Effect of copper on biofilm formation DAR isolates.....	196
6.2.6	Effect of copper on BH1CC biofilm formation and its biofilm composition	198
6.3	Discussion	200
6.4	Results Chapter 4 Summary.....	205
Chapter 7	Discussion	206
Bibliography	218

List of Tables

Table 1.1 Abbreviations Used.....	xviii
Table 2.1. Bacterial Strains used in this study	45
Table 2.2 Plasmids used in this study.....	46
Table 2.3 Primers used in this study.....	49
Table 2.4 Antibodies used in this study	55
Table 4.1. The 13 additional genes deleted in MRSA252 14 gene KO....	122

List of Figures

Figure 1.1. Schematic diagram of <i>S. aureus</i> biofilm formation	11
Figure 1.2. Schematic of copper tolerance mechanisms in MRSA252	22
Figure 1.3. Proposed mechanism of CueO cuprous oxidase activity	28
Figure 1.4. Sec system secretion in Gram-positive bacteria.....	35
Figure 1.5. The Tat system of Gram-positive bacteria.....	38
Figure 3.1 Alignment of <i>S. aureus</i> Mco and <i>E. coli</i> CueO	66
Figure 3.2. Mco1-56 is found in <i>Staphylococcus</i> and <i>Listeria</i> genera, and is predicted to contain a Sec signal peptide.....	67
Figure 3.3. <i>S. aureus</i> Mco model based on <i>E. coli</i> CueO superimposed on CueO.....	69
Figure 3.4 Generation of pIMAY:: Δmco	71
Figure 3.5 Deletion of <i>mco</i> using pIMAY mediated allelic exchange.	73
Figure 3.6. Integration and excision of pIMAY:: Δmco leading to MRSA252 Δmco generation.....	75
Figure 3.7. Confirmation that MRSA252 Δmco was not compromised during mutagenesis procedure.....	77
Figure 3.8 Generation of pCL55::UCMF	79
Figure 3.9. Construction of MRSA252 Δmco ::pCL55::UCMF Δmco 2-53....	81
Figure 3.10 Mco is membrane located in <i>S. aureus</i>	83
Figure 3.11. Expression of Mco3XFLAG in response to copper supplementation of growth media.	85
Figure 3.12 Mco contributes to copper tolerance in MRSA252.	87
Figure 3.13. The C-terminal 3X-FLAG tag does not disrupt the function of Mco	89
Figure 3.14 <i>S. aureus</i> is more sensitive to copper in anaerobic conditions	91

Figure 3.15 Growth of <i>S. aureus</i> on copper supplemented agar in anaerobic conditions	92
Figure 3.16. Growth of <i>S. aureus</i> in TSBd supplemented with copper	94
Figure 3.17. Growth of MRSA252 Δ <i>mco</i> in RPMI	97
Figure 3.18. Generation of pRMC2::D3D4::Mco1-56, WTSP and NoSP .	100
Figure 3.19. Mco1-56 transports D3D4 to the supernatant.....	103
Figure 3.20. Design and Generation of pRMC2::D3D4Mco1-26 and pRMC2::D3D4Mco27-56.....	105
Figure 3.21. Mco1-26 contains a supernatant localising signal peptide...	107
Figure 3.22. KK-KQ substitution of Mco signal peptide does not affect secretion of the reporter protein	109
Figure 3.23 Deletion of <i>tatAC</i> from <i>S. aureus</i> does not affect Mco signal peptide delivery of reporter protein to the supernatant	111
Figure 4.1 Whole genome sequencing identified a clone with three unintended regions of DNA deletion during the mutagenesis process to generate MRSA252 Δ <i>mco</i>	121
Figure 4.2. Schematic of the genes deleted in MRSA252 14 gene KO ...	127
Figure 4.3 The off target gene deletions of 14 gene KO were not detectable by conventional mutant confirmation procedures	129
Figure 4.4 MRSA252 14 gene KO is more sensitive to copper than MRSA252 and MRSA252 Δ <i>mco</i>	131
Figure 4.5 Growth of MRSA252 14 gene KO on copper supplemented TSA and its minimum inhibitory concentration of copper.....	134
Figure 4.6 Growth of MRSA252 14 gene KO on copper supplemented agar in anaerobic conditions.....	135
Figure 4.7. Schematic diagram of isogenic mutants generated between the <i>copB</i> and <i>sar0725</i> locus in MRSA252 to investigate the role of the <i>cadAC</i> operon in copper tolerance.....	137

Figure 4.8. Growth of <i>cadAC</i> deletion mutants in liquid media supplemented with copper.....	140
Figure 4.9. Growth of <i>cadAC</i> deletion mutants on TSA supplemented with copper.....	142
Figure 5.1 Survival of MRSA252 in murine macrophages	154
Figure 5.2 Survival of MRSA252 and its mutants in whole human blood and growth in plasma	156
Figure 5.3 Survival of copper sensitive MRSA252 deletion mutants in whole human blood and growth in plasma.....	158
Figure 5.4 Survival of <i>S. aureus</i> in whole blood and growth in plasma when the initial inocula is changed	161
Figure 5.5 Whole blood survival and growth in plasma of <i>S. aureus</i> that had been grown in sub-inhibitory copper before incubation with whole human blood or plasma.....	163
Figure 5.6. Expression of copper transporting genes in primary human neutrophils in response to copper and TNF- α	166
Figure 5.7 Survival of copper sensitive <i>S. aureus</i> mutants when incubated with primary human neutrophils in RPMI.....	168
Figure 5.8. Survival of <i>mco</i> mutant derivatives of <i>S. aureus</i> when incubated with primary human neutrophils in HBSS	170
Figure 5.9 Survival of copper sensitive <i>S. aureus</i> deletion mutants when incubated with primary human neutrophils in HBSS	172
Figure 5.10 Survival of control <i>S. aureus</i> strains JE2 and 14-2533T with human neutrophils.....	174
Figure 6.1 Copper reduces biofilm formation of MRSA252	187
Figure 6.2 Copper induces formation of a protein-mediated biofilm in ED83	190
Figure 6.3 Effect of copper on biofilm formation of cystic fibrosis clinical isolates CF10 and CF15.....	193

Figure 6.4 The effect of copper supplementation on biofilm formation of clinical <i>S. aureus</i> isolates from device related infections.....	195
Figure 6.5 The effect of copper supplementation on biofilm formation of DAR clinical isolates	197
Figure 6.6 Copper reduces <i>fnbAB</i> mediated biofilm formation of BH1CC 199	
Figure 7.1 Mco is localised to the membrane of <i>S. aureus</i>	210

Key to Abbreviations

Table 1.1 Abbreviations Used

Abbreviation	Full Name
Amp	Ampicillin
ATc	Anhydrotetracycline
BHI	Brain Heart Infusion
bp	Base pairs
Cm	Chloramphenicol
DPI	Diphenyleneiodonium
DMEM	Dulbecco's Modified Eagle Medium
h	Hours
kb	Kilobase pairs
KO	Knock Out
Mco	Multicopper Oxidase
LB	Luria Burtani
MCS	Multiple Cloning Site
PCR	Polymerase Chain Reaction
ROS	Reactive Oxygen Species
RPMI	Roswell Park Memorial Institute
SLIC	Sequence and Ligase Independent Cloning
<i>sbi</i>	The second immunoglobulin binding protein of <i>S. aureus</i>
<i>spa</i>	Staphylococcal immunoglobulin binding protein A
TSA	Tryptic Soy Agar
TSBd	Tryptic Soy Broth (difco)
WT	wild-type

Chapter 1

Introduction

1.1 The Biology of Staphylococci

1.1.1 Classification and Identification

Staphylococcus aureus was first identified by Sir Alexander Ogston when he identified micrococci in pus. He subsequently named these 'staphylococci' upon observing the grape-like etiological agent of suppurative abscesses (Ogston, 1882). Shortly afterwards, Friedrich Rosenbach coined the term *Staphylococcus aureus* to describe its characteristic yellow/gold colonies and to differentiate it from another staphylococcal commensals that formed dull white/grey colonies (*Staphylococcus albus*, now *Staphylococcus epidermidis*) (Rosenbach, 1884).

The staphylococci belong to the family *Staphylococcaceae*, order *Bacillales*, class *Bacilli* (Becker, Skov and Eiff, 2015). They are most closely related to *Enterococcus*, *Bacillus* and *Listeria*, and their genomes have DNA of a characteristically low G+C content (30-39%) (Stackebrandt and Teuber, 1988).

Bacteria of the genus *Staphylococcus* are Gram-positive organisms that characteristically divide in three planes to form grape-like structures (Tzagoloff and Novick, 1977). They are extremely halotolerant, growing in up to 3.5 M NaCl and can ferment mannitol allowing their selection by growth on mannitol salt agar.

The production of coagulases can divide the staphylococci into two further groups: coagulase-positive and coagulase-negative staphylococci. *Staphylococcus aureus*, *Staphylococcus pseudintermedius*, *Staphylococcus delphini* and *Staphylococcus intermedius* make up the coagulase positive group, while *Staphylococcus epidermidis* and *Staphylococcus lugdunensis* are typical coagulase negative staphylococci. *Staphylococcus aureus* is a facultative anaerobe, Gram-positive, coagulase-positive, catalase-positive, DNase-positive, non-motile coccus that forms smooth round colonies when grown on solid media (Missiakas and Schneewind, 2013). *S. aureus* produces a carotenoid pigment called staphyloxanthin, which gives *S. aureus* its characteristic golden/yellow colony colour.

1.1.2 Colonisation and Disease

S. aureus is both a commensal and a deadly human pathogen. *S. aureus* persistently colonizes the nares of about 20% of healthy humans while the remainder are colonized transiently (Mulcahy and McLoughlin, 2016). The reason

for this is not properly understood but is in part due to variation in innate immune defences and competition with members of the nasal microbiota such as *S. epidermidis*, *S. hominis* and *S. lugdunensis*. Nasal carriage by *S. aureus* is an established risk factor for *S. aureus* infection, and infected individuals are usually infected with the strain that they carry (Perl *et al.*, 2002; Van Belkum *et al.*, 2009). However, *S. aureus* nasal carriage has also been associated with an increased survival or reduced morbidity of *S. aureus*-mediated bacteraemia related deaths (Van Belkum *et al.*, 2009). This suggests that nasal colonisation contributes to immunological memory aiding in resolution of subsequent infection with *S. aureus*.

Between 10-30% of *S. aureus* bacteraemia patients die from their infection (van Hal *et al.*, 2012). Bacteraemia accounts for a greater number of deaths than acquired immune deficiency syndrome (AIDS), tuberculosis and viral hepatitis combined (van Hal *et al.*, 2012) in the USA. In 2017 there were 119,247 recorded *S. aureus* bacteraemia cases with 19,832 deaths (Kourtis *et al.*, 2019).

The burden on healthcare facilities caused by *S. aureus* is further complicated by the growth of antimicrobial resistance which reduces the available treatment options for patients. If the rise of antimicrobial resistance continues it is predicted to cost global economies 100 trillion USD by 2050 (Rice, 2010).

1.1.3 Methicillin-resistant *Staphylococcus aureus*

Penicillin resistance in *S. aureus* was detected within 2 years of the routine use of penicillin (Kirby, 1944). This was mediated by a plasmid encoded penicillinase (β -lactamase) (Rountree and Freeman, 1955). Methicillin-resistant *S. aureus* (MRSA) emerged in the healthcare setting in 1958 shortly after introduction of the β -lactamase insensitive derivative methicillin (Barber, 1961; Jevons, 1961). Methicillin resistance is mediated by the production of novel PBP2a protein by the *mecA* or *mecC* genes, conferring resistance to the majority of β -lactam antibiotics that have since been developed (Katayama, Ito and Hiramatsu, 2000). MRSA infection increases mortality rates, increases length of hospital stays and increases economic costs more than methicillin sensitive *S. aureus* (Whitby, McLaws and Berry, 2001; Antonanzas, Lozano and Torres, 2015).

1.1.4 Mobile Genetic Elements of *S. aureus*

Mobile genetic elements are regions of DNA that can move within or between genomes. The most common types of mobile genetic elements seen in *S. aureus* are bacteriophages, pathogenicity islands, plasmids, transposons and staphylococcal cassette chromosomes (Lindsay, 2010). Mobile genetic elements can harbour genes coding for antimicrobial resistance, virulence factors, and heavy metal resistance.

Most *S. aureus* harbour at least one lysogenic bacteriophage and some have as many as four (Lindsay and Holden, 2004). Bacteriophages can carry virulence genes like enterotoxin A (*sea*), Panton-Valentine leukocidin (*lukSF*), complement inhibitory protein (*scin*), chemotaxis inhibitory protein (*chip*) and staphylokinase (*sak*) (Betley and Mekalanos, 1985; Kaneko *et al.*, 1998; Lindsay and Holden, 2006).

Plasmids can be either large or small in size, and often harbour resistance genes to antibiotics like erythromycin, penicillin, trimethoprim, and heavy metals like cadmium and arsenic (Berg *et al.*, 1998; Lindsay, 2010). Plasmids may contain transposons which specify antimicrobial and heavy metal resistance genes.

Transposons are relatively small regions of DNA that often confer resistance to antibiotics or heavy metals (Bruins, Kapil and Oehme, 2000). Transposons also integrate into staphylococcal cassette chromosomes (Rowland and Dyke, 1989).

Staphylococcal cassette chromosomes are segments of DNA that insert specifically into the *orfX* gene of *S. aureus* (Liu *et al.*, 2016). They can carry small transposons and plasmids. All harbour a *mecA*, *mecB* or *mecC* gene (Katayama, Ito and Hiramatsu, 2000) which code for a novel penicillin binding protein PBP2a, which results in resistance to beta-lactam antibiotics (Katayama, Ito and Hiramatsu, 2000). A *mecD* gene also exists, but is only found in *Micrococcus caseolyticus* (Schwendener, Cotting and Perreten, 2017). There are at least thirteen different Staphylococcal chromosomal cassette *mec* (SCC*mec*) (types I-XIII) (Lakhundi and Zhang, 2018). SCC*mec* type-IV is a relatively small SCC*mec* present in the successful USA300 lineage of Community Acquired-MRSA (CA-MRSA) (Diep *et al.*, 2006). These CA-MRSA strains also harbour the Panton-Valentine leukocidins *lukS* and *lukF* and frequently cause devastating skin and soft tissue infections and

necrotising fasciitis in individuals outside of the hospital setting (Chambers, 2005; Miller et al., 2005; Diep et al., 2006).

The Arginine Catabolic Mobile Element (ACME) and Copper and Mercury (COMER) resistance elements are distinct mobile genetic elements that are located adjacent to the *SCCmec* element of USA300 CA-MRSA (Planet *et al.*, 2015). *SCCmec* type IX contains cadmium, copper and arsenic resistance operons (Liu *et al.*, 2016), the *copXcopL* operon associates with the ACME element in North American *SCCmec* type IV (Planet *et al.*, 2015; Rosario-Cruz *et al.*, 2019), and the *merAB*, *copX*, *mco* and *copL* genes occur in the COMER element in the Latin America variant of the *SCCmec* type IV (Planet *et al.*, 2015). The ACME element contributes to fitness and virulence of *S. aureus* in a rabbit model of bacteraemia (Diep *et al.*, 2008).

Hospital Acquired-MRSA (HA-MRSA) describe MRSA strains that cause nosocomial infections in hospitals. They rarely harbour the Panton-Valentine leukocidins, are often heavily resistant to antibiotics, and are life threatening associated with device related infections, bacteraemia, necrotising pneumonia, osteomyelitis and endocarditis (Johnson *et al.*, 2001; McDougal *et al.*, 2003; Holden *et al.*, 2004).

The prevalence of metal resistance genes in a multitude of mobile genetic elements found in a diverse background of successful *S. aureus* lineages, indicating that they provide a survival advantage to *S. aureus*.

Clinically relevant *S. aureus* strains often harbour multiple mobile genetic elements carrying an array of genes specifying virulence factors and resistance to antibiotics and toxic metals. MRSA252, a CC30 HA-MRSA clinical isolate harbours a *SCCmec* type II cassette, bacteriophages, an *S. aureus* pathogenicity island, as well as an integrated plasmid and transposons (Lindsay and Holden, 2004). The mobile genetic elements carry genes encoding virulence factors (*sea*, *sak*, *set*, *spl* and *hysA*); antimicrobial resistance (*mecA*, *ble*, *kan*, *ermA*, *spc* and *blaZ*) and heavy metal resistance (*cadAC* and *arsBC*) (Lindsay and Holden, 2004).

In summary, the success of *S. aureus* as a pathogen can be attributed in part to its ability to harbour a diverse array of mobile genetic elements which can

specify antimicrobial resistance, heavy metal resistance, and virulence mechanisms (Lindsay, 2010).

1.2 *S. aureus* virulence factors

S. aureus expresses a diverse array of secreted and surface-located proteins that contribute to its ability to cause infections (Cheung, Bae and Otto, 2021). This section focusses on those that are important for helping the organism avoid neutrophils, the first line of defence against *S. aureus* infection.

1.2.1 Chemotaxis inhibition by *S. aureus*

S. aureus has developed a number of defence mechanisms to combat neutrophil killing (Guerra *et al.*, 2017). Neutrophil defence against *S. aureus* begins with migration of neutrophils in peripheral blood to the site of infection. This is triggered by cytokines, chemokines, and host derived products such as damage associated molecular patterns and complement (Petri and Sanz, 2018). The C5a component of the complement system is recognised by the C5aR on the surface of neutrophils. The chemotaxis inhibitory protein of *S. aureus* (CHIPS) binds to the C5aR on neutrophils and prevents neutrophil activation and migration (De Haas *et al.*, 2004). Similarly, activation of the formyl peptide receptor-like-1 (FPRL1) on the surface of human neutrophils results in chemotaxis towards the site of infection. *S. aureus* secretes chemotaxis inhibiting proteins, FPRL1 inhibitory protein (FLIPr) and FLIPr-like protein, which inhibit chemotaxis by binding and antagonising FPRL1 (Prat *et al.*, 2009).

1.2.2 Opsonisation inhibition by *S. aureus*

S. aureus has defence mechanisms against opsonisation which in turn protect it from phagocytic killing. Effective phagocytosis requires opsonisation of pathogens by complement and immunoglobulins. *S. aureus* has defence mechanisms against both. Staphylococcal immunoglobulin binding protein A is a cell wall anchored protein that binds the F_c region of IgG (Forsgren and Sjöquist, 1966). Binding of protein A to IgG prevents neutrophil phagocytosis (Dossett *et al.*, 1969). Protein A also acts as a B cell superantigen by binding the F_{ab} region of IgM and causing B cell apoptosis, and can prevent complement activation by the classical pathway (Goodyear and Silverman, 2003). It also triggers plasma B cell

production of antibodies that do not provide protection against *S. aureus* (Pauli *et al.*, 2014).

The second binding protein of immunoglobulin (Sbi) can bind the F_c region of immunoglobulins via its N-terminal D1 and D2 immunoglobulin binding domains (Smith *et al.*, 2011). This impairs phagocytosis of *S. aureus*. The D3 and D4 domains of Sbi bind to the C3 component of the complement system (Smith *et al.*, 2011). Sbi binding to complement components C3 and Factor H inhibits activation of the alternate complement pathway (Haupt *et al.*, 2008).

The staphylococcal complement inhibitory (SCIN) protein binds and inhibits human C3 convertases, preventing C3b mediated opsonisation of *S. aureus* and preventing phagocytosis (Rooijackers *et al.*, 2005).

These are just three of the virulence factors in *S. aureus* that contribute to immune evasion by disrupting opsonisation pathways, evading phagocytosis of *S. aureus* by professional phagocytes. Other virulence factors that impede opsonophagocytosis by *S. aureus* include proteins collagen adhesin (Cna) (Kang *et al.*, 2013), serine-aspartate repeat containing protein E (SdrE) (Zhang *et al.*, 2017), extracellular adherence protein (Eap) (Woehl *et al.*, 2014), staphylococcal superantigen-like protein 7 (SSL7) (Langley *et al.*, 2005), staphylococcal serine protease (SspA) and aureolysin (Aur) (Dubin, 2002; Cheung, Bae and Otto, 2021).

1.2.3 Toxin mediated killing of neutrophils

S. aureus expresses a number of toxins that can kill neutrophils to augment its virulence. Some of the most well characterised are bi-component leucocidins and phenol soluble modulins (Periasamy *et al.*, 2012; Berube and Wardenburg, 2013; Alonzo and Torres, 2014).

The cytolytic α -toxin has multiple functions in *S. aureus* virulence (Berube and Wardenburg, 2013). It's a 33 kDa protein that oligomerises into a heptameric membrane spanning pore. α -toxin targets a disintegrin and metalloprotease 10 (ADAM10) protein in the cellular membrane (Wilke and Wardenburg, 2010). ADAM10 is high affinity receptor for α -toxin and explains its tropism for cells expressing the ADAM10 protein such as erythrocytes, leukocytes, platelets, endothelial and epithelial cells (Tam and Torres, 2019). Binding of α -toxin to ADAM10 stimulates protease activity which degrades tight junctions causing

damage to the epithelium, which has been shown in murine lung infection (Powers *et al.*, 2012). ADAM10 has been shown to be required for α -toxin mediated virulence in mice, as disruption of the *ADAM10* gene from lung epithelial cells protected mice from fatal pneumonia (Inoshima *et al.*, 2011). α -toxin induces cell death of B cells and T cells, but not polymorphonuclear leukocytes (Nygaard *et al.*, 2012; Tam and Torres, 2019).

The bicomponent leucocidins lyse and kill immune cells by creating an octameric β -barrel pore in their phospholipid membrane (Alonzo and Torres, 2014). All strains of *S. aureus* are capable of producing at least three bicomponent leucocidins (HlgAB, HlgCB, and LukAB/HG). Of the six known leucocidins, the most virulent *S. aureus* strains produce five (HlgAB, HlgCB, and LukAB/HG, Panton-Valentine leucocidin (PVL)/LukSF, and LukED) (Alonzo and Torres, 2014; Tam and Torres, 2019). LukMF is only found in *S. aureus* isolated from ruminants. PVL is only present in 2-3% of all *S. aureus* strains (Vandenesch *et al.*, 2003), but has garnered significant attention due to its association with CA-MRSA isolates and considerable contribution to virulence in a rabbit lung model of infection (Diep *et al.*, 2010). Host cell receptors determine the host tropism of the bicomponent leucocidins. HlgAB targets human erythrocytes, neutrophils, monocytes and macrophages by binding to CXCR1, CXCR2, CCR2 and the Duffy antigen receptor for chemokine (DARC) (Spaan *et al.*, 2014; Spaan, Reyes-Robles, *et al.*, 2015). The PVL/LukSF toxins target human and rabbit leukocytes by targeting the human and rabbit G-protein-coupled-receptors (GPCRs) C5aR1 and C5aR2 (Spaan *et al.*, 2013; Spaan, Schiepers, *et al.*, 2015). The LukED toxins target human neutrophils, monocytes, macrophages, dendritic cells, NK cells, T cells and red blood cells by binding to the GPCRs CXCR1, CXCR2, CCR5 and DARC (Alonzo *et al.*, 2013; Reyes-Robles *et al.*, 2013; Spaan, Reyes-Robles, *et al.*, 2015).

Phenol soluble modulins (PSMs) are a family of amphipathic α -helical peptides which can disrupt and lyse immune cells (Cheung *et al.*, 2014). They have cytolytic activity against neutrophils which is most clear with the PSM α 3 peptide (Wang *et al.*, 2007). The α -type PSMs are approximately 20-25 amino acids in length while the β -type PSMs are approximately 44 amino acids in length (Wang *et al.*, 2007). PSMs exert their function after phagocytosis and can facilitate escape from the

phagolysosome (Grosz *et al.*, 2014). This property is likely because PSMs are inactivated in the extracellular environment by serum lipoproteins (Surewaard *et al.*, 2012), meaning they can only function when intracellular.

S. aureus has relatively recently been accepted to be an intracellular pathogen. Immunofluorescence studies showed that USA300 strains of *S. aureus* can survive and replicate inside the phagolysosome of murine macrophages (Flannagan, Heit and Heinrichs, 2016). This reinforces the importance for *S. aureus* to have mechanisms of resisting phagocytic killing for its survival in immune cells. The phagolysosome of immune cells is an extremely harsh environment with antimicrobial peptides, and ROS-like nitric oxide, superoxide and hydrogen peroxide (Flannagan, Cosío and Grinstein, 2009). Resistance of *S. aureus* to oxidative stress is important for its survival in host phagocytes. Known *S. aureus* mechanisms for combating oxidative stress include the production of catalase KatA and alkyl hydroperoxide reductase AhpC (Cosgrove *et al.*, 2007), superoxide dismutases SodA and SodM (Karavolos *et al.*, 2003), and the carotenoid staphyloxanthin (Liu *et al.*, 2005).

1.2.4 Neutrophil disorders and increased susceptibility to *S. aureus* infection

The importance of neutrophils in eradication of *S. aureus* from the host can be seen in human neutrophil disorders. For example, Chronic Granulomatous Disease (CGD) is an X-linked or autosomal recessive disease where neutrophils have impaired generation of ROS due to a defective NADPH oxidase gene (Segal *et al.*, 2011). CGD is characterised by recurrent bacterial and fungal infections, of which *S. aureus* is the most common infectious bacterium (Buvelot *et al.*, 2017). In CGD patients, *S. aureus* causes skin and soft tissue abscesses, pneumonia, hepatic granulomas and abscesses, lymphadenitis, bacteraemia and osteomyelitis (van den Berg *et al.*, 2009; Song *et al.*, 2011). This reinforces the importance of neutrophils and their ROS-mediated defences against *S. aureus*.

Archer and colleagues examined the immune response to nasal colonisation of mice with *S. aureus* and found that neutrophil depletion increased *S. aureus* colonisation, implicating neutrophils in *S. aureus* clearance from the nasal cavity. Furthermore, *S. aureus* clearance was T-cell dependent, suggesting that a Th17-

associated immune response is required for neutrophil influx and elimination of murine nasal colonisation (Archer, Harro and Shirtliff, 2013).

1.3 Biofilm Formation by *Staphylococcus aureus*

S. aureus biofilms pose a significant challenge to healthcare as they cause infections associated with implanted medical devices such as catheters, cardiovascular devices and prosthetic joints (O’Gara and Humphreys, 2001; Zimmerli, Trampuz and Ochsner, 2009). Biofilms are complex multicellular communities of bacteria embedded in an extracellular matrix that are able to form on biotic or abiotic surfaces (Schilcher and Horswill, 2020). The life cycle of a biofilm can be broadly divided into three parts namely the attachment, proliferation/maturation and detachment phases (O’Toole, Kaplan and Kolter, 2000; Otto, 2018; Schilcher and Horswill, 2020).

The attachment phase of biofilm formation describes the process by which planktonic bacteria initially attach to the abiotic or biotic surface (Fig. 1.1). The attachment of *S. aureus* to implanted devices often does not require binding to the abiotic surface itself as host matrix molecules like fibrinogen and fibronectin quickly cover the surface of implant (Vaudaux *et al.*, 1995; Heilmann, 2011). Binding can be mediated by the Microbial Surface Component Recognising Adhesive Matrix Molecules (MSCRAMM) family of cell wall anchored (CWA) proteins. Many members of the MSCRAMM family can bind host factors such as fibrinogen and fibronectin, mediating biofilm formation (Foster, 2019). The MSCRAMMs consist an N-terminal signal peptide, a ligand-binding domain, an extended repeated sequence, a cell wall anchoring region, a membrane-spanning region and a positively charged tail (Clarke and Foster, 2006). There is a LPXTG motif at the C-terminus that promotes covalent linkage to the cell wall peptidoglycan by sortase A (Mazmanian *et al.*, 1999). Some of the most notable MSCRAMMs are clumping factor A (ClfA), clumping factor B (ClfB), fibronectin binding protein A (FnbpA), fibronectin binding protein B (FnbpB) and the serine-aspartate repeat (Sdr) family of proteins (Josefsson *et al.*, 1998; Clarke and Foster, 2006).

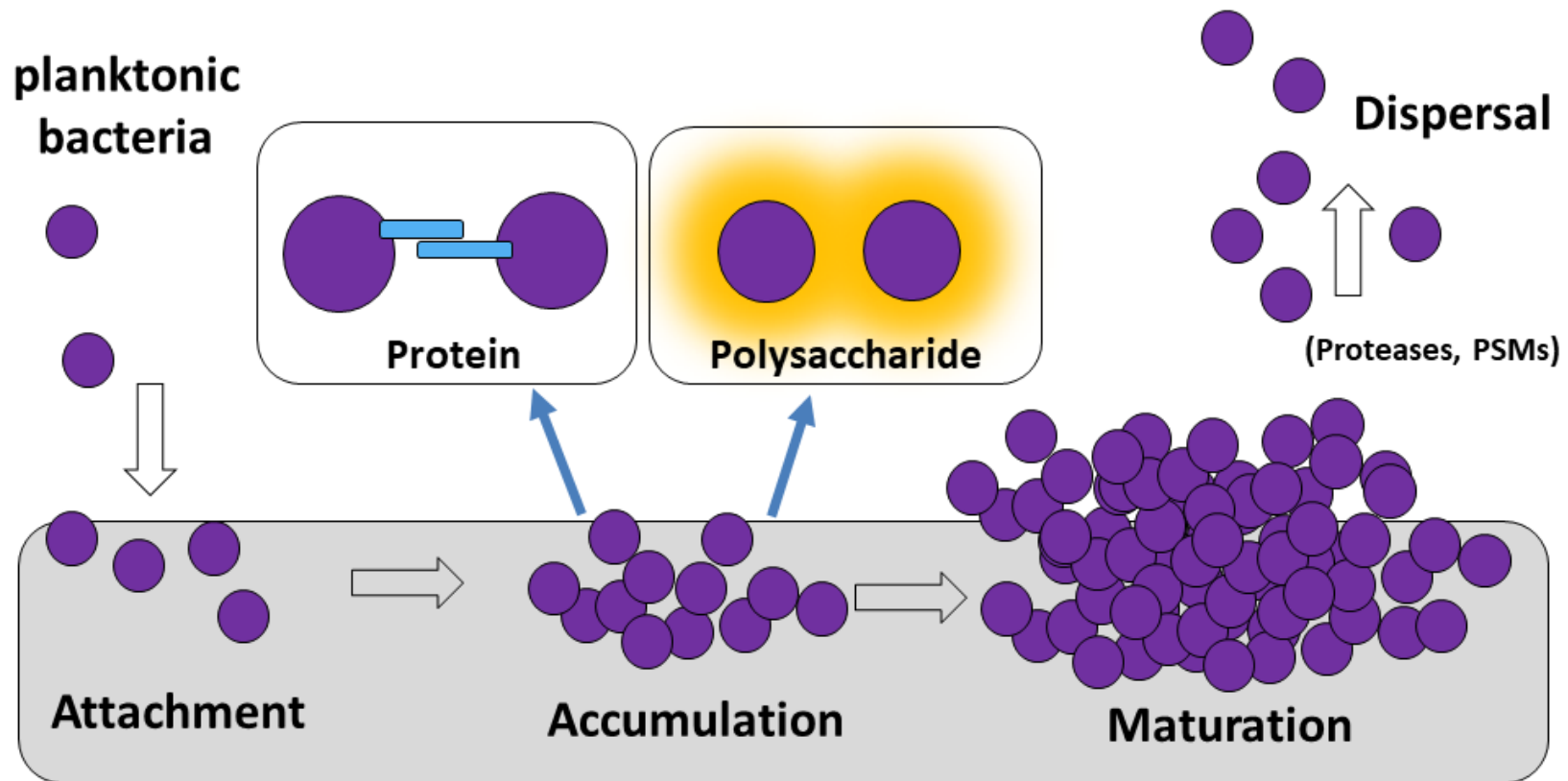


Figure 1.1. Schematic diagram of *S. aureus* biofilm formation

Diagram showing the main phases of *S. aureus* biofilm formation. Planktonic bacteria initially attach to the biotic or abiotic surface. Then the accumulation phase begins as bacteria divide on the surface developing into either a cell well anchored protein-mediated biofilm or a secreted extracellular polysaccharide matrix mediated biofilm. When the mature biofilm is formed, proteases and PSMs are secreted which permit disassociation and dispersal of cells from the biofilm. These can disseminate to develop infection at a different location.

The accumulation/maturation phase of biofilm consists of generation of the extracellular polymeric substance, eventually generating the biofilm matrix. This consists of polysaccharides, proteins, teichoic acids, and eDNA (Schilcher and Horswill, 2020). The composition of the biofilm matrix can divide *S. aureus* biofilms into those with a polysaccharide matrix, and those with a proteinaceous matrix (Fig. 1.1). The polysaccharide produced by staphylococci is called poly-N-acetylglucosamine (PNAG) or alternatively the polysaccharide intercellular adhesin (PIA) (Mack *et al.*, 1996). PNAG is synthesized by the products of the *icaADBC* operon, which is under the control of the transcriptional repressor IcaR (Conlon, Humphreys and O’Gara, 2002).

The accumulation phase involves low affinity homophilic interactions between cell wall anchored proteins on adjacent cells. It is often mediated by protein-protein interactions, rather than relying on the production of extracellular polymeric substances. Fibronectin binding proteins are the dominant cell-wall anchored proteins involved in biofilm formation by some MRSA strains (O’Neill *et al.*, 2007). MSSA isolates usually produce polysaccharide mediated biofilms, but not always (O’Neill *et al.*, 2007). *Staphylococcus epidermidis* often produces a polysaccharide mediated biofilm (Rohde *et al.*, 2007; Otto, 2018), but many clinical *S. epidermidis* isolates lack the *icaADBC* operon and form a proteinaceous biofilm matrix with the accumulation associated protein (Aap) (Rohde *et al.*, 2005). Aap is closely related to the SasG protein of *S. aureus*, and both are important for biofilm formation (Hussain *et al.*, 1997; Rohde *et al.*, 2005; Geoghegan *et al.*, 2010) and adhesion to nasal epithelial squamous cells (Roche, Meehan and Foster, 2003). Proteins that are important in Staphylococcal biofilm formation include Aap (Hussain *et al.*, 1997; Rohde *et al.*, 2005), SasG (Geoghegan *et al.*, 2010), Bap (Taglialegna *et al.*, 2016), SdrC (Feuillie *et al.*, 2017), FnbpA and FnbpB (O’Neill *et al.*, 2008).

Non-protein extracellular polymers involved in biofilm formation include wall teichoic acids and extracellular DNA (Whitchurch *et al.*, 2002; Otto, 2018). A mutant deficient in AtlA, an autolysin responsible for extracellular DNA release and is important for primary attachment, shows reduced biofilm production (Bose *et al.*, 2012). A mutant deficient in the staphylococcal thermonuclease had enhanced biofilm forming ability (Kiedrowski *et al.*, 2011). *S. aureus* biofilms are sensitive to

externally added DNase (Mann *et al.*, 2009). These data together indicate that extracellular DNA is a component of the biofilm matrix.

The architecture of a mature biofilm is a three-dimensional structure with high mushroom-like towers with fluid-filled channels (Otto, 2013; Schilcher and Horswill, 2020). These are generated by enzymes and proteins such as proteases and phenol soluble modulins that shape the mature biofilm (Fig. 1.1). The dispersal phase of biofilm formation involves the release of bacteria from a mature biofilm back into the planktonic state which facilitates dissemination and infection at other sites. The metalloprotease aureolysin (Aur) (Banbula *et al.*, 1998), cysteine proteases SspB and ScpA (Golonka *et al.*, 2004), and serine protease SspA can disrupt and disperse protein-mediated biofilms (Rice *et al.*, 2001). Phenol soluble modulins disperse mature biofilms due to their surfactant properties (Wang *et al.*, 2007; Periasamy *et al.*, 2012; Otto, 2013).

Biofilm associated cells show low metabolic activity similar to small colony variants. This and low levels of ATP are presumed to contribute to the antimicrobial tolerance of biofilms, contributing to complicated and long-term infections in patients. The difficulty of eradication of biofilms usually leads to surgical removal of biofilm-infected implanted devices (Conlon *et al.*, 2016; Waters *et al.*, 2016; Bui, Conlon and Kidd, 2017; Guo *et al.*, 2022). *S. aureus* biofilm formation is not only implicated in hospital implanted medical device related and prosthetic joint infections (Otto, 2018), but is also the suspected cause of menstrual staphylococcal toxic shock syndrome, where *S. aureus* secretes the pyrogenic toxin superantigen TSS toxin 1 (Schlievert and Davis, 2020).

1.4 Copper Biology

Metals are ubiquitous in living cells being functionally required as a bound cofactor for 40% of all proteins (Waldron *et al.*, 2009). Copper is a required cofactor for important human cuproenzymes such as cytochrome-c oxidase, ceruloplasmin, superoxide dismutase, lysyl oxidase and dopamine- β -mono-oxygenase (Linder and Hazegh-Azam, 1996). There is an extremely low level of free copper in cells (Rae *et al.*, 1999). Newly absorbed copper from the gut is quickly bound to proteins such as albumin, transcuprein and ceruloplasmin (Linder *et al.*, 1998).

1.4.1 Copper homeostasis disorders in humans

There are two notable disorders of copper homeostasis in humans, Menkes disease and Wilson's disease. These disorders are due to defects in the human copper transporting P-Type ATPase genes *ATP7A* and *ATP7B* (Bull and Cox, 1994).

Menkes disease is a fatal X-linked copper deficiency disorder due to mutation of the *ATP7A* gene producing a defective ATP7A protein. It affects primarily infant males, who suffer cuproenzyme related deficiencies, hypotonia, neurological defects and seizures, often resulting in death by the age of three. However early diagnosis and treatment can improve clinical outcomes significantly (Mercer, 2001; Kaler *et al.*, 2008).

Wilson's disease is a copper toxicity disorder due to a defective *ATP7B* gene, resulting in the inability to correctly package and export copper from the liver (Mercer, 2001). It is a rare disease with a prevalence of 30 cases per million (I. H. Scheinberg and I. Sternlieb Philadelphia, 1984). Left untreated it results in liver failure due to copper toxicity to hepatocytes. Current treatment options include copper chelation therapy, or zinc supplementation as an inducer of methallothioneins (Mercer, 2001; Rodriguez-Castro, Hevia-Urrutia and Sturniolo, 2015).

The expression of the human *ATP7A* gene was detected in cells from the heart, brain, placenta, lung, muscle, kidney and pancreas but not the liver (Vulpe *et al.*, 1993). The expression of the *ATP7B* gene was detected in heart, brain, placenta, lung, liver, muscle, kidney and pancreas, but a marked increase in expression was observed in the liver and placenta (Tanzi *et al.*, 1993). This is congruent with the copper toxicity caused to hepatic cells seen in Wilson's disease patients, as they have defective copies of the *ATP7B* genes.

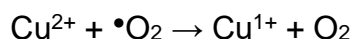
Both the Menkes and Wilson's diseases give insight into the importance of correct copper homeostasis mechanisms in eukaryotes, and how disruption of these P-Type ATPase mediated copper homeostatic mechanisms alone, are detrimental for human health.

1.4.2 The bactericidal properties of copper

The bactericidal nature of copper has long been known. The use of copper as an antimicrobial to sterilise chest wounds and drinking water was recorded in one of the oldest texts ever discovered, written by the ancient Egyptians (Dollwet and Sorenson, 1985; Grass, Rensing and Solioz, 2011). The ancient Greeks, Romans, Aztecs and others have recorded using copper and copper based compounds to treat headaches, burns, intestinal worms, ear infections and for cleaning and hygienic purposes (Dollwet and Sorenson, 1985). However the molecular mechanisms of copper toxicity are only being understood with the advent of modern medicine.

1.4.3 Copper catalysed generation of hydroxyl radicals

One mechanism of copper toxicity lies in the ability of copper to catalyse the production of reactive oxygen species such as hydrogen peroxide, superoxide anions and most notably hydroxyl radicals via the Fenton and Haber-Weiss reactions summarised below (Haber and Weiss, 1934; Liochev and Fridovich, 2002).



Due to the high standard reduction potential of $\bullet\text{OH}$ ($> 2 \text{ V}$) (Freinbichler *et al.*, 2011) copper catalysed production of $\bullet\text{OH}$ can cause oxidative damage to macromolecules (Yoshida, Furuta and Niki, 1993; Freinbichler *et al.*, 2011). The half-life of $\bullet\text{OH}$ is extremely short (10^{-9} s) so macromolecule damage will be diffusion limited to the molecules closest in proximity to the copper. This is congruent with data showing the $\bullet\text{OH}$ generation occurs in the periplasm of *E. coli*, the cellular compartment where copper is most enriched (Macomber, Rensing and Imlay, 2007). These reactive oxygen species generated by copper via Fenton and Haber-Weiss reactions can cause lipid peroxidation, inhibit respiration, and cause oxidative damage to proteins (Yoshida, Furuta and Niki, 1993; Nandakumar *et al.*, 2011).

1.4.4 Copper and mismetallation

Copper can cause damage to proteins by mismetallation. Mismetallation is the displacement of the desired metal ion from a metalloprotein and replacement with an undesired metal ion which can render that metalloprotein non-functional.

Most cases of mismetallation can be explained by the Irving-Williams series (Irving and Williams, 1953) which describes how the stability of complexes formed by different divalent metals is ordered, as is shown below.



The presence of a particular divalent metal ion higher up the Irving-William series can displace a metal ligand lower ranked in the series from its location in the protein (Foster, Osman and Robinson, 2014; Imlay, 2014). Bacterial mechanisms of protecting from mismetallation include metallochaperones and metal cofactor loading during protein folding (Waldron and Robinson, 2009; Stewart *et al.*, 2019).

1.4.5 Copper and disruption of iron sulphur clusters

Another mechanism of copper damage is via disruption of iron sulphur clusters. Cu^{1+} ions disrupt the iron sulphur cluster of the SufU protein of *Bacillus subtilis* (Chillappagari *et al.*, 2010). The expression of the PerR regulon which is involved in oxidative stress defence was not induced by copper, suggesting that copper toxicity was not due to oxidative stress (Chillappagari *et al.*, 2010). Copper damaged the iron-sulphur cluster enzyme fumarate reductase and reduced iron-sulphur cluster biogenesis in *E. coli* grown in anaerobic and amino acid limited conditions (Fung *et al.*, 2013). Furthermore, expression of the CusCFBA copper efflux pump and additional iron-sulphur cluster biogenesis systems was increased in response to anaerobic conditions (Fung *et al.*, 2013). Additional evidence indicates that Cu^{1+} ions are more toxic than Cu^{2+} ions due to their higher thiophilicity and avidity for sulphhydryl groups (Abicht *et al.*, 2013). Iron-sulphur biogenesis is disrupted when *E. coli* is exposed to copper in anaerobic conditions, which indicates that iron-sulphur cluster disruption is a mechanism of copper toxicity that does not require oxygen (Tan *et al.*, 2017).

1.4.6 Metallic copper proposed mechanisms of bactericidal activity

The killing of microbes placed on metallic copper surfaces occurs within minutes to hours. Killing is exceptionally fast when bacteria encounter dry metallic copper. The mechanisms of killing by metallic copper are less understood than in media supplemented with copper salts. The currently proposed model of contact killing by copper is that copper is rapidly dissolved by liquid on the surface of the metal. This causes severe membrane damage lysing the membrane, reactive

oxygen species are generated further damaging the cell, and finally any remnants of DNA left on the copper are destroyed (Grass, Rensing and Solioz, 2011). Metallic copper causing damage by dissolving in the solution applied to its surface is supported by the fact that the use of Tris buffer as the suspension solution for applying bacteria dramatically enhanced bacterial killing on metallic copper, and that more copper is dissolved by Tris buffer than PBS or water (Molteni, Abicht and Solioz, 2010). Furthermore, addition of copper chelators protected *E. coli* from metallic copper killing, and the *pco* copper resistance operon did not protect *E. coli* from killing (Espírito Santo *et al.*, 2008).

Interestingly, Gram-positive bacteria are the most prominent group of bacteria isolated from copper coins (Espírito Santo, Morais and Grass, 2010). These bacteria were as sensitive to liquid copper ions as copper resistant bacteria, indicating that the mechanisms of resistance to metallic copper are completely different to liquid copper ions. There was no increased association with antimicrobial resistance and strains that survived on pure metallic copper, indicating that dry metallic copper resistance does not appear to co-select for antimicrobial resistance (Espírito Santo, Morais and Grass, 2010).

1.4.7 GSH and copper

Glutathione is a small thiol-containing tripeptide that is found in all eukaryotes, and many prokaryotes. It protects cells from toxic free metal ions. Deletion of the genes responsible for the glutathione transporting protein GshT, or glutathione reductase, increases the sensitivity of *Streptococcus pneumoniae* to the ROS-generating compound paraquat, and the metals copper, cadmium and zinc (Potter, Trappetti and Paton, 2012).

Glutathione has been shown to play an important role in buffering excess copper in *Streptococcus pyogenes* when its copper detoxification system has been overloaded (Stewart *et al.*, 2020). Some Gram-positive bacteria lack glutathione, but it is usually replaced by another small thiol containing homologue, bacillithiol (Gaballa *et al.*, 2010). Although the role of bacillithiol in copper resistance in *S. aureus* is undetermined, bacillithiol has been shown to improve survival of *S. aureus* in murine macrophages (Pöther *et al.*, 2013), and has been shown to contribute to

oxidative stress resistance, H₂O₂ resistance and whole blood survival (Posada *et al.*, 2014).

1.4.8 Copper and the human immune system

Copper plays an important and complex role in optimal innate immune function (Djoko *et al.*, 2015). Rats fed copper deficient diets had impaired neutrophil function including reduced superoxide dismutase activity, reduced superoxide generation, and reduced ability to kill *Candida albicans*. There was no reduction in phagocytosis between copper fed and deficient rats. The reduction in neutrophil function were restored in these rats within 1 week of supplementation of feed with copper (Babu and Failla, 1990).

Similarly, cattle fed a copper deficient diet had reduced neutrophil counts and a reduced killing capacity for phagocytosed *S. aureus* compared to cattle fed a copper sufficient diet. Superoxide dismutase function was reduced in copper deficient cattle, and there was no reduction in phagocytosis seen between copper fed and deficient cattle (Xin *et al.*, 1991).

A study examining polymorphonuclear leukocyte function in hypocupraemic infants before and after intervention with a copper supplemented diet (Heresi *et al.*, 1985) found that phagocytic killing was significantly improved for babies after dietary intervention with supplementary copper, indicating that copper deficiency reduces neutrophil function in humans, and that this can be restored with dietary copper supplementation (Heresi *et al.*, 1985).

Copper deficiency in humans that is not due to Wilson's disease most often presents as a result of bariatric surgery. Bariatric surgical intervention can lead to nutritional absorption defects, including copper. The resulting cupraemia causes neutropoenia and anaemia, indicating the importance of copper for maintaining normal haematological function (Halfdanarson *et al.*, 2008). Neutropoenia, reduced granulocyte maturation and erythrocyte hypoplasia have also been observed in cupraemic infants where dietary copper supplementation reduced peripheral blood neutropoenia and improved granulocyte maturation (Cordano, Placko and Graham, 1966).

1.4.9 Copper use by macrophages to enhance intracellular bacterial killing

Research into how macrophages kill intracellular bacteria has advanced greatly in recent years, including the discovery that macrophages employ copper in their arsenal to enhance intracellular killing of phagocytosed bacteria. It was observed that upon exposure to mycobacteria species, IFN- γ activated peritoneal macrophages accumulated copper in their phagolysosomes (Wagner *et al.*, 2005). This indicated that infection triggers the import of copper into the phagolysosomes of professional phagocytes.

White and colleagues observed that the murine macrophage RAW264.7 cells increased both ATP7A and CTR1 expression in response to IFN- γ and LPS resulting in the import of copper into cytoplasm and phagolysosome (White, Lee, *et al.*, 2009). The copper transporter ATOX1 delivers copper to ATP7A in the Golgi apparatus which in turn localises to the phagolysosomal membrane to transport copper into the phagolysosome (White, Kambe, *et al.*, 2009; White, Lee, *et al.*, 2009). This suggests that copper is employed by macrophages during inflammation in response to both IFN- γ and LPS resulting in copper being imported into the cytoplasm and phagolysosome.

To investigate if ATP7A transported copper enhances bacterial killing in macrophages, RAW264.7 cells were transfected with a 29 bp short hairpin RNA interference (RNAi) plasmid against ATP7A, which provided robust silencing of the *ATP7A* gene. Survival of *E. coli* in IFN- γ activated macrophages was improved from 16% to 45% upon silencing of ATP7A with *ATP7A* RNAi. This demonstrates that ATP7A mediated copper transport enhances intracellular bacterial killing (White, Lee, *et al.*, 2009).

To investigate if bacterial copper tolerance genes improve survival inside macrophages the intracellular survival of an *E. coli* mutant lacking a copper exporter was examined. Survival of *E. coli* strain W3110 Δ *copA* was lower (15%) than its wild-type (43%) after 1 hour in RAW264.7 macrophages (White, Lee, *et al.*, 2009). This indicates that *copA* contributes to intracellular survival of *E. coli* in macrophages. This discovery suggests that copper hypertolerance could be a general virulence mechanism for bacteria to enhance survival in the host. However more studies are required to thoroughly investigate this.

1.5 Copper tolerance genes in *S. aureus*

S. aureus harbours a number of genes that contribute to copper tolerance (Fig. 1.2). The *copA* and *copZ* genes are conserved in all *S. aureus* strains, and are co-localised together on the *copAZ* operon. Expression of the *copAZ* operon is under the control of the CsoR protein (Baker *et al.*, 2011). CsoR is a transcriptional repressor which binds the promoter region upstream of *copAZ*. When copper is present, it binds CsoR, causing derepression of transcription of the *copAZ* operon. CopA is a copper transporting P_{1B}-Type ATPase. CopZ is a copper binding metallochaperone (Sitthisak *et al.*, 2007) (Fig. 1.2). P_{1B}-Type ATPases belong to the superfamily of P-Type ATPases which transport cations and lipids (Palmgren and Nissen, 2011). P_{1B}-Type ATPases typically consist of six to eight transmembrane helices, an ATP binding domain, and an actuator domain. P_{1B}-Type ATPases couple ATP-hydrolysis at the ATP binding domain to metal ion transport across the membrane by cycling between low and high affinity metal binding states within the metal binding sites in the transmembrane helices (Albers, 1967; Smith, Smith and Rosenzweig, 2014; Purohit *et al.*, 2018).

The *copB* and *mco* genes are found in all CC30 strains of *S. aureus* as part of a plasmid that is integrated into the chromosome that also harbours heavy metal resistance genes (Zapotoczna *et al.*, 2018). The *copBmco* operon is expressed under the control of the copper sensitive transcriptional repressor CsoR, which controls transcription of *copBmco* in the same manner it controls expression of *copAZ* (Baker *et al.*, 2010) (Fig. 1.2). CopB is another copper transporting P_{1B}-type ATPase that has been shown to confer copper tolerance, to improve intracellular survival in murine macrophages, and to improve survival when incubated in whole human blood (Zapotoczna *et al.*, 2018). Mco is a multicopper oxidase, which contributes to copper tolerance (Sitthisak *et al.*, 2005). The *mco* gene has also been shown to contribute to copper tolerance, improve intracellular survival in murine macrophages, and improve survival in human blood, when it was introduced into a CC22 strain of *S. aureus* on a replicating plasmid alongside other heavy metal resistance genes (Zapotoczna *et al.*, 2018).

The copper tolerance genes *copX* and *copL* are found in *S. aureus* isolates of the USA300 lineage. The *copX* and *copL* genes occur together as part of the

ACME element of North American USA300 isolates. They are also part of the COMER element in South American USA300 isolates (Planet *et al.*, 2015; Saenkham-Huntsinger *et al.*, 2021). The *copX* gene codes for another copper transporting P_{1B}-Type ATPase. CopX and CopB are two copper transporting P-Type ATPases that share a high degree of sequence homology. Sometimes CopX is called CopB in the literature due to this homology, but for the remainder of this thesis CopX and CopB are described as two different proteins (Purves *et al.*, 2018; Rosario-Cruz *et al.*, 2019).

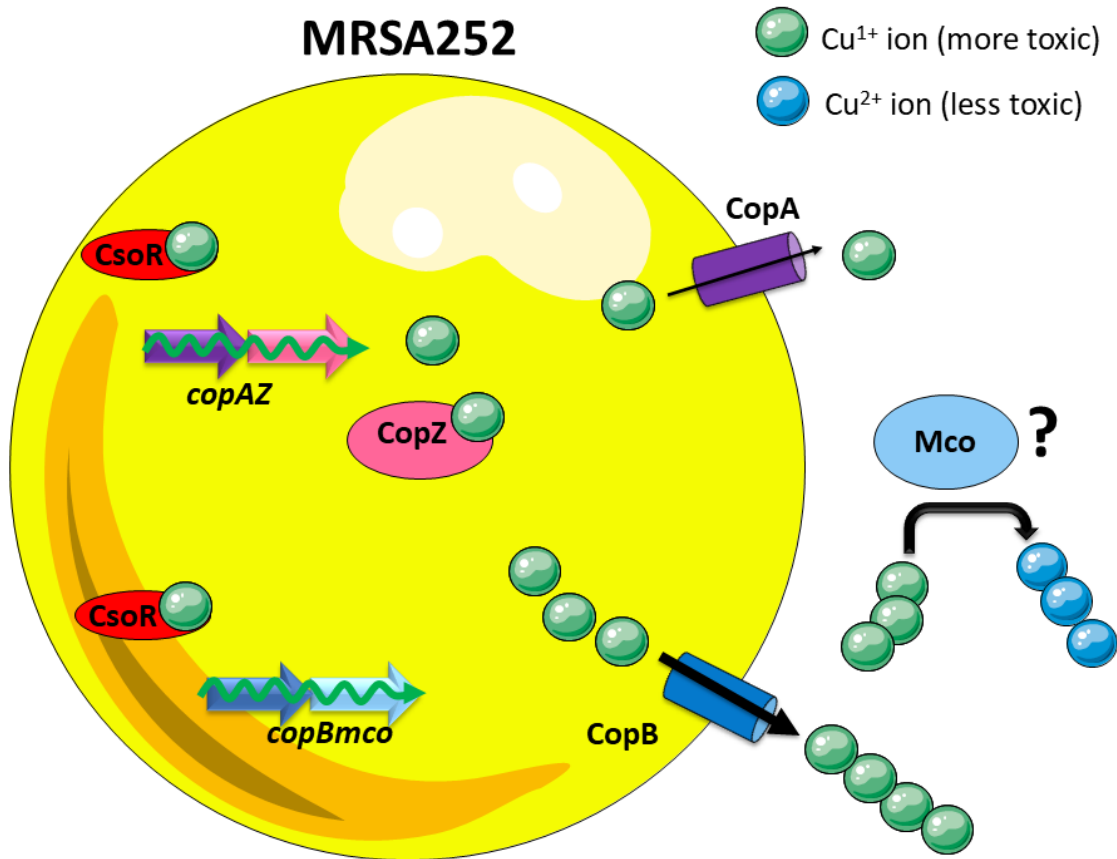


Figure 1.2. Schematic of copper tolerance mechanisms in MRSA252

Schematic of the copper tolerance for MRSA252 (yellow sphere). The *copA* and *copZ* genes (purple and pink arrows respectively) form an operon that is under the control of CsoR. CsoR (red oval) derepresses transcription upon Cu^{1+} ion (green sphere) binding. CopA (purple barrel) is a P_{1B} -Type Cu^{1+} transporting ATPase depicted exporting Cu^{1+} ions out of the cell. CopZ (pink oval) is a Cu^{1+} binding metallochaperone, binding free Cu^{1+} in the cytoplasm.

The *copB* and *mco* genes (blue and light blue arrows respectively) form an operon that is under the control of CsoR. CsoR derepresses transcription upon Cu^{1+} ion binding. CopB (blue barrel) is a high efficiency P_{1B} -Type Cu^{1+} transporting ATPase. It is depicted exporting more Cu^{1+} ions than CopA to indicate higher efficiency. Mco (light blue oval) is a multicopper oxidase of unknown location (indicated with '?') that putatively contributes to copper tolerance by oxidising toxic Cu^{1+} ions to less toxic Cu^{2+} ions (blue spheres).

The *copL* gene codes for a copper binding lipoprotein that contributes to copper tolerance and virulence in *S. aureus* (Rosario-Cruz *et al.*, 2019; Saenkham-Huntsinger *et al.*, 2021). It is found in USA300 lineage CA-MRSA strains, and not HA-MRSA strains like MRSA252 (Planet *et al.*, 2015; Purves *et al.*, 2018; Zapotoczna *et al.*, 2018). CopL is a membrane-associated, surface-exposed lipoprotein that can bind up to 4 Cu⁺ ions. It is co-transcribed with *copX*, and can confer copper tolerance independently of *copA* and *copX*. Mutation of the copper ligand binding sites of CopL attenuates copper tolerance to the same extent as a deletion mutant, indicating that copper binding was required for conferring copper tolerance (Rosario-Cruz *et al.*, 2019). The *copL* gene has been shown to contribute to intracellular survival in murine macrophages (Purves *et al.*, 2018), suggesting it may augment virulence of *S. aureus* during infection. CopL contributes to copper tolerance when plated on copper supplemented agar only in iron restricted conditions, revealing a connection between copper tolerance and iron homeostasis (Saenkham-Huntsinger *et al.*, 2021). CopL also contributes to fitness of *S. aureus* during urinary tract infection in a mouse model (Saenkham-Huntsinger *et al.*, 2021).

Transcriptional profiling of *S. aureus* grown in copper supplemented media showed an increase in expression of genes involved in copper resistance (*copAZ*), oxidative stress resistance (*ahpF*, *sodM*), and misfolded protein response (*clpB*, *clpC*) (Baker *et al.*, 2010). These data indicate that copper can damage *S. aureus* by the generation of ROS. This aligns with the proposed mechanism of bactericidal activity of copper via Fenton and Haber-Weiss reactions where the breakdown of H₂O₂ into superoxide and hydroxyl radicals is catalysed by copper. Expression of oxidative stress response genes indicates *S. aureus* battles copper toxicity by reducing H₂O₂ content in the cell, preventing copper catalysed formation of hydroxyl radicals.

Proteomic analysis of *S. aureus* grown in copper supplemented media showed that the SodM, AhpC, AhpK and KatA proteins involved in oxidative stress resistance were induced in response to copper (Tarrant *et al.*, 2019). The proteomic investigation is congruent with the previously mentioned transcriptional response of *S. aureus* to copper (Baker *et al.*, 2010).

1.6 Multicopper oxidases – a widely conserved family of proteins

Multicopper oxidases are a widely conserved family of enzymes found in bacteria, fungi, plants and mammals (Solomon, Sundaram and Machonkin, 1996). The family of multicopper oxidases includes laccases, ferroxidases, ascorbate oxidase and ceruloplasmin (Hoegger *et al.*, 2006). Multicopper oxidases in turn belong to the family of blue copper proteins which contain from 1-6 copper ions per molecule.

All multicopper oxidases function by coupling four one-electron substrate oxidation steps to the four-electron reduction of dioxygen to water (Solomon, Sundaram and Machonkin, 1996). Substrate oxidation occurs at the type 1 (T1) copper centre. The electrons are then transferred to the trinuclear copper centre (T2/T3) where dioxygen binds and is reduced to water (Solomon, Sundaram and Machonkin, 1996). Multicopper oxidases can oxidise a number of different substrates such as copper and iron ions to organic compounds. Fungal laccases are involved in lignin degradation (Leonowicz *et al.*, 2001), ascorbate oxidase oxidises ascorbate in plants (Messerschmidt and Huber, 1990), ceruloplasmin oxidises Fe^{2+} to the more readily transportable Fe^{3+} in iron homeostasis (Takahashi, Ortel and Putnam, 1984).

Multicopper oxidases are proteins that form complexes with copper. Cysteines, histidines and methionines are most frequently found as the ligand donor for copper complexes. A selection of copper complexes in multicopper oxidases are described in Fig. 2 in the review by Sakurai and Kataoka (Sakurai and Kataoka, 2007).

Ceruloplasmin is a well characterised human multicopper oxidase found in blood. It harbours 90-95% of the copper found in blood. It functions as a ferroxidase oxidising Fe^{2+} to Fe^{3+} which is required for transferrin uptake of iron (Hellman and Gitlin, 2003). It binds 6 or 7 cuprous ions per protein (Solomon, Sundaram and Machonkin, 1996) and is the primary source of copper for copper transport and homeostasis in humans. Ceruloplasmin is mobilised to the urinary tract of mice during urinary tract infection. Copper resistant *S. aureus* have improved fitness during urinary tract infection (Saenkham-Huntsinger *et al.*, 2021).

There is a membrane bound multicopper oxidase in *Saccharomyces cerevisiae* called Fet3 (De Silva *et al.*, 1995). It is a homologue of ceruloplasmin (De Silva *et al.*, 1997) and it contributes to copper tolerance (Shi *et al.*, 2003).

1.7 Bacterial multicopper oxidases

1.7.1 *Escherichia coli* multicopper oxidase

The most well described bacterial multicopper oxidase is *Escherichia coli* CueO. Prior to 2000, it was called YakK. It was subsequently designated the Cu efflux oxidase CueO by Outten *et al.* (Outten *et al.*, 2000). It was shown that *copA* (a P-Type ATPase) and *cueO* are both under the transcriptional control of the MerR homologue CueR (Outten *et al.*, 2000). A *cueO* disrupted mutant had a reduced MIC to copper (2.75 mM compared to 3.5 mM) (Grass and Rensing, 2001b).

CueO binds 4 copper atoms per molecule and has spectroscopic properties similar to blue copper oxidases suggesting it has copper centres T1 and T2/T3. CueO has *para*-phenylenediamine (pPD) oxidase activity, 2, 6-dimethoxyphenol (DMP) oxidase activity and ferroxidase activity (Grass and Rensing, 2001a). CueO oxidises 2,3-dihydroxy benzoic acid (DHB) (Grass *et al.*, 2004). Silver ions are a potent inhibitor of CueO, as 5 μ M silver is enough to suppress copper resistance in *E. coli* (Singh *et al.*, 2011). Silver can inhibit cuprous oxidase activity *in vitro* as it can bind all three copper binding sites in the methionine rich helix of CueO. This prevents substrate binding and electron transfer to the T1 nuclear centre (Singh *et al.*, 2011).

The methionine rich helix of CueO incorporates an extra three copper ligand sites, named Cu5, Cu6 and Cu7 (Fig. 1.3)(Cortes, Wedd and Xiao, 2015). The functional role of the additional sites associated with the methionine rich region has been elucidated by introducing amino acid substitutions at copper binding residues (Cortes, Wedd and Xiao, 2015). The Cu5 site connects the surface exposed copper sites Cu6 and Cu7 to the buried T1 copper centre. The methionine rich helix of CueO is a flexible alpha helix that blocks the access of a substrate to the T1 copper centre in CueO (Singh *et al.*, 2011). Oxidation of the substrate is instead performed by the surface exposed Cu6 and/or Cu7 sites (Cortes, Wedd and Xiao, 2015). The donated electron is then transferred from Cu7 to Cu5, or Cu6 to Cu7 and then to Cu5, or Cu6 straight to Cu5 as indicated by red arrows (Fig. 1.3). Electron transfer

occurs at the Cu5 site and the electron is donated to the T1 copper centre, which transfers it to the T2/T3 trinuclear cluster. The T2/T3 site is responsible for the reduction of O₂ to H₂O (Fig. 1.3).

A second multicopper oxidase is found in the plasmid-borne *pco* system of *E. coli* and *Pseudomonas syringae*, named PcoA (Rensing and Grass, 2003). It functions with the metallochaperone PcoC. PcoC can bind both Cu¹⁺ and Cu²⁺ ions. PcoA can oxidise PcoC bound Cu¹⁺ to Cu²⁺ (Djoko, Xiao and Wedd, 2008). Additionally, PcoC that is bound to Cu²⁺ only, suppresses cuprous oxidation of PcoA, reinforcing that PcoA oxidises bound Cu¹⁺ ions, and that PcoA and PcoC interact (Djoko, Xiao and Wedd, 2008). Other bacterial multicopper oxidases are reviewed and discussed below.

1.7.2 *Salmonella enterica* serovar Typhimurium multicopper oxidase

The multicopper oxidase from *Salmonella enterica* Serovar Typhimurium CueO (also known as CuiD) contributes to copper tolerance, has DMP oxidase activity and cuprous oxidase activity (Lim *et al.*, 2002; Achard *et al.*, 2010). The virulence of a *cueO* deletion mutant in a mouse model of infection was attenuated as a reduced number of bacteria were recovered from the liver and spleen, but not from Peyers patches or lymph nodes. There was no difference in survival for the *cueO* mutant in IFN- γ activated RAW264.7 macrophages (Achard *et al.*, 2010).

1.7.3 *Acinetobacter baumannii* multicopper oxidase

Williams and colleagues generated 21 transposon mutants of copper tolerance genes found in *Acinetobacter baumannii* and characterised their contribution to copper tolerance, copper transport, and virulence in a *Galleria mellonella* model of infection (Williams *et al.*, 2020). There are two multicopper oxidases in *A. baumannii*, PcoA and CueO. Both are homologues to *E. coli* CueO. Transposon mutants of both CueO and PcoA had reduced growth in copper supplemented media. However complementation of these mutants was unsuccessful (Williams *et al.*, 2020). ICP-MS analysis showed that the CueO, but not PcoA mutant, had an increased intracellular copper concentration when compared to WT, implicating CueO but not PcoA in copper homeostasis and transport (Williams *et al.*, 2020). In a *Galleria mellonella* model of infection, larvae infected with PcoA or CueO mutants had ~ 70 and ~ 90% survival after 5 days

respectively, compared to ~ 20% survival for WT. These data together indicate that the multicopper oxidases PcoA and CueO of *A. baumannii* contribute to copper tolerance and virulence (Williams *et al.*, 2020).

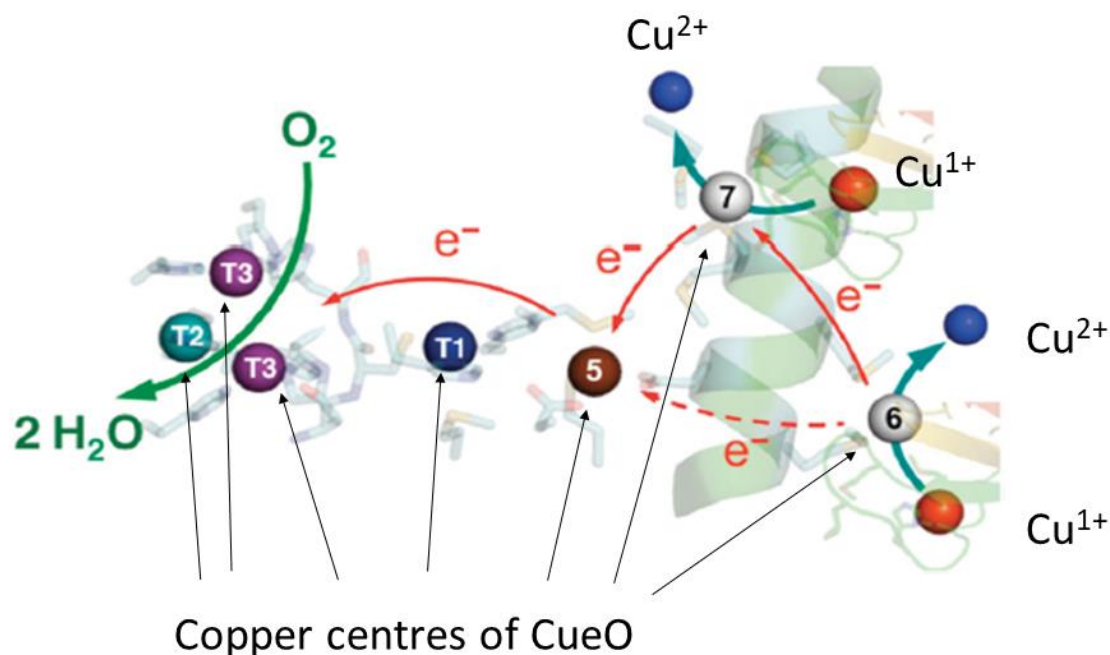


Figure 1.3. Proposed mechanism of CueO cuprous oxidase activity

Partial model of the crystal structure of CueO with copper centres emphasised (black arrows). The copper centres associated with multicopper oxidase activity (T1, blue; T2, teal; binuclear T3, purple), and the copper centres associated with the methionine-rich insert are shown (Cu5, brown; Cu6 and Cu7, grey). Cu6 and Cu7 are the two proposed reaction sites for Cu¹⁺ ion (orange) loading and oxidation to Cu²⁺ ions (blue). The function of Cu6 site depends primarily on electron transfer to the Cu7 site. Electron transfer occurs from the Cu5 site to T1, then from T1 to T2/T3 trinuclear cluster where the electron is used to reduce O₂ to H₂O. The Cu5 site is required for electron transfer from Cu6 and Cu7 to the T1 copper centre. This figure was taken and adapted from (Cortes, Wedd and Xiao, 2015).

1.7.4 *Pseudomonas aeruginosa* multicopper oxidase

The multicopper oxidase of *P. aeruginosa* was identified with the first sequenced genome of *P. aeruginosa* in 2000 but its properties remained undefined (Stover *et al.*, 2000). The *pcoA* gene of *P. aeruginosa* codes for a 72 kDa multicopper oxidase (Huston, Jennings and McEwan, 2002). All of the critical amino acids required for Type 1 and trinuclear copper centres in *E. coli* CueO are conserved in PcoA. Ferroxidase activity was detected in periplasmic preparations of *P. aeruginosa*, and purified PcoA exhibited ferroxidase activity. Sodium fluoride is the classical inhibitor of multicopper oxidases. It caused ~75% reduction in ferroxidase activity, further reinforcing the role of PcoA in ferroxidase activity.

1.7.5 *Mycobacterium tuberculosis* multicopper oxidase

The multicopper oxidase of *Mycobacterium tuberculosis* was examined by Rowland and Niederweis and named MmcO (Rowland and Niederweis, 2013). It is a 56 kDa membrane-associated protein that exhibits azino-bis(3-ethylbenzothiazoline-6-sulfonic acid) (ABTS), para-phenylenediamine and dimethoxyphenol (DMP) oxidase activity, and low levels of ferroxidase activity. It confers copper tolerance to *M. tuberculosis* and is conserved amongst almost all mycobacteria (Rowland and Niederweis, 2013). Mutants defective in MmcO had a marked attenuation in growth when plated on copper supplemented agar (Shi *et al.*, 2014). Copper tolerance is important for virulence in *M. tuberculosis* in both a guinea pig and mouse model of infection (Wolschendorf *et al.*, 2011). However the *mmcO* deletion alone did not contribute to virulence in mouse models of infection (Shi *et al.*, 2014; Shi and Darwin, 2015).

1.7.6 *Staphylococcus aureus* multicopper oxidase

The first report describing the multicopper oxidase of *S. aureus* was in 2005 (Sitthisak *et al.*, 2005). In this study, a Tn917 insertion disrupted the *mco* gene in the CC8 strain ATCC12600. The *mco* gene was cloned and overexpressed in *E. coli* and Mco multicopper oxidase activity was established as it could oxidise 3,3'-dimethoxybenzidine. This oxidase activity was copper dependent. Purified Mco had an activity of 9.7 U/mg and low levels of ferroxidase (1.58 U/mg) and phenoloxidase activity (2.3 U/mg). The *mco* mutant grew more slowly in copper and had increased

resistance to H₂O₂. This indicated that Mco is a multicopper oxidase that contributes to copper tolerance in *S. aureus* strain ATCC12600 (Sitthisak *et al.*, 2005).

This group attempted to complement the insertion mutant by cloning a 1.8 kb fragment of DNA containing *mco* into the expression plasmid pLI50. This failed to restore copper resistance, but seemed to restore H₂O₂ sensitivity (Sitthisak *et al.*, 2005). They postulated that the inability to complement the *mco* mutant was due to unintended disruption of *copA* since the cellular copper content was higher in the complemented mutant (10 pmol/10⁸ cells) than in the *mco* mutant (5 pmol/10⁸ cells). This increased intracellular copper content suggests that the *mco* mutant was attenuated in its ability to export copper, suggesting disruption of CopA function (Sitthisak *et al.*, 2005).

The Northern blot analysis indicated that 3 transcripts are produced in the wild-type after exposure to 200 µM copper, 3.5 kb, 2 kb and 1.3 kb. These are likely to specify *copB-mco*, *copB* and *mco*, respectively. The *copBmco* operon in MRSA252 is 3.5 kb in length, with *copB* being 2046 bp and *mco* 1434 bp. This suggests that *copB-mco* are co-transcribed as a 3.5 kb transcript, which is subsequently processed into separate *copB* and *mco* transcripts. Unfortunately Northern blot analysis of the complemented strain was not published, so analysis of the transcription of the *mco* gene on pLI50 cannot be determined (Sitthisak *et al.*, 2005).

The *mco* gene was also examined by Zapotoczna and colleagues (Zapotoczna *et al.*, 2018). The copper hypertolerance locus *copB-mco* is located on a mobile genetic element that is integrated into the chromosome in all CC30 strains tested. In contrast the operon is located on a plasmid named pSCBU in 50% of CC22 strains (Zapotoczna *et al.*, 2018). A precise *mco* deletion was made in pSCBU and transformed into the CC22 strain 14-2533T. The strain 14-2533T (pSCBUΔ*mco*) had a reduced MIC to copper sulphate compared to 14-2533T (pSCBU). The mutant also had impaired growth in a subinhibitory concentration of copper (4 mM). Furthermore, the mutant had a reduced intracellular survival in IFN-γ activated RAW264.7 macrophages, and reduced survival in whole human blood. This paper indicates that plasmid-borne *mco* in a CC22 background contributes to

copper tolerance as well as intracellular survival in activated macrophages and in whole human blood.

Zapotoczna and colleagues also show using recombinant CsoR in an electrophoretic mobility shift assay that CsoR does not bind immediately upstream of *mco*, but instead binds immediately upstream of *copA* and *copB*, suggesting that *copB* and *mco* are co-transcribed as a single transcript (Zapotoczna *et al.*, 2018).

1.7.7 *Listeria monocytogenes* multicopper oxidases

Multicopper oxidases are frequently specified by *Listeria monocytogenes* plasmids (Hingston *et al.*, 2019). In strain Lm106, plasmid located heavy metal resistance genes including its multicopper oxidase named MCO were upregulated ≥ 2 fold when grown in salt or acid stress conditions, suggesting involvement in improving growth of *Listeria* under environmental stress. Due to the potential role of MCO in iron homeostasis, and the coordination between iron homeostasis and oxidative stress, Hingston and colleagues speculated that MCO may be involved in oxidative stress resistance in high salt and acidic environments (Hingston *et al.*, 2019). Naditz and colleagues showed that the *L. monocytogenes* plasmid R479a specifies an MCO that is 95% identical to *S. aureus* Mco which improved survival in high salt, H₂O₂ and temperature (Naditz *et al.*, 2019). This suggests the involvement of MCO in oxidative stress resistance. Furthermore, 32% of ST87 *L. monocytogenes* isolates which are the most predominant in China contain a 90 kb plasmid that harbours metal resistance genes including *mco* (Wang *et al.*, 2019). This is consistent with MCO supporting *L. monocytogenes* survival under environmental stress.

1.7.8 *Rhodococcus erythropolis* multicopper oxidase

Multicopper oxidases are of biotechnological significance as they have uses in dye colouration, wood fibre delignification, bioremediation, polymer synthesis and food processing (Rodríguez, Pickard and Vazquez-Duhalt, 1999; Riva, 2006; Classen, Pietruszka and Schuback, 2013). *R. erythropolis* multicopper oxidase CueO displays 35% amino acid identity with *E. coli* CueO. It contains a twin arginine translocation motif, a methionine rich region similar to *E. coli* CueO, and it displays robust cuprous oxidase and DMP oxidase activity (Classen, Pietruszka and Schuback, 2013).

1.7.9 *Rhodobacter capsulatis* multicopper oxidase

The multicopper oxidase of photosynthetic purple bacterium *Rhodobacter capsulatis* was identified in 2000 (Alexandre and Zhulin, 2000) and was examined in 2006 (Wiethaus, Wildner and Masepohl, 2006). The multicopper oxidase gene *cutO* occurs in a three-gene operon *orf635-cutO-cutR*. The function of *orf635* was not determined. The *cutR* gene codes for a copper dependent repressor. CutO shares a 21% identity with *E. coli* CueO and contains an N-terminal Twin arginine translocation motif. These three genes are transcribed together. Unlike *E. coli* CueO, CutO lacks a methionine rich sequence. It binds 3.6 to 4.13 copper atoms per molecule as determined by atomic absorption spectroscopy and total reflection X-ray fluorescence spectrophotometry. CutO activity is reduced in the absence of the copper binding metallochaperone CopZ or the copper exporting ATPase CopA, indicating a link between CutO maturation and potential CopA-CopZ mediated copper export (Öztürk *et al.*, 2021). CutO contributes to copper tolerance in both aerobic and anaerobic conditions (Wiethaus, Wildner and Masepohl, 2006; Öztürk *et al.*, 2021), This is the first report of a multicopper oxidase contributing to copper tolerance under anaerobic conditions.

1.7.10 *Alphaproteobacteria* multicopper oxidase

A strain of *Alphaproteobacteria* isolated from iodine rich environments in Japan (Amachi *et al.*, 2005) expresses an extracellular multicopper oxidase system (IOX) that oxidises iodide ions (I^-) to molecular iodine (I_2), exhibits 2, 6-dimethoxy phenol and *p*-phenylenediamine activity, is inhibited by KCN, NaN_3 , EDTA and a copper chelator *o*-phenanthroline (Suzuki *et al.*, 2012). The IOX system can kill many Gram-positive and Gram-negative bacteria by generating toxic iodine (Yuliana *et al.*, 2015). It comprises *loxA* and *loxC*. *loxA* shows significant homology to the multicopper oxidases *CotA*, *CueO*, *CumA* and *CopA* (Suzuki *et al.*, 2012). This is a unique multicopper oxidase as it can oxidise molecular iodide to iodine with anti-bacterial activity (Yuliana *et al.*, 2015).

1.7.11 *Desulvibrio* multicopper oxidase

Desulvibrio sp. A2 isolated from a mining and smelting area in Russia can grow in culture containing 40 mM copper (Karnachuk *et al.*, 2008). It harbours a 71 kDa multicopper oxidase called DA2_CueO that has cuprous oxidase, ferroxidase

and phenol oxidase activity (Mancini *et al.*, 2017). DA_CueO expressed in *E. coli* $\Delta cueO$ could complement the copper sensitive phenotype of *E. coli* $\Delta cueO$ (Mancini *et al.*, 2017).

1.7.12 *Pseudomonas syringae* pathovar *tomato* multicopper oxidase

The plant pathogen *Pseudomonas syringae* pv. *tomato* appears in tomato fields in California that are heavily sprayed with copper as a disease control mechanism (Cha and Cooksey, 1991). *P. syringae* pv. *tomato* grows as blue colonies when grown on copper supplemented agar. Its multicopper oxidase CopA is a 72 kDa periplasmic protein that can bind up to 11 copper atoms per molecule (Cha and Cooksey, 1991).

The acquisition of mobile genetic elements containing heavy metal resistance genes, including multicopper oxidases, has been documented in environmental bacterial species in copper polluted agricultural soils in Chile, indicating that mobile genetic element transfer of heavy metal resistance genes occurs in metal polluted environments (Altimira *et al.*, 2012).

In summary, the prevalence and function of bacterial multicopper oxidases is diverse and complex. Multicopper oxidases are found in food borne pathogens such as *Listeria* and *Salmonella*, healthcare associated pathogens such as *S. aureus*, *E. coli*, *Acinetobacter baumannii* and *Pseudomonas aeruginosa*, in plant pathogen *Pseudomonas syringae* and mining environmental bacterial species isolates. Bacterial multicopper oxidases have a diverse substrate oxidation ability including phenol-oxidase, cuprous oxidase, ferroxidase and iodide oxidase activity. They have been implicated in resistance to toxic heavy metals such as copper, homeostatic acquisition of iron, response and resistance to oxidative, salt and acid stress, and can contribute to virulence *in vitro* and *ex vivo*, and in a multitude of host-niches *in vivo*.

1.8 Protein translocation across bacterial membranes

The transport of proteins across biological membranes is catalysed by membrane bound transport machinery. Protein export is most often mediated by one of two main transport systems, the conserved general secretion (Sec) system or the twin-arginine translocation (Tat) system (Freudl, 2013). The Sec system

transports proteins in an unfolded state, which are then folded following export through the SecYEG pore. By contrast, proteins transported via the Tat system are typically transported in their folded state.

The majority of proteins exported out of the cytosol of Gram-positive bacteria are transported via the Sec system (Tsirigotaki *et al.*, 2017). Proteins transported via the Sec system are usually synthesised with an N-terminal Sec signal peptide, which directs protein secretion through the Sec system (Freudl, 2018). The Sec signal peptide comprises a positively-charged amino-terminal (n-region), a central hydrophobic core (h-region), and a polar carboxyl-terminal domain (c-region) that contains the signal peptidase recognition site (AXA) (Freudl, 2018). In staphylococci, the Sec signal peptide is recognised and cleaved by signal peptidase I (SpsB) (Cregg, Wilding and Black, 1996). Sec protein transport can occur either in a co- or post-translational manner.

The co-translational pathway is used mainly for proteins that are integral to the cytoplasmic membrane. A ribosome-ribosome nascent chain (RNC) complex is targeted to the SecYEG pore by the signal recognition particle (SRP)/FtsY targeting system so that the ribosomal exit site is in close proximity to the SecYEG translocation pore (Fig. 1.4)(Freudl, 2013).

The post-translational mode of export is driven by the motor protein SecA. The translocation ATPase SecA interacts with the SecYEG pore and pushes the protein stepwise through it via repeated ATP hydrolysis (Pugsley, 1993; Lycklama a Nijeholt and Driessen, 2012). Accessory factors SecD and SecF exert a proton-motive-force (pmf)-dependent pulling force on the substrate from the external side of the membrane (Fig. 1.4) (Tsukazaki *et al.*, 2011; Freudl, 2013). The majority of research done on the Sec system has been performed in *E. coli*. The core components SecYEG and SecA are conserved in *S. aureus*, as well as homologues of the SecD and SecF proteins (Sibbald *et al.*, 2006).

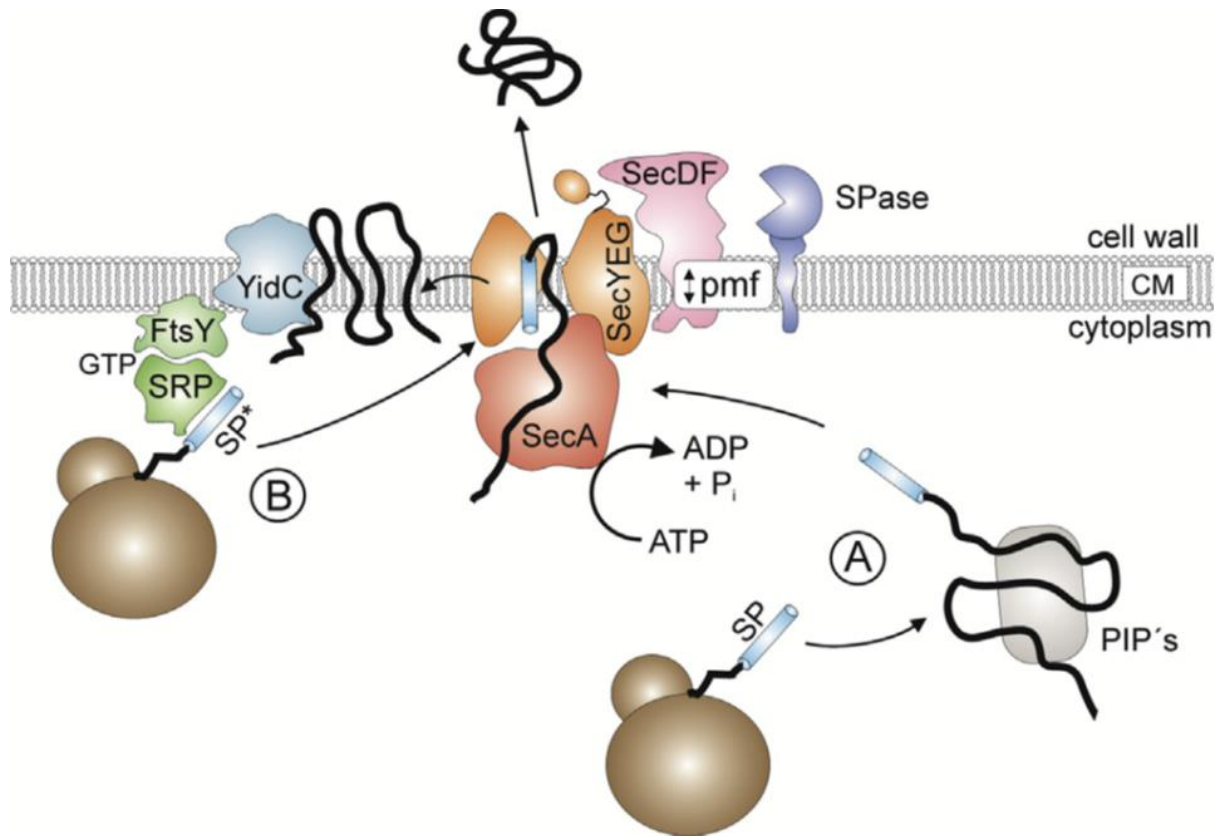


Figure 1.4. Sec system secretion in Gram-positive bacteria

(A) Translated Sec secreted proteins are bound by post-translationally interacting proteins (PIPs) to facilitate appropriate delivery of the translated and unfolded protein to the SecA protein. SecA recognises the signal peptide (SP) of this protein, and then pushes the protein through the SecYEG pore in a stepwise ATP-hydrolysis dependent manner. The SecDF complex assists with protein transport by exerting a proton motive force (pmf) from the extracytosolic face of the membrane. Signal peptidase cleaves the signal peptide from the Sec transported protein during or after SecYEG transport, releasing the mature Sec secreted protein on the extracytosolic face of the membrane. (B) Sec transport substrates that harbour a highly hydrophobic signal peptide or a transmembrane domain (SP*) are recognised by the signal peptide recognition particle (SRP) while still being translated by the ribosome. This ribosome-sec secreted protein-SRP complex docks to the SRP-receptor FtsY, which transports the sec signal peptide containing protein to the SecYEG pore. The transmembrane segments of a sec secreted transmembrane protein can be released through a laterally located gate within the SecYEG pore. SecA can also assist in the stepwise ATP-mediated pumping of these protein chains through the SecYEG pore. Membrane insertion and membrane protein folding can be assisted by the YidC. Taken from (Freudl, 2013).

The Tat system exports pre-folded proteins. Usually the proteins transported by the Tat system require a co-factor before they become functional. The Tat system has been primarily studied in *E. coli*, but research on the Tat system in Gram-positive bacteria indicates that they are similar (Freudl, 2013). Proteins transported by the Tat system have an N-terminal signal peptide that almost always contains the canonical Tat consensus motif 'S/T-R-R-X-F-L-K', where X is often a polar amino acid' at the border between the n-domain and h-domain (Berks, Palmer and Sargent, 2003; Freudl, 2018). Tat signal peptides consist of a similar tripartite structure to Sec signal peptides with an N-terminal n domain, a central hydrophobic h-domain and a carboxyl-terminal c-domain. Some characteristic differences between Sec and Tat signal peptides include Tat signal peptides having a less hydrophobic h-domain (Cristóbal *et al.*, 1999) and basic residues are often found in the c-domain which assist in avoiding the Sec systems machinery (Cristóbal *et al.*, 1999; Blaudeck *et al.*, 2003).

In *E. coli*, the Tat system is comprised of three proteins TatA, TatB and TatC (Fig. 1.5). The TatB and TatC proteins form the TatBC complex which recognises and binds Tat substrates via the Tat consensus motif (Lausberg *et al.*, 2012). Following this, recruitment of multiple TatA proteins occurs in a pmf-dependent manner (Fig. 1.5) (Mori and Cline, 2002). Membrane pores of different sizes are likely to be generated by the multimeric TatA complexes, with different sizes for differently sized Tat secreted proteins (Gohlke *et al.*, 2005). After Tat transport across the membrane, cleavage of the Tat signal peptide occurs via signal peptidase I (Fig. 1.5) (Lüke *et al.*, 2009).

A very similar Tat system is present in Gram-positives. Generally organisms with high-GC-content genomes have a TatABC system (Fig. 1.5A) (Freudl, 2013). Gram-positive bacteria with a low-GC-content genomes have a TatAC system (Fig. 1.5B). In the TatAC system of *S. aureus* and *B. subtilis*, the function of the TatB protein is replaced by a bifunctional homologue of TatA. This is supported by evidence that *B. subtilis* TatA can functionally replace both the TatA and TatB proteins in *E. coli* (Barnett *et al.*, 2008). The use of the Tat system by Gram-positive bacteria varies greatly. *B. subtilis* only exports a few proteins via Tat, while *Streptomyces coelicolor* has over one hundred Tat exported proteins (Widdick *et*

al., 2006; Freudl, 2013). The only known Tat transported protein in *S. aureus* is the iron dependent ferroxidase FepB (Biswas *et al.*, 2009).

E. coli CueO is secreted via Tat, so it was assumed that that copper cofactor assembly occurred in the cytoplasm prior to or during protein folding in order to export a copper-loaded, folded and functional protein. However this was shown not to be the case (Stolle, Hou and Brüser, 2016). Cytoplasmic CueO is not loaded with copper but is loaded upon transport to the periplasm. Binding of copper to Apo-CueO greatly stabilised the protein as assessed by protease sensitivity of Apo-CueO and Holo-CueO (Stolle, Hou and Brüser, 2016). This indicates transformation from a flexible domain structure with accessible copper sites to a closed structure with deeply buried copper ions (Stolle, Hou and Brüser, 2016). This represents the first known Tat secreted protein that is transported in an incompletely folded state. The majority of multicopper oxidases in Gram-negative bacteria contain a signal peptide with a twin arginine translocation motif responsible for membrane translocation (Palmer, Sargent and Berks, 2010; Rowland and Niederweis, 2013; Stolle, Hou and Brüser, 2016).

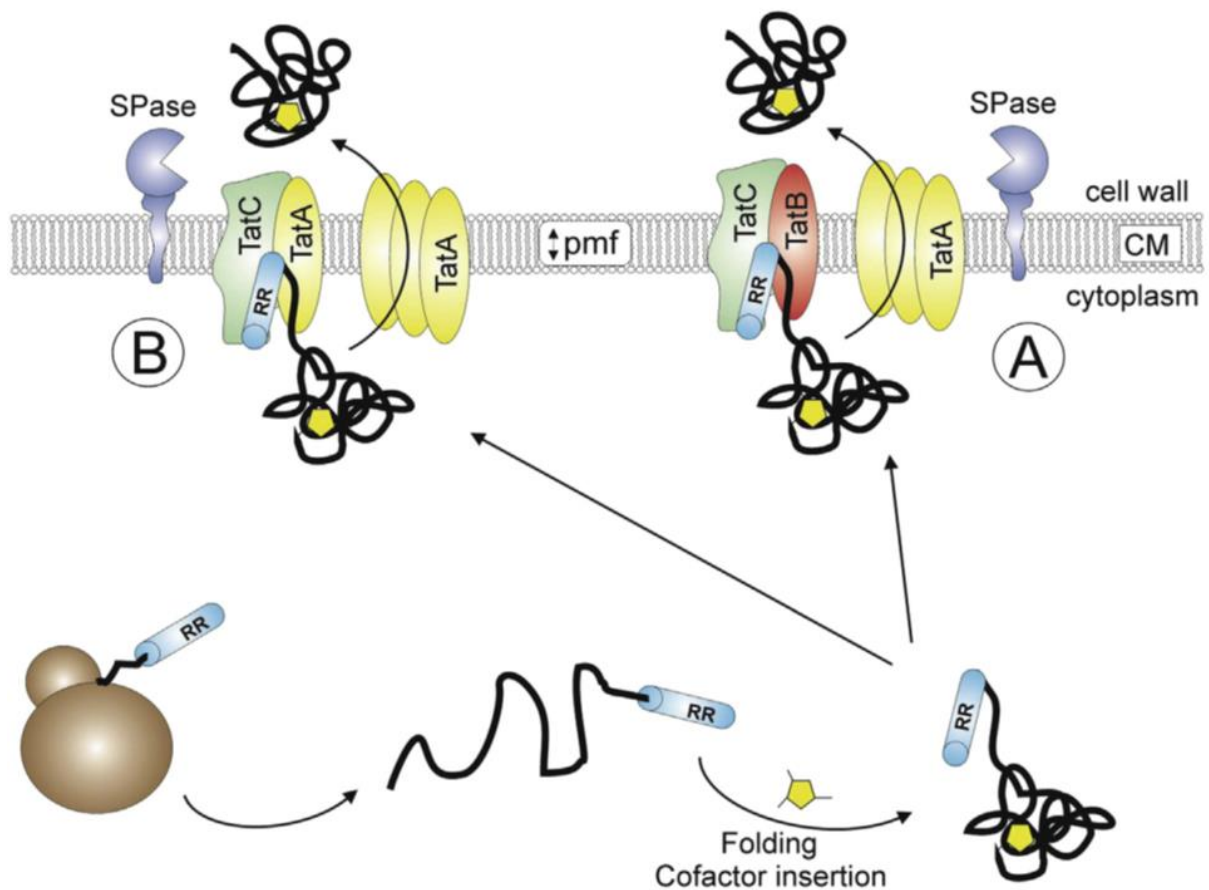


Figure 1.5. The Tat system of Gram-positive bacteria

After translation, the Tat signal peptide containing protein is folded and any required cofactors (yellow pentagon) are inserted into the folding protein while in the cytoplasm. The Twin arginine motif of the folded Tat protein is recognised by either the TatBC complex in Gram-positives with high-GC-content genomes (A) or by the TatAC complex in Gram-positives with low-GC-content genomes (B). In both cases, homo-oligomeric complexes of TatA are recruited to the membrane, and Tat protein transport occurs across the membrane. It is not yet understood how exactly this happens, but it is proposed that TatA multimers form a substrate-fitted protein-transporting channel. After membrane translocation, the Tat signal peptide is cleaved by signal peptidase one and the mature protein is released from the extracytosolic face of the membrane. Figure taken from (Freudl, 2013).

1.9 Metals and Biofilm Formation in *Staphylococcus aureus*

Given the potent bactericidal properties of heavy metals such as copper and the difficulty in treating biofilm associated infections, the potential for metal-based anti-biofilm therapy should be investigated further. However, there is little information concerning the effect of copper on staphylococcal biofilm formation.

The effect of copper on gene expression in *S. aureus* has been examined (Baker *et al.*, 2010). Genes involved in biofilm formation in iron-restricted conditions *eap* and *emp* are positively regulated by Agr and Sae. Exposure to copper downregulated the virulence gene regulators and reduced biofilm formation. Biofilm formation was not affected by exposure to manganese, magnesium or calcium (Baker *et al.*, 2010).

The effect of copper on pre-formed *Acinetobacter baumannii* biofilms *in vitro* was examined using copper tolerance gene mutants (Williams *et al.*, 2020). The sensitivity of the mutants to copper shock was similar in biofilm growth and planktonic growth, suggesting that copper resistance in planktonic growth is preserved in biofilm conditions.

The generation of *Streptococcus mutans* oral biofilms requires zinc as a nutrient. Disruption of the conserved zinc import system AdcABC of *S. mutans*, or chelation of zinc from growth media, severely attenuated the generation of *S. mutans* biofilms. This ability to generate a biofilm was restored with zinc supplementation to the media, indicating that zinc is required for biofilm formation (Ganguly *et al.*, 2021).

Biofilm formation of *S. mutans* is reduced by copper supplementation (Singh *et al.*, 2015). This was reduced further by deletion of the copper resistance operon *copYAZ*. A *copYAZ* mutant had reduced biofilm formation in the presence of 0.5 mM copper when compared to no copper, and had reduced biofilm at 0.5 mM when compared to the WT at 0.5 mM (Singh *et al.*, 2015). The *gtf* genes (*gtfB*, *gtfC*, and *gtfD*) and *gbp* genes (*gbpB* and *gbpC*) contribute to biofilm formation in *S. mutans* (Mattos-Graner *et al.*, 2006; Koo *et al.*, 2010). Supplementation of growth media with 0.5 mM copper was shown to reduce transcription of the *gtf* and *gbp* genes,

suggesting that copper may be reducing biofilm formation in *S. mutans* by reducing transcription of biofilm forming genes (Singh *et al.*, 2015).

These two studies show that *S. mutans* biofilm formation is sensitive to heavy metals. Zinc starvation or copper supplementation both reduce biofilm formation (Singh *et al.*, 2015; Ganguly *et al.*, 2021).

1.10 Aims and objectives of this thesis

The contribution of multicopper oxidases to copper tolerance in Gram-negative bacteria such as *E. coli* is well understood. By comparison, very little is known about Gram-positive multicopper oxidases such as *S. aureus* Mco. A limited number of studies have focused on investigating the contribution of copper tolerance genes to survival in human blood and neutrophils. Information regarding the effect of copper on biofilm formation is also limited, particularly for *S. aureus*.

The major aims of this project were to:

- Determine the cellular location of Mco
- Determine the contribution of Mco to copper tolerance in *S. aureus*
- Investigate a selection of uncharacterised genes that putatively contribute to copper tolerance in MRSA252, including the cadmium resistance genes *cadAC*
- Investigate the contribution of copper tolerance genes in *S. aureus* to survival in whole human blood and purified human neutrophils
- Examine the effect of copper on biofilm formation in *S. aureus*

Chapter 2

Materials and Methods

2.1 Bacterial growth conditions

Bacterial strains used in this study are listed in table 2.1. *S. aureus* strains were grown in tryptic soy broth (Difco)(TSBd), at 37°C with shaking or in brain heart infusion broth (BHI, Oxoid) or on tryptic soy agar (TSA, Sigma) at 37°C. *Escherichia coli* strains were grown at 37°C in lysogeny broth (LB, Difco) at 37°C with shaking or on lysogeny agar (Difco) at 37°C. Ampicillin (100 µg/ml) or chloramphenicol (10 µg/ml) were added to growth media where necessary for plasmid selection. Anhydrotetracycline (ATc) (312.5 ng/ml) was used to induce expression of pRMC2 vector. Unless otherwise stated, all reagents were obtained from Sigma.

2.2 Plasmids and primers in this study

All plasmids, both obtained from other labs and generated in this study, are listed in table 2.2. All primers used in this study are described in table 2.3.

2.3 DNA manipulation

2.3.1 Isolation of genomic and plasmid DNA

Genomic DNA was isolated using the EdgeBio PurElute Bacterial Genomic Kit.

Plasmid DNA was isolated using the Wizard® Plus SV DNA Purification System kit for all plasmids except pIMAY, which was purified using the Qiagen® Plus Midi Kit.

Pellet Paint® Co-Precipitant (Merck) was used to further concentrate and purify plasmid DNA as needed.

2.3.2 Polymerase Chain Reaction (PCR)

DNA amplification was performed in reaction volumes of 50 µl consisting of 5-10 ng of plasmid DNA or 150 ng of genomic DNA, 200 nM forward and reverse primers, 250 µM dNTPs (Bioline), 1 U of Velocity polymerase (Bioline) and 1X HI-FI reaction buffer (Bioline) in molecular biology grade nuclease free water. Primers (Table 2.) were synthesised by Integrated DNA Technologies (Leuven, Belgium). PCR was carried out in a thermocycler (Techne) with cycling conditions as per the Velocity polymerase manufacturers guidelines.

2.3.3 Colony PCR screening of *E. coli* and *S. aureus*

Colony PCR was performed to screen transformants. A single colony was suspended in 20 µl of molecular biology grade nuclease free water for *E. coli* screens, and 40 µl of Tris-Acetate EDTA buffer for *S. aureus* screens. This suspension was boiled for 10 min at 100°C, and the debris was pelleted by centrifugation at 3,500 x *g*. 2 µl of the supernatant was used as template for the colony PCR. Each 25 µl PCR reaction contained 1X Phire buffer (Finnzymes), 200 µM dNTPs, 200 nM forward and reverse primers and Phire hot start II polymerase (Finnzymes).

PCR products that were used for cloning purposes were treated with 1U of DpnI (NEB) to digest parental template DNA. PCR products for cloning or sequencing purposes was treated further by cleaning up with Bioline PCR Clean up kit (Bioline).

2.3.4 Agarose Gel Electrophoresis

PCR products were separated by electrophoresis through a 1% w/v agarose gel in Tris-Acetate-EDTA (TAE) buffer (Invitrogen). Nucleic acid staining was achieved by addition of SYBERSAFE red stain (Invitrogen) to the molten agarose gel. PCR products were viewed under UV or blue light and images were captured using an Alpha imager.

2.4 Plasmid construction

2.4.1 Sequence and Ligase-independent Cloning

Plasmids were frequently constructed by sequence and ligase independent cloning (SLIC) as described by Li and Elledge (Li and Elledge, 2007). Briefly, both vector and insert were amplified by PCR. The primers used to amplify the insert contained 5' extensions that were typically 24 base pairs (bp) which were homologous to the end regions of the vector. Both vector and insert DNA (1 µg) were incubated with T4 polymerase (3U; NEB) in a final reaction volume of 40 µl containing NEB Buffer 2, molecular grade BSA (NEB), dithiothreitol (DTT; 5 mM) and urea (200 mM). This reaction was incubated at 23°C for 20 min and stopped by the addition of EDTA (25 mM), followed by a further 20 min incubation at 75°C. 5 µl of each resulting vector and insert containing single stranded ends were mixed to

permit annealing of vector and insert. This reaction was incubated at 65°C for 10 min followed by a slow decrease in temperature from 65 – 25 °C with 1 min old time for each degree. The entire reaction was used for transformation into *E. coli* IM08B or IM30B.

2.4.2 Generation of pRMC2::D3D4::NoSP

Generation of plasmids used to express chimaeric protein fusions of a reporter protein and different signal peptide sequences was performed using a combination of SLIC and blunt end ligation. The plasmid pRMC2::D3D4WTSP was used as template to delete the native signal peptide of Sbi, present on this plasmid. Primers pRMC2 D3D4 SS delete F and pRMC2 D3D4 SS delete R were used to amplify 6810 bp of DNA which removed the signal sequence of Sbi from pRMC2::D3D4WTSP by inverse PCR. This PCR product was ligated by blunt end ligation to create pRMC2::D3D4NoSP and transformed into IM08B.

2.4.3 Generation of pRMC2::D3D4::Mco1-56

The 168 bp of DNA encoding residues 1-56 of Mco were amplified by PCR using primers Mco 1-56 SLIC F and Mco 1-56 SLIC R. These primers were designed to have overhang extensions homologous to the terminal regions of pRMC2::D3D4::NoSP which had been linearised by PCR using primers pRMC2::D3D4 SS delete F and pRMC2::D3D4 SS delete R. These two PCR amplimers were ligated by SLIC to generate pRMC2::D3D4::Mco1-56.

2.4.4 Generation of pRMC2::D3D4::Mco1-26

Primers Mco 27-56 del F and Mco 27-56 del R were used to delete residues 27-56 from Mco1-56 by amplifying 6888 bp of DNA from pRMC2::D3D4::Mco1-56 by inverse PCR. This linearised product was ligated by blunt end ligation to generate pRMC2::D3D4::Mco1-26.

2.4.5 Generation of pRMC2::D3D4::Mco27-56

Primers Mco 2-26 del F and Mco 2-26 del R were used to delete residues 2-26 from Mco1-56 by amplifying 6903 bp of DNA from pRMC2::D3D4::Mco1-56 by inverse PCR. This linearised product was ligated by blunt end ligation to generate pRMC2::D3D4::Mco27-56.

Table 2.1. Bacterial Strains used in this study

Strain	Description	Reference
MRSA252	CC30 HA-MRSA isolated from fatal post-operative septicaemia patient	(Holden <i>et al.</i> , 2004)
MRSA252Δ <i>mco</i>	Isogenic <i>mco</i> deletion mutant	This study
MRSA252Δ <i>mco</i> ::pCL55	<i>mco</i> deletion mutant with empty pCL55 integrated into <i>geh</i> locus	This study
MRSA252Δ <i>mco</i> ::pCL55::UCMF	<i>mco</i> deletion mutant with <i>mco</i> 3X-FLAG under the transcriptional control of CsoR	This study
MRSA252Δ <i>mco</i> ::pCL55::UCMFΔ2-53	<i>mco</i> deletion mutant with <i>mco</i> 3X-FLAGΔ <i>Mco</i> 2-53 under the transcriptional control of CsoR	This study
MRSA252Δ <i>mco</i> ::pCL55::UCM	<i>mco</i> deletion mutant with <i>mco</i> under the transcriptional control of CsoR	This study
LAC* <i>spa sbi</i>	Erythromycin sensitive version of LAC with <i>spa</i> :: <i>Erm</i> ^r and <i>sbi</i> :: <i>Kan</i> ^r disruptions	(O'Halloran, Wynne and Geoghegan, 2015)
LAC* <i>spa sbi</i> Δ <i>tatAC</i>	Derivative of LAC* <i>spa sbi</i> deficient in <i>tatAC</i> . Δ <i>tatAC</i> .	This study
MRSA252 14 gene KO	Deletion mutant lacking <i>mco</i> and 13 genes downstream of <i>mco</i> , including <i>cadA</i> and <i>cadC</i>	This study
MRSA252Δ <i>cadA</i>	Isogenic deletion mutant of <i>cadA</i>	This study
MRSA252Δ <i>cadAC</i>	Isogenic deletion mutant of <i>cadAC</i>	This study
MRSA252Δ <i>mco</i> Δ <i>cadA</i>	Isogenic deletion mutant of <i>mco</i> and <i>cadA</i>	This study
MRSA252Δ <i>mco</i> Δ <i>cadAC</i>	Isogenic deletion mutant of <i>mco</i> and <i>cadAC</i>	This study
MRSA252Δ <i>copZ</i>	Isogenic deletion mutant of <i>copZ</i>	(Oisin Gilmartin & Joan. A Geoghegan, unpublished)
MRSA252 CHC	MRSA252 expressing the CsoR CHC variant (CsoR C41A/H66A/C70A)	(Zapotoczna <i>et al.</i> , 2018)
14-2533T	CC22 MRSA clinical isolate, was isolated without pSCBU, so was used as a negative background	(Zapotoczna <i>et al.</i> , 2018)
14-2533T pSCBU	CC22 MRSA clinical isolate with pSCBU transformed into it, to represent CC22 MRSA strains that harbour pSCBU as a replicating plasmid	(Zapotoczna <i>et al.</i> , 2018)
JE2	USA-300 lineage CA-MRSA, representative of the most prominent CA-MRSA lineage in the USA	(Fey <i>et al.</i> , 2013)
JE2 <i>rexB</i> :: <i>erm</i>	JE2 with <i>rexB</i> gene disrupted by <i>erm</i> cassette insertion	(Ha <i>et al.</i> , 2020)
BH1CC	CC8 HA-MRSA isolated from device related infection at Beaumont Hospital Dublin	(O'Neill <i>et al.</i> , 2007)
BH1CCΔ <i>fnbAfnbB</i>	BH1CC deficient of <i>fnbA</i> and <i>fnbB</i> due to <i>fnbAB</i> :: <i>Tc</i> ^r	(O'Neill <i>et al.</i> , 2008)
ED83	CC30 MSSA isolated from lung sputum of chronically infected cystic fibrosis patient	(McAdam <i>et al.</i> , 2011)
CF10	<i>S. aureus</i> isolated from lung sputum of cystic fibrosis patient in Vincent's Hospital	(Kirsten Schaffer, unpublished)
CF15	<i>S. aureus</i> isolated from lung sputum of cystic fibrosis patient in Vincent's Hospital	(Kirsten Schaffer, unpublished)
BH3	MRSA clinical isolate from device related infection from patient in Beaumont Hospital, Ireland	(O'Neill <i>et al.</i> , 2008)

BH4	MRSA clinical isolate from device related infection from patient in Beaumont Hospital, Ireland	(O'Neill <i>et al.</i> , 2008)
BH10	MRSA clinical isolate from device related infection from patient in Beaumont Hospital, Ireland	(O'Neill <i>et al.</i> , 2008)
BH10(03)	MRSA clinical isolate from device related infection from patient in Beaumont Hospital, Ireland	(O'Neill <i>et al.</i> , 2008)
BH18	MRSA clinical isolate from device related infection from patient in Beaumont Hospital, Ireland	(O'Neill <i>et al.</i> , 2008)
BH48(04)	MSSA clinical isolate from device related infection from patient in Beaumont Hospital, Ireland	(O'Neill <i>et al.</i> , 2008)
DAR113	MRSA clinical isolate from device related infection from patient in Beaumont Hospital, Ireland	(Robinson and Enright, 2003)
DAR217	MRSA clinical isolate from device related infection from patient in Beaumont Hospital, Ireland	(Robinson and Enright, 2003)
DAR70	MRSA clinical isolate from device related infection from patient in Beaumont Hospital, Ireland	(Robinson and Enright, 2003)
DAR70 Δ <i>fnbAB</i>	DAR70 with isogenic deletion of <i>fnbAB</i> genes	(Leanne Hays, Marta Zapotoczna & Joan A. Geoghegan, unpublished)
IM30B	<i>E. coli</i> strain for high efficiency plasmid transformation into CC30 <i>S. aureus</i> strains	(Monk <i>et al.</i> , 2015)
IM08B	<i>E. coli</i> strain for high efficiency plasmid transformation into CC08 <i>S. aureus</i> strains	(Monk <i>et al.</i> , 2015)

Table 2.2 Plasmids used in this study

Plasmid	Description	Reference
pIMAY	Thermosensitive vector used for allelic exchange. Confers chloramphenicol resistance in both <i>E. coli</i> and <i>S. aureus</i>	(Monk <i>et al.</i> , 2012)
pIMAY:: Δ <i>mco</i>	pIMAY with ~550 bp up- and down-stream of <i>mco</i> cloned into MCS	This study
pCL55	Single copy integrating vector. Confers chloramphenicol resistance in <i>S. aureus</i> , and ampicillin resistance in <i>E. coli</i> .	(Lee, Buranen and Zhi-Hai, 1991)
pCL55::UCMF	pCL55 with Upstream of <i>copB</i> including the CsoR binding site to <i>mco3XFLAG</i> cloned into the MCS of pCL55.	This study
pCL55::UCMF Δ Mco2-53	pCL55::UCMF with in-frame deletion of residues 2-53 of Mco	This study
pCL55::UCM	pCL55::UCMF with in-frame deletion of the C-terminal 3X-FLAG tag	This study

pRMC2	High copy inducible vector, confers ampicillin resistance in <i>E. coli</i> , chloramphenicol resistance in <i>S. aureus</i> , inducible expression of MCS using anhydrotetracycline	(Corrigan and Foster, 2009)
pRMC2::D3D4 NoSP	pRMC2 with just the D3D4 subunits of Sbi cloned into the MCS	This study
pRMC2::D3D4 WTSP	pRMC2 with the D3D4 subunits of Sbi and its native N-terminal sec signal peptide sequence cloned into the MCS	(O'Halloran, Wynne and Geoghegan, 2015)
pRMC2::D3D4Mco1-56	pRMC2::D3D4 with Mco1-56 fused to the N-terminal region of D3D4.	This study
pRMC2::D3D4Mco1-26	pRMC2::D3D4 with Mco1-26 fused to the N-terminal region of D3D4.	This study
pRMC2::D3D4Mco27-56	pRMC2::D3D4 with Mco27-56 fused to the N-terminal region of D3D4.	This study
pRMC2::D3D4Mco1-56 KQ	pRMC2::D3D4Mco1-56 with McoK4Q amino acid substitution in the premier residues of Mco1-56	This study
pRMC2::D3D4Mco1-26 KQ	pRMC2::D3D4Mco1-56 with McoK4Q amino acid substitution in the premier residues of Mco1-26	This study
pIMAY:: Δ tatAC	pIMAY with ~550 bp up- and down-stream of <i>tatAC</i> cloned into MCS	This study
pIMAY:: Δ cadA	pIMAY with ~550 bp up- and down-stream of <i>cadA</i> cloned into MCS	This study
pIMAY:: Δ cadAC	pIMAY with ~550 bp up- and down-stream of <i>cadAC</i> cloned into MCS	This study

2.4.6 Generation of pRMC2::D3D4::Mco1-56 KQ and pRMC2::D3D4::Mco1-26 KQ

Site direct mutagenesis was performed by designing primers annealing to the N-terminus of Mco1-56, containing a signal nucleotide mismatch to change a 'T' to a 'G' resulting the change of McoK₄ to McoQ₄. A PCR using primers McoKK-KQ sub F and McoKK-KQ sub R was performed using pRMC2::D3D4::Mco1-56 as template to generate pRMC2::D3D4::Mco1-56 KQ.

Similarly, a PCR was performed using pRMC2::D3D4::Mco1-26 as template using primers McoKK-KQ sub F and McoKK-KQ sub R to generate pRMC2::D3D4::Mco1-26 KQ.

2.4.7 Generation of pCL55:UCMF

Primers UpcopB F and Mco3X-FLAG Full R were used to generate a DNA construct of 3747 bp beginning from just upstream region of copB (including its promoter site) all the way to the C terminus of *mco* encoding a 3X-FLAG onto the C-terminus of *mco*, using purified genomic DNA from MRSA252 as template. This DNA construct was named UCMF for short. The plasmid pCL55 was linearised at

its MCS by inverse PCR using primers pCL55 inv F and pCL55 inv R. The UCMF DNA construct was inserted into the MCS of pCL55 by SLIC as described previously, to generate pCL55::UCMF.

2.4.8 Generation of pCL55:UCMF Δ Mco2-53

A PCR using primers Mco 2-53 del F and Mco 2-53 del R was performed using pCL55::UCMF as template to amplify 9156 bp of DNA, removing residues 2-53 of Mco from UCMF. This PCR amplicon was ligated by blunt end ligation to generate pCL55::UCMF Δ Mco2-53.

2.4.9 Generation of pCL55:UCM

A PCR using primers UCM del F and UCM del R was performed using pCL55::UCMF as template to amplify 9235 bp of DNA, removing the 3X-FLAG tag from the C-terminus of *mco*. This PCR amplicon was ligated by blunt end ligation to generate pCL55::UCM.

2.5 Strain construction by allelic exchange

MRSA252 Δ *mco*, LAC* *spa sbi* Δ *tatAC*, MRSA252 14 gene KO, MRSA252 Δ *cadA*, MRSA252 Δ *cadAC*, MRSA252 Δ *mco* Δ *cadA*, and MRSA252 Δ *mco* Δ *cadAC* were generated by allelic exchange as described previously (Monk *et al.*, 2012).

2.5.1 Generation of MRSA252 Δ *mco*

Deletion of the *mco* gene was achieved by generation of the plasmid pIMAY:: Δ *mco*. The 513 bp immediately upstream of *mco* were amplified by PCR using primers Mco A and Mco B to generate the AB product. The 503 bp immediately downstream of *mco* were amplified by PCR using primers Mco C and Mco D primers to generate the CD product. The Mco C primer was designed to have an overhanging extension homologous to the Mco B primer, so that an overlapping extension PCR could be performed using primers Mco A and Mco D with PCR products AB and CD as template, to generate the continuous AD product with a length of 1074 base pairs. This AD product was cloned into the MCS of pIMAY by SLIC as described earlier (Li and Elledge, 2007). The resulting plasmid (pIMAY:: Δ *mco*) was transformed into IM30B and verified by DNA sequencing. Plasmid was purified from this IM30B background and transformed into electrocompetent MRSA252 and deletion of *mco* was achieved by allelic exchange

(Monk *et al.*, 2012). Deletion of *mco* from the genome was confirmed by DNA sequencing of a PCR amplicon. The mutant was confirmed phenotypically identical to the parent strain when growth rate and haemolysis on sheep blood agar were analysed (Traber and Novick, 2006; Sun, Li, *et al.*, 2010). Confirmation of δ -haemolysin production confirmed that no non-synonymous mutations were made in these global virulence regulation systems so we could conclude that any virulence defects seen in this mutant were due to *mco* deletion alone.

Table 2.3 Primers used in this study

Primer	Sequence (5'-3')
Mco A	CCTCACTAAAGGGAACAAAAGCTGGGTACCAAGTGGCACAAACAGTGGCTG
Mco B	GAAAATAACGTAATTTAAATTGTG
Mco C	TCACAATTTTAATTACGTTATTTTCTTATA
Mco D	CGACTCACTATAGGGCGAATTGGAGCTCTATGCAAACCGTAATGATAGATAT G
Mco Out F	ACATTACGCCAGTCATGCTTAC
Mco Out R	ACGAGAAAAGTTTAAAAGTGAC
pIMAY MCS F	TACATGTCAAGAATAAACTGCCAAAGC
pIMAY MCS R	AATACCTGTGACGGAAGATCACTTCG
pIMAY SLIC F	GGTACCCAGCTTTTGTCCCTTTAGTGAGG
pIMAY SLIC R	GAGCTCCAATTCGCCCTATAGTGAGTCG
UpcoB F	GCCGGTACCTCCTATATCCATCATTAGTGATC
Mco3X-FLAG full R	TTATTTATCGTCATCATCTTTATAATCTATATCGTGATCTTTATAATCTCCATCGT GATCTTTATAATCTTTTGTACTTTTATTTGTCCCA
UCMF SLIC F	CGTCTCAAGAATTCGAGCTCGGTACCTCCTATATCCATCATTAGTGATACC
UCMF SLIC R	ACCACATTTTACATCCCTCCGGATCCTTATTTATCGTCATCATCTTTATAATC
pCL55 inv F	GGATCCGGAGGGATGTAATAATG
pCL55 inv R	GGTACCGAGCTCGAATTCTTG
pCL55 MCS Screen R	TGATATTCAAGCCATTCATC
pCL55 MCS Screen F	AATAGGCGTATCAGGAGGC
pCL55 int screen R	GCGCATAGGTGAGTTATTAGC
geh F	GTTGTTTTGTACATGGATTTTTAG
Mco3XFLAG Screen F	GTATGGACGATAATGTTACTATTAATG
pRMC2 MCS F	ATTCAGGCTGCGCAAC
pRMC2 MCS R	TTGTTGACATTATATCATTG
pRMC2 D3D4 SS delete R	AGTGAAAACACGCAACAACTTC
pRMC2 D3D4 SS delete F	GTGTATTCCTTTCTTTGGGTA
Mco1-56 SLIC R	GAAGTTTGTGCGTGTTCCTCAAAATTTTTCTTCGTCATGACTT
Mco1-56 SLIC F	TACCCAAAAGAAAGGGAATACACATGTATAAAAAATGTTCACAATTTTAA
Mco 2-26 del F	CATGTGTATTCCCTTTCTTTTGG
Mco 2-26 del R	GGTAAGCACAACATGATGGACA
Mco 27-56 del F	TTCTGCAAAAAGTATCATTAGGAAC
Mco 27-56 del R	AGTGAAAACACGCAACAACTTC
Mco 2-53 del F	AAAAATTTGAATTCCTCAAAAGGAA
Mco 2-53 del R	CATTATATTTACCTTTTTATTTAAT
Mco 2-53 seq R	GTTATCTTTTTTAGGATCCAAAACCTTTGGGAAATG
UCM del F	AGGGATGTAAAATGTGGTTTGAAA
UCM del R	TTATTTTGTACTTTTATTTGTCCCA
McoKK-KQ Sub F	CACATGTATAAACAATGTTAC
McoKK-KQ Sub R	GTGAACATTTGTTTATACATGTG
dtatAC A	CCTCACTAAAGGGAACAAAAGCTGGGTACCGCATTCTAATTTTAGTATGATGC

dtatAC B	GATAATCAACCTCACTCATAAG
dtatAC C	CTACTTATGAGTGAGGTTGATTATCCTTATACGAATCAATGCTGTG
dtatAC D	CGACTCACTATAGGGCGAATTGGAGCTCCAAACGTTCAAATGCAAAACG
Out tatAC F	GAAACAAACACCTCAACGCC
Out tatAC R	CATATTAATGTTTATCGTTGGTG
dcadA A	CCTCACTAAAGGGAACAAAAGCTGGGTACCCGACCAGAAAATACAGATTGAG
dcadA B	TACTATATGTGTGCAATTTACGG
dcadA C	CTCCGTAAATTGCACACATATAGTACGGTAAACCTGTTTATCTTCTG
dcadA D	CGACTCACTATAGGGCGAATTGGAGCTCCTAACGGGGCAGTTATGTTTAAAG
dcadAC C	CTCCGTAAATTGCACACATATAGTATATCCTCCTTATTCAAATGACTG
dcadAC D	CGACTCACTATAGGGCGAATTGGAGCTCGTACGTTTGGCGAAGCAGAAATC
Out cadA F	CATCATTCGAATACTGTCATGA
Out cadAC R	CATTGGAAGTTTGACGGGGT

2.5.2 Generation of LAC* *spa sbi* Δ *tatAC*

Deletion of the *tatAC* genes in LAC* *spa sbi* was achieved by generation of the plasmid pIMAY:: Δ *tatAC*. The 561 bp immediately upstream of *tatAC* was amplified with primers dtatAC A and dtatAC B. The 574 bp immediately downstream of *tatAC* was amplified with primers dtatAC C and dtatAC D. An overlapping extension PCR was performed using these AB and CD products to generate the AD product, which was cloned into the MCS of pIMAY by SLIC to generate the plasmid pIMAY:: Δ *tatAC*. This plasmid was first transformed into IM08B, confirmed by DNA sequencing, and subsequently transformed into LAC* *spa sbi* by electroporation. Deletion of *tatAC* from the genome was confirmed by DNA sequencing of a PCR amplicon. The mutant was confirmed phenotypically identical to the parent strain when growth rate and haemolysis on sheep blood agar were analysed.

2.5.3 Generation of MRSA252 14 gene KO

MRSA252 14 gene KO was generated during the excision step of allelic exchange when generating MRSA252 Δ *mco*. In total, there were five clones negative for *mco* when screened by colony PCR after the excision step. Whole genome sequencing was performed and it was discovered that one of the clones had lost an extra 13 genes downstream of *mco* in addition to *mco*, and was named MRSA252 14 gene KO (See Chapter 4 for details).

2.5.4 Generation of MRSA252 Δ *cadA* and MRSA252 Δ *mco* Δ *cadA*

Deletion of *cadA* was achieved generation of the plasmid pIMAY:: Δ *cadA*. The 582 bp immediately upstream of *cadA* was amplified with primers dcadA A and dcadA B. The 596 bp immediately downstream of *cadA* was amplified with primers

dcadA C and dcadA D. An overlapping extension PCR was performed using these AB and CD products to generate the AD product, which was cloned into the MCS of pIMAY by SLIC to generate the plasmid pIMAY:: Δ cadA. This plasmid was first transformed into IM30B, confirmed by DNA sequencing, and subsequently transformed into MRSA252 and MRSA252 Δ mco by electroporation. Deletion of cadA from the genome was confirmed by DNA sequencing of a PCR amplicon. The mutant was confirmed phenotypically identical to the parent strain when growth rate and haemolysis on sheep blood agar were analysed.

2.5.5 Generation of MRSA252 Δ cadAC and MRSA252 Δ mco Δ cadAC

Deletion of cadAC was achieved generation of the plasmid pIMAY:: Δ cadAC. The 582 bp immediately upstream of cadA was amplified with primers dcadA A and dcadA B. The 579 bp immediately downstream of cadC was amplified with primers dcadAC C and dcadAC D. An overlapping extension PCR was performed using these AB and CD products to generate the AD product, which was cloned into the MCS of pIMAY by SLIC to generate the plasmid pIMAY:: Δ cadAC. This plasmid was first transformed into IM30B, confirmed by DNA sequencing, and subsequently transformed into MRSA252 and MRSA252 Δ mco by electroporation. Deletion of cadAC from the genome was confirmed by DNA sequencing of a PCR amplicon. The mutant was confirmed phenotypically identical to the parent strain when growth rate and haemolysis on sheep blood agar were analysed.

2.6 Transformation

2.6.1 Preparation of chemical competent *E. coli*

Chemically competent *E. coli* IM30B or IM08B cells were made by the calcium-chloride method as described previously (Chan *et al.*, 2013). Briefly, 400 ml of LB in a 2 L baffled flask was inoculated with 4 ml of an overnight culture of *E. coli* and incubated at 37°C with shaking (200 rpm) until an OD_{600nm} of 0.5 was achieved (2-2.5 h). The culture was chilled on ice for 20 min, harvested by centrifugation at 8,000 x g for 10 min at 4°C and resuspended in 30 ml of ice-cold MgCl₂ (100 mM). Cells were harvested again by centrifugation at 8,000 x g for 10 min at 4°C and resuspended in 50 ml ice-cold CaCl₂/PIPES solution (60 mM CaCl₂, 10 mM PIPES, 15% glycerol) and left on ice for 30 min. Cells were harvested again

by centrifugation at 8,000 x *g* for 10 min at 4°C and resuspended in 30 ml ice-cold CaCl₂/PIPES solution. 500 µl aliquots were immediately stored at -80°C.

2.6.2 Preparation of electrocompetent *S. aureus*

Electrocompetent *S. aureus* were made as described previously (Löfblom *et al.*, 2007). Briefly, a 10 ml overnight culture of BHI broth was inoculated with *S. aureus* and grown for 16 h at 37°C with shaking (200 rpm). This overnight culture was diluted to an OD_{570nm} of 0.5 in 50 ml of prewarmed BHI broth and incubated at 37°C with shaking for 30 min. This culture was cooled in an ice-water slurry for 10 min. Cells were harvested by centrifugation at 3900 x *g* for 10 min at 4°C. The supernatant was removed, and the pellet was resuspended in 50 ml of ice-cold sterile H₂O. Cells were harvested by centrifugation again and resuspended in decreasing volumes of 10% (v/v) ice-cold glycerol (5 ml, 1 ml, 250 µl). 50 µl aliquots were stored at -80°C.

2.6.3 Transformation of *E. coli* by heat shock

Plasmid DNA (150-200 ng) was incubated with 200 µl of chemically competent *E. coli* cells on ice for 10 min, were heat shocked at 42°C in a heat block for precisely 2 min, and followed by incubation on ice for 2 min before being transferred to 1 ml of LB broth and incubated at 37°C for 1 h shaking at 200 rpm for recovery. Following recovery, cells were plated onto LB agar with appropriate selective antibiotic added.

2.6.4 Transformation of *S. aureus* by electroporation

Electrocompetent cells were thawed on ice for 5 min, incubated at room temperature for 5 min, and pelleted by centrifugation at 5000 x *g* for 1 min. The pelleted cells were resuspended in 50 µl of 10% glycerol/500 mM sucrose. Plasmid DNA (1-5 µg) was added to bacteria in a volume of no greater than 5 µl. Cells were electroporated at 2.1 kV/cm, 100 Ω and 25 µF. After electroporation cells were allowed recover in 1 ml brain-heart infusion/500 mM sucrose and incubated at 37°C with shaking 200 rpm for 1 h. Cells were then plated on TSA with appropriate selective antibiotic. Transformants were screened by colony PCR.

2.6.5 Transformation of *S. aureus* with pCL55 plasmids

IM30B was used as the host strain for growing and purifying plasmids pCL55, pCL55::UCMF, pCL55::UCMFΔMco2-53 and pCL55::UCM that would readily

transform into MRSA252 Δ *mco* (Monk *et al.*, 2015). MRSA252 Δ *mco* was transformed with these pCL55 constructs by electroporation as described previously and transformants were selected for by growth on TSA with chloramphenicol (10 μ g/ml) at 37°C for 24 - 48 h. Amplification by colony PCR using primers pCL55 int screen R and geh F confirmed pCL55 integration. Amplification by colony PCR using primers Mco3XFLAG Screen F and pCL55 MCS R confirmed the presence and absence of the C-terminal 3X-FLAG tag pCL55::UCMF and pCL55::UCM respectively. Amplification by colony PCR using primers pCL55 MCS F and PCL55 MCS R on pCL55 containing clones confirmed it was an empty vector control. All strains of *S. aureus* that harboured integrated pCL55 constructs were confirmed by DNA sequencing of a PCR amplicon.

2.7 Fractionation of *S. aureus*

Cultures were grown for 16 h in TSB supplemented with CuCl₂ as appropriate. Cultures were pelleted at 4000 x *g* for 10 min and the supernatant was carefully removed for trichloroacetic acid (TCA) precipitation of supernatant proteins. To extract cell wall-associated proteins, pellet was washed in PBS and pelleted by centrifugation. The supernatant was discarded and the pellet was resuspended in 1 ml PBS. The OD₆₀₀ was measured and the volume of cells required to give an OD₆₀₀ of 10 was pelleted by centrifugation at 14,000 x *g* for 10 min. Pellet was resuspended in lysis buffer (50 mM Tris-HCl, 20 mM MgCl₂, pH 7.5) supplemented with raffinose pentahydrate (30% w/v; Sigma), and complete protease inhibitors (40 μ l/ml; Roche). Cell wall proteins were solubilised with lysostaphin (100 μ g/ml; AMBI, New York, NY) and incubated at 37°C for precisely 8 min before centrifugation at 14,000 x *g* for 5 min. The supernatant (Cell wall fraction) was removed. To extract membrane and cytoplasmic proteins, the protoplast pellet was washed once with lysis buffer and resuspended in ice-cold lysis buffer complete with protease inhibitor, DNaseI (33 μ g/ml). Protoplasts were lysed by vigorous vortexing followed by 10 min incubation on ice three times. Membrane and cytoplasmic fractions were separated by centrifugation at 18,500 rpm in Sorvall with rotor SS34 (SORVALL, RC 5C PLUS) at 4°C for 1 h. The supernatant (cytoplasmic fraction) was removed and the membrane pellet was resuspended in lysis buffer. Both the membrane and cytoplasmic fractions were

pelleted by centrifugation at 18,500 rpm in Sorvall at 4°C for 1 h. The supernatant was removed from the cytoplasmic fractions and added to a clean microcentrifuge tube. The supernatant of the membrane fractions was discarded and the pellet was resuspended in Tris/MgCl₂ solution (Tris-HCl pH 7.5; MgCl₂). All fractions were resuspended to a final volume of 300 µl, 300 µl of 2X Laemmli-buffer was added.

2.8 TCA Precipitation of Supernatant Proteins

S. aureus supernatants were filtered through a 0.22 µm membrane filter. Supernatant harvested from an OD_{600nm} of 10 was used for protein precipitation. 1 vol of ice-cold 100% Trichloro-acetic acid solution was added to 19 vol of supernatant and incubated on ice for 10 min. Proteins were pelleted by centrifugation at 14,000 g for 5 min, the pellet was washed with 100% ice-cold acetone and pelleted by centrifugation twice. The remaining acetone was removed by placing the microcentrifuge tube on a heating block at 95°C for 20 min. The protein pellet was resuspended in 300 µl Tris/MgCl₂ solution and 300 µl 2X Laemmli buffer.

2.9 SDS-PAGE and Western Blotting

Protein samples were boiled at 100°C for 10 min to denature all proteins. 14 µl of each sample was loaded onto polyacrylamide gels (4.5% stacking gel, 12.5% separating gel) and separated by SDS-PAGE at 35 mA for 1 h 45 m. The separated proteins were transferred to a polyvinylidene difluoride (PVDF) or nitrocellulose membrane using electrophoresis at 100 V for 1 h and blocked in Marvel skimmed milk (10% w/v) in TS buffer (10 mM Tris-HCl, 0.9% (w/v) NaCl₂, pH 7.4) at 4°C for 16 h. Blots were probed with a primary antibody for 45 min at room temperature. The blot was washed three times with TS buffer before incubation in secondary antibody for 30 min at room temperature. The blot was washed three times with TS buffer. The blot was developed in 1X chemiluminescent agent (LumiGLO[®] Reagent and peroxide detection system, Cell Signalling Technology) for 1 min before imaging with an ImageQuant LAS4000 luminescent image analyser (GE Life Sciences). All antibodies used in this study are listed and described in table 2.4.

Table 2.4 Antibodies used in this study

Antibody	Description	Working Dilution	Reference
Mouse α -FLAG IgG	Monoclonal anti-FLAG M2 mouse antibody used as primary antibody	1:800	Sigma-Aldrich
Goat α -mouse HRP IgG	Goat anti-mouse HRP conjugated F(ab') fragments used as secondary antibody to detect mouse α -FLAG antibody	1:1000	Thermo Fisher Scientific
Rabbit α -D3D4 IgG	Polyclonal rabbit anti-SbiD3D4 serum used as primary antibody	1:250	(Smith <i>et al.</i> , 2011)
Rabbit α -V8 IgG	Polyclonal rabbit anti-V8 protease serum used as primary antibody	1:250	Martin McGavin, Toronto, Canada
Rabbit α -EbpS IgG	Polyclonal rabbit anti-EbpS serum used as primary antibody	1:500	(Downer <i>et al.</i> , 2002)
PAP	Protein-A Peroxidase, used to detect bound polyclonal rabbit primary antibodies	1:500	DAKO

2.10 Growth of *S. aureus* in subinhibitory concentrations of copper in TSB

Bacteria were grown for 12-16 hours at 37°C in TSB and adjusted to an OD₆₀₀ of 0.025 in TSB supplemented with CuCl₂. 100 μ l of bacteria were added in triplicate to round bottom 96-well sterile plates (Sarstedt). Plates were incubated in EPOCH² microplate reader (Biotek) for 18 h at 37°C with shaking 200 rpm, with OD₆₀₀ readings taken every 30 minutes.

2.11 Growth of *S. aureus* in subinhibitory concentrations of copper in RPMI

Bacteria were grown for 18 hours at 37°C in Roswell Park Memorial Institute Medium (RPMI) and sub-cultured 1:100 into RPMI for a further 24 h of growth. Cultures were then adjusted to an OD₆₀₀ of 0.025 in RPMI supplemented with CuCl₂. 100 μ l of bacteria were added in triplicate to round bottom 96-well sterile plates (Sarstedt). Plates were incubated in EPOCH² microplate reader (Biotek) for 18 h at 37°C with shaking 200 rpm, with OD₆₀₀ readings taken every 30 minutes. A second plate was incubated statically in 5% CO₂ incubator with OD₅₉₅ readings taken at 8 and 24 hours.

2.12 Growth of *S. aureus* on TSA supplemented with CuCl₂

Bacteria were grown for 12-16 hours at 37°C in TSB and pelleted by centrifugation at 4000 x g for 10 minutes. Bacteria were resuspended in 1X sterile PBS and adjusted to an OD₆₀₀ of 3 in PBS. This suspension was serially diluted 10-fold and 5 µl volumes were spotted onto TSA containing 0.01-8 mM CuCl₂. Plates were incubated aerobically for 18 hours, or anaerobically in an anaerobic jar for 24 hours.

2.13 Macrophage survival assay

RAW264.7 macrophages were seeded in 24 well plates at 2x10⁵ cells per well with Dulbecco's Modified Eagle Medium (DMEM) +10% FBS supplemented with IFN-γ (40 ng/ml) and CuSO₄ (40 µM) for 16 h prior to infection. Macrophages were infected with *S. aureus* at a multiplicity of infection of 10 in DMEM. Phagocytosis was allowed for 30 min followed by killing of extracellular bacteria with gentamycin and lysostaphin for 30 min. At 1 hour post-infection (T1) and 4 hours post-infection (T4), macrophages were lysed with ice-cold water and lysates were plated on agar to calculate CFUs/ml. The percentage survival after 3 hours was calculated as ((CFU per ml at T4/CFU per ml at T1) x 100).

2.14 Whole blood survival assay

The whole blood survival assay was performed as described previously (Visai *et al.*, 2009). Bacteria were grown for 16 h at 37°C with 200 RPM orbital shaking in TSBd. Bacteria were subsequently sub-cultured 1:100 into RPMI for a further 16 h growth at 37°C with 200 RPM orbital shaking. Bacteria were washed 3 times in RPMI before adjusting to the desired optical density (to an OD₆₀₀ that gave 2 x 10⁶ CFU/ml unless otherwise stated). Blood was obtained from healthy volunteers and treated with the anticoagulant Hirudin (50 µg/ml, Repludin, Pharmion). 25 µl of bacteria was added to 475 µl of blood and incubated in a table-top orbital incubator at 37°C with 400 RPM shaking. Immediately 100 µl of each sample was added to 900 µl of ice cold endotoxin-free water, and 100 µl was plated in triplicate on TSA for CFU enumeration. This was the T0 time point. Samples were incubated for 3 h at 37°C with 200 RPM orbital shaking with manual inversion of tubes every 30 mins. After 3 h, 100 µl of each sample was added to 900 µl of ice

cold endotoxin-free water and 100 µl was plated in triplicate on TSA for CFU enumeration. This was T3 time point. Percentage survival of bacteria was calculated as $(\text{mean CFU/ml at T3})/(\text{mean CFU/ml at T0}) \times 100$. Ethical approval for research with human blood was obtained from the TCD Faculty of Health Sciences ethics committee. Only blood donors that gave $\geq 10\%$ survival of wild-type *S. aureus* were used in this experiment.

2.15 Bacterial growth in purified human plasma

Bacteria were grown for 16 h at 37°C with 200 RPM orbital shaking in TSBd. Bacteria were subsequently sub-cultured 1:100 into RPMI for a further 16 h growth at 37°C with 200 RPM orbital shaking. Bacteria were washed 3 times in RPMI before adjusting to the desired optical density (to an OD₆₀₀ that gave 2×10^6 CFU/ml unless otherwise stated). Blood was obtained from healthy volunteers and treated with the anticoagulant Hirudin (50 µg/ml), before centrifugation at 3000 RPM ($\sim 1200 \times g$) for 10 mins. Following sedimentation of blood cells, the plasma layer was aspirated and used immediately. Similar to as done with whole blood, 25 µl of bacteria were added to 475 µl of plasma. 100 µl was added to 900 µl of ice cold endotoxin-free water, and 100 µl was plated in triplicate on TSA for CFU enumeration. This was the T0 time point. Samples were incubated for 3 h at 37°C with 200 RPM orbital shaking with manual inversion of tubes every 30 mins. After 3 h, 100 µl of each sample was added to 900 µl of ice cold endotoxin-free water and 100 µl was plated in triplicate on TSA for CFU enumeration. This was T3 time point. Percentage survival of bacteria was calculated as $(\text{mean CFU/ml at T3})/(\text{mean CFU/ml at T0}) \times 100$.

2.16 Neutrophil isolation from whole human blood

Freshly drawn human blood from healthy donors was heparinised and mixed 2:1 with 3% dextran and left to sediment for 30-40 min to stimulate red blood cell sedimentation. The top layer was very gently aspirated and layered onto 10 ml of Ficol-Paque PLUS (GE Healthcare) and centrifuged at $300 \times g$ for 20 min with the brake off. The supernatant was removed, and the remaining red blood cells were lysed by the addition of 3 ml ACK lysing buffer (Gibco) for 7 min. Prewarmed DMEM supplemented with 10% freshly prepared human serum was added to this mixture, inactivating the ACK lysing buffer. Neutrophils were pelleted by centrifugation at $300 \times g$ for 10 min before resuspension in DMEM + 10% serum. Neutrophils were

counted using a haemocytometer (Bright line, Neubauer) and adjusted to 5×10^6 cells/ml in DMEM + 10% autologous serum. Neutrophils were incubated at 37°C for 30 min to adjust to this medium before neutrophil infection experiments.

2.17 Serum isolation from whole human blood

Freshly drawn human blood from healthy donors was clotted by drawing blood into serum clot activator vacuettes (Greiner) and incubating statically at room temperature for 5 min. Human serum was separated from the clotted blood by centrifugation at $1,200 \times g$ for 10 min. Serum was used immediately, or stored on ice until needed.

2.18 Neutrophil survival assay

S. aureus were grown in TSBd for 16 h, before 1:100 dilution into RPMI medium and 18 further growth. *S. aureus* was washed twice in RPMI or HBSS as required, and adjusted to an OD_{600nm} of 0.0025 ($\sim 1 \times 10^6$ CFU/ml). 250 μ l of *S. aureus*, 250 μ l of neutrophils (5×10^6 cells/ml), 400 μ l of RPMI or HBSS and 100 μ l of autologous human serum were combined in a sterile 1.5 ml microcentrifuge tube. 40 μ l of this mixture was immediately added to 360 μ l of ice cold endotoxin-free water to lyse neutrophils and enumerate the input CFU/ml of *S. aureus* at T0. The sample tubes were incubated at 37°C with 600 rpm shaking in a tabletop incubator. At 30, 60, 120, 180 and 240 min, 40 μ l was removed from the sample tubes and added to 360 μ l of ice-cold endotoxin-free water, and serial diluted in a 96 well plate with ice-cold endotoxin-free water before spot plating these lysates on TSA to enumerate CFU/ml over the course of the infection. Sample lysates were spotted in on TSA in triplicate for each time point, and the average CFU/plate was calculated. Survival was calculated as the percentage of surviving bacteria compared to the number of bacteria at T0. $((T(x \text{ min}) \text{ CFU/ml}) / (T0 \text{ CFU/ml})) \times 100$.

2.19 Neutrophil activation for gene expression analysis

Neutrophils were purified from whole human blood as described above, and incubated for one hour at 37°C with 10 ng/ml TNF- α and/or 40 μ M CuSO₄ before RNA extraction.

2.20 RNA extraction using Norgen Biotek corp RNA kit

RNA was isolated as per the manufactures protocol. Cell suspension was transferred to an RNase free tube and centrifuged for 200 x *g* for 10 min to pellet the cells. 350 µl of buffer RL (guanidinium salts) and 200 µl of 100% ethanol was added, vortexed and added to the RNA column. The column was spun at 3500 x *g* to allow the RNA to bind. The RNA was subsequently washed three times with a wash buffer before being eluted in an RNase free tube.

2.21 Reverse transcription (cDNA synthesis)

250 ng of total RNA from each sample was reverse transcribed into cDNA using the SensiFAST reverse transcription cDNA kit (Bioline, MSC, Dublin), using the following reaction: 0.25 µl of reverse transcriptase and 2.25 µl of 5X Transamp buffer was added to 250 ng RNA and made up to 17.5 µl in RNase free DNase free H₂O (Sigma). Following this, the reaction was placed on the thermocycler at 25°C for 10 min (annealing), 42°C for 15 min (reverse transcription), 85°C for 5 min (inactivation of the enzyme) and 4°C hold. cDNA was quantified using the NanoDrop ND-1000 spectrophotometer.

2.22 Quantitative RealTime-Polymerase Chain Reaction (qRT-PCR)

Each qRT-PCR reaction was carried out in Triplicate in a 96-well PCR plate. Total volume per well was 10 µl: 1 µl of a 1 in 10 dilution of cDNA, 4 µl of SYBR green PCR master mix (Biorad), 0.5 µl of forward and reverse primer and 4 µl of H₂O. qRT-PCR was performed using the Biorad quantitative PCR system using the following cycling parameters: 95°C for 15 min, 92°C for 30 s, 65°C for 1 min, 72°C for 30 s. The cycle was repeated 40 times. All gene amplifications were normalised to β-Actin.

Neutrophil activation, RNA extraction, reverse transcription and qRT-PCR were all performed by Richard Wubben, from the Nigel Stephenson Lab, Trinity Biomedical Sciences Institute, Trinity College Dublin, Ireland.

2.23 Microtitre plate biofilm assay

Bacteria were grown for 12-16 hours in TSB and diluted 1:200 in BHI supplemented with glucose (1% w/v) or NaCl₂ (4% w/v) and supplemented with

CuCl₂ (1 mM) when appropriate. Diluted bacteria (200 µl) were added to a Nunclon™ Delta Surface 96 well flat-bottomed plate (Thermo Scientific, Denmark) and incubated statically at 37° C for 24 h. Wells were washed gently three times with PBS and dried by inversion for 30 min at room temperature. Adherent cells were stained with crystal violet (0.5% w/v). Plates were washed gently five times with PBS and crystal violet was solubilised with 100 µl 5% acetic acid. The A_{570nm} was measured using a *MULTISKAN EX* luminometer (Biosciences).

2.24 Minimum Inhibitory Concentration Assay

Minimum inhibitory concentration assay was performed as recommended by the Clinical Laboratory Standards Institute guidelines (Weinstein *et al.*, 2020), adapted to achieve a desired copper range of 0, 1, 2, 4, 6, 8, 10, 12, 14, 16 mM CuCl₂ in a single 96 well plate. This was done to enhance the resolution of the concentrations of CuCl₂ examined so that a difference could be detected. Briefly, 5 µl of 20X copper stock was added to each well of a 96-well plate, and 95 µl of Muller-Hinton broth was added to dilute to the desired working concentration. This permitted the examination of a precise range of concentrations of copper. The first concentration with no signs of visible growth was considered the MIC of that strain. MIC plates were read independently by two scientists.

2.25 *in silico* data analysis and statistical tests

Graphical analysis and statistical tests were performed using Graphpad prism 8 software. Phyre2 was used to generate predicted molecular model of Mco (Kelley *et al.*, 2015). Chimera 1.14 was used to generate images of CueO and Mco (Pettersen *et al.*, 2004). SignalP6.0 was used to predict if Mco1-56 contained a signal peptide (Teufel *et al.*, 2022). Image Studio™ Lite version 5.2 - Free Western Blot Quantification Software (LI-COR Biosciences) was used to quantify intensities of western blot bands. Benchling.com was used for primer design, plasmid cloning and construction design, analysis of sequencing data and genome interrogation. The Kyoto Encyclopedia of Genes and Genomes (KEGG) was used as the database to retrieve publicly available genome sequences (Kanehisa and Goto, 2000). Whole genome sequencing data was analysed using Integrative Genome Viewer (IGV) 2.8.9 software (Thorvaldsdóttir, Robinson and Mesirov, 2013). The Basic Local Alignment Search Tool (BLAST) and corresponding NCBI public

database of DNA and amino acid sequences was used for searching for homologous DNA and proteins throughout the project (Altschul *et al.*, 1990). The software 'GrowthRates' was used to mathematically calculate the exponential growth rate/doubling time of *S. aureus* growth curves (Hall *et al.*, 2014).

Chapter 3

Results Chapter 1 - Mco is a membrane localised protein in *S. aureus* that contributes to copper tolerance in aerobic conditions

3.1 Introduction

Multicopper oxidases are a family of enzymes found in Eukaryotes, Bacteria and Archaea (Quintanar *et al.*, 2007). Their active sites most often contain four copper atoms, which are required for the enzyme to oxidise their substrate, and use that electron to reduce dioxygen to water (Solomon, Sundaram and Machonkin, 1996). The vast majority of the research on bacterial multicopper oxidases has been done on *E. coli* CueO (Grass and Rensing, 2001a; Roberts *et al.*, 2002; Djoko *et al.*, 2010). By comparison however, very little is known about multicopper oxidases in Gram-positive bacteria such as *S. aureus*.

The initial characterisation of Mco found that it could oxidise 3,3'-dimethoxybenzidine, had low levels of ferroxidase and phenoloxidase activity, and that it contributed to copper tolerance (Sitthisak *et al.*, 2005). Data has also been published showing that Mco contributes to copper tolerance and promotes survival of *S. aureus* in human blood (Zapotoczna *et al.*, 2018).

Much remains unknown about Mco. Its cellular location is unknown. In comparison, other characterised bacterial multicopper oxidases including *E. coli* CueO and *M. tuberculosis* MmcO, contain a canonical twin-arginine protein translocation (Tat) signal peptide, and are translocated by the Tat pathway to the periplasm where they are active (Outten *et al.*, 2000; Palmer, Sargent and Berks, 2005; Rowland and Niederweis, 2013; Stolle, Hou and Brüser, 2016). Proteins secreted by the Tat pathway are characterised by the presence of two consecutive arginines towards the N-terminus of the signal peptide and an AXA (alanine-any amino acid-alanine) motif where signal peptidase I cleaves. *S. aureus* and other Gram-positive bacteria lack the periplasm found in Gram-negative bacteria and the cellular location of *S. aureus* Mco remains undetermined.

Clonal complex 30 (CC30) strains of *S. aureus* are one of the most prevalent clonal lineages present in hospitals in the UK and Ireland. The copper hypertolerance locus *copBmco* is present in all CC30 strains of *S. aureus*. It is located within a mobile genetic element called p2-hm, which is integrated into the chromosome (Zapotoczna *et al.*, 2018).

Here, to investigate the role of *mco* in *S. aureus*, an isogenic *mco* deletion mutant was generated in the CC30 hospital-associated methicillin resistant *S. aureus* (HA-MRSA) strain, MRSA252. MRSA252 was chosen as a clinically relevant strain of *S. aureus* that is representative of HA-MRSA isolates that frequently occur in the UK and Ireland. Uncovering more about *copB* and *mco* in clinically relevant strains will hopefully uncover novel avenues for treatment for multidrug resistant *S. aureus*. This chapter begins by analysing the similarities and differences between the relatively uncharacterised *S. aureus* Mco with the most well understood bacterial multicopper oxidase *E. coli* CueO. The cellular location and contribution of Mco to copper tolerance is investigated in detail.

3.2 Similarities and differences between *S. aureus* Mco and *E. coli* CueO.

The sequence of Mco was compared to the most well characterised bacterial multicopper oxidase, *E. coli* CueO. An amino acid sequence alignment was generated to compare the residues of Mco to CueO (Fig. 3.1).

Mco and CueO share 39% amino acid identity and the four copper ligand binding sites characteristic of all blue copper oxidases are fully conserved (Solomon, Sundaram and Machonkin, 1996). The amino acid residues of the copper ligand binding sites are highlighted in Fig. 3.1 with blue boxes. This suggests that Mco likely functions as a multicopper oxidase similar to CueO, where substrate oxidation occurs at the type-1 copper centre, and electron transfer to the type-2/3 tri-nuclear cluster results in reduction of dioxygen to H₂O.

Mco lacks the methionine-rich region that CueO harbours (amino-acids 356-402). The exact molecular protein structure of this methionine rich region of CueO has never been successfully crystallised. It is likely to be a highly flexible and disordered loop (Roulling, Godin and Feller, 2022). However it is believed to assist in substrate copper acquisition in the environment and promote direction of substrate copper to the type-1 copper centre where substrate oxidation can begin.

A unique N-terminal region was identified in Mco that is absent in other bacterial multicopper oxidases. This N-terminal region does not contain the twin arginine motif that occurs in CueO (Fig.3.1). The N-terminal 56 residues of Mco align extremely poorly with CueO. These residues were interrogated further by an amino acid BLAST search (Fig.3.2A). This sequence of amino acids only appears in the *Staphylococcus* and *Listeria* genera, hinting that perhaps this novel N-terminal region is required for monoderm multicopper oxidases to function.

A signal peptide prediction software SignalP6.0 was used to predict if this unique 56 residue N-terminal region contained a signal peptide (Fig.3.2B). SignalP6.0 predicted that residues 1-26 contain a Sec signal peptide that would be cleaved by signal peptidase I between residues A₂₅ and E₂₆. A sec signal peptide is not typical of bacterial multicopper oxidases and warranted empirical

experimentation to discern if residues 1-26 of Mco truly contained a Sec signal peptide. This is presented later in this chapter (Fig. 3.21A).

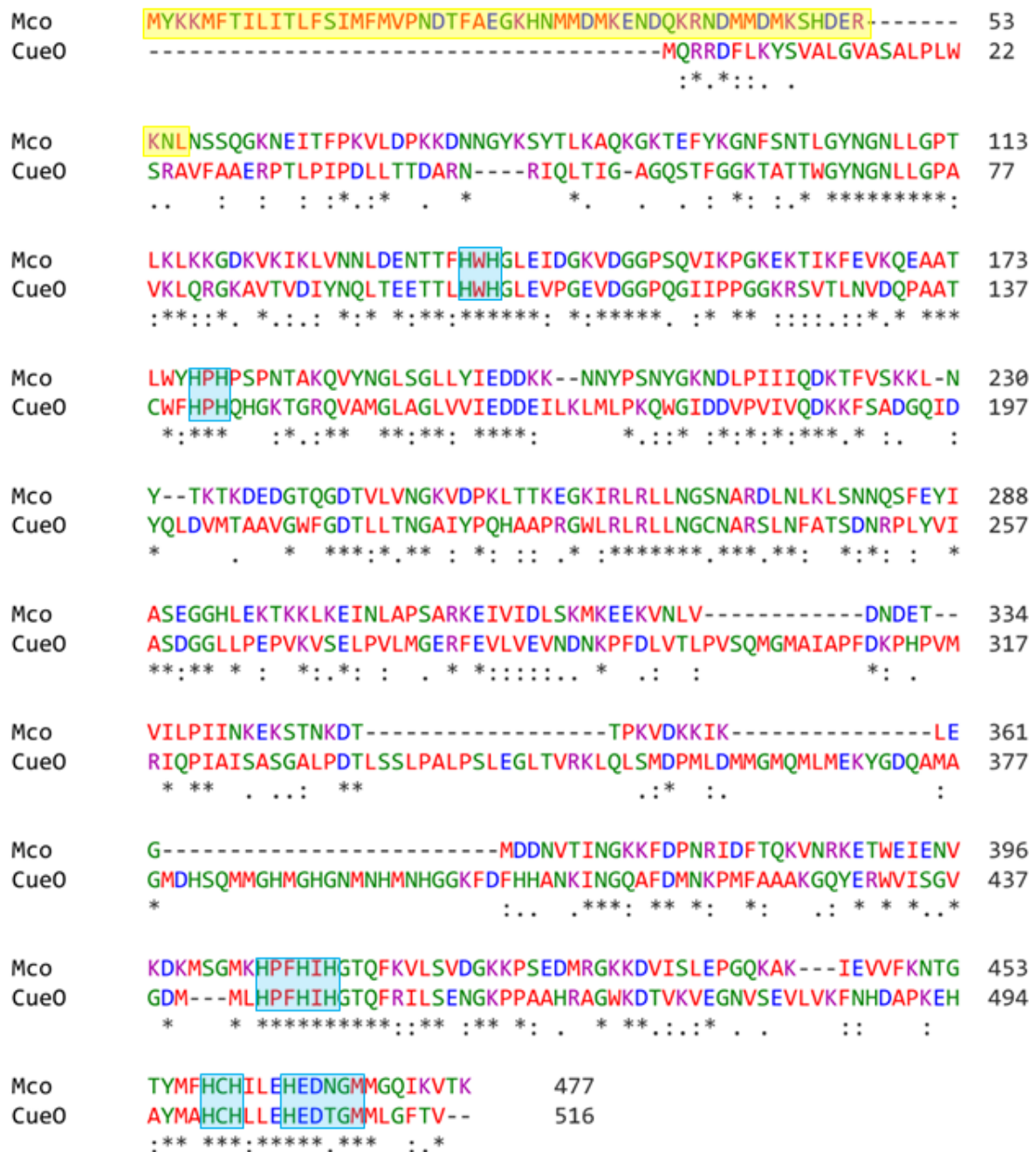


Figure 3.1 Alignment of *S. aureus* Mco and *E. coli* CueO

Alignment of *S. aureus* Mco and *E. coli* CueO. Conservation of the copper binding ligand sites HxH, HxH, HxxHxH, HCH and HxxxxM are highlighted in blue boxes. Residues 1-56 of Mco are highlighted in yellow. The first 56 residues of Mco align poorly with CueO, while residues 57 to 477 align with much greater identity similarity. “*” indicates fully conserved residue, “:” indicates conservation between groups of strongly similar properties, “.” Indicates conservation between groups of weakly similar properties. Red = small and hydrophobic, blue = acidic, magenta = basic, green = hydroxyl, sulfhydryl and amine, grey = other amino acids.

3.3 Modelling the structure of Mco

Our knowledge of the molecular structure and function of multicopper oxidases is aided by the crystal structure of *E. coli* CueO (Roberts *et al.*, 2002). *S. aureus* Mco has not been crystallised and as a result the mechanisms of action of the *S. aureus* enzyme are best predicted by modelling the structure based on that of CueO and related proteins whose X-ray crystal structures have been solved, using Phyre2 software (Kelley *et al.*, 2015).

Models (n=78) were generated. Of these, 51 were multicopper oxidases with homology largely based on 2 or 3 of the 3 cupredoxin domains. Models of the 20 proteins with the highest raw alignment score were generated by Phyre2. The models with the highest raw alignment scores to *S. aureus* Mco were bilirubin oxidase from *Myrothecium verrucaria*, bilirubin oxidase from *Myrothecium verrucaria* by X-ray crystal analysis using a twin crystal, multicopper oxidase from *Campylobacter jejuni*, Sufl from *E. coli*, CotA from *Bacillus subtilis*, CueO from *E. coli* and CueO from *Ochrobactrum* sp..

The protein with highest percentage amino-acid identity to Mco is *E. coli* CueO at 39%. The model of *S. aureus* Mco based on the crystal structure of *E. coli* CueO was superimposed onto CueO (Fig. 3.3A). The model begins at residue 57 of Mco and does not include residues 1-56. The superimposition gives a representation of the similarity between Mco and CueO (Fig. 3.3A). An enlarged view of the copper centres was generated (Fig. 3.3B). By showing the copper binding residues of both Mco and CueO in ball and stick configuration the homology between their copper binding centres is evident. This suggests that Mco and CueO function in the same way. The cuprous oxidation likely occurs at the relatively exposed T1 copper centre, where the electron is transferred to the T2/3 trinuclear cluster which reduces dioxygen to water in a similar fashion to CueO. However the methionine rich region of CueO is absent in Mco, suggesting the methionine rich region is not required for function of Mco (Roberts *et al.*, 2002; Djoko *et al.*, 2010; Cortes, Wedd and Xiao, 2015).

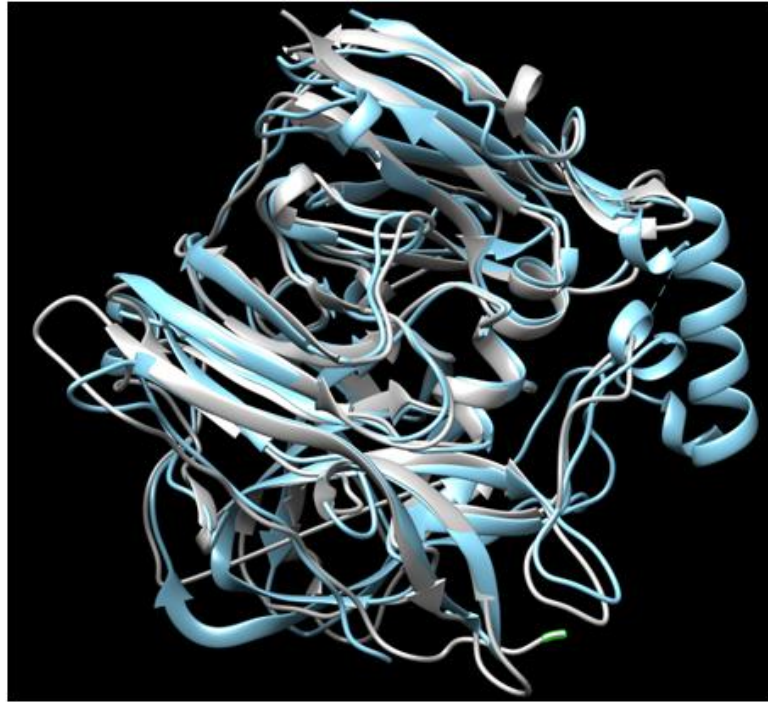
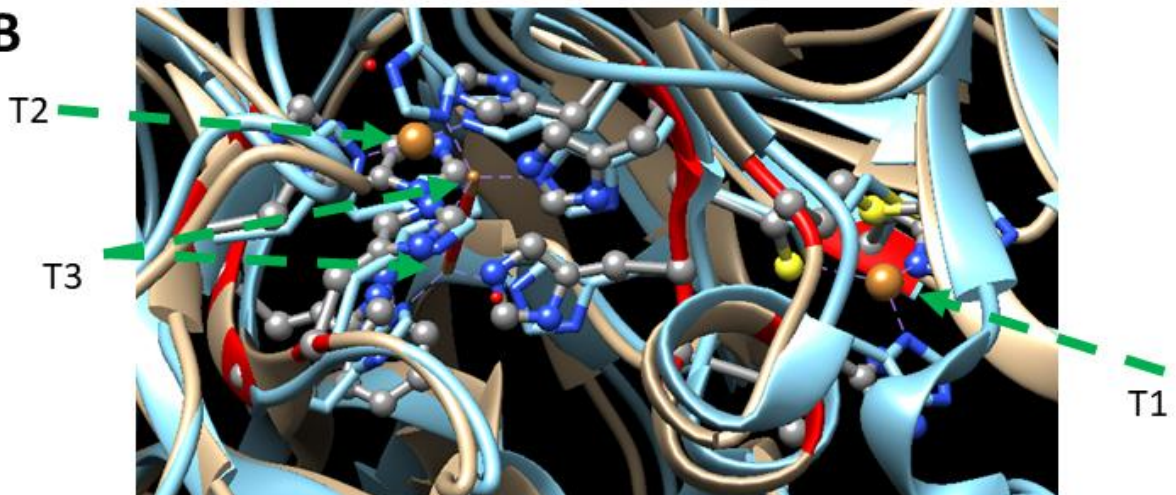
A**B**

Figure 3.3. *S. aureus* Mco model based on *E. coli* CueO superimposed on CueO

(A) Ribbon representation of Mco (grey) superimposed onto CueO (light blue).

(B) Enlarged view of the molecular structure of the T1, T2 and T3 copper centres of CueO and Mco. The copper ligand binding sites are represented in a ball and stick configuration for both CueO and Mco, with the ligand binding sites of Mco highlighted in the ribbon (red). The 4 copper ligands shown as gold balls with their bonds (light purple dashed line) indicated. The T1, T2 and T3 copper centres are indicated by the green dashed arrows.

3.4 Generation of pIMAY:: Δmco by allelic exchange

To begin investigation and characterisation of *S. aureus* Mco, an isogenic *mco* deletion mutant was generated by allelic exchange (Monk *et al.*, 2012).

The 472 base pairs immediately upstream of *mco*, and the first 41 nucleotides of *mco* were amplified by PCR using primers Mco A and Mco B to generate the 513 base pair AB product. The first 41 nucleotides of *mco* were intentionally left on the chromosome of MRSA252 to reduce the likelihood of *copB* transcription disruption in an isogenic *mco* deletion mutant. The 3' end of *copB* terminates only 14 base pairs before the 5' end of *mco*. The 503 base pairs immediately downstream of *mco* were amplified by PCR using primers Mco C and Mco D to generate the CD product (Fig. 3.4A and B).

The Mco C primer was designed to have an overhanging extension homologous to the Mco B primer, so that an overlapping extension PCR could be performed using primers Mco A and Mco D with PCR products AB and CD as template, to generate the continuous AD product with a length of 1074 base pairs (Fig. 3.4C and D).

The empty vector pIMAY was linearised using primers pIMAY SLIC F and pIMAY SLIC R. These primers were designed to linearise pIMAY at its multiple cloning site (MCS) (Fig. 3.4E and F).

The primers Mco A and Mco D were designed to have overhanging extensions homologous to pIMAY SLIC F and pIMAY SLIC R respectively. This permitted the use of the high efficiency plasmid cloning strategy sequence and ligase independent cloning (SLIC) (Li and Elledge, 2007).

SLIC was performed on linearised pIMAY and the AD product which joined these two products together creating pIMAY:: Δmco (Fig. 3.4G). The high efficiency cloning *E. coli* strain IM30B (Monk *et al.*, 2015) was transformed with pIMAY:: Δmco , and plated on LB agar supplemented with chloramphenicol (10 $\mu\text{g/ml}$) to select for *E. coli* harbouring the plasmid pIMAY which confers resistance to chloramphenicol. A colony screen was performed using PCR primers pIMAY MCS F and pIMAY MCS R to confirm the presence of pIMAY:: Δmco (Fig. 3.4H).

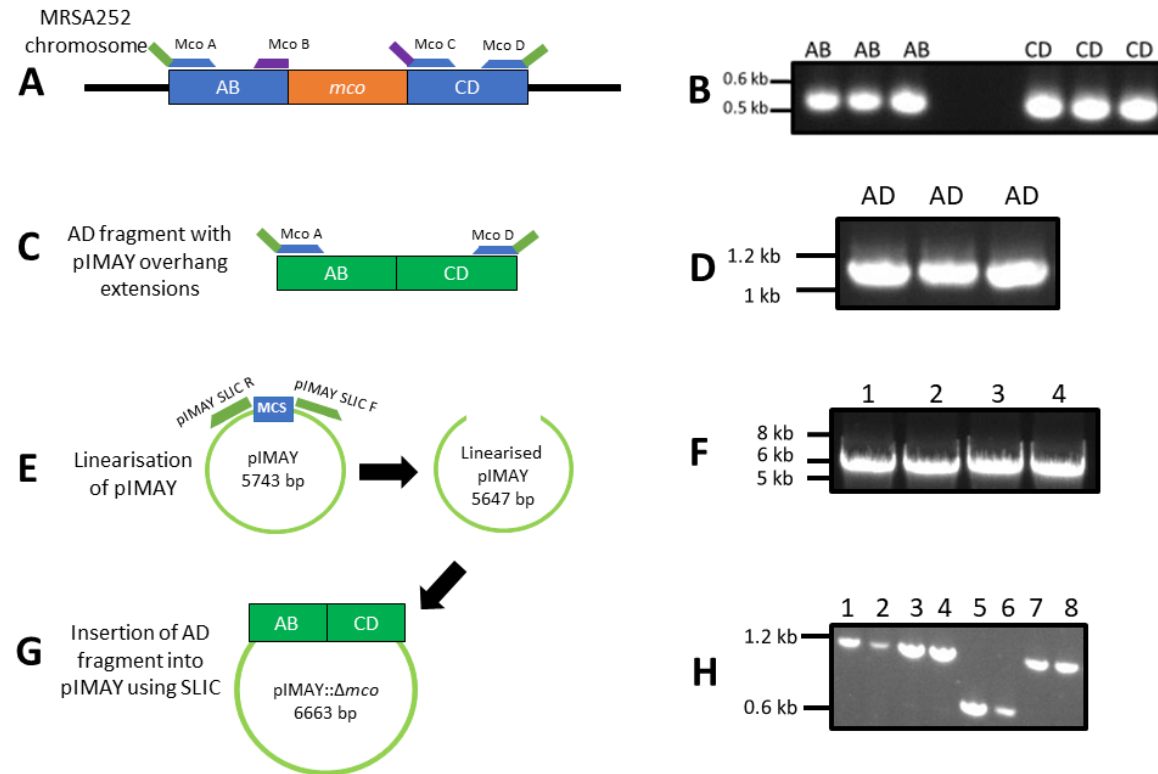


Figure 3.4 Generation of pIMAY:: Δmco .

Schematic of *AB* and *CD* region design for deletion of *mco* by allelic exchange (A). Agarose gel showing amplified *AB* and *CD* region of 503 and 413 base pairs respectively (B). Schematic representation of amplification of *AD* product using primers Mco A and Mco D including overhangs homologous to linearised pIMAY (C). Agarose gel showing the 1074 base pair *AD* product (D). Schematic representation of inverse PCR linearising pIMAY at its multiple cloning site (E). Agarose gel showing 4 PCR products of linearised pIMAY at 5743 base pairs in length (F). Schematic representation of pIMAY:: Δmco showing the *AD* product insertion (G). Agarose gel showing colony screen of 8 *Cm*^r IM30B clones where clones 1-4 and 7-8 contained the desired PCR product length of 1203 base pairs (H), indicating successful insertion of *AD* into pIMAY using SLIC.

3.5 Generation of MRSA252 Δ *mco* by allelic exchange with pIMAY:: Δ *mco*

The plasmid pIMAY:: Δ *mco* was purified and the integrity of the AD region was confirmed by DNA sequencing (data not shown). MRSA252 made electrocompetent was transformed with pIMAY:: Δ *mco* and deletion of *mco* was achieved by allelic exchange (Monk *et al.*, 2012).

This mutagenesis process achieves deletion by designing a pIMAY plasmid with ~550 bp of homology upstream and downstream of the gene of interest (Fig. 3.5A). This facilitates integration of the plasmid into the chromosome of *S. aureus* at the location of the gene of interest (Fig. 3.5B). Then excision of pIMAY was selected for, which will sometimes remove the gene of interest from the chromosome along with pIMAY (Fig. 3.5C).

Briefly, transformants grown at 28°C on agar containing chloramphenicol were screened by PCR for the presence of replicating plasmid using primers pIMAY MCS F and pIMAY MCS R. Colonies positive for pIMAY:: Δ *mco* yielded a band of approximately 1.1 kb. These clones were grown at 37°C which is not permissive for plasmid replication in order to select for colonies where the plasmid had integrated into the chromosome of MRSA252.

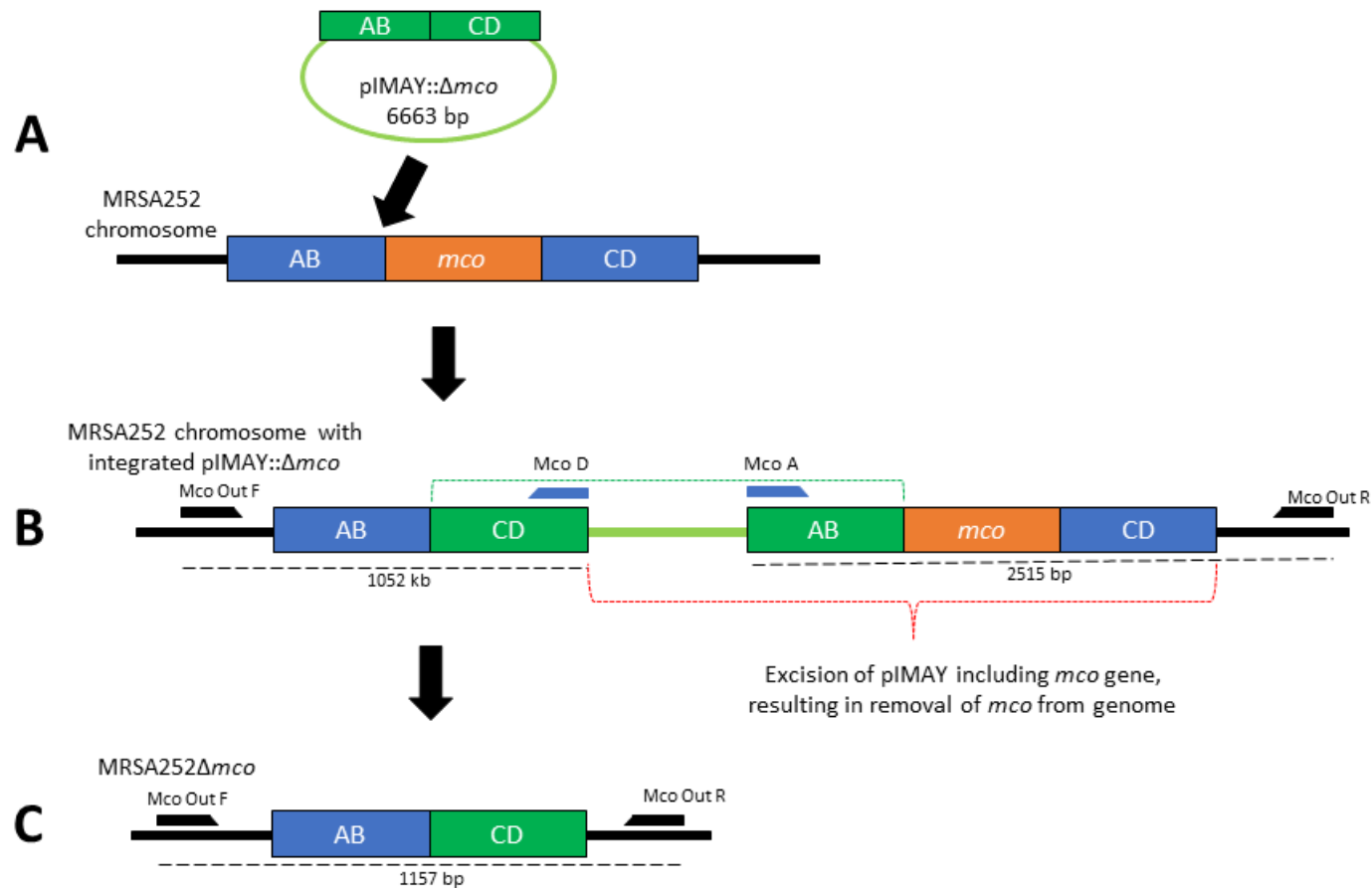


Figure 3.5 Deletion of *mco* using pIMAY mediated allelic exchange.

Schematic representation of pIMAY:: Δmco integrating into the chromosome of MRSA252 upstream of *mco* (A). Schematic representation of pIMAY:: Δmco integrated upstream of *mco*, including the four primers used to determine the side of integration (B). Excision of pIMAY resulting in the loss of *mco* is indicated with the red dotted bracket. Schematic representation of the chromosome of MRSA252 Δmco upon successful excision of pIMAY:: Δmco (C). PCR product length of primer pairs is indicated by the black dotted line below the schematics.

The larger colonies growing at 37°C were chosen for colony screening for replicating pIMAY using primers pIMAY MCS F and R (Fig. 3.6A). Clones giving no band or a weak band were considered integrants.

Another colony screen was performed on clones negative for replicating pIMAY using primer pairs Mco out F and Mco D, and Mco out R and Mco A to screen for upstream and downstream integrants of *mco* respectively (Fig. 3.6B).

Clones carrying plasmids that had integrated either up or downstream of *mco* were chosen for growth for 16 h at 28°C in TSBd without any antibiotic to encourage excision of pIMAY:: Δ *mco*. The broth cultures were plated on L agar containing anhydrotetracycline (ATc, 1 µg/ml) and incubated at 28°C for 48 h. This induced expression of the anti-*secY* antisense RNA present on pIMAY in any clones that still harboured pIMAY. The *secY* gene product is essential in *S. aureus* so expression of this antisense RNA selects for clones where pIMAY has excised. Big colonies on the ATc plates were toothpicked onto TSA supplemented with Cm (10 µg/ml) to confirm pIMAY absence. Cm^S clones were chosen for excision colony screening.

When the excision event occurs, it may excise pIMAY including the gene of interest (*mco* in this case) or it may excise without the gene of interest. Cm^S excisants were screened by colony PCR for the loss of *mco* using primers Mco out F and Mco out R (Fig. 3.6C). A band of 1157 bp was amplified from isogenic *mco* mutants. Genomic DNA from these clones was purified and the flanking regions of *mco* were amplified using primers Mco out F and Mco out R (Fig. 3.6D). The integrity of the deletion of *mco* was confirmed by DNA sequencing of this PCR amplicon (data not shown).

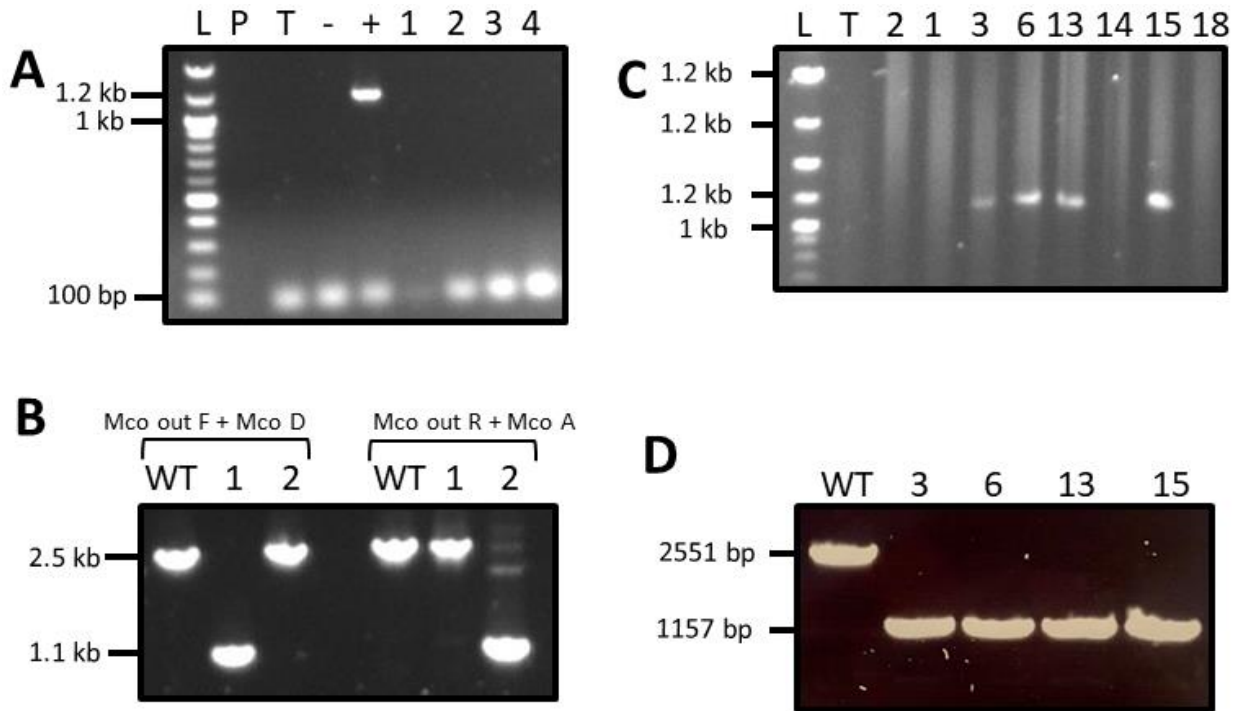


Figure 3.6. Integration and excision of pIMAY:: Δ mco leading to MRSA252 Δ mco generation.

(A) Agarose gel showing no replicating pIMAY which was detected in clones grown at 37°C e.g. clones 1-4. pIMAY was detectable in the positive control (+) which was MRSA252 carrying pIMAY:: Δ mco grown at 28°C. L indicates ladder, P indicates no polymerase control, T no template DNA control, - WT MRSA252 with no pIMAY.

(B) Integration screen of MRSA252 without pIMAY (WT), one upstream (1) and one downstream (2) integrant.

(C) Out Mco colony screen of clones that were large on TSA supplemented with ATc (1 μ g/ml) and were Cm^S when toothpicked onto TSA supplemented with chloramphenicol (10 μ g/ml). Clones where *mco* had been deleted presented with a band of 1157 bp in length, e.g. clones 3, 6, 13 and 15. L = ladder, T = no template DNA control.

(D) Out Mco PCR screen using purified genomic DNA from the 4 independently isolated MRSA252 Δ mco clones including WT MRSA252 as a control.

3.6 Growth or haemolysis of MRSA252Δ*mco*

No change in the growth profile of any of the MRSA252Δ*mco* clones was detected when compared to MRSA252 (Fig. 3.7A). MRSA252Δ*mco* clone 3 was used for the remainder of this work and is named MRSA252Δ*mco*. There was no change in the haemolytic profile (delta or alpha toxin activity) of MRSA252Δ*mco* when streaked onto Columbia sheep blood agar plates when compared to MRSA252 (Fig. 3.7B). Since the gene encoding delta toxin is encoded within *agr* RNAIII, this indicates the integrity of the *agr* operon and supports the conclusion that any changes in phenotype were not due to potential off target disruption of the *agr* operon during the mutagenesis procedure.

Occasionally during the pIMAY mutagenesis process off target mutations can occur elsewhere in the genome. To control for the possibility of off target mutations being responsible for the phenotype of the *mco* mutant, whole genome sequencing was carried out on MRSA252Δ*mco* and the sequence was compared to the parent strain MRSA252. No additional mutations were detected (data not shown).

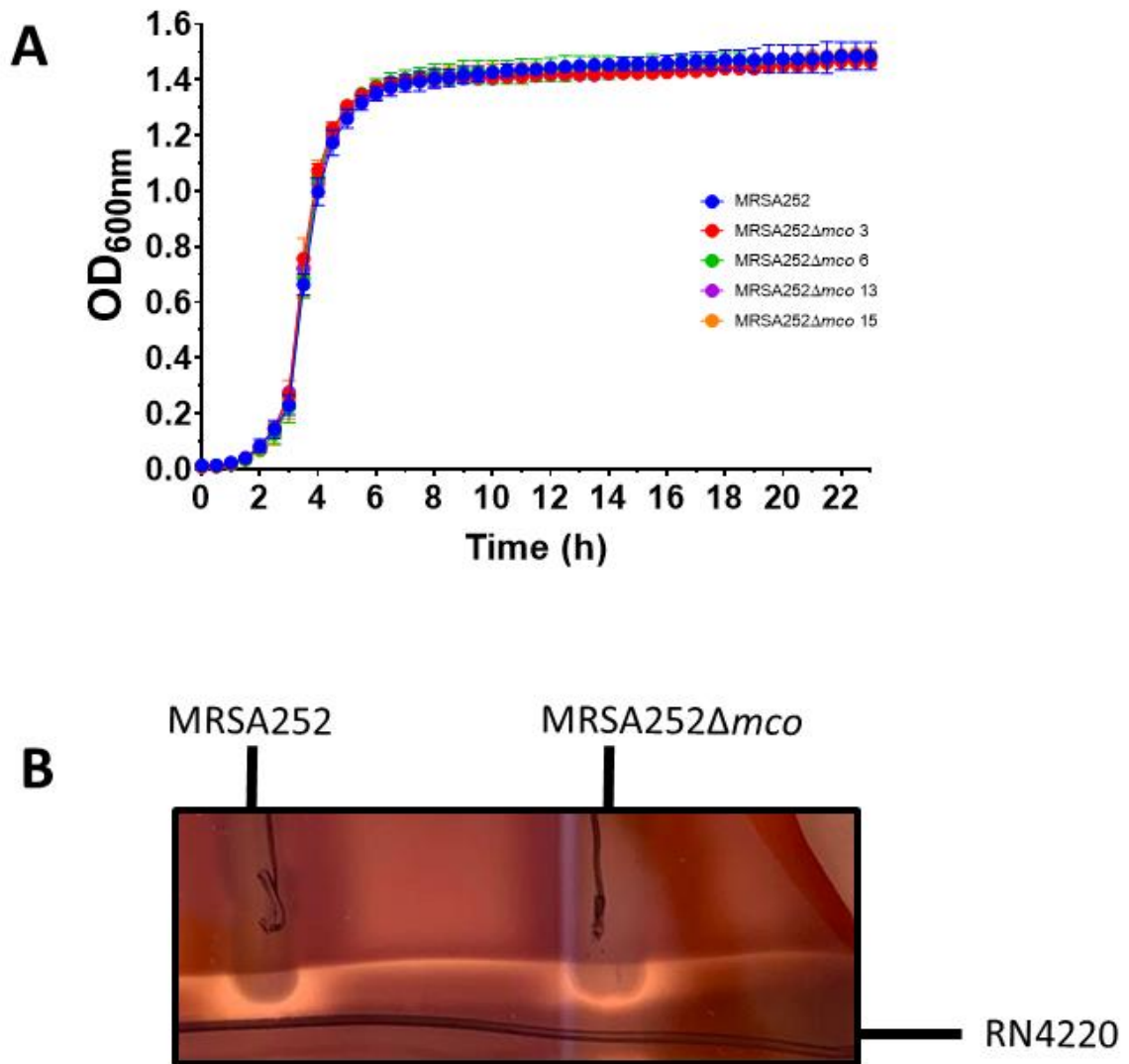


Figure 3.7. Confirmation that MRSA252Δmco was not compromised during mutagenesis procedure.

(A) Growth of the 4 independently isolated MRSA252Δmco clones (clones 3, 6, 13 and 15) was monitored in TSBd over 23 h in a 96 well plate with orbital shaking. Error bars represent +/- SD (n=3).

(B) Growth of MRSA252 and MRSA252Δmco on sheep blood agar plate cross-streaked with RN4220. The haemolysis profile produced by MRSA252Δmco is the same as MRSA252, indicating disruption of the virulence operon *agr* has not been compromised (n=1).

3.7 Expression of Mco with an N-terminal 3X-FLAG tag in response to copper supplementation.

3.7.1 Generation of pCL55::UCMF

To determine the location of Mco in *S. aureus*, the expression of the protein with a C-terminal 3X-FLAG tag under conditions closest to how it is expressed in nature was pursued. Native *mco* is expressed under the control of the copper sensitive operon repressor (CsoR). Under copper restricted conditions the operon is repressed by CsoR. When copper is present, it binds CsoR and derepresses the *copBmco* operon permitting transcription of the copper resistance genes.

A DNA construct extending from 180 bp upstream of the CsoR binding site of *copB* to the 3' end of *mco*. DNA encoding the 3X-FLAG tag was cloned into the 3' end of *mco* (Fig. 3.8A). This DNA construct was named UpCopBMco3XFLAG (UCMF). Next, UCMF was inserted into the single copy integrating vector pCL55. This plasmid is unable to replicate in *S. aureus* so it only survives in *S. aureus* after integration into the chromosome. It harbours both the integrase gene (*int*) and the *attP* site that is required for integration into the *attB* site within the *geh* gene in the chromosome of *S. aureus* (Fig. 3.8B).

Integration of pCL55::UCMF and an empty vector control (pCL55 empty) was confirmed by colony screen using a primer that anneals to *geh* (*geh* F) and a primer that anneals to pCL55 (pCL55 int screen R). This primer pair would only amplify a product if the plasmid was integrated into the chromosome at the *geh* locus (Fig. 3.8C). To confirm that the pCL55::UCMF clones in Fig. 3.8C truly contained UCMF, a colony screen was performed where primers amplified from within the *mco* gene just before the 3X-FLAG tag (Mco3XFLAG Screen F) and the pCL55 vector (pCL55 MCS screen R) to confirm that *mco*3XFLAG was present in the *S. aureus* clones containing integrated pCL55::UCMF (Fig. 3.8D).

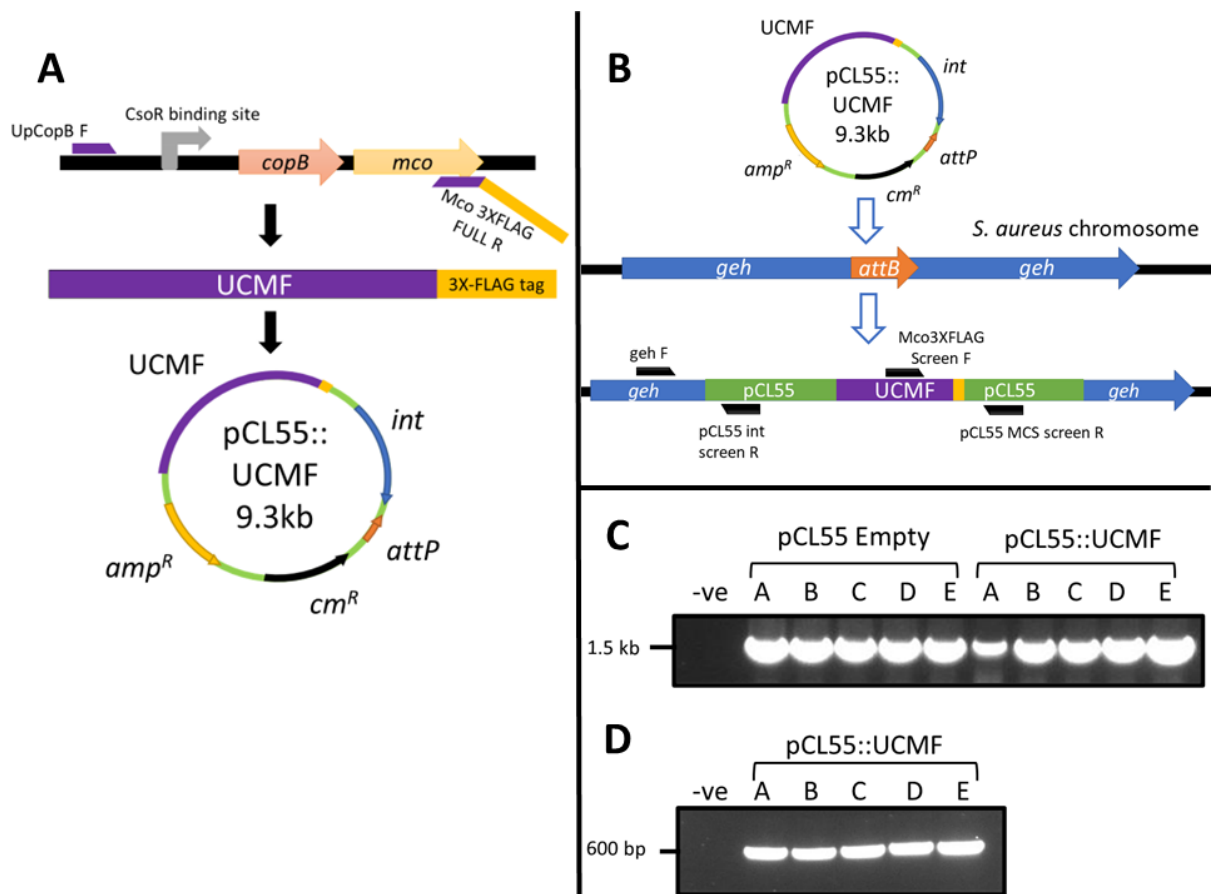


Figure 3.8 Generation of pCL55::UCMF

(A) Schematic detailing how a DNA construct was designed to express *mco*3X-FLAG under control of its native promoter which contains the CsoR binding site. UCMF was inserted into the MCS of pCL55. This schematic is not drawn to scale. *int* = integrase gene, *amp^R* = ampicillin resistance cassette, *cm^R* = chloramphenicol resistance cassette.

(B) Illustration of how pCL55::UCMF integrated into the chromosome of *S. aureus*. The *attP* site in pCL55 recognises the *attB* site and integrates at this site in the *geh* locus. The *geh* gene is disrupted and pCL55::UCMF is now irreversibly integrated into the chromosome of *S. aureus*. Screening primers are depicted in black. Primers *geh* F and pCL55 int screen R confirm chromosomal integration, and primers Mco3XFLAG Screen F and pCL55 MCS screen R confirm UCMF presence in the MCS of pCL55.

(C) Agarose gel of colony screen on successful pCL55 empty and pCL55::UCMF integrants using primers *geh* F and pCL55 int screen R. -ve indicates negative control of MRSA252Δ*mco* without pCL55 integration.

(D) Agarose gel of colony screen on successful pCL55::UCMF integrants confirming UCMF presence using primers Mco3XFLAG Screen F and pCL55 MCS screen R. -ve indicates negative control of MRSA252Δ*mco* without pCL55 integration.

3.7.2 Generation of pCL55::UCMF Δ Mco2-53

Residues 1-56 of Mco are (Fig. 3.1) likely to be unique to *Listeria* and *Staphylococcal* genera (Fig. 3.2A) and are predicted to contain a Sec signal peptide (Fig. 3.2B). In order to test this, residues 2-53 of Mco were deleted from pCL55::UCMF (Fig. 9). Residues 53-56 of Mco were intentionally omitted from the deletion strategy in order to reduce the risk of inappropriate folding of the mature Mco protein. The first residue of Mco was retained as the protein requires a methionine encoded by the start codon in order to be translated.

The strategy employed to make an in-frame deletion removing residues Mco2-53 in pCL55::UCMF generating pCL55::UCMF Δ Mco2-53 is outlined schematically (Fig. 3.9A). Inverse PCR with primers Mco2-53 del F and Mco2-53 del R using pCL55::UCMF as template successfully linearised pCL55::UCMF deleting DNA encoding residues Mco2-53 (Fig. 3.9B). This PCR amplicon was ligated by blunt end ligation, transformed into IM30B, and clones were screened for the presence of pCL55::UCMF Δ Mco2-53 using primers Mco A F and Mco 2-53 seq R (Fig. 3.9C). The integrity of the Mco2-53 deletion was confirmed by DNA sequencing (data not shown).

Plasmid from clones with carrying the deletion was purified and transformed into MRSA252 Δ mco made electrocompetent and plated on TSA supplemented with Cm (10 μ g/ml). Cm^R clones were screen by colony PCR with primers pCL55 int screen R and geh F to confirm integration of pCL55 into the chromosome of *S. aureus* (Fig. 3.9D). Purified genomic DNA from clones positive for pCL55 were screened by PCR with primers pCL55 MCS F and R (Fig. 3.9E). The integrity of the Mco2-53 deletion was confirmed by DNA sequencing of this PCR amplicon (data not shown).

This confirmed that MRSA252 Δ mco::pCL55::UCMF Δ Mco2-53 had been successfully generated thus facilitating a thorough investigation of the cellular location of Mco in *S. aureus*.

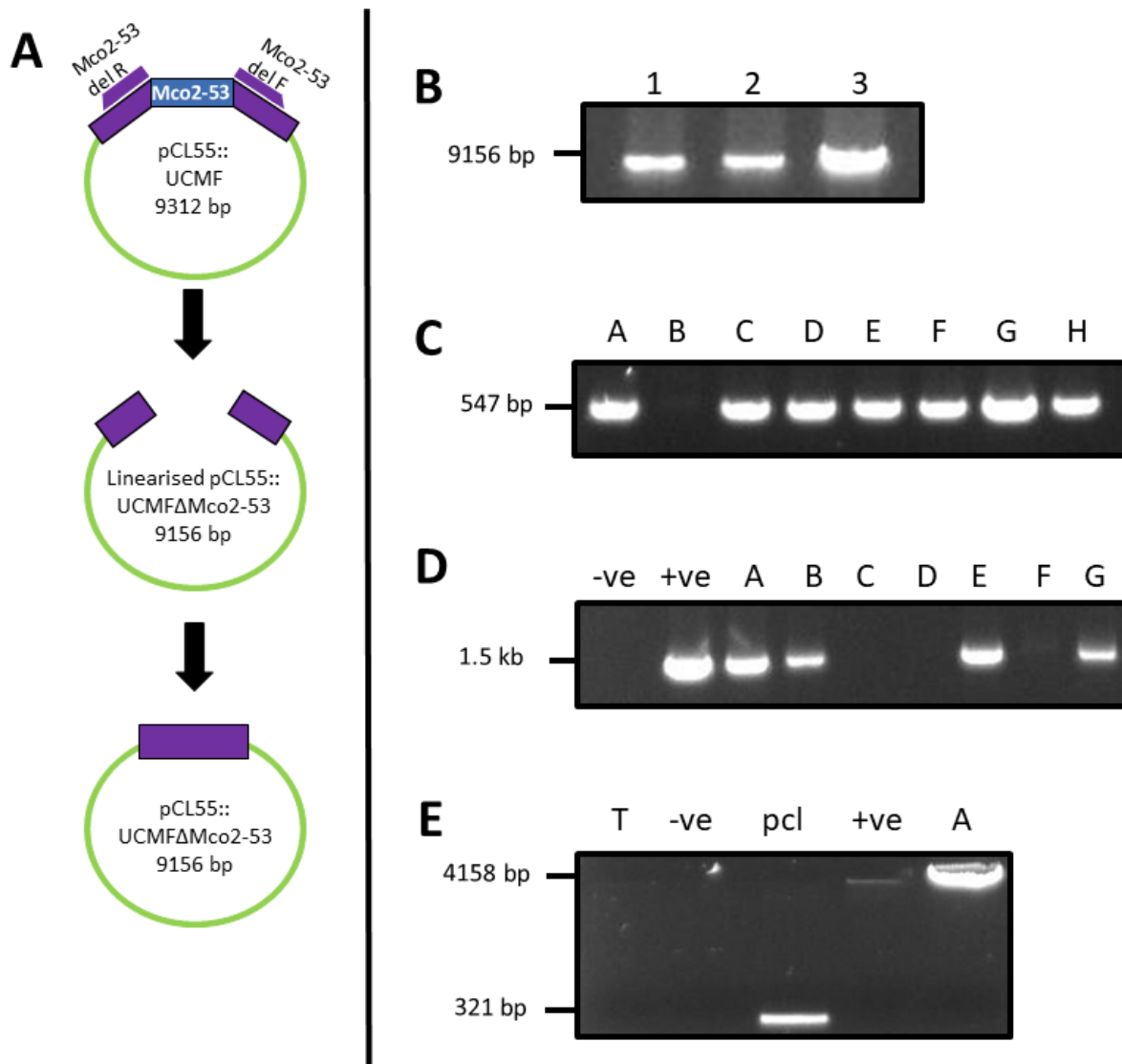


Figure 3.9. Construction of MRSA252Δmco::pCL55::UCMFΔMco2-53.

(A) Schematic detailing how primers were used for inverse PCR to delete Mco2-53 from pCL55::UCMF. This schematic is not drawn to scale.

(B) Agarose gel of three successful PCR amplifiers of linearised pCL55::UCMFΔMco2-53.

(C) Agarose gel of colony screen of pCL55::UCMFΔMco2-53 harbouring clones of IM30B using Mco A F and 2-53 seq R.

(D) Agarose gel of colony screen on successful pCL55::UCMFΔMco2-53 integrants confirming pCL55 presence using primers pCL55 in screen R and geh F. -ve indicates MRSA252Δmco not harbouring pCL55, +ve indicates positive control of MRSA252Δmco::pCL55::UCMF.

(E) Agarose gel of on purified genomic DNA amplifying UCMFΔMco2-53 using primers pCL55 MCS F and R. T indicates template DNA negative control, -ve indicates MRSA252Δmco without pCL55, pcl indicates MRSA252Δmco::pCL55 empty, +ve indicates MRSA252Δmco::pCL55::UCMF.

3.8 Mco is a membrane-located protein in *S. aureus*

Having generated strains MRSA252 Δ *mco*::pCL55, MRSA252 Δ *mco*::pCL55::UCMF and MRSA252 Δ *mco*::pCL55::UCMF Δ Mco2-53, the location of *S. aureus* Mco and the role of its predicted signal peptide region could then be determined by fractionation of bacterial cells into distinct compartments. The empty pCL55 containing strain was required to ensure that the incorporation of pCL55 or *geh* disruption was not responsible for any alteration in phenotype. Cultures were grown overnight in the presence of 1 mM CuCl₂ and fractionated into 4 cellular compartments namely the supernatant, cell wall, membrane and cytoplasm. These fractions were probed by Western immunoblotting with α -FLAG IgG.

Mco3X-FLAG was detected in the membrane fraction of *S. aureus* UCMF migrating at the expected molecular weight of ~ 57 kDa (Fig. 3.10A), but not in the empty vector control.

The other immunoreactive bands appearing in the cell wall, cytoplasm and supernatant fractions (including the empty pCL55 control) are most likely the immunoglobulin binding staphylococcal protein A which binds to the Fc region of IgG (Becker *et al.*, 2014; O'Halloran, Wynne and Geoghegan, 2015).

As a control, samples were probed for the membrane protein EbpS with anti-EbpS IgG. A ~90 kDa band representing EbpS was detected only in the membrane fractions (Fig. 3.10B), verifying that the membrane samples contained membrane-located antigens, and that there was no contamination of the supernatant, cell wall or cytoplasmic fractions with membrane proteins.

As another control the samples were probed for the supernatant-located protein V8 protease with anti-V8 protease IgG (O'Halloran, Wynne and Geoghegan, 2015). V8 protease was detected only in the supernatant (Fig. 3.10C), confirming that supernatant material did not contaminate any of the other fractions.

In conclusion, these data indicate that Mco is localised to the membrane of *S. aureus*.

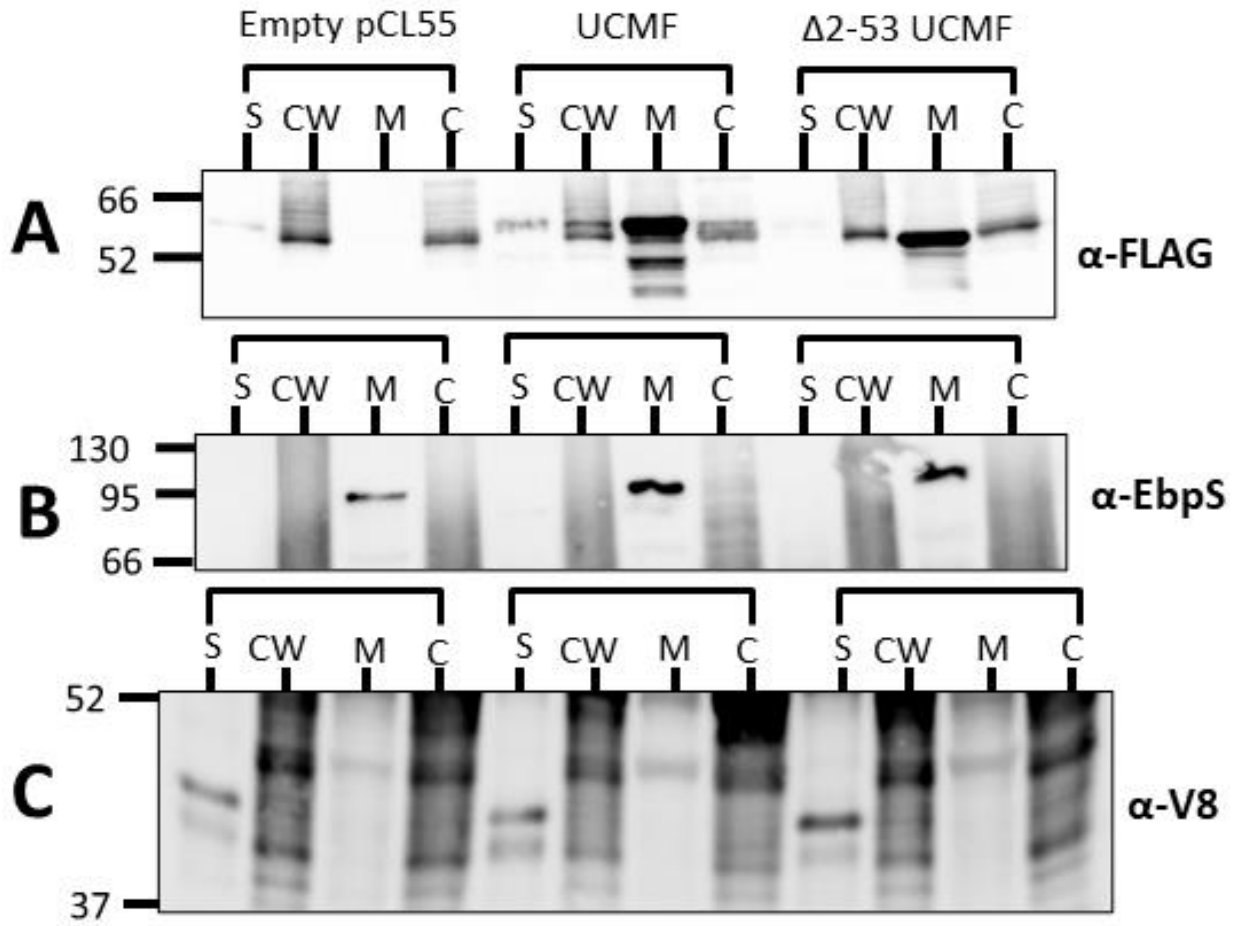


Figure 3.10 Mco is membrane located in *S. aureus*

Subcellular protein fractions of MRSA252 Δ *mco*::pCL55 empty (Empty pCL55), MRSA252 Δ *mco*::pCL55::UCMF (UCMF) and MRSA252 Δ *mco*::pCL55::UCMF Δ Mco2-53 (Δ 2-53 UCMF) cultured overnight in the presence of CuCl₂ (1 mM) were transferred to a nitrocellulose membrane and probed with anti-FLAG IgG (A), anti-EbpS IgG (B) and anti-V8 IgG (C) Bound antibody was detected using HRP-conjugated goat anti-mouse Fab fragments (A) and protein-A peroxidase (B + C). Size markers are indicated at the side (kDa). S = supernatant, CW = Cell wall, M = membrane, C = cytoplasm.

Importantly, testing that the band representing Mco3X-FLAG in the membrane fraction of *S. aureus* was a result of copper induced expression was required to confirm that the UCMF DNA construct expressed a copper inducible protein as expected. The expression of *mco3X-FLAG* was confirmed to be in response to copper addition by performing western immunoblotting on membrane fractions of *S. aureus* with and without supplementation of growth media with 1 mM CuCl₂ (Fig. 3.11). Mco3X-FLAG was detectable without the addition of copper. However this band was much weaker than the band representing Mco3X-FLAG in the culture grown with 1 mM CuCl₂ supplementation. This indicated that *mco3X-FLAG* was expressed poorly in the absence of copper, but was strongly expressed in the presence of copper. This confirmed the DNA construct worked as designed and that UCMF expressed *mco3X-FLAG* in response to copper.

The N-terminal truncated form of Mco, McoΔ2-53, was also investigated (Fig. 3.11). McoΔ2-53-3X-FLAG was detected with a weaker band in the absence of copper, when compared to the band in the presence of 1 mM copper.

Lastly, to control for background non-specific immunoglobulin binding, membrane proteins of the empty vector control MRSA252Δ*mco*:pCL55 grown in media supplemented with 1 mM CuCl₂ were also purified, transferred to a nitrocellulose membrane and probed with α-FLAG IgG. No band was detected at 57 or 53 kDa, indicating that the bands representing Mco3X-FLAG and McoΔ2-53-3XFLAG were not due to non-specific immunoglobulin binding.

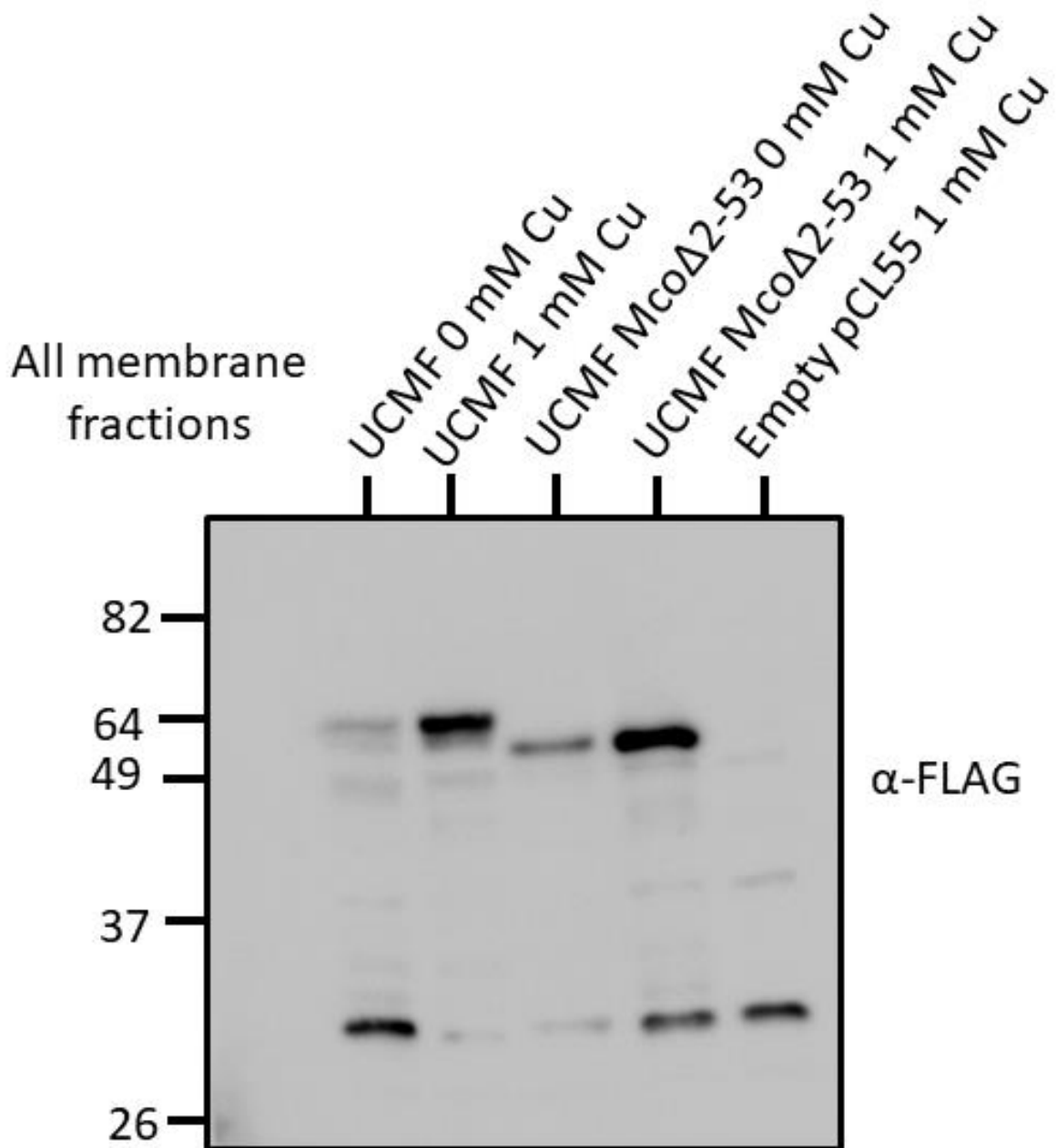


Figure 3.11. Expression of Mco3XFLAG in response to copper supplementation of growth media.

Cultures of MRSA252Δ*mco*::pCL55::UCMF (UCMF), MRSA252Δ*mco*::pCL55::UCMFΔ*Mco*2-53 (UCMF McoΔ2-53) and MRSA252Δ*mco*::pCL55 empty (Empty pCL55) were grown overnight in the presence of 0 or 1 mM CuCl₂ as indicated. Membrane fractions were transferred to a nitrocellulose membrane and probed with anti-FLAG IgG and detected with HRP-conjugated goat anti-mouse IgG in a Western immunoblot. Size markers are indicated at the side (kDa).

3.9 Mco confers copper tolerance to MRSA252

Under aerobic conditions, bacterial multicopper oxidases often contribute to a copper tolerant phenotype (Outten *et al.*, 2001; Sitthisak *et al.*, 2005; Rowland and Niederweis, 2013; Zapotoczna *et al.*, 2018; Williams *et al.*, 2020). It was hypothesised that deletion of *mco* would render MRSA252 more sensitive to copper. This was examined by analysing the growth of *S. aureus* on Tryptic Soy Agar supplemented with 6 mM CuCl₂ in both aerobic conditions and with 5% CO₂ at 37°C (Fig. 3.12).

MRSA252Δ*mco* grew poorly on TSA supplemented with CuCl₂ compared to the wild-type strain MRSA252, demonstrating that *mco* contributes to copper tolerance in MRSA252. Similarly to MRSA252Δ*mco*, the mutant carrying empty vector (MRSA252Δ*mco*::pCL55) grew weakly on medium supplemented with CuCl₂ compared to MRSA252. Copper tolerance was restored in MRSA252Δ*mco*::UCMF, indicating that the copper sensitive phenotype could be complemented and that 3X-FLAG tagged Mco is functional in *S. aureus* (Fig. 3.12). These phenotypes were observed both when bacteria were incubated aerobically and with 5% CO₂, suggesting enrichment with CO₂ does not affect the copper detoxification mechanism of Mco.

Deletion of the putative N-terminal signal peptide-containing region of Mco rendered the strain copper sensitive (Fig. 3.12). MRSA252Δ*mco*::UCMF McoΔ2-53 grew identically to MRSA252Δ*mco*, indicating that the signal peptide containing region of Mco is required for conferring copper tolerance. No difference in growth was detected between any strain in the absence of copper, indicating deletion or disruption of *mco* did not affect the growth phenotype of MRSA252 on TSA.

These data together indicate that *mco* contributes to the growth and resistance to copper of *S. aureus* in aerobic and CO₂ enriched conditions. The copper resistance phenotype was abolished upon deletion of the N-terminal region of Mco (amino acids 2-53), indicating it is required for Mco to confer copper tolerance.

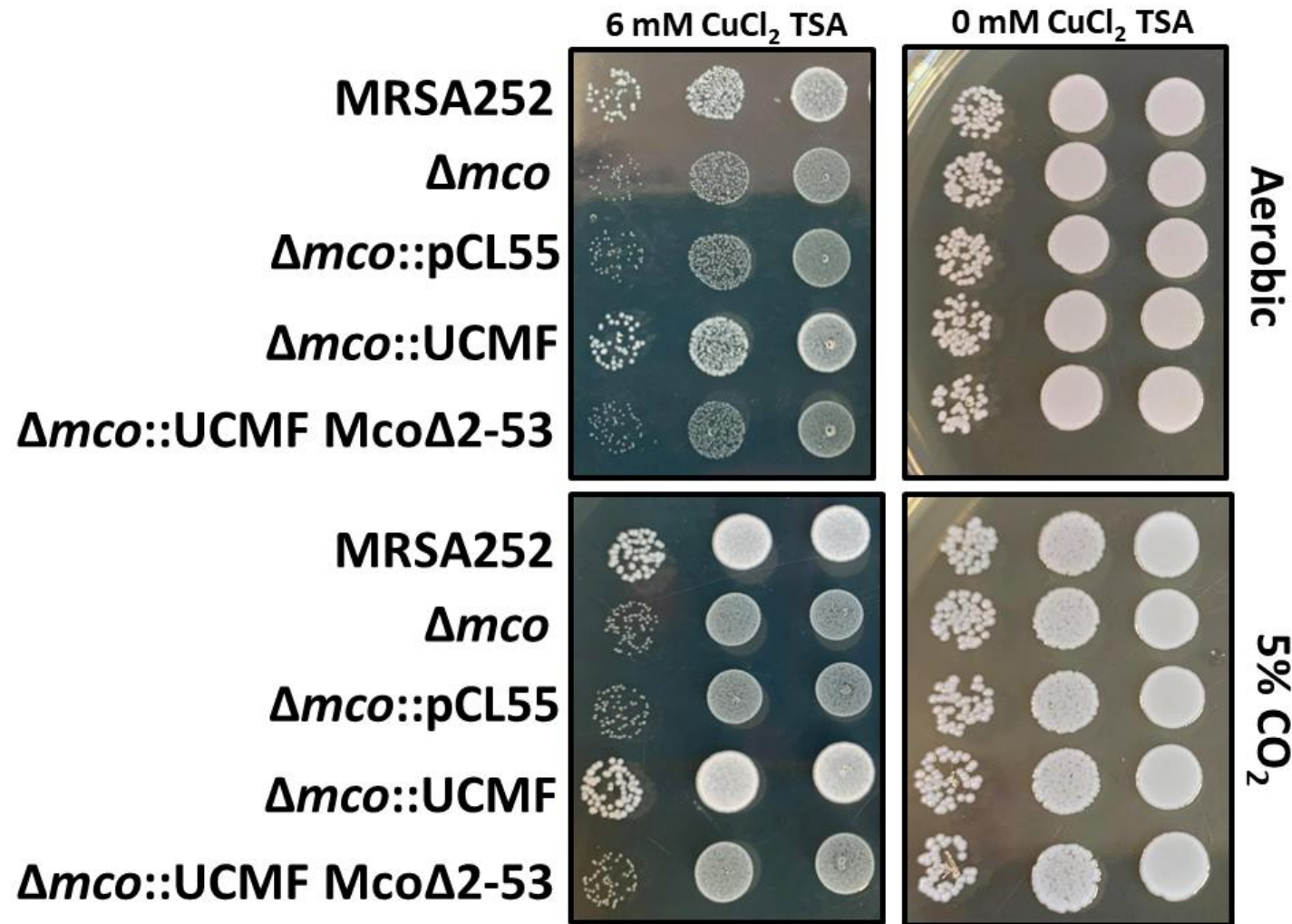


Figure 3.12 Mco contributes to copper tolerance in MRSA252.

Overnight cultures were washed in PBS and adjusted to an OD₆₀₀ of 3. 10-fold dilutions of the suspension were spotted onto TSA supplemented with CuCl₂ (6 mM) and incubated at 37°C aerobically, or in 5% CO₂. Data is representative of 3 independent biological replicates.

There was as distinct possibility that the 3X-FLAG tag disrupted the function of Mco3X-FLAG. If this was the case, then perhaps the second chromosomal copy of *copB* was responsible for the restoration of copper tolerance in MRSA252 Δ *mco*::pCL55::UCMF.

To control for this, the 3X-FLAG tag was deleted from pCL55::UCMF using inverse PCR to generate a version of pCL55 harbouring a construct named UpCopBMco (UCM). This plasmid was transformed into MRSA252 Δ *mco*, and its growth on agar supplemented with copper was monitored as described previously (Fig. 3.13). The UCM harbouring strain was able to complement the copper sensitive phenotype of the *mco* mutant exactly like the UCMF harbouring strain, indicating that the FLAG tag did not disrupt the copper detoxifying properties of Mco. MRSA252, Δ *mco*, UCMF Δ Mco2-53 were included as controls for comparison with MRSA252 Δ *mco*::pCL55::UCM. No difference in growth was detected for any strain when plated in the absence of copper, indicating that the transformation of MRSA252 Δ *mco* with pCL55 plasmids did not reduce its growth on TSA.

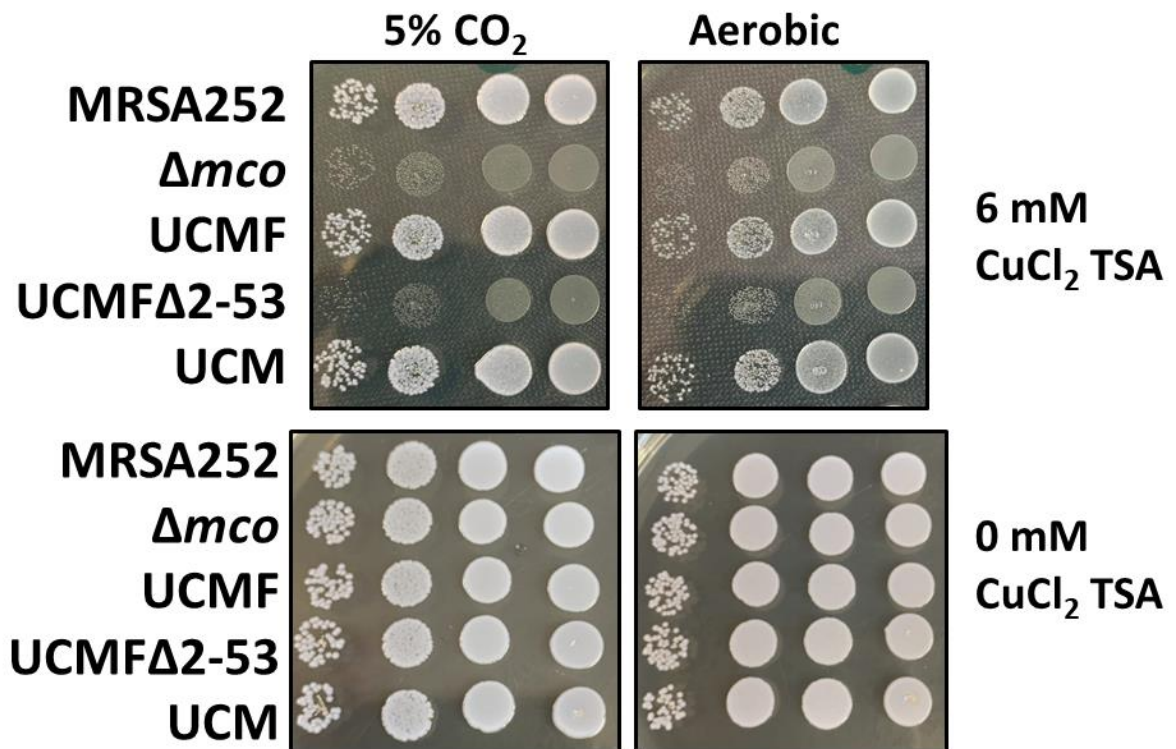


Figure 3.13. The C-terminal 3X-FLAG tag does not disrupt the function of Mco

Cells from overnight cultures were washed in PBS and adjusted to an OD₆₀₀ of 3. 10-fold serial dilutions of the suspension were spotted onto TSA supplemented with and without CuCl₂ (6 mM) and incubated at 37°C aerobically, or in 5% CO₂. Data is representative of 2 independent biological replicates.

3.10 Growth of *S. aureus* in copper supplemented anaerobic conditions

To determine if *mco* contributes to copper tolerance in anaerobic conditions, *S. aureus* was grown in an anaerobic jar on TSA supplemented with 0, 1, 2 and 4 mM CuCl₂ (Fig. 3.14).

Firstly, it was observed that none of the *S. aureus* strains were able to grow to form single colonies on TSA supplemented with ≥ 1 mM CuCl₂ under anaerobic conditions indicating an unexpected reduction in copper tolerance. Importantly, *S. aureus* grown on TSA without copper was able to form single colonies at the appropriate dilution (Fig. 3.14). This indicates that copper tolerance of *S. aureus* is reduced in anaerobic conditions.

Next, the level of sensitivity of *S. aureus* to copper under anaerobic conditions was examined by identifying the concentration that permitted the growth of single colonies (Fig. 3.15). The lowest concentration that resulted in single colony formation under anaerobic conditions was 0.05 mM CuCl₂ while no single colonies were detectable at 0.1 mM CuCl₂ or higher (Fig. 3.15).

Growth of *S. aureus* was detectable only at a high cell density. This growth was extremely poor in comparison to that in the absence of copper. This may indicate that if a large population density of *S. aureus* is present, it is more resistant to copper than less dense populations. This phenotype was only detected in anaerobic conditions.

Lastly, no difference in growth of *S. aureus* was detected when *mco* was deleted (Fig. 3.15), indicating that *mco* was unable to contribute to copper tolerance under anaerobic conditions (Fig. 3.15).



Figure 3.14 *S. aureus* is more sensitive to copper in anaerobic conditions

Overnight cultures were washed in PBS and adjusted to an OD₆₀₀ of 3. 10-fold serial dilutions of the suspension were spotted onto TSA supplemented with CuCl₂ and incubated at 37°C in an anaerobic jar. Data is representative of 3 independent biological replicates.

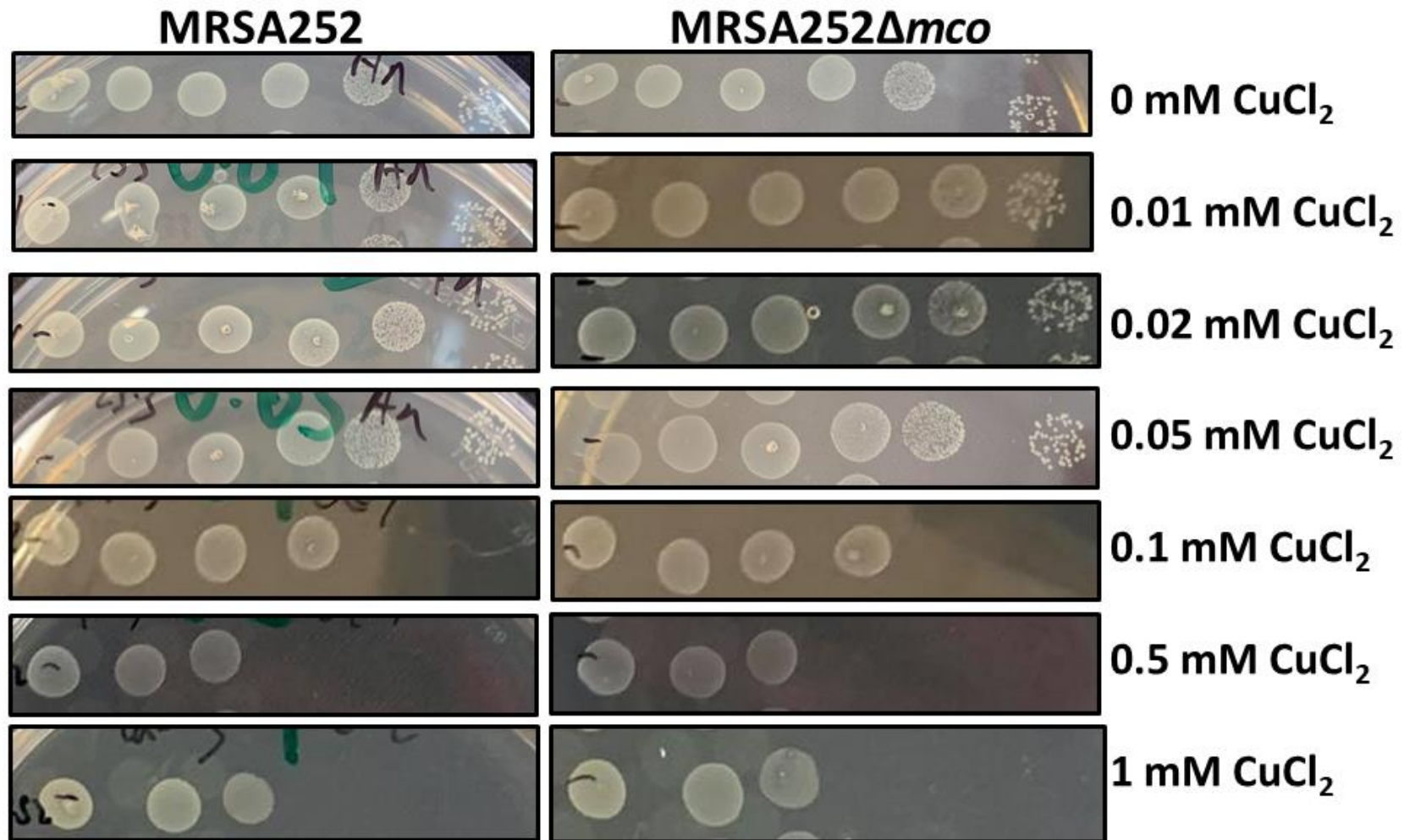


Figure 3.15 Growth of *S. aureus* on copper supplemented agar in anaerobic conditions

Overnight cultures were washed in PBS and adjusted to an OD₆₀₀ of 3. 10-fold serial dilutions of the suspension were spotted onto TSA supplemented with CuCl₂ and incubated at 37°C in an anaerobic jar. Data is representative of 3 independent biological replicates.

3.11 Growth of MRSA252 Δ *mco* in TSBd supplemented with copper.

Next, the growth of MRSA252 Δ *mco* in a nutrient rich liquid growth medium namely TSB (Difco, TSBd) supplemented with copper was analysed (Fig. 3.16). Bacteria from an overnight culture were adjusted to an OD₆₀₀ of 0.025 in TSBd incorporating the indicated concentration of CuCl₂.

Growth of MRSA252 was almost unaffected by CuCl₂ concentrations up to 0.5 mM under standard conditions involving a x/y dilution of a stationary phase starter culture. A defect in growth was detected at 1 mM CuCl₂, but MRSA252 was still able to achieve the same final maximum optical density as MRSA252 grown in the absence of copper. At concentrations of 2 and 4 mM however a greater attenuation in growth was observed, and the bacterium was unable to achieve the same optical density as the control after 22 hours. The maximum OD₆₀₀ was 0.8 and 0.4 respectively, compared to 1.55 in media without added copper (Fig. 3.16). This indicated that MRSA252 can grow normally in up to 0.5 mM CuCl₂ with little or no attenuation of growth. Also 1 mM could slow growth, but the same OD₆₀₀ as the control was eventually achieved after 22 hours.

Surprisingly, no difference in growth between MRSA252 and MRSA252 Δ *mco* at any of the concentrations tested was observed. Growth of MRSA252 Δ *mco* was unaffected at up to 0.5 mM CuCl₂, and was attenuated in a similar fashion to the wild type control at 1, 2 and 4 mM CuCl₂. This indicated that *mco* likely did not contribute to copper tolerance under in these conditions.

A large variation was detected at 1 and 2 mM CuCl₂. The error bars for both WT and *mco* mutant are relatively small in CuCl₂ concentrations up to 0.5 mM, but they widened considerably at 1 and 2 mM CuCl₂, and tightened again for 4 mM CuCl₂ (Fig. 3.16).

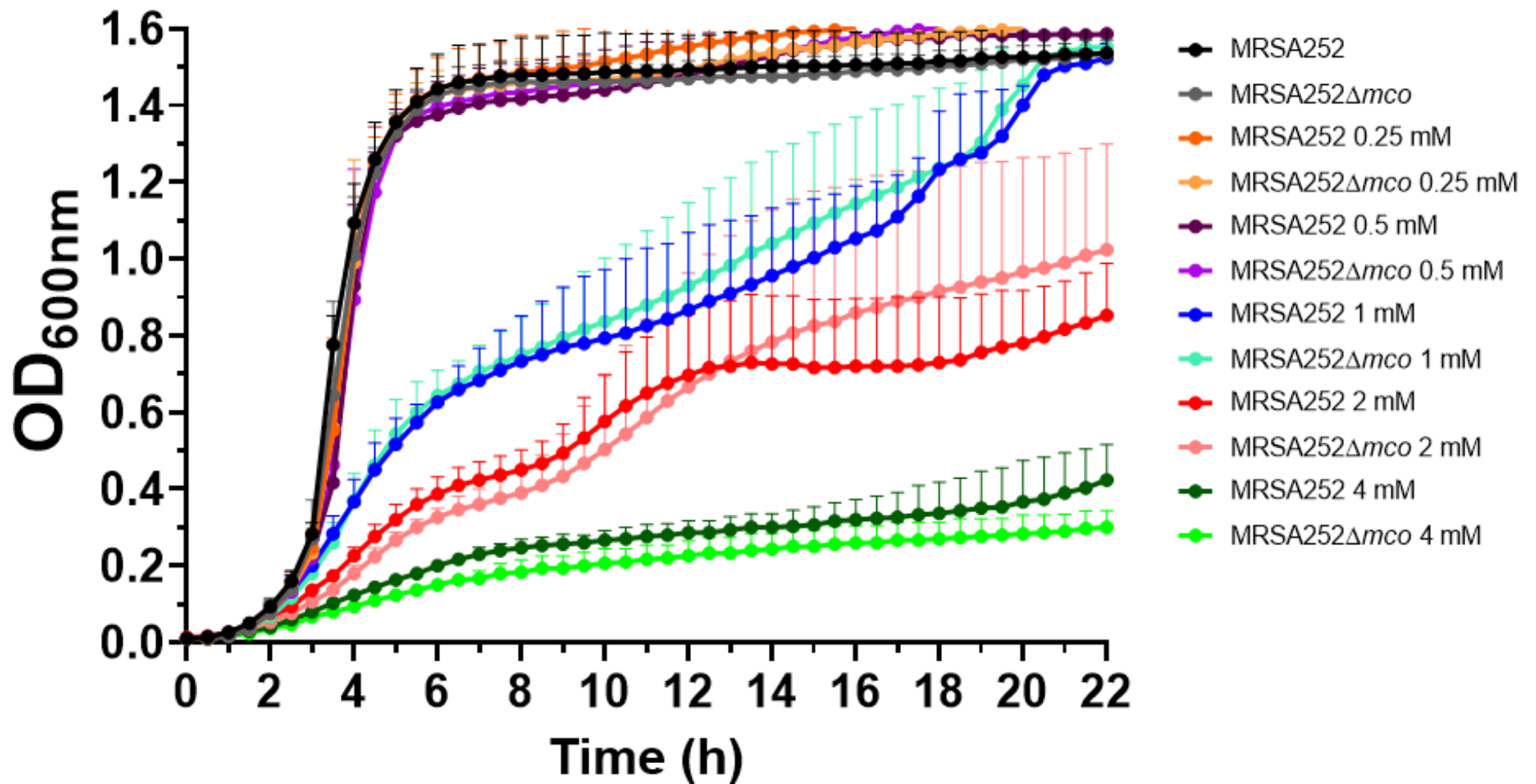


Figure 3.16. Growth of *S. aureus* in TSBd supplemented with copper

Growth of MRSA252 and MRSA252Δmco in TSBd supplemented with CuCl₂ (0, 0.25, 0.5, 1, 2 and 4 mM) was monitored for 22 hours. Error bars represent + standard deviation. n=3

3.12 Growth of MRSA252 Δ *mco* in RPMI supplemented with copper.

Copper tolerance levels might vary depending on the growth media. Generally, the more nutrient rich the media, the greater the concentration of copper the bacteria can withstand. Conversely bacteria are more sensitive to copper in nutrient poor media (Tarrant *et al.*, 2019). RPMI was chosen as a nutrient deficient medium because it had been used previously in *S. aureus* copper tolerance studies (Baker *et al.*, 2010; Purves *et al.*, 2018).

Growth of MRSA252 and MRSA252 Δ *mco* was compared in RPMI supplemented with copper (Fig. 3.17). Firstly, MRSA252 was much more sensitive to copper in RPMI than in TSBd. A defect in growth was detected in RPMI at 6.25 μ M CuCl₂ (Fig. 3.17A), while a defect was only detected at 1 mM and above in TSBd (Fig. 3.16). This indicates that MRSA252 is 160-times more sensitive to copper when grown in RPMI compared to TSBd, highlighting the importance of nutrient availability for *S. aureus* to detoxify copper.

Next, the growth of MRSA252 and MRSA252 Δ *mco* was compared (Fig. 3.17A). There was little difference in the growth of MRSA252 and MRSA252 Δ *mco* in the absence of copper. However the variation and resulting error bars in these conditions are larger than was observed when *S. aureus* was grown in TSBd. No significant difference in growth was detected at 6.25 μ M between MRSA252 and MRSA252 Δ *mco*. A significant growth defect was detected at 12.5 μ M, where MRSA252 grew noticeably better than MRSA252 Δ *mco* between hours 8 and 15. However the growth of MRSA252 Δ *mco* recovered in a similar fashion to MRSA252 by 22 h. Similarly, growth of MRSA252 Δ *mco* was attenuated when compared to MRSA252 at 100 μ M CuCl₂, as it grew more slowly than MRSA252 and achieved a lower maximum optical density (0.2 vs 0.4).

Growth of both MRSA252 and MRSA252 Δ *mco* was heavily reduced by the presence of 100 μ M CuCl₂ in RPMI. However the attenuation of growth was more severe for the *mco* mutant, suggesting that Mco provides an advantage to growth of *S. aureus* in nutrient restricted conditions (Fig. 3.17A).

The growth of MRSA252 and MRSA252 Δ *mco* in static conditions in the presence of 5% CO₂ was monitored (Fig. 3.17B and C). A significant difference in

growth was detected between MRSA252 and MRSA252 Δ *mco* after 8 hours of growth in the presence of 100 μ M CuCl₂ (Fig. 3.17B). No significant difference was detected at 0, 6.25 or 25 μ M CuCl₂. No significant difference was detected between the growth of MRSA252 and MRSA252 Δ *mco* after 24 hours of growth with 0, 6.25, 25 or 100 μ M CuCl₂ (Fig. 3.17C).

In summary, a defect in growth of MRSA252 Δ *mco* compared to MRSA252 can be detected in RPMI with aeration in the absence of CO₂ supplementation at 25 and 100 μ M CuCl₂ (Fig. 3.17A). In contrast in CO₂ supplementation without aeration (static conditions), MRSA252 Δ *mco* achieved a lower optical density than MRSA252 after 8 hours of growth, but this attenuation recovered after 24 hours (Fig. 3.17B+C).

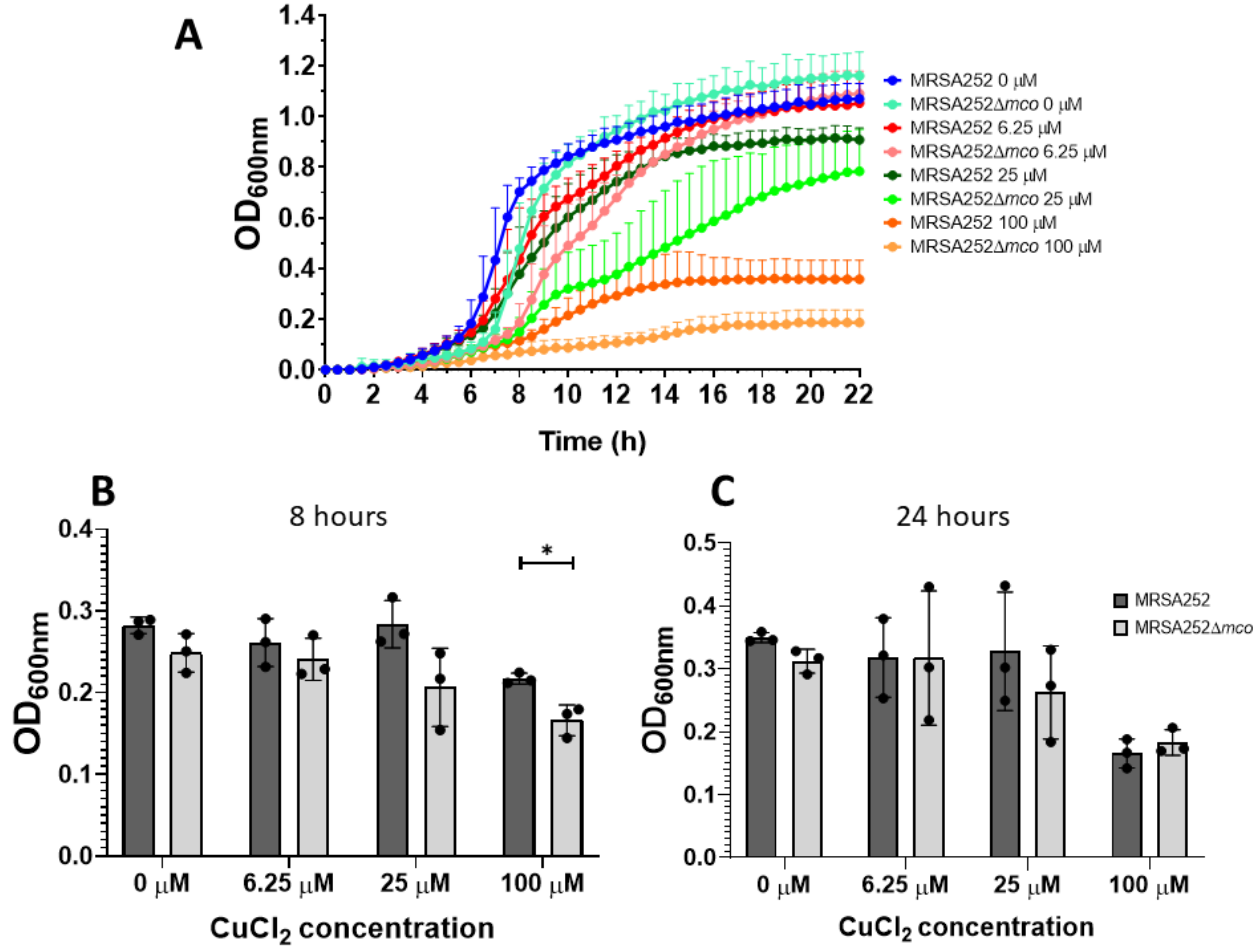


Figure 3.17. Growth of MRSA252 Δmco in RPMI

Growth of MRSA252 and MRSA252 Δmco in RPMI supplemented with CuCl₂ (0, 6.25, 25, and 100 μM) at 37°C with orbital shaking was monitored for 22 h (A). Growth of MRSA252 and MRSA252 Δmco in RPMI supplemented with CuCl₂ (0, 6.25, 25, and 100 μM) at 37°C in static conditions with 5% CO₂ was monitored (B+C). Error bars represent + standard deviation. Significance was determined by multiple T-tests comparing MRSA252 to MRSA252 Δmco at each time point and copper concentration. *, $P < 0.05$. $n=3$.

3.13 Generation of reporter protein expression constructs

Having established that residues 2-53 were not necessary for membrane localisation of Mco (Fig. 3.10A), but were required for proper functioning of Mco in copper tolerance (Fig. 3.12), the importance of the N-terminal region of Mco in the protein's export to the membrane was investigated.

To determine if Mco harboured an N-terminal signal peptide, a plasmid expressing a chimaeric protein where residues 1-56 of Mco were fused to the D3D4 domains of the Sbi protein was constructed. Sbi is an *S. aureus* protein that harbours an N-terminal Sec signal sequence and is normally found both in the culture supernatant and associated with the cytoplasmic membrane (Smith *et al.*, 2011). It was used previously as reporter protein for investigating sorting signal activity (O'Halloran, Wynne and Geoghegan, 2015).

Plasmid pRMC2 was chosen as for expression of D3D4 constructs because the promoter upstream of the MCS is strongly repressed in the absence of the inducing agent anhydrotetracycline (ATc) (Corrigan and Foster, 2009). LAC *spa sbi* was chosen as the host strain because it lacks immunoglobulin binding proteins protein A (*spa*), and the second immunoglobulin-binding protein of *S. aureus* (*sbi*) which interfere with interpretation of data when fractions are probed by Western immunoblotting.

In order to determine if residues 1-56 and 1-26 of Mco contain a signal peptide, fusion proteins were generated where the putative signal sequence was fused to Sbi D3D4.

Primers Mco1-56 SLIC F and R were used to amplify Mco1-56 and include overhangs with homology to the beginning of the D3D4 encoding region of Sbi and the pRMC2 MCS (Fig. 3.18A). The PCR amplicon was 168 bp (Fig. 3.18B). The plasmid pRMC2::D3D4WTSP was used as template to generate pRMC2::D3D4::NoSP by inverse PCR using primers pRMC2 SS delete F and R (Fig. 3.17C). The PCR amplicon was the expected size of 6.8 kb (Fig. 3.18D). The Mco1-56 amplicon was inserted into the linearised pRMC2::D3D4::NoSP using SLIC to generate pRMC2::D3D4Mco1-56 (Fig. 3.18E). In addition, blunt end ligation was used to close the linearised pRMC2::D3D4::NoSP resulting in a control plasmid

pRMC2::D3D4::NoSP that harboured D3D4 with no signal peptide. *E. coli* host IM08B was transformed with plasmids pRMC2::D3D4::WTSP, pRMC2::D3D4Mco1-56 and pRMC2::D3D4::NoSP. A colony screen was performed on three transformants of each (Fig. 3.18F). Clone A of WT SP, clone C of Mco1-56, and clone A of No SP amplified PCR amplimers of the expected lengths. Plasmids from these clones were purified, confirmed by DNA sequencing (data not shown) and transformed into LAC* *spa sbi*.

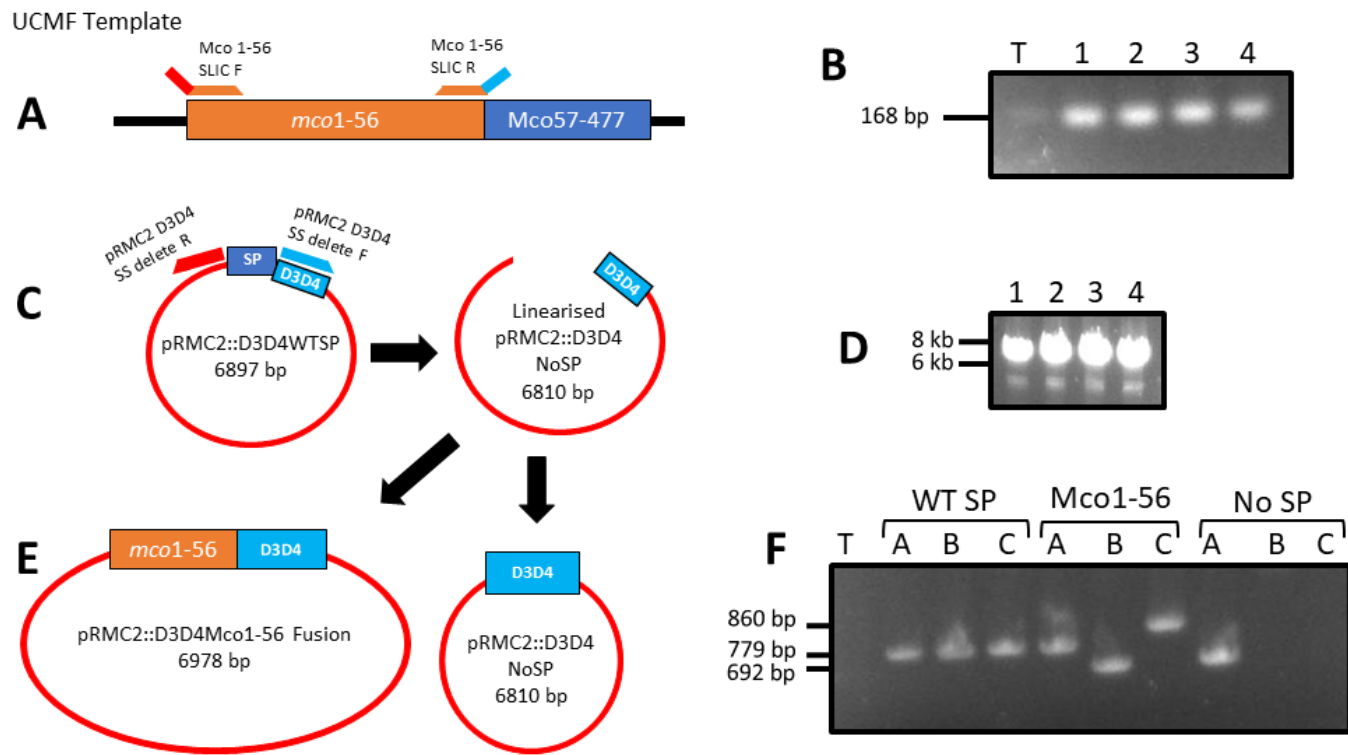


Figure 3.18. Generation of pRMC2::D3D4::Mco1-56, WTSP and NoSP

- (A) Schematic diagram of amplification of *mco1-56* using primers Mco1-56 SLIC F and R.
- (B) Agarose gel of four PCR amplimers of *mco1-56*. T = no template control PCR reaction.
- (C) Schematic diagram of deletion of the native Sbi signal peptide (SP) region present in pRMC2::D3D4WTSP by inverse PCR.
- (D) Agarose gel of four PCR amplimers of deletion of the Sbi SP present in pRMC2::D3D4WTSP, resulting in linear pRMC2::D3D4NoSP
- (E) Schematic diagram of pRMC2::D3D4Mco1-56 which was generated by inserting the Mco1-56 amplimer into the MCS of pRMC2 by SLIC. The plasmid pRMC2::D3D4NoSP was also generated, but by blunt end ligation of the linearised pRMC2::D3D4NoSP.
- (F) Agarose gel of colony screen of three putative IM08B clones of each plasmid construct pRMC2::D3D4WTSP, pRMC2::D3D4Mco1-56 and pRMC2::D3D4NoSP. T = no template control PCR reaction.

3.14 Residues 1-56 of Mco contains a cleavable signal peptide that delivers a reporter protein to the supernatant

Generating a fusion protein allowed investigation of the requirement of the N-terminal region of Mco for protein targeting to the membrane. LAC *spa sbi* harbouring pRMC2 expressing D3D4 with no signal peptide, D3D4 with the native Sbi signal peptide, and D3D4 harbouring the Mco1-56 putative signal peptide containing region were supplemented with ATc were grown for 18 h and fractionated to the four cellular compartments namely supernatant, cell wall, cytoplasmic membranes and cytoplasm. Fractions were analysed by Western immunoblotting by probing with anti-D3D4 IgG (Fig. 19A).

A very strong band representing SbiD3D4Mco1-56 was present in the supernatant fraction of *S. aureus*, along with much weaker bands in the cell wall and membrane fractions (Fig. 19A) showing that the majority of the protein is located in the supernatant. Densitometric analysis of relative band intensity indicated that the cell wall and membrane fractions contained approximately 4 and 10% of the protein compared to the supernatant fraction respectively (Fig. 3.19A). This demonstrates that Mco1-56 contains a signal peptide capable of delivering a reporter protein to the supernatant.

The band representing SbiD3D4Mco1-56 in the membrane fraction migrated with a higher apparent molecular weight than the most prominent band found in the supernatant fraction suggesting that SbiD3D4Mco1-56 harbours a cleavable signal peptide. A band corresponding to the putative precursor protein was also apparent in the supernatant. The faint band isolated in the cell wall fraction is the size of the putative mature processed form.

Immunoreactive SbiD3D4 protein was not detected in any fraction of the strain expressing SbiD3D4 with no signal peptide. This indicates that the protein was either not translated or is highly unstable and rapidly degraded. In the strain harbouring SbiD3D4 with its native Sec signal peptide, a band was detected only in the supernatant fraction. Sbi is non-covalently bound to lipoteichoic acid, but the D3D4 domains of Sbi lack the lipoteichoic acid binding region, hence SbiD3D4 was only found in the supernatant.

As a control for the purity of the membrane fraction, samples were probed with anti-EbpS IgG (Fig. 19B). EbpS was detected primarily in the membrane fractions, with a small amount in the cell wall and cytoplasmic fractions. Densitometric analysis determined that only 2-5% EbpS was present in the cell wall and cytoplasmic fractions compared to the membrane fraction, indicating that contamination of these fractions was low.

As a supernatant fraction purity control, fractions were probed with anti-V8 protease IgG (Fig. 19C). V8 protease was detected primarily in the supernatant fractions which demonstrated their integrity.

Expression SbiD3D4 was maximal at 312.5 ng/ml of ATc. To determine if membrane or supernatant localisation was a result of over expression of pRMC2::D3D4Mco1-56, cultures were grown in the presence of 0, 78.125, 156.25 and 312.5 ng/ml ATc and fractionated as described previously. Supernatant and membrane fractions were probed for D3D4 with anti-D3D4 IgG (Fig. 3.19D). A dose-dependent reduction in band strength was observed for D3D4Mco1-56 in both the membrane and supernatant fractions in response to a reduction in ATc concentration. This indicated that expression of D3D4Mco1-56 was regulated by ATc induction. Densitometric analysis indicated that 6-15% of D3D4Mco1-56 was present in the membrane fraction compared to the supernatant. This suggests that Mco1-56 primarily delivers SbiD3D4 to the supernatant.

In summary, these data show that there is a cleavable signal peptide capable of delivery of a reporter protein to the culture supernatant located within the first 56 amino acids of Mco.

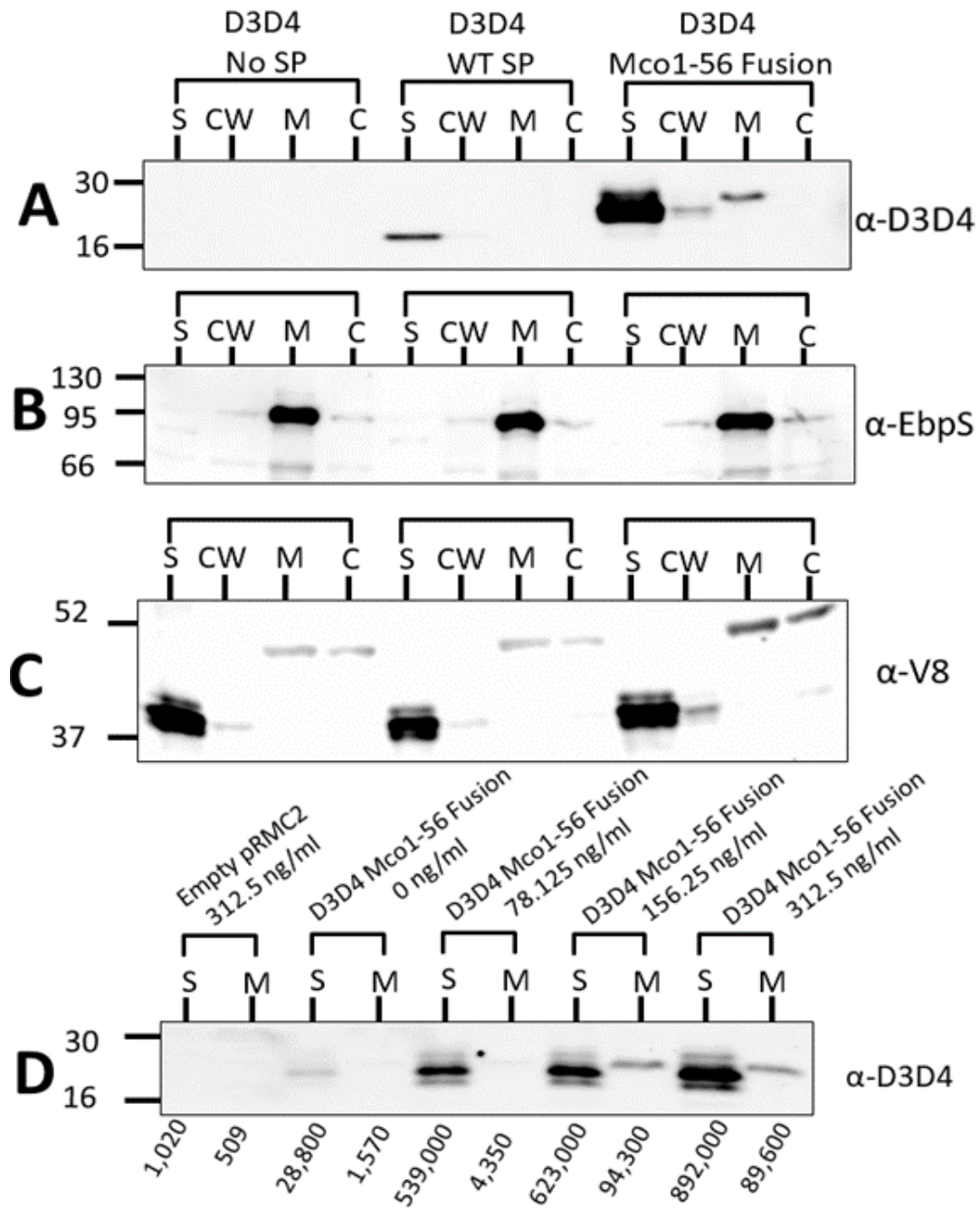


Figure 3.19. Mco1-56 transports D3D4 to the supernatant
 Subcellular fractions of LAC *spa sbi* harbouring pRMC2::D3D4NoSP (D3D4 No SP), pRMC2::D3D4WTSP (D3D4 WT SP) and pRMC2::D3D4Mco1-56fusion, (D3D4 Mco1-56 Fusion) were separated by SDS-PAGE (12.5% acrylamide), transferred to a nitrocellulose membrane and probed with a rabbit anti-D3D4 (A), rabbit anti-EbpS (B), and rabbit anti-V8 (C) sera. Antibody bound proteins were detected with HRP-conjugated goat anti-mouse IgG (A), or protein-A peroxidase (B+C). LACΔ*spa sbi* harbouring empty pRMC2 or D3D4 Mco1-56 Fusion were grown with doubling concentrations of the inducing agent ATc and supernatant and membrane fractions were probed for SbiD3D4 with arbitrary densitometric values for each band shown underneath (D). Size markers are indicated at the side (kDa). S = supernatant, CW = cell wall, M = membrane, C = cytoplasm. Blots (A-C) are representative of data obtained from 2 independent biological experiments. Blot (D) is from a single experiment performed just once.

3.15 Generation of pRMC2::D3D4Mco1-26 and pRMC2::D3D4Mco27-56

The data described above suggests that Mco1-56 contains a cleavable secretory signal peptide. Next, further refinement of this hypothesis was performed to confirm that the signal peptide prediction software SignalP 6.0 was correct in suggesting that Mco1-26 contained the signal sequence (Fig. 3.2B).

Two additional plasmids were constructed: pRMC2::D3D4Mco1-26 and pRMC2::D3D4Mco27-56. This was accomplished by inverse PCR using pRMC2::D3D4Mco1-56 as the template and deleting DNA encoding residues 27-56 and 2-26 using primer pairs Mco27-56 del F and R, and Mco 2-26 del F and R, respectively (Fig. 3.20A). The cloning strategy employed left the putative translational start codon intact which is indicated with a grey box labelled 'Mco1' in Fig. 3.20A.

The PCR amplimers of linearised pRMC2::D3D4Mco1-26 (Fig. 3.19B) and pRMC2::D3D4Mco27-56 (Fig. 3.20C) were ligated by blunt end ligation and the resulting DNA transformed into IM08B. Four Cm^R clones of each were chosen for colony PCR using the pRMC2 MCS F and R primers (Fig. 3.20D). Clone 2 exhibited a band of the desired length indicating successful generation of pRMC2::D3D4Mco1-26 and clones 2 and 3 were of the correct size for pRMC2::D3D4Mco27-56. The integrity of these plasmids was confirmed by DNA sequencing before transforming *S. aureus* LAC* *spa sbi* with purified plasmid.

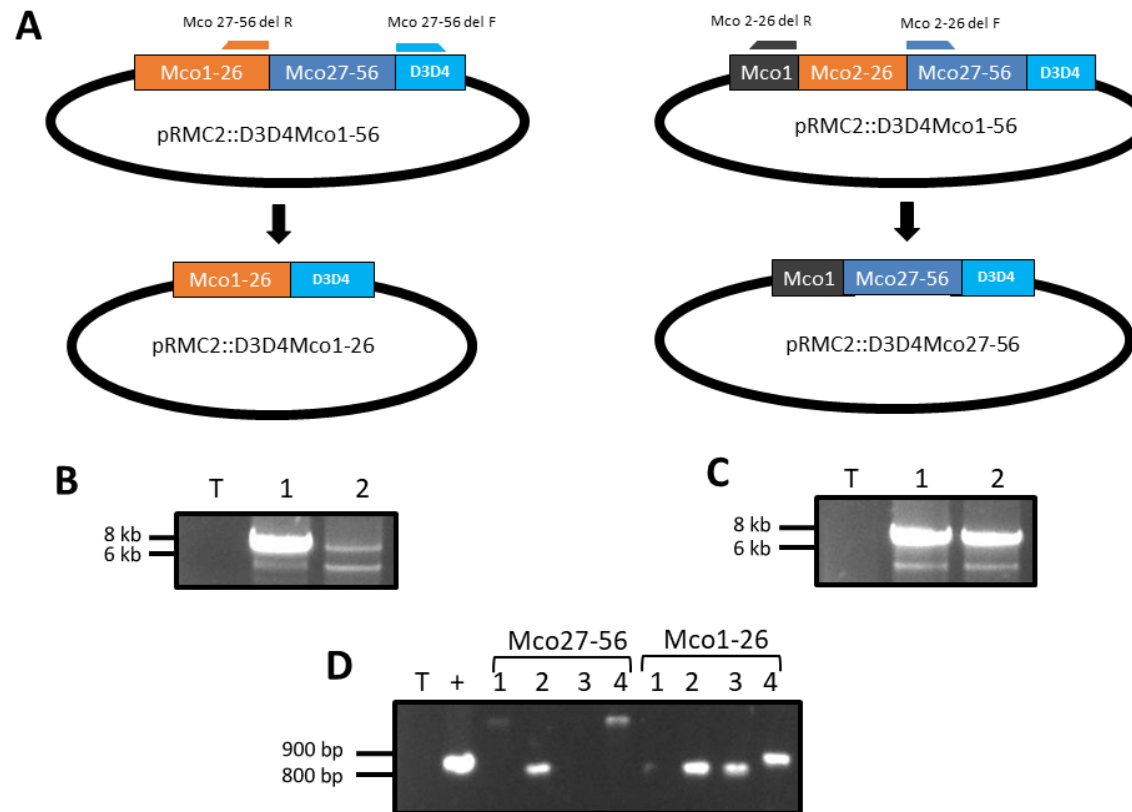


Figure 3.20. Design and Generation of pRMC2::D3D4Mco1-26 and pRMC2::D3D4Mco27-56.

(A) Schematic diagram demonstrating the cloning strategy employed to remove Mco27-56 to generate pRMC2::D3D4Mco1-26, and Mco2-26 to generate pRMC2::D3D4Mco27-56. This is not drawn to scale. The start codon of Mco (Mco1) is included in diagram of pRMC2::D3D4Mco27-56 to indicate the start codon was left intact as a part of the cloning strategy. (B) Agarose gel of Inverse PCR of pRMC2::D3D4Mco1-56 using primers to delete residues 27-56 of Mco1-56. (C) Agarose gel of Inverse PCR of pRMC2::D3D4Mco1-56 using primers to delete residues 2-26 of Mco1-56. (D) Agarose gel of colony screen using pRMC2 MCS primers on four putative IM08B clones of each pRMC2::D3D4Mco27-56 and pRMC2::D3D4Mco1-26. Clone 2, and clone 2 and 3 exhibit bands of the expected amplicer length indicative of pRMC2::D3D4Mco27-56 and pRMC2::D3D4Mco1-26 respectively. T = no template control PCR reaction, + = positive control of pRMC2::D3D4Mco1-56.

3.16 Mco1-26 contains a cleavable secretory signal sequence

To determine if residues 1-26 of Mco are sufficient for secretion of D3D4, cells expressing a variant of D3D4 fused to Mco1-56, Mco1-26 and Mco27-56 were fractionated and probed for D3D4 by Western immunoblotting using anti-D3D4 IgG (Fig. 3.21A).

D3D4Mco1-26 had a lower molecular weight compared to D3D4Mco1-56. The majority of the D3D4Mco1-26 protein was detected in the supernatant with faint bands in the cell wall and membrane fractions, in a similar manner to D3D4Mco1-56 (Fig. 3.21A). The faint bands are slightly larger than that present in the supernatant, suggesting that un-cleaved D3D4Mco1-26 remained in the membrane, in a similar fashion to D3D4Mco1-56.

No immunoreactive bands were present in any fraction from the D3D4Mco27-56 construct (Fig. 3.21A), in a similar fashion to D3D4 t lacking a signal peptide (Fig. 3.19A).

These data indicate that residues 1-26 are necessary and sufficient for protein export, because that deletion of residues 2-26 (D3D4Mco27-56) abolished secretion.

The controls with anti-EbpS and anti-V8 protease IgG (Fig. 3.21B and C) demonstrated the integrity and purity of the membrane and supernatant fractions as in previous experiments.

In conclusion, Mco1-26 contains a cleavable secretory signal sequence that can deliver a reporter protein to the supernatant of *S. aureus*.

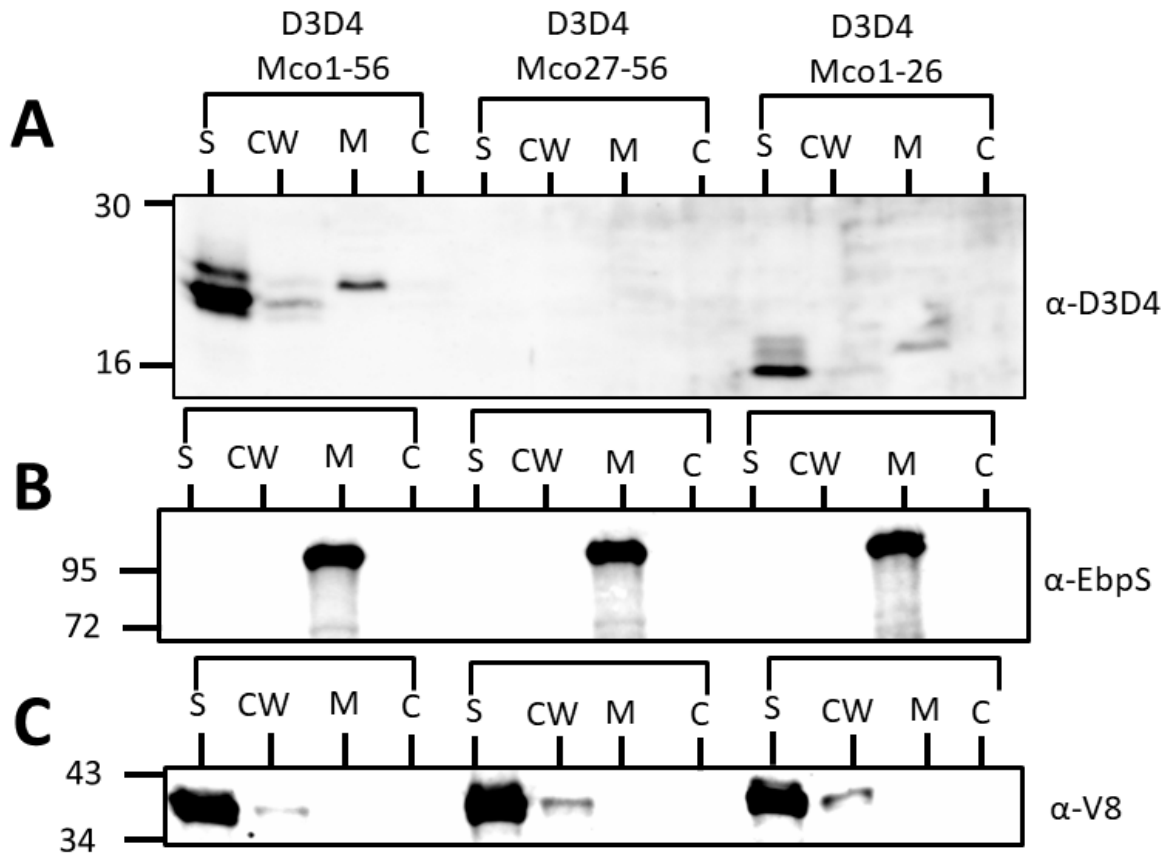


Figure 3.21. Mco1-26 contains a supernatant localising signal peptide
 Subcellular fractions of LAC *spa sbi* harbouring pRMC2::D3D4Mco1-56 (D3D4 Mco1-56), pRMC2:: D3D4Mco27-56 (D3D4 Mco27-56) and pRMC2::D3D4Mco1-26 (D3D4 Mco1-26) were separated by SDS-PAGE (12.5% acrylamide), transferred to a nitrocellulose membrane, and probed with rabbit anti-D3D4 IgG (A), rabbit anti-EbpS IgG (B), or rabbit anti-V8 IgG (C). Antibody bound proteins were detected with protein-A peroxidase (A-C). Size markers are indicated at the side (kDa). S = supernatant, CW = cell wall, M = membrane, C = cytoplasm. Blots are representative of data obtained from 2 independent experiments.

3.17 Mco residues 1-26 do not direct protein secretion through the TatAC pathway

The data presented above suggests that residues 1-26 of Mco directs protein export through the Sec pathway (Fig. 3.2B). However, the well characterised bacterial multicopper oxidases in other bacterial genera contain a canonical twin-arginine motif and are translocated by the Tat pathway.

The closest homologue of Mco is CueO from *E. coli*. This contains a twin arginine motif and is translocated by the TatABC system. Mco has two lysines at the position where two arginines occur in other TatAC translocated protein in *S. aureus* (Biswas *et al.*, 2009; Frain, Robinson and van Dijk, 2019).

Despite the lack of a twin-arginine motif at the N-terminus of the Mco precursor protein (Fig. 3.1) it was decided to investigate if twin lysines at positions 3 and 4 (K₃K₄) can function in place of the 'RR' motif in Tat transport, as has been described for a Tat substrate in *E. coli* (Kreutzenbeck *et al.*, 2007). Substitution of 'KK' with 'KQ' in the signal peptide prevented Tat transport in *E. coli* (Kreutzenbeck *et al.*, 2007). A K4Q substitution was generated in both pRMC2::D3D4::Mco1-56 and pRMC2::D3D4::Mco1-26. Cells were fractionated as above and probed with anti-D3D4 IgG by Western immunoblotting (Fig. 3.22).

The K4Q substitution did not affect secretion of D3D4 fused to Mco1-56 because immunoreactive bands were present in the supernatant and membrane fractions in a similar fashion to the parental construct (Fig. 3.22A). In contrast the V8 protease control was detected predominately in the supernatant (Fig. 3.22B).

Similarly, the K4Q substitution did not prevent secretion of D3D4 fused to Mco1-26, as D3D4Mco1-26 and D3D4Mco1-26 KQ immunoreactive bands were present in the supernatant and membrane fractions (Fig. 3.22C). Again the V8 protease control was detected predominately in the supernatant (Fig. 3.22D).

These data indicate that a K4Q substitution within the Mco signal sequence did not prevent secretion or cleavage by signal peptidase.

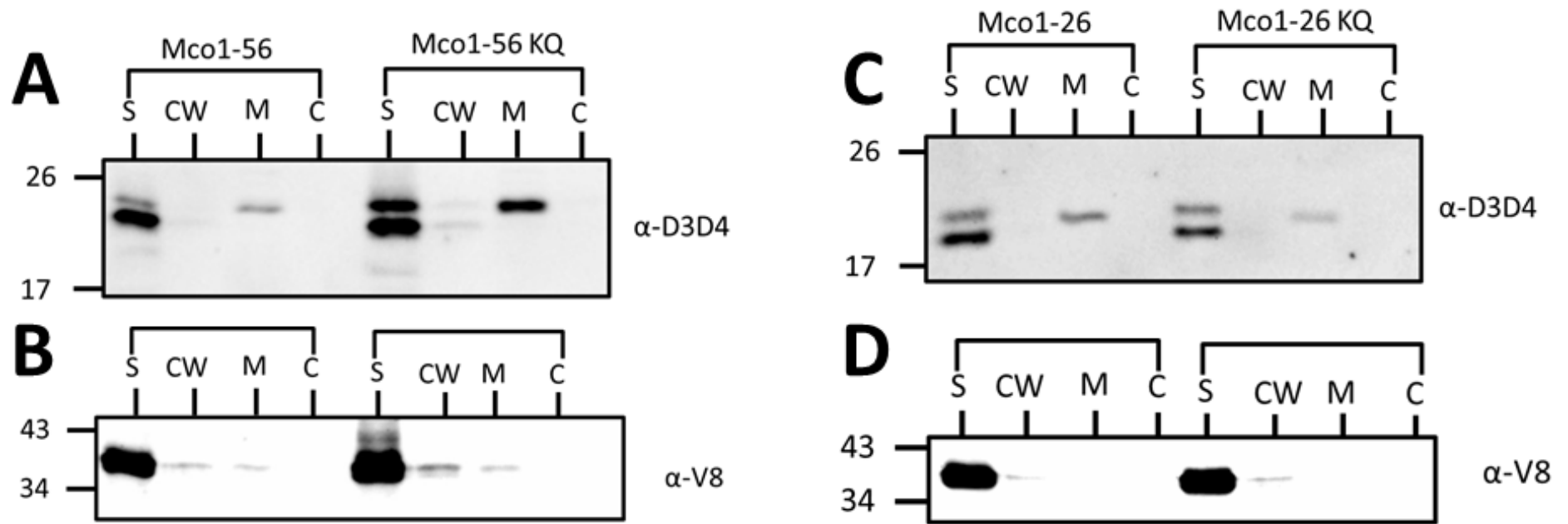


Figure 3.22. KK-KQ substitution of Mco signal peptide does not affect secretion of the reporter protein

Subcellular fractions of LAC *spa sbi* harbouring pRMC2::D3D4Mco1-56 (Mco1-56) and pRMC2::D3D4Mco1-56 KQ (Mco1-56 KQ), pRMC2::D3D4Mco1-26 (Mco1-26) and pRMC2::D3D4Mco1-26 KQ (Mco1-26 KQ) were separated by SDS-PAGE (12.5% acrylamide), transferred to a nitrocellulose membrane and probed with rabbit anti-D3D4 IgG (A+C) and rabbit anti-V8 IgG (B+D). Antibody bound proteins were detected with protein-A peroxidase (A-D). Size markers are indicated at the side (kDa). S = supernatant, CW = Cell wall, M = membrane, C = cytoplasm. Blots are representative of data obtained from 2 independent experiments.

Although the data presented in Fig. 3.22 suggest that Mco1-26 is not translocated by the TatAC system, the possibility could not be excluded that the Tat system of *S. aureus* has slightly different signal peptide requirements to that of *E. coli*. To determine if the Mco signal peptide directed export through the Tat pathway in *S. aureus*, a *tatAC* deletion mutant was generated in LAC *spa sbi* forming LAC *spa sbi* Δ *tatAC*. The construct expressing D3D4Mco1-56 was introduced into the mutant and each of the four cellular compartments were analysed by Western immunoblotting probing with anti-D3D4 IgG (Fig. 3.23A).

Immunoreactive bands were present in the supernatant fractions of both LAC *spa sbi* and LAC *spa sbi* Δ *tatAC* (Fig. 3.23A) indicating that export of the fusion protein did not rely on a functional TatAC system. A faint band was observed in the membrane fractions of both LAC *spa sbi* and LAC *spa sbi* Δ *tatAC*, indicative of the un-cleaved form of D3D4Mco1-56 similar that observed in Fig. 3.23A. This suggests that residues 1-56 of Mco are sufficient to mediate protein export in a TatAC-independent manner.

As before these fractions were probed with anti-EbpS IgG and anti-V8 protease IgG (Fig. 3.23B and C). EbpS was detected only in the membrane fractions, while V8 was detected only in the supernatant fractions, demonstrating their purity and integrity.

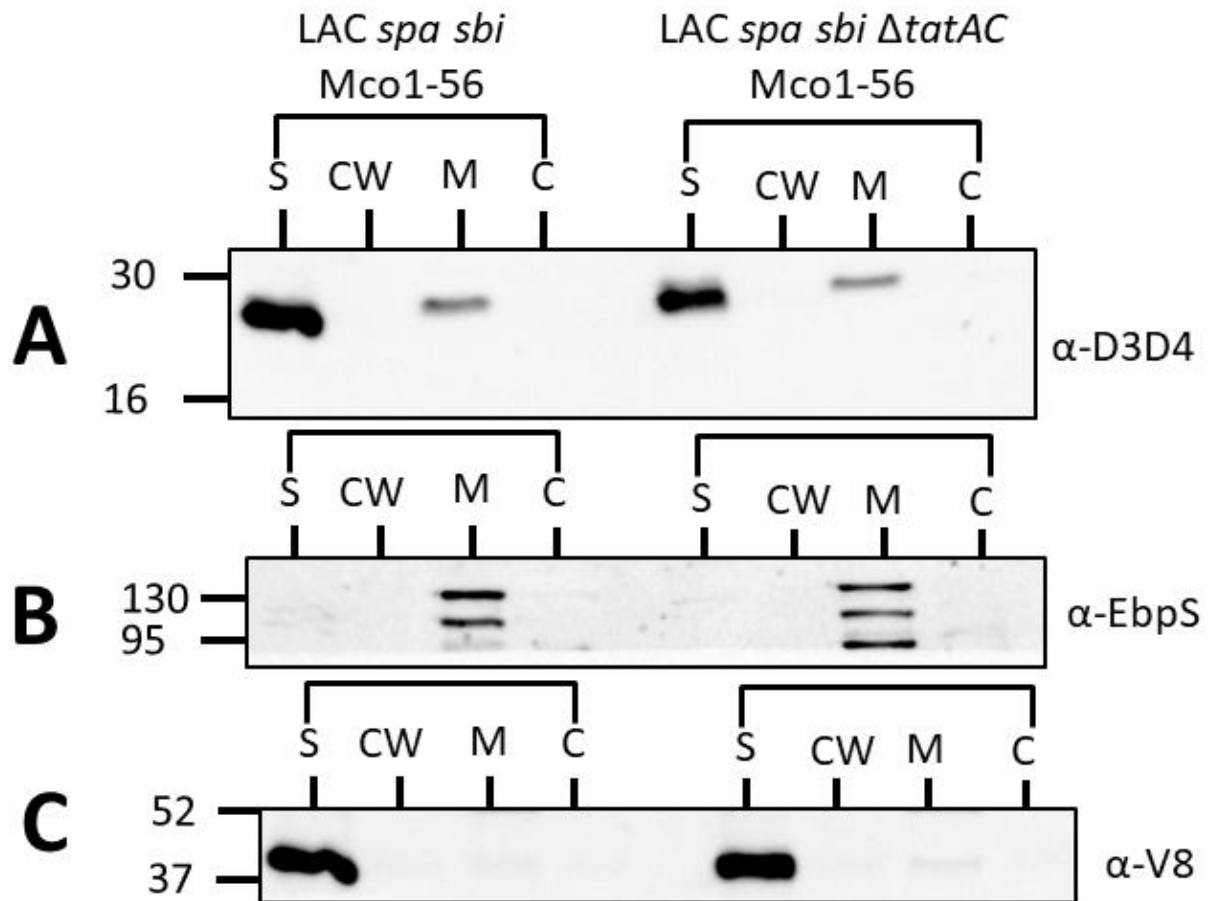


Figure 3.23 Deletion of *tatAC* from *S. aureus* does not affect Mco signal peptide delivery of reporter protein to the supernatant

Subcellular fractions of LAC *spa sbi* harbouring pRMC2::D3D4Mco1-56 (LAC *spa sbi* Mco1-56) and LAC *spa sbi* Δ *tatAC* harbouring pRMC2::D3D4Mco1-56 (LAC *spa sbi* Δ *tatAC* Mco1-56) were separated by SDS-PAGE (12.5% acrylamide), transferred to a nitrocellulose membrane, and probed with rabbit anti-D3D4 IgG (A), rabbit anti-EbpS IgG (B), and rabbit anti-V8 IgG (C). Antibody bound proteins were detected with protein-A peroxidase (A, B+C). Size markers are indicated at the side (kDa). S = supernatant, CW = Cell wall, M = membrane, C = cytoplasm. Blots are representative of data obtained from 2 independent experiments.

3.18 Discussion

This study showed that Mco is a membrane located protein in *S. aureus* and that it does not require the N-terminal residues Mco2-53 for membrane localisation (Fig. 3.10). It was found that residues 1-56 of Mco are unique to the *S. aureus* Mco protein when compared to *E. coli* CueO, that Mco lacks the methionine rich region present in CueO, and that the copper ligand binding domains are fully conserved between Mco and CueO (Fig. 3.1). An isogenic *mco* deletion mutant was more sensitive to copper than the wild-type when plated on TSA containing copper, and this defect was complemented by a vector expressing Mco3X-FLAG under control of its native copper inducible promoter. Truncation of the novel N-terminal region of Mco rendered *S. aureus* sensitive to copper similar to an *mco* deletion mutant, indicating that the N-terminal region of Mco is essential for copper tolerance (Fig. 3.12). Mco contributed to copper tolerance in aerobic and 5% CO₂ conditions (Fig. 3.12), but not anaerobic conditions (Fig. 3.14 and 3.15). Furthermore, Mco1-26 contains a cleavable secretory signal sequence that delivers a reporter protein to the culture supernatant (Fig. 3.20). This signal peptide was not recognized by the TatAC system of *S. aureus* because substitution of the 'KK' motif to 'KQ' did not prevent secretion of the reporter protein (Fig. 3.22). Also Mco1-56 mediated export of a reporter protein to the supernatant was not impaired by deletion of *tatAC* in *S. aureus* (Fig. 3.23). These data indicate that Mco1-26 does not contain a Tat signal peptide which is consistent with the data indicating that it is a Sec dependent signal sequence. This represents the first bacterial multicopper oxidase that is not trafficked through the Twin-arginine translocation system.

Signal peptides are typically responsible for localisation of proteins to a specific cellular compartment (Freudl, 2018). In this study, a signal peptide was detected in Mco. However it did not deliver Mco to the supernatant as occurred with the reporter protein SbiD3D4. The reason for this is likely to be the inherent characteristics of the Mco protein which results in its integration into the membrane. Mco exhibits properties typical of membrane proteins. 15.5% of the residues of Mco are lysines. Given the electrochemical negativity of membranes, positively charged lysines can result in proteins being integrated into the membrane. Mco contains many hydrophobic residues which also encourage integration into the phospholipid

membrane. Membrane proteins often have hydrophobic residues flanking their positively charged residues as occurs with Mco. It is difficult to interrogate this by genetic manipulation as extensive substitution of hydrophobic regions would be both technically challenging and would likely result in an unstable protein. The signal peptide of Mco likely assists in studding Mco to the external face of the membrane, where it could oxidise Cu^{1+} ions to the less toxic Cu^{2+} in a similar fashion to CueO in the periplasm of *E. coli* (Grass and Rensing, 2001a; Singh *et al.*, 2004; Stolle, Hou and Brüser, 2016). If this is the case, then the type 1 copper centre of Mco is likely to be exposed on the outer surface of the membrane. The attenuation of copper tolerance observed in the $\Delta 2-53$ truncation of Mco can be explained if the absence of the signal peptide prevents the correct orientation of Mco in the membrane, rendering the type 1 copper centre inaccessible to external Cu^{1+} ions.

This chapter reports the first successful attempt to complement an *mco* mutant in *S. aureus*. Sitthisak and colleagues (Sitthisak *et al.*, 2005) failed to complement an *mco* mutant by expressing the gene on a multicopy plasmid. Here complementation was achieved by integrating the entire *copB-mco* operon into the chromosome. Successfully complementing a phenotype provides robust evidence that the *mco* gene causes the phenotype in question. Here complete restoration of Mco protein and its associated activity occurred in the complemented mutant.

There is large variation of growth between replicates at 1 and 2 mM copper seen in Figure 3.16. This phenotype can not be entirely explained, but variation was consistently large at these concentrations but not others, perhaps indicating that there is some degree of spontaneity, chance or random event that occurs on a population, cellular, biochemical, or molecular level when *S. aureus* is exposed to copper levels in the threshold between no growth attenuation and severe growth attenuation, and this random event, either its presence or absence, can lead to an increase or decrease in copper tolerance. Further in depth research is required to fully elucidate this phenomenon. There was little variation seen at other concentrations of copper (0-0.5 and 4 mM), indicating that the experimental error is unlikely to be the source of the variation. If experimental error was the source, it would be seen at all concentrations of copper.

It remains a possibility that 2 copies of *copB* in the complemented mutant could result in the restoration of copper tolerance. However, this is unlikely because deletion of residues 2-53 rendered the complemented *S. aureus* strain copper sensitive to the same extent as the *mco* mutant. This indicates that only loss of *mco* and not duplication of *copB* was affecting growth. This strain harboured two copies of *copB* but was still sensitive to copper similar to the *mco* deletion mutant which harboured a single copy of *copB*. Perhaps two copies of *copB* resulted in a greater level of *copB* transcript.

There was insufficient data to determine if Mco and CopB cooperate to detoxify copper. Additional deletion mutants of *copB* and *copB-mco* would be required to begin to investigate this phenomenon. However, it is unlikely that CopB and Mco do cooperate because constructs of *S. aureus* carrying both *copB* and *mco*, Δmco and $\Delta copB$ each have different MICs of CuCl₂ and different growth phenotypes in TSB supplemented with 4 mM CuCl₂ (Zapotoczna *et al.*, 2018). If two genes act cooperatively, their copper resistance profiles would be identical, which is not what was observed previously (Zapotoczna *et al.*, 2018).

A low molecular weight band is present for all samples in figure 3.11. Given the band is present in the empty vector control, this band is not degraded Mco3X-FLAG. This band is expected to be a non-specific IgG binding, potentially the second immunoglobulin binding protein Sbi. To confirm this, a no anti-FLAG IgG control western immunoblot could be performed. This experiment would confirm if this band is only binding to the HRP-conjugated secondary antibody, or if the anti-FLAG primary antibody is responsible for this off target binding.

In order to reduce the risk of the FLAG tag disrupting Mco function, the C-terminus of protein was chosen for its location instead of the N-terminus. This was because the N-terminus is the location of signal peptides of secreted proteins. Even so, it remained a possibility that the C-terminal 3X-FLAG tag affected localisation of Mco. However this was unlikely to have been the case because the 3X-FLAG tag containing construct restored copper tolerance to MRSA252 Δmco (Fig. 3.12). If Mco was mislocalised due to the C-terminal FLAG tag, it would most likely be rendered non-functional. The FLAG tag was deleted from pCL55::UCMF and the FLAG tag-less derivative had the same copper tolerance phenotype to the FLAG tagged strain

(Fig. 3.13). Taken together, the C-terminal 3X-FLAG tag does not affect the localisation of Mco or its ability to detoxify copper. It was somewhat surprising to find that Mco is not secreted by the Tat pathway as occurs in Gram-negative bacteria. The answer may lie in the basic differences of the Gram-negative and Gram-positive bacterial cell architecture. Gram-negative bacteria have a periplasmic compartment which acts like a molecular gatekeeper controlling which molecules can enter and leave the cell. Thus, the periplasmic space is uniquely suited for proteins with detoxification functions which act before the toxic compounds enter the cytoplasm. CueO is found in the periplasm, where it can detoxify cuprous ions before they can reach the cytoplasm and cause damage. Gram-positive bacteria like *S. aureus* do not have a periplasm. The cytoplasmic membrane and the thick cell wall are the only barriers to uptake of toxic molecules. The membrane likely represents the most effective place for the detoxification protein Mco, so that it can detoxify toxic copper at the surface of the membrane before the it can reach the cytoplasm. This chapter does not investigate the orientation of Mco in the membrane, but hypothesises that it is extracellularly facing.

Combining all of the data gathered in this study, it is postulated that Mco protects *S. aureus* from copper damage by detoxifying toxic cuprous ions in the external environment. Detoxifying the copper on the surface of the bacteria would prevent lethal damage to sensitive cytoplasmic cellular machinery. It is proposed that Mco is properly orientated into the membrane of *S. aureus* by its Sec signal peptide. Removal of the signal sequence results in the incorrect orientation of Mco in the membrane. This incorrect orientation probably results in the burial of its substrate oxidation site in the membrane and its inability to oxidise its substrates in the external environment.

In conclusion, the *S. aureus* Mco protein has been analysed by identifying a novel N-terminal region which traffics Mco through the Sec secretion system and not the Tat pathway. This is the first bacterial multicopper oxidase that does not have a canonical Tat signal peptide and that is not transported by the Tat system. Mco resides in the membrane of *S. aureus* and contributes to copper tolerance. This study is the first report of complementation of the copper sensitive phenotype of an

Mco mutant by expression of *mco* from a single copy genomic locus under control of CsoR.

3.19 Results Chapter 1 Summary

- Mco shares 39% amino-acid identity with CueO, contains a novel N-terminal signal peptide region, and lacks a methionine rich region.
- Mco is membrane localised in *S. aureus*.
- *S. aureus* Mco contains a novel N-terminal region of 56 amino acids, of which residues 1-26 are a Sec signal peptide which is capable of delivering a reporter protein to the supernatant in a cleavable manner from the membrane. This is the first bacterial multicopper oxidase to be transported by the Sec system, and not the Tat system.
- Loss of *mco* results in copper sensitivity of *S. aureus* when plated on copper containing agar, and the copper sensitive phenotype of an *mco* mutant was complemented by restoring the *mco* gene onto a different chromosomal locus, under the control of its native promoter CsoR.

Chapter 4

Results Chapter 2 - Investigation into novel genes involved in copper tolerance in *S. aureus*

4.1 Introduction

There are a limited number of genes whose products have been shown to contribute to copper tolerance in *S. aureus*. These are the *copAZ* operon and its regulator *csoR* which are conserved in all *S. aureus* strains, the *copB-mco* operon present in all CC30 and many CC22 *S. aureus* lineages (Zapotoczna *et al.*, 2018), the *copXL* operon mostly prevalent in the CC8 USA300 lineage CA-MRSA in North America but also in livestock associated CC398 strains. The accessory copper tolerance genes can also occur in different combinations such as the *copX-mco-copL* operon found in the CC8 USA300 South America clone of CA-MRSA (Purves *et al.*, 2018). As a result, only seven unique genes have been implicated thus far in copper tolerance in *S. aureus*, three of which are copper exporting P-type ATPases (*copA*, *copB*, *copX*) one multicopper oxidase (*mco*), one copper binding lipoprotein (*copL*), and one copper sensitive operon repressor (*csoR*), responsible for transcription of all of the above genes (Purves *et al.*, 2018). Given the toxicity of copper, and its ubiquitous presence in the environment, it is unlikely that these are the only factors that protect *S. aureus* from copper damage.

During the mutagenesis process for generating MRSA252 Δ *mco*, a mutant was generated that contained an additional 13 unintended gene deletions downstream of *mco*. This mutant was more sensitive to copper than any other copper sensitive strains of *S. aureus* in our strain collection. As a result, this mutant presented an opportunity to investigate how this clone was so copper sensitive, and potentially discover novel uncharacterised copper tolerance gene/genes in *S. aureus*.

The hypothesis for this chapter was that the copper sensitive phenotype of this mutant was due to a defect in one or more additional unknown copper tolerance genes. The genes deleted in this mutant were identified by whole genome sequencing, and two of these genes were investigated for their ability to contribute to copper tolerance.

4.2 Whole genome sequence analysis of MRSA252 Δ *mco* clones

During the mutagenesis process to generate MRSA252 Δ *mco* in Chapter 3 of this thesis, one of the isolated putative MRSA252 Δ *mco* clones that was sent for whole genome sequencing had an extra 13 genes deleted immediately downstream of *mco*, resulting in a total of 14 genes deleted from that clone (Fig. 4.1). This clone is named MRSA252 14 gene Knock Out (KO) for the remainder of this thesis.

The *mco* gene was deleted as intended by pIMAY mediated allelic exchange, (Fig. 4.1). However, three unintended genomic deletions were also made downstream of *mco*, and are emphasised with red arrows (Fig. 4.1). The first deletion removed 3397 bp of DNA, which resulted in deletion of the cadmium resistance genes *cadA* and *cadC*. The second deletion removed 41 bp of intergenic DNA, which has no annotated function associated with it on the KEGG genome database for MRSA252. The third deletion removed 7541 bp of DNA, which contained 10 genes which code for mostly uncharacterised and hypothetical proteins. The gene deletions that occurred were located between the *copB* and *cydC* genes (*copB-cydC* locus) and are summarised in table 4.1.

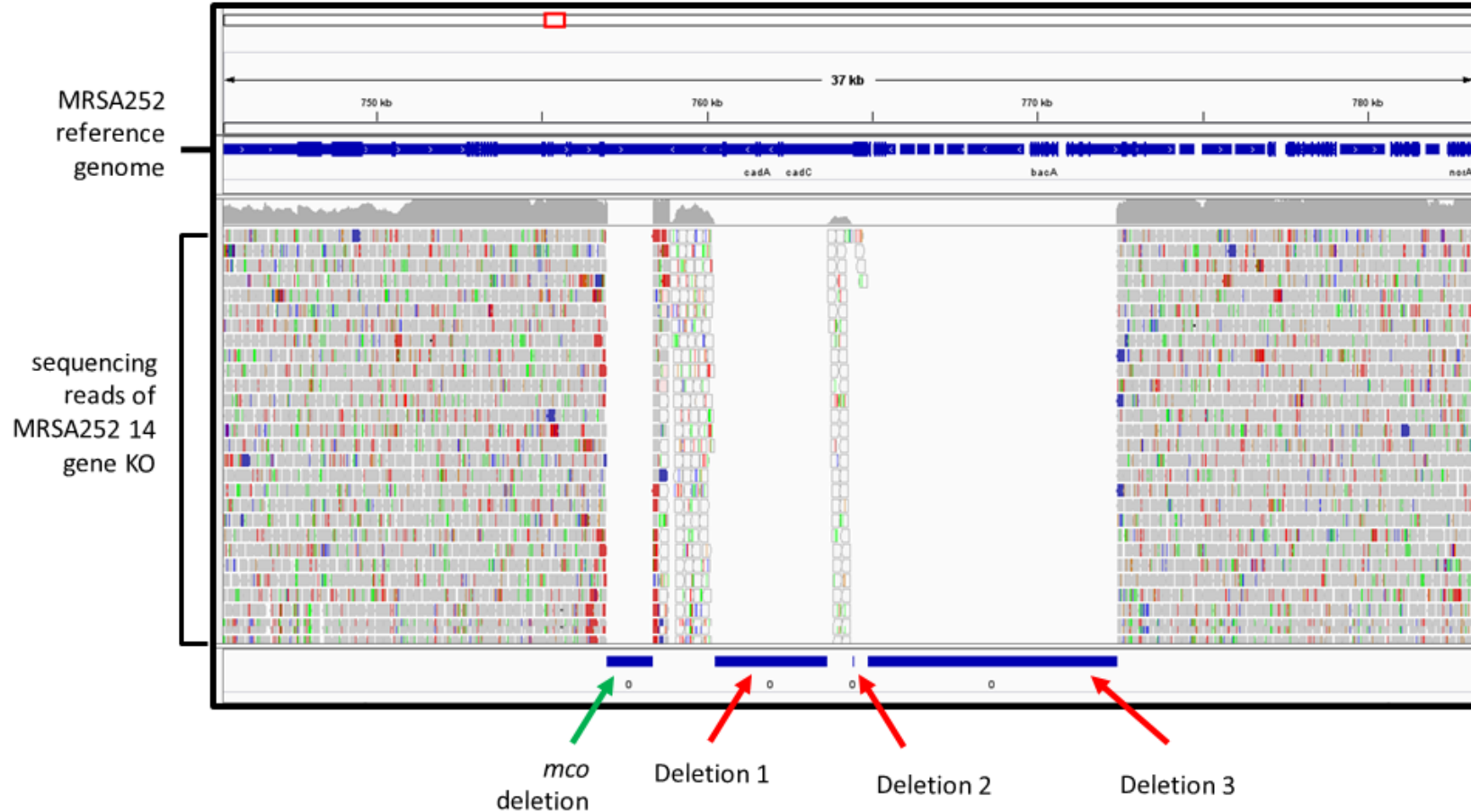


Figure 4.1 Whole genome sequencing identified a clone with three unintended regions of DNA deletion during the mutagenesis process to generate MRSA252 Δ *mco*

Integrated genome browser visualisation of the deletions discovered in MRSA252 14 gene KO. The blue bars at the bottom of the figure represent regions where no sequencing reads matched the reference genome MRSA252. They are labelled with green and red arrows to indicate the desired deletion of *mco* (green arrow) and the three unintended deletions (three red arrows).

Table 4.1. The 13 additional genes deleted in MRSA252 14 gene KO

Gene name	Description	GenBank ID
<i>cadA</i>	High efficiency Cd ²⁺ ATPase transporter	CAG39734.1
<i>cadC</i>	Cd ⁵ transcriptional repressor	CAG39735.1
<i>sar0725</i>	98.4% amino acid identity to <i>S. aureus</i> transposase C of transposon <i>Tn554</i>	CAG39736.1
<i>sar0728</i>	Putative membrane protein with poor database matches	CAG39738.1
<i>sar0729</i>	Putative acetyltransferase	CAG39739.1
<i>sar0730</i>	Putative lipoprotein with poor database matches	CAG39740.1
<i>sar0731</i>	Hypothetical protein with poor database matches	CAG39741.1
<i>sar0732</i>	Putative acetyltransferase. 45% amino acid identity to <i>Proteus mirabilis</i> acetyltransferase Pat	CAG39742.1
<i>sar0733</i>	Conserved hypothetical protein. 49% amino acid identity to <i>Bacillus halodurans</i> hypothetical protein	CAG39743.1
<i>sar0734</i>	Conserved hypothetical protein. 34% amino acid identity to a <i>Listeria monocytogenes</i> hypothetical protein.	CAG39744.1
<i>sar0735</i>	Putative exported protein with poor database matches	CAG39745.1
<i>bacA</i>	putative undecaprenol kinase. 97% amino acid identity to <i>Staphylococcus aureus</i> bacitracin resistance protein, putative undecaprenol kinase BacA.	CAG39746.1
<i>cydD</i>	ABC transporter ATP-binding protein. Involved in cytochrome bd biosynthesis.	CAG39747.1

Gene names were obtained from NCBI protein database, GenBank IDs are provided for each gene, the descriptions in the above table was written using data directly submitted to the NCBI protein database by M.T.G. Holden on behalf of the Pathogen Sequencing Unit, Sanger Institute, Wellcome Trust Genome Campus, Hinxton, Cambridge (Holden *et al.*, 2004).

4.3 Gene deletion profile of MRSA252 14 gene KO

In order to generate hypotheses about why the 14 gene KO was more sensitive to copper, bioinformatic analysis was carried out to determine if any of the genes could be linked to copper tolerance. A protein BLAST search was performed using the predicted amino acid sequence of each gene and the proteins with the greatest amino acid identity to the search query were analysed for any ascribed functions.

The gene *sar0722* remains intact just downstream of *mco* in MRSA252 14 gene KO (Fig. 4.2). A protein BLAST against the NCBI database of proteins found that it shares 99.8% amino acid identity to IS1182 family transposase proteins. Transposase genes are commonly located within or flanking their specific transposon. The proximity of this transposase to the DNA deletions in MRSA252 14 gene KO may suggest that activation of this transposase was responsible for a DNA deletion, possibly deletion 1. Deletion 1 (Fig. 4.2).

There were three genes deleted in Deletion 1, *cadA*, *cadC* and *sar0725*. The *cadA* and *cadC* genes are well described and characterised as conferring cadmium, zinc and lead resistance to *S. aureus* (Endo and Silver, 1995; Ye *et al.*, 2005). The *cadA* gene codes for a P-type ATPase that is a high efficiency exporter of cadmium, zinc and lead. CadA is found in the membrane, and contains eight transmembrane segments (Wong, Fan and Rosen, 2005). An amino acid BLAST comparing CopB and CadA showed that they share 30% amino acid identity indicating some homology between these two metal transporting ATPases. The *cadC* gene codes for an ArsR/SmtB family transcription regulator which derepresses from the *cad* promoter following binding of a heavy-metal ion to its ligand site (Ye *et al.*, 2005). The *sar0725* gene codes for another putative transposase, the second one found in the *copB-cydC* locus. This transposase gene was removed as part of Deletion 1 (Fig. 4.2 and table 4.1). A protein BLAST of its amino acid sequence indicated it had 99.2% amino acid identity to transposase for transposon *Tn554*. Transposon *Tn554* can be found in both *S. aureus* and *S. epidermidis* and is typically known for conferring resistance to macrolides-lincosamides-streptogramin B (Tillotson *et al.*, 1989; Chikramane *et al.*, 1991). No association with copper or metal resistance was determined by reviewing these publications on this transposase.

The gene *sar0726* remains intact just upstream of Deletion 3 (Fig. 4.2). This gene codes for a third putative transposase that is similar to 'S. aureus transposase for insertion sequence-like element IS431mec'. A protein BLAST of the amino acid sequence found that it shares 99.5% amino acid identity to IS6-like element ISSau6 family transposase. This proximity of this transposase may mean that this transposase was activated during the allelic exchange process and was responsible for a DNA deletion, possibly Deletion 3 (Fig. 4.2). No additional information regarding this transposase and metal tolerance was found in the literature.

A protein BLAST search of the amino acid sequence of *sar0728* found that it shared 99.56% identity with the hypothetical DUF1129 family of proteins in *S. aureus*. These are a conserved family of proteins with no known function.

A protein BLAST search of the amino acid sequence of *sar0729* indicated that it shared 100% amino acid identity to aminoglycoside 6'-N-Acetyltransferase of *S. aureus*. This protein is a member of the GCN5-related N-acetyltransferase (GNAT) family of N-acetyltransferases. It confers resistance to aminoglycosides by acetylating aminoglycoside compounds, reducing their affinity for the acceptor tRNA site on the 30S ribosome, conferring resistance to aminoglycosides (Vetting *et al.*, 2005). There is no reason to believe this protein contributes to copper tolerance.

A protein BLAST search of the amino acid sequence of *sar0730* did not result in homology to any known proteins or families, only hypothetical lipoproteins found in other *S. aureus* strains. The CopL lipoprotein contributes to copper tolerance in *S. aureus* (Rosario-Cruz *et al.*, 2019). The amino acid sequence of CopL was compared to the amino acid sequence of *sar0730* by protein BLAST, and no significant similarity between these two proteins was found, indicating this putative lipoprotein is not a homologue of the copper binding lipoprotein of *S. aureus* CopL.

A protein BLAST search of the amino acid sequence of *sar0731* found that this protein is a hypothetical protein with no assigned function. It shares a 100% amino acid identity similarity with hypothetical proteins from bovine and ovine mastitis, perhaps suggesting a role for this protein in ruminant mastitis (Le Maréchal *et al.*, 2011; Cormican and Keane, 2018).

A protein BLAST search of the 180 amino acid sequence of *sar0732* indicated that it shares 100% identity with a hypothetical protein that contains a GNAT family acetyltransferase domain between residues 8 and 152. The same gene has been identified in *Staphylococcus schleiferi* isolated in the UK (Genbank accession number: SUN30646.1), and in *S. aureus* isolated from a cystic fibrosis patient in Atlanta, USA (Genbank accession number: RNH11141.1). No additional information was available on this hypothetical protein with a GNAT family acetyltransferase domain, and no connection to metal tolerance could be found.

A protein BLAST search of the amino acid sequence of *sar0733* indicated that it shares 100% amino acid identity to the predicted TIGR00730 family Rossmann fold protein found in isolates of *S. aureus*, *S. schleiferi* and *Staphylococcus hyicus*. In *S. schleiferi* and *S. hyicus* it is described as a lysine decarboxylase family protein. No direct connection between this protein and metal tolerance could be found.

A protein BLAST search of the amino acid sequence of *sar0734* indicated that it shared 100% amino acid identity with the putative Yail/YqxD family protein found in isolates of *S. aureus* and *S. schleiferi*. There are no reports in the literature of Yail/YqxD family proteins being involved in metal tolerance.

A protein BLAST search of the 227 amino acid sequence of *sar0735* did not result in homology to any known proteins or families, only hypothetical and uncharacterised proteins from *S. aureus* strains isolated from bovine mastitis. Amino acid residues 60-205 were predicted to contain a 'recombination and DNA strand exchange inhibitor protein' domain, perhaps implicating this protein in a transfer of DNA in this mobile genetic element. No connection could be determined between this protein and metal tolerance.

A protein BLAST search of the amino acid sequence of *bacA* indicated that it shared a 100% identity with undecaprenyl-diphosphate phosphatase from isolates of *S. aureus* and *S. schleiferi*. This protein confers bacitracin resistance by increasing the pool of undecaprenol monophosphate available for cell wall biosynthesis, therefore overcoming the undecaprenol monophosphate sequestering properties of bacitracin (Chalker *et al.*, 2000). As a result of this investigation, no evidence that *bacA* contributes to metal resistance could be found.

A protein BLAST search of the amino acid sequence of *cydD* indicated that it shared a 100% identity with ABC transporter ATP-binding protein/permease or cysteine ABC transporter ATP-binding protein CydD isolated from both *S. aureus* and *S. schleiferi*. The *cydCD* operon has been shown to be important for the export of low molecular weight thiols such as glutathione and cysteine in *E. coli* (Shepherd, 2015; Poole, Cozens and Shepherd, 2019). The contribution of *cydD* or the *cydCD* operon to copper tolerance has not been investigated in *E. coli*. No studies investigating the function of the *cydCD* operon have been carried out in Gram-positive bacteria, including *S. aureus*.

4.4 Mutagenesis leading to generation of MRSA252 14 gene KO

In order to determine how MRSA252 14 gene KO was generated, the mutagenesis process of this mutant was analysed. The *cadAC* operon confers resistance to toxic CdCl₂, and so freezer stocks of MRSA252, MRSA252Δ*mco*, MRSA252 14 gene KO, MRSA252/pIMAY::Δ*mco* and MRSA252::pIMAY::Δ*mco* were toothpicked onto TSA supplemented with CdCl₂ to identify when in the mutagenesis process were these genes lost (Data not shown). Cadmium resistance was observed for all strains except MRSA252 14 gene KO, indicating that the integrity of the *cadAC* operon remained up to the excision stage of pIMAY mutagenesis, suggesting that the deletion of the extra 13 genes occurred at the excision step of pIMAY mutagenesis. It is hypothesised that transposon activation of *sar0722* and *sar0726* occurred at the excision stage and removed these genes.

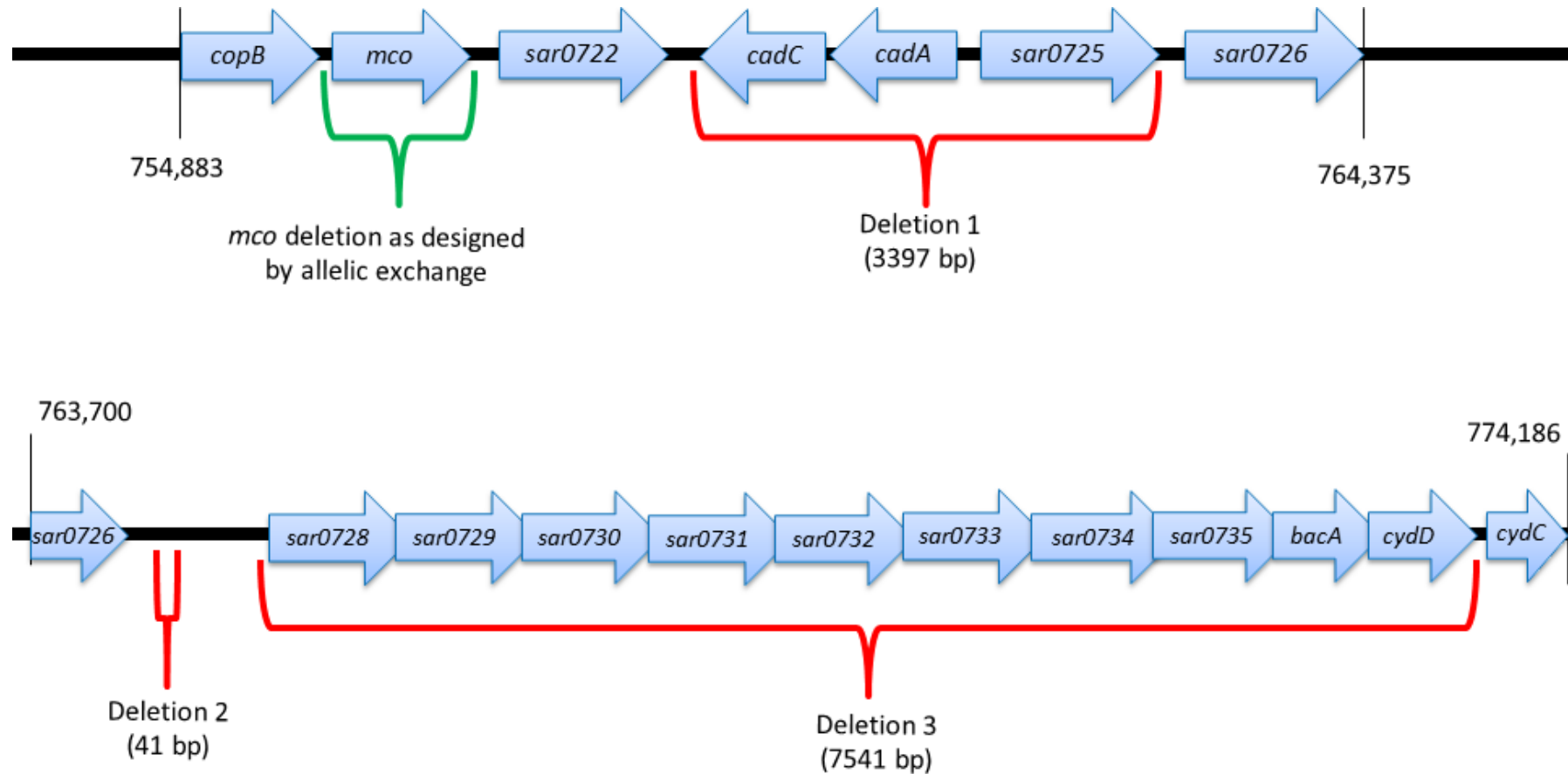


Figure 4.2. Schematic of the genes deleted in MRSA252 14 gene KO

Schematic diagram of the genome of MRSA252 and annotation of the genes that were deleted downstream of *mco* in MRSA252 14 gene KO. The pIMAY mediated deletion of *mco* is indicated with a green brackets. Deletion 1, Deletion 2 and Deletion 3 are indicated with red brackets. Deletion 1 and Deletion 3 resulted in removal of 3 and 10 genes from the chromosome respectively. The integrity of genes *copB*, *sar0722*, *sar0726* and *cydC* remained intact, as a result they are not indicated with brackets. Chromosomal coordinates (MRSA252) are indicated with horizontal black lines.

Detection of the deletion of the extra 13 genes was undetectable by conventional and phenotypic confirmation of the isogenic mutant. In the first attempted round of excising pIMAY:: Δmco from the chromosome of MRSA252::pIMAY:: Δmco , MRSA252 14 gene KO was isolated and mistaken for an *mco* deletion mutant due to confirmation by the conventional methods (Fig. 4.3). A batch of Cm^S MRSA252 excisants that grew well on TSA supplemented with ATc (1 μ g/ml) were screened for *mco* presence using primers out Mco F and out Mco R (Fig. 4.3A). Of 10 clones, only clone number 6 presented with a band of 1.1 kb indicating *mco* deletion, while the other 9 clones presented with a band of 2.5 kb, indicating excision resulting in Wild-Type *mco* presence on the chromosome. Genomic DNA was isolated from this clone and a PCR was performed using primers Mco out F and Mco out R and once again, a band indicating the desired deletion of *mco* was observed (Fig. 4.3B). This PCR amplicon was confirmed for deletion of *mco* by DNA sequencing (data not shown). The growth of this clone was monitored in TSBd and compared to Wild-Type MRSA252, and no substantial difference in growth was detected (Fig. 4.3C). In addition to this, the growth of this clone was analysed on sheep blood agar as a phenotypic assay to check for *agr* operon integrity by haemolysis profiling (Fig. 4.3D). The haemolysis profile of this clone was identical to Wild-Type, indicating integrity of the *agr* operon.

In summary, the extra 13 gene deletions would not have been detected without whole genome sequencing analysis. This provides robust evidence that whole genome sequencing should be performed on all mutants generated by pIMAY mediated allelic exchange in *S. aureus*, as deletions can occur and be phenotypically undetectable by the conventional phenotypical confirmation methods of growth analysis in TSBd and haemolysis analysis (Fig. 4.3).

Furthermore, this discovery has highlighted the importance of examining the surrounding gene profile of the gene to be deleted for any potential transposase genes or sites. There is a chance that these transposases could activate during the pIMAY mutagenesis procedure and disrupt other genes on the chromosome of *S. aureus*.

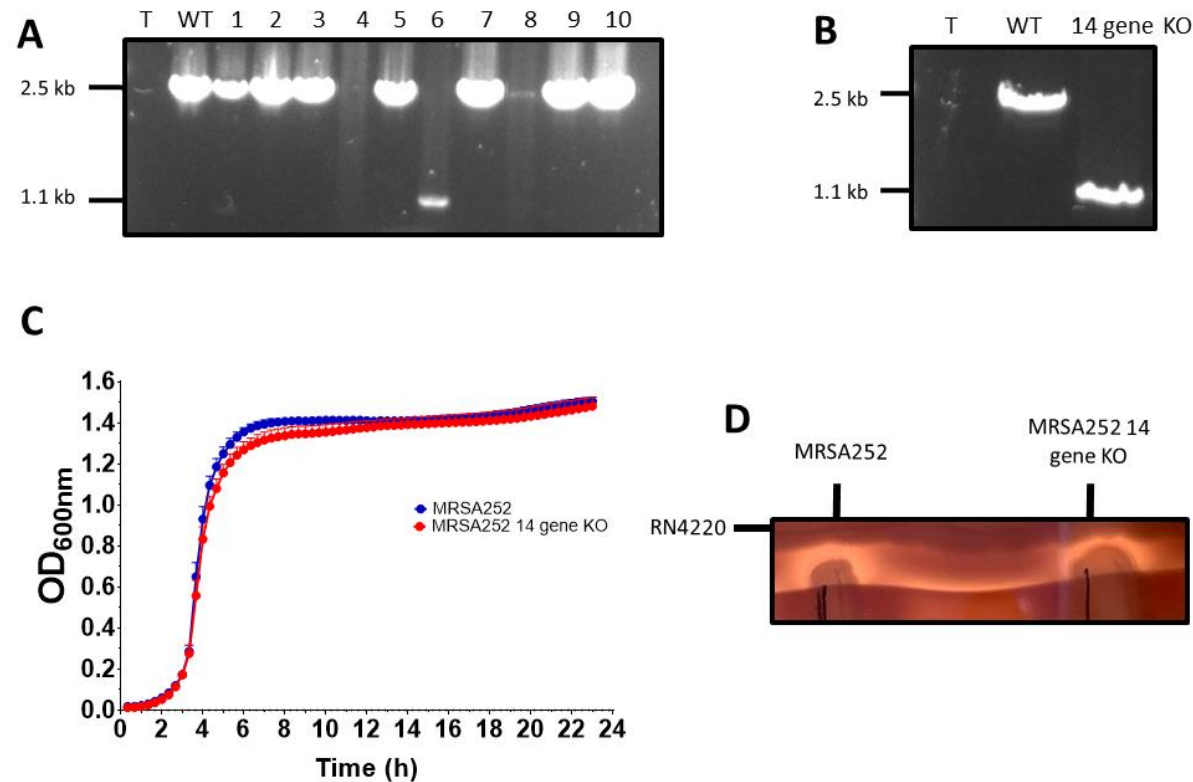


Figure 4.3 The off target gene deletions of 14 gene KO were not detectable by conventional mutant confirmation procedures

(A) Colony screen of excisants that were large on TSA supplemented with ATc (1 μ g/ml) and were Cm^S when toothpicked onto TSA supplemented with chloramphenicol (10 μ g/ml). T = no template DNA control, WT = MRSA252 positive control.

(B) Out Mco PCR screen using purified genomic DNA from the MRSA252 13 gene KO including WT MRSA252 as a control.

(C) Growth of the MRSA252 and MRSA252 14 gene KO was monitored in TSBd over 24 h in a 96 well plate with orbital shaking. Error bars represent + SD (n=3).

(D) Growth of MRSA252 and MRSA252 13 gene KO on sheep blood agar plate with RN4220. The haemolysis profile produced by MRSA252 13 gene knockout is the same as MRSA252, indicating disruption of the virulence operon *agr* has not been compromised (n=1).

4.5 Analysis of the growth profile of MRSA252 14 gene KO in copper supplemented media

The copper tolerance profile of MRSA252 14 gene KO was investigated by comparing its growth in TSBd medium supplemented with copper to the growth of MRSA252 and MRSA252 Δ *mco* under the same conditions (Fig. 4.4).

MRSA252 achieved an OD₆₀₀ of 0.9 after 8 h of growth and an OD₆₀₀ of 1.3 after 18 h. MRSA252 Δ *mco* reached an OD₆₀₀ of 0.66 after 8 h of growth in 1 mM CuCl₂, and an OD₆₀₀ of 1 after 18 h. By comparison, growth of MRSA252 14 gene KO was significantly attenuated in media supplemented with 1 mM CuCl₂. It reached a maximum OD₆₀₀ of 0.5 after 8 h of growth. This indicated that MRSA252 14 gene KO was more sensitive to 1 mM CuCl₂ than both its parent strain MRSA252, and MRSA252 Δ *mco*. Furthermore, the OD₆₀₀ of the culture of MRSA252 14 gene KO did not increase after 8 h, while the OD₆₀₀ of the MRSA252 and MRSA252 Δ *mco* cultures continued to increase after 8 h (Fig. 4.4).

MRSA252, MRSA252 Δ *mco* and MRSA252 14 gene KO all reached similar OD₆₀₀ values after 8 h of growth in 2 mM CuCl₂, but interestingly both MRSA252 and MRSA252 Δ *mco* continued growth after 8 h to reach a maximum OD₆₀₀ of 0.83 after 18 h (Fig. 4.4). The growth of MRSA252 14 gene KO appeared to be severely attenuated in the presence of 2 mM CuCl₂ as it reached a maximum OD₆₀₀ of 0.32 after 8 h, although this difference was not statistically significant (Fig. 4.4). This may indicate that MRSA252 14 gene KO is more sensitive to copper than both the wild-type MRSA252, and the copper sensitive MRSA252 Δ *mco*.

The growth profiles of MRSA252, MRSA252 Δ *mco* and MRSA252 14 gene KO were very similar in the absence of copper (Fig. 4.4), indicating that the differences between strains seen in the presence of copper are not due to a difference in growth, but due to a change in copper sensitivity.

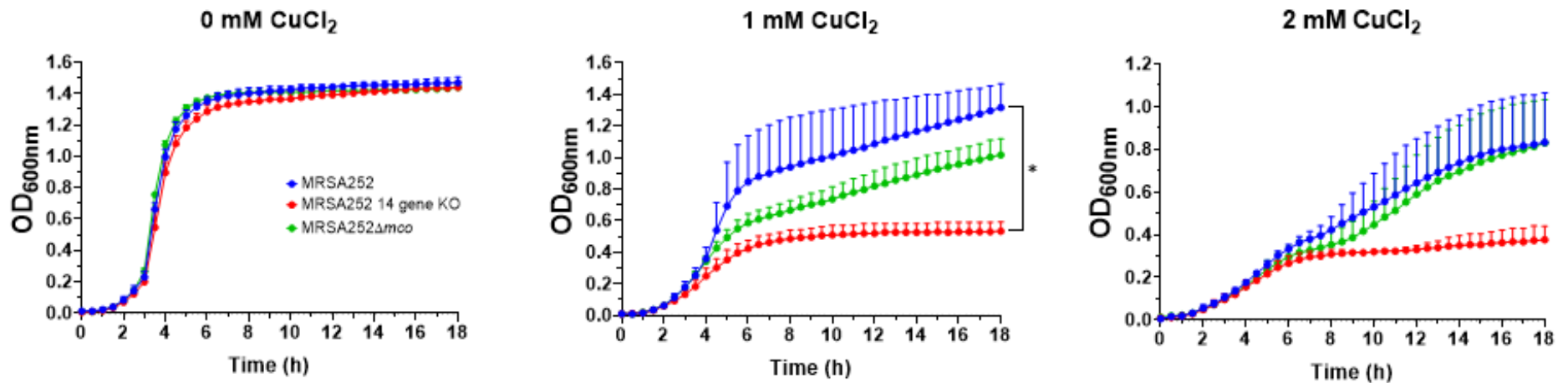


Figure 4.4 MRSA252 14 gene KO is more sensitive to copper than MRSA252 and MRSA252Δ*mco*.

Growth of MRSA252 (blue curves), MRSA252Δ*mco* (green curves) and MRSA252 14 gene KO (red curves) in TSBd supplemented with CuCl₂ (0, 1, and 2 mM) was monitored for 18 h in a 96 well plate with orbital shaking (200 rpm) at 37°C. Error bars represent + standard deviation. Statistical significance was determined at 18 h by students t-test. *; $P = \leq 0.05$. $n=3$.

The growth of MRSA252 14 gene KO was monitored on TSA supplemented with 6 mM CuCl₂ (Fig. 4.5A). The wild-type MRSA252, *mco* deletion mutant MRSA252Δ*mco*, *mco* mutant harbouring empty vector pCL55 MRSA252Δ*mco*::pCL55 empty, the *mco* complemented mutant MRSA252Δ*mco*::pCL55::UCMF, and the mutant complemented with a truncated, defective *mco* gene MRSA252Δ*mco*::pCL55::UCMF*mco*Δ2-53 (see section 3.9-12) were included as controls.

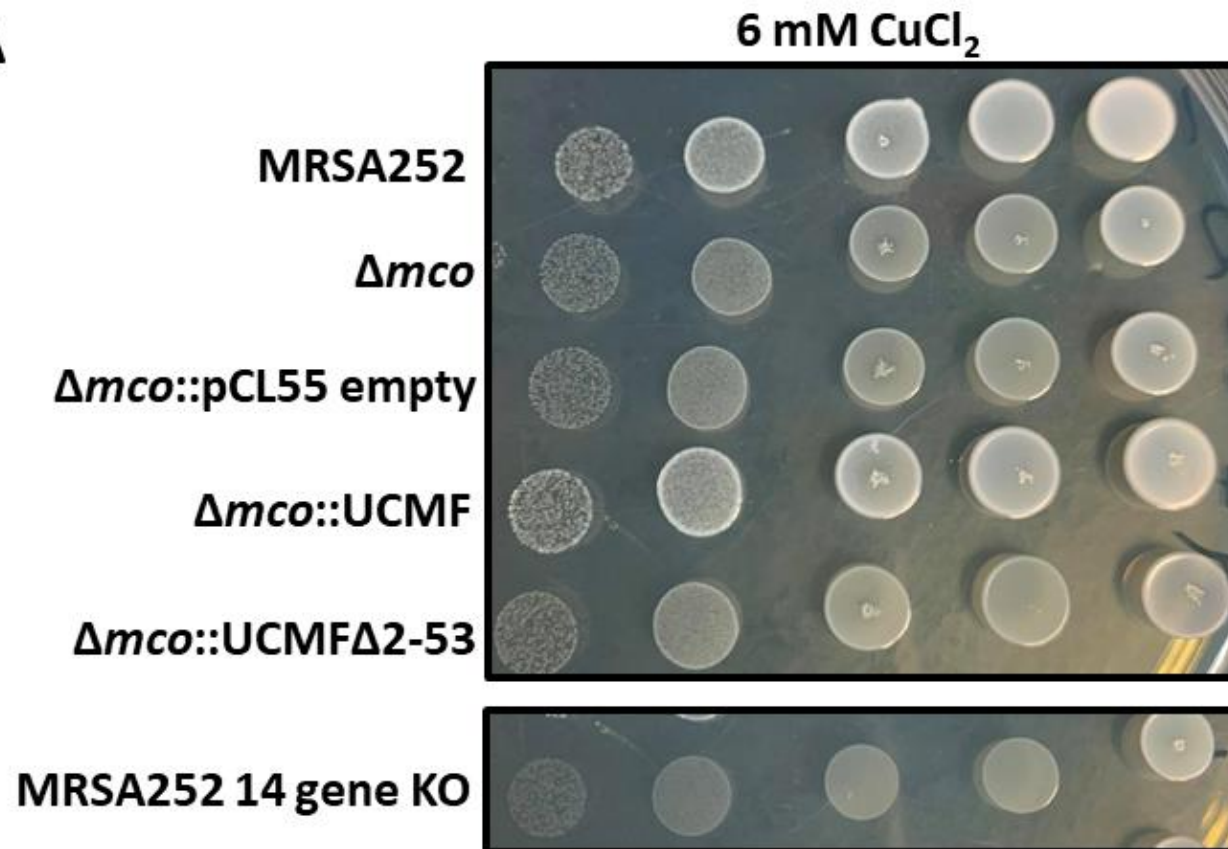
MRSA252 grew well on copper supplemented TSA forming big bright white colonies. The *mco* mutant MRSA252Δ*mco* and the empty vector control MRSA252Δ*mco*::pCL55 empty both grew more poorly on copper supplemented TSA as expected, as they had smaller, paler colonies compared to wild type. The copper sensitive phenotype was restored similar to wild-type using the mutant derivative MRSA252Δ*mco*::pCL55::UCMF which expresses *mco*3X-FLAG. The mutant expressing truncated Mco (McoΔ2-53) had a similar sensitivity to copper to MRSA252Δ*mco*.

The MRSA252 14 gene KO formed smaller, paler colonies on TSA supplemented with CuCl₂ (6 mM) than both wild-type MRSA252 and MRSA252Δ*mco*, indicating that it grew more slowly. This indicated that MRSA252 14 gene KO was even more sensitive to copper than MRSA252Δ*mco*.

The minimum inhibitory concentration of copper for MRSA252 and MRSA252 14 gene KO was determined (Fig. 4.5B). MRSA252 14 gene KO had a lower MIC (6 mM) than MRSA252 (8 mM), further indicating that MRSA252 14 gene KO was more sensitive to copper than MRSA252.

In chapter 3, it was found that *mco* did not contribute to copper tolerance under anaerobic conditions (Fig. 3.15). Here, growth of MRSA252 14 gene KO was monitored on copper supplemented agar in anaerobic conditions to investigate if genes deleted in this mutant contributed to copper tolerance in anaerobic conditions (Fig. 4.6). Growth of MRSA252 and MRSA252 14 gene KO was identical at all concentrations of copper tested in anaerobic conditions. Growth was similar for both strains on plates containing no added copper or with 0.05 mM CuCl₂. Growth was inhibited at 0.1 mM CuCl₂ for the two lowest dilutions (10⁻⁴ and 10⁻⁵), while *S. aureus*

could not form colonies at the 10^{-3} , 10^{-4} and 10^{-5} dilutions on medium supplemented with 0.5 mM copper. These data indicate that none of the deletions in MRSA252 14 gene KO contributed to copper tolerance in anaerobic conditions, as both MRSA252 and MRSA252 14 gene KO grew similarly on medium containing copper in anaerobic conditions.

A**B**

Strain	MIC
MRSA252	8 mM CuCl ₂
MRSA252 14 gene KO	6 mM CuCl ₂

Figure 4.5 Growth of MRSA252 14 gene KO on copper supplemented TSA and its minimum inhibitory concentration of copper

(A) Overnight cultures were washed in PBS and adjusted to an OD₆₀₀ of 3. 10 fold Serial dilutions of the suspension were spotted onto TSA supplemented with CuCl₂ (6 mM) and incubated at 37°C aerobically. Data is representative of 2 independent biological replicates.

(B) The minimum inhibitory concentration (MIC) of MRSA252 and MRSA252 14 gene KO to CuCl₂ was obtained by minor adaptation of the CLSI protocol for MIC determination as described in the methods section. Results were read by two scientists independently. The same result was obtained in 3 biological replicates.

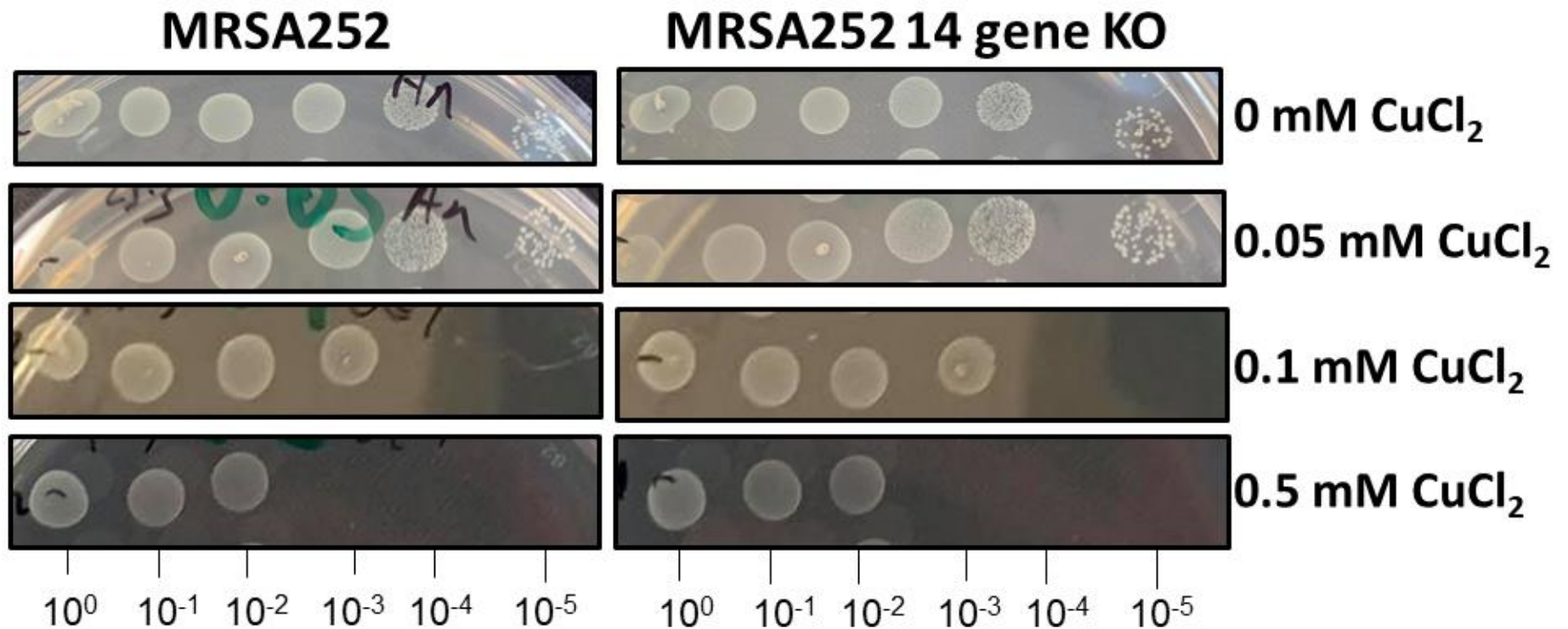


Figure 4.6 Growth of MRSA252 14 gene KO on copper supplemented agar in anaerobic conditions

Overnight cultures were washed in PBS and adjusted to an OD₆₀₀ of 3. 10 fold Serial dilutions of the suspension were spotted onto TSA supplemented with CuCl₂ and incubated at 37°C in an anaerobic jar. Concentration of copper in agar is indicated at the side. Dilution of the bacterial suspension is indicated at the bottom. Data is representative of 2 independent biological replicates.

4.6 Generation of MRSA252 Δ *cadA*, MRSA252 Δ *cadAC*, MRSA252 Δ *mco* Δ *cadA* and MRSA252 Δ *mco* Δ *cadAC*.

Given that the MRSA252 14 gene KO is more sensitive to copper than MRSA252 Δ *mco* (Fig. 4.4), it was hypothesised that at least one other gene missing in MRSA252 14 gene KO contributed to copper tolerance. The data presented in Table 4.1 indicate that there are no other genes with a known role in copper tolerance missing from the 14 gene KO mutant. Additional bioinformatic analysis on each delete gene did not find a direct link to copper tolerance in *S. aureus*. The *cydCD* operon is important in small molecular weight thiol transport in *E. coli* (Poole, Cozens and Shepherd, 2019), However its function in Gram-positive bacteria has not been studied. Additionally, the CydCD ABC-transporter exports thiols to the periplasm, and *S. aureus* does not have a periplasm like *E. coli*.

However, the absence of *cadA* and *cadC* in the mutant was interesting as these genes are known to confer resistance to the heavy metals cadmium, cobalt and zinc (Tynecka, Gos and Zajac, 1981; Zapotoczna *et al.*, 2018). The *cadA* gene codes for a high efficiency Cd²⁺, Zn²⁺ and Co²⁺ exporting ATPase, and the *cadC* gene codes for a Cd²⁺ sensitive transcriptional repressor of the *cadAC* operon (Endo and Silver, 1995). A role for *cadA* and *cadC* in copper tolerance has not been investigated. Given that *cadAC* has already been described to confer resistance to multiple heavy metals, it was hypothesised that the *cadAC* operon could also contribute to copper tolerance, and that loss of the *cadAC* operon contributed to the increased copper sensitivity of MRSA252 14 gene KO. To empirically determine this, isogenic deletion mutants of *cadA* and *cadAC* were generated by allelic exchange in both MRSA252 and MRSA252 Δ *mco*, leading to the generation of four new isogenic deletion mutants; MRSA252 Δ *cadA*, MRSA252 Δ *cadAC*, MRSA252 Δ *mco* Δ *cadA* and MRSA252 Δ *mco* Δ *cadAC* (Fig. 4.7). The integrity of these mutants was confirmed by whole genome sequencing and analysis of haemolytic profile on sheep blood agar (data not shown).

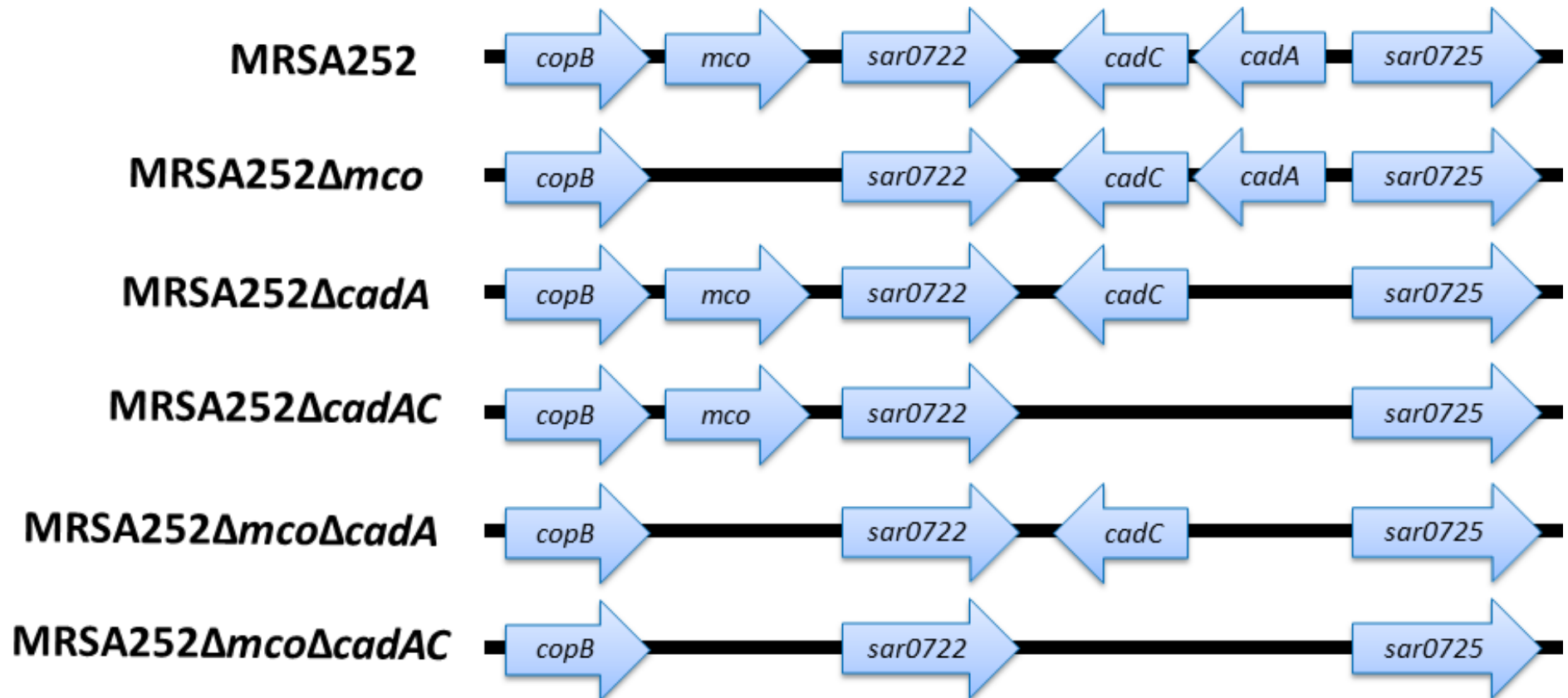


Figure 4.7. Schematic diagram of isogenic mutants generated between the *copB* and *sar0725* locus in MRSA252 to investigate the role of the *cadAC* operon in copper tolerance

Arrows are representative of the gene orientation on the chromosome of MRSA252. Arrows are not drawn to scale of the length of the gene. Each gene deletion was precisely its opening reading frame only. The promoter regions upstream of *copB* and *cadA* remain intact in all mutants, to ensure preservation of expression of the downstream genes *mco* and *cadC* respectively.

4.7 Investigation of the contribution of the *cadAC* operon to copper tolerance of MRSA252

The copper sensitivity profile of these mutants was investigated by growth in TSBd supplemented with subinhibitory concentrations of CuCl₂ (Fig. 4.8).

MRSA252Δ*mco*, MRSA252Δ*cadA*, MRSA252Δ*cadAC*, MRSA252Δ*mco*Δ*cadA* and MRSA252Δ*mco*Δ*cadAC* all exhibited similar growth in the presence of 1 mM copper. These strains achieved an OD₆₀₀ of 0.94 at 8 h of growth, and reached a final optical density of ~ 1.5 at 22 h. This growth is attenuated when compared to the parent strain MRSA252, which achieved an OD₆₀₀ of 1.21 at 8 h, and reached a final optical density of 1.6 at 22 h. However this difference was not statistically significant. MRSA252Δ*mco*, MRSA252Δ*cadA*, MRSA252Δ*cadAC*, MRSA252Δ*mco*Δ*cadA* and MRSA252Δ*mco*Δ*cadAC* achieved a greater final OD₆₀₀ than MRSA252 14 gene KO in TSBd supplemented with 1 mM copper (Fig. 4.7). Growth of MRSA252 14 gene KO reached an OD₆₀₀ of ~ 0.67 at 8 h, and an optical density of 0.84 at 22 h. This indicated that MRSA252 14 gene KO was more sensitive to copper than all other strains tested, and had a reduced ability to recover its growth in copper after ~ 8 h similar to MRSA252Δ*mco*, MRSA252Δ*cadA*, MRSA252Δ*cadAC*, MRSA252Δ*mco*Δ*cadA* and MRSA252Δ*mco*Δ*cadAC*. Statistical significance was only achieved upon comparing the final optical density of strains MRSA252 and MRSA252 14 gene KO (Fig. 4.8).

Growth of MRSA252, MRSA252Δ*mco*, MRSA252Δ*cadA*, MRSA252Δ*cadAC*, MRSA252Δ*mco*Δ*cadA* and MRSA252Δ*mco*Δ*cadAC* in TSBd supplemented with 2 mM copper had significant variation between biological replicates rendering it difficult to distinguish any meaningful phenotypes between these strains in this experiment. However the growth of MRSA252 14 gene KO was significantly attenuated in comparison to other strains, again demonstrating that this strain is much more copper sensitive than all other strains in this copper concentration (Fig. 4.8).

Growth of all strains was severely attenuated at 4 mM CuCl₂, with Wild-Type MRSA252 growing slightly better than all other strains at this copper concentration. Although variation is high at 4 mM copper, all of strains MRSA252Δ*mco*,

MRSA252 Δ *cadA*, MRSA252 Δ *cadAC*, MRSA252 Δ *mco* Δ *cadA*, MRSA252 Δ *mco* Δ *cadAC* and MRSA252 14 gene KO all exhibit a similar growth attenuation, potentially indicating that loss of any copper tolerance gene/genes results in copper sensitivity compared to Wild-Type MRSA252, indicating that all of these genes in combination contribute to a greater overall copper resistant phenotype TSBd (Fig. 4.8).

Growth of all strains was similar in the absence of copper, confirming all phenotypes described were in response to copper, and not due to attenuation of growth in TSBd (Fig. 4.8).

Together, these data suggested that *cadA* contributed to copper tolerance similar to *mco*, and that *cadAC* was not responsible for the extreme growth defect in the presence of copper seen in MRSA252 14 gene KO (Fig. 4.8).

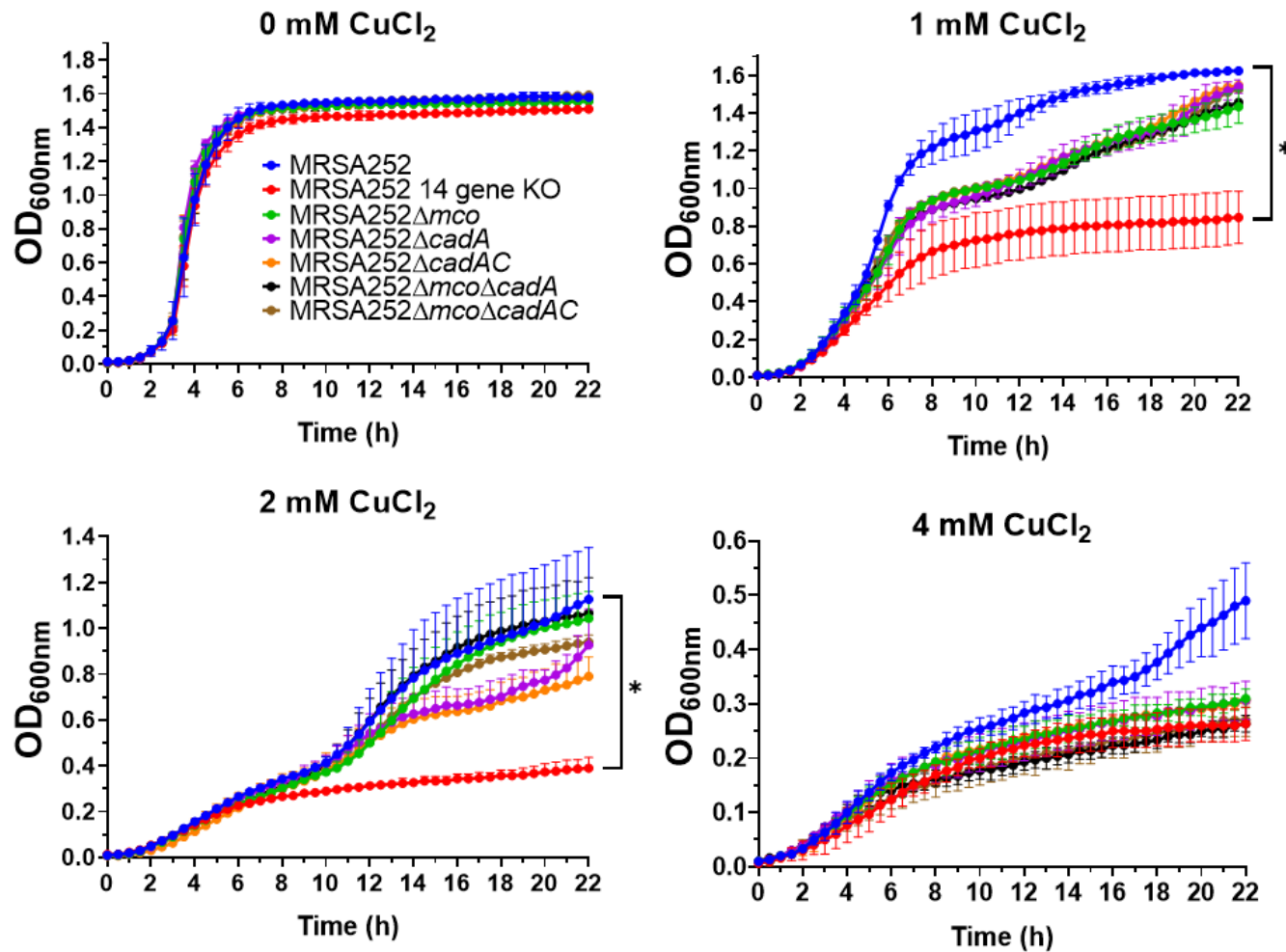


Figure 4.8. Growth of *cadAC* deletion mutants in liquid media supplemented with copper

Growth of various MRSA252 mutants in TSBd supplemented with subinhibitory concentrations of CuCl_2 (0, 1, 2, 4 mM) was monitored for 22 h in a 96 well plate with orbital shaking. Error bars represent standard deviation. Statistical significance was determined at 22 h by students t-test. *; $P = \leq 0.05$. $n=3$.

The growth of MRSA252, MRSA252 Δ *mco*, MRSA252 Δ *cadA*, MRSA252 Δ *cadAC*, MRSA252 Δ *mco* Δ *cadA*, MRSA252 Δ *mco* Δ *cadAC* and MRSA252 14 gene KO was monitored on TSA supplemented with 4 mM copper (Fig. 4.9). There was no growth defect detected for MRSA252 Δ *cadA* or MRSA252 Δ *cadAC* when compared to growth of MRSA252, indicating that the *cadAC* operon did not contribute to copper tolerance in these conditions using solid media. The mutants MRSA252 Δ *mco* Δ *cadA* and MRSA252 Δ *mco* Δ *cadAC* exhibited the same growth phenotype as MRSA252 Δ *mco*, suggesting that only the *mco* gene was contributing to copper tolerance in these conditions.

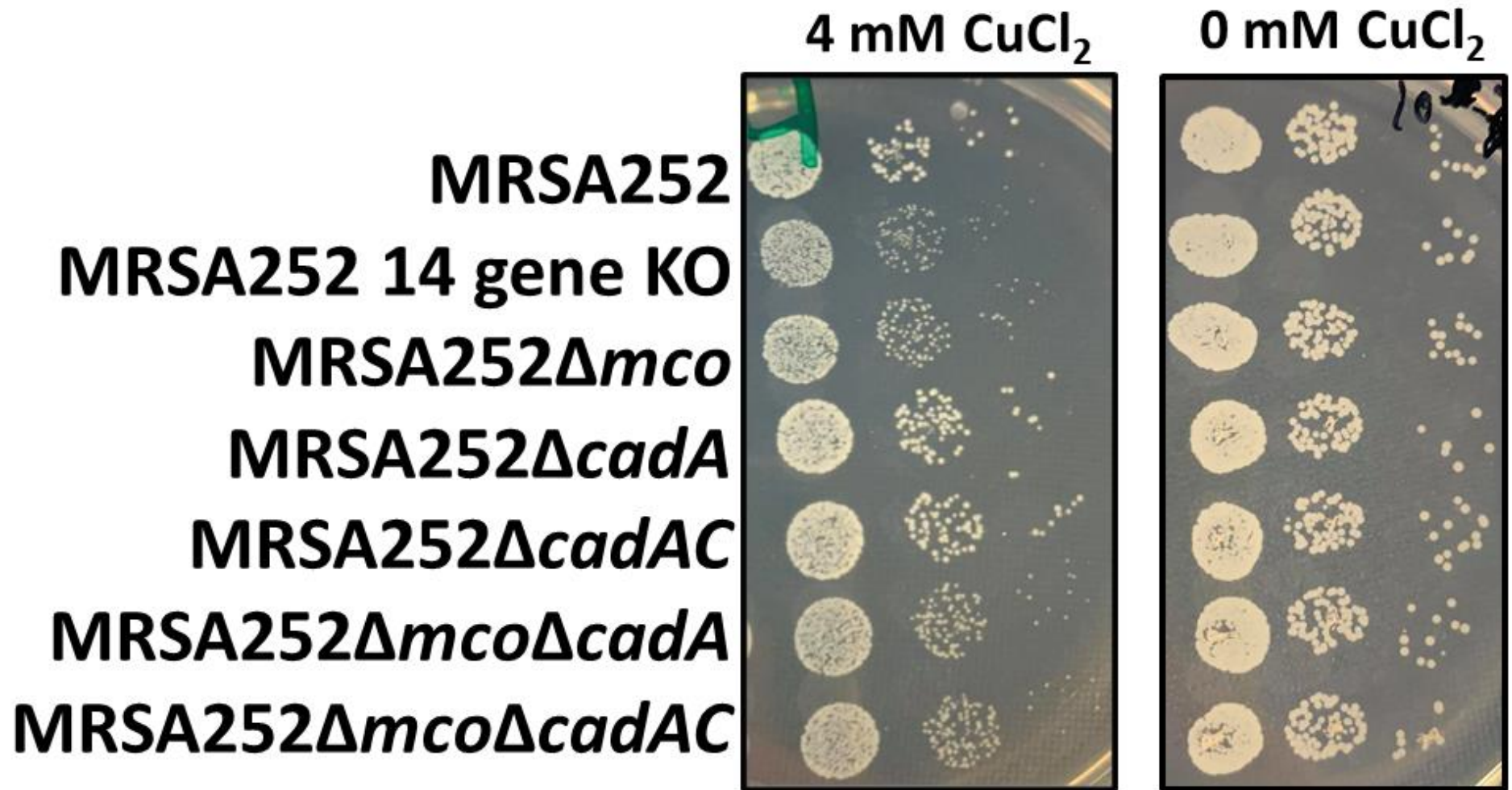


Figure 4.9. Growth of *cadAC* deletion mutants on TSA supplemented with copper. Overnight cultures were washed in PBS and adjusted to an OD₆₀₀ of 3. 10 fold serial dilutions of the suspension were spotted onto TSA supplemented with (4 mM) or without CuCl₂ (0 mM) and incubated at 37°C aerobically. Data is representative of 2 independent biological replicates.

4.8 Discussion

This chapter described an unintended deletion of 13 extra genes during the pIMAY-mediated allelic exchange process, which generated the mutant MRSA252 14 gene KO (Fig. 4.2). This deletion of 13 extra genes was likely the result of activation of two transposases immediately downstream of *mco*, at the excision step of pIMAY-mediated mutagenesis. This strain with 14 genes deleted was more sensitive to copper than an isogenic *mco* mutant alone (Fig. 4.4-5), indicating that one or more of the deleted genes contributed to copper tolerance, indicating the presence of a novel copper tolerance factor in *S. aureus*. Of the 13 extra genes deleted in MRSA252 14 gene KO, the *cadAC* operon was hypothesised to contribute to copper tolerance. Isogenic deletion mutants were generated in *cadA*, *cadAC*, *mco* and *cadA*, *mco* and *cadAC*, to determine if these genes were responsible for the extremely copper sensitive phenotype of MRSA252 14 gene KO. The *cadA* gene contributed to copper tolerance in liquid media but not solid media conditions (Fig. 4.8-9), and deletion of both *mco* and *cadA* did not result in the extremely copper sensitive phenotype of MRSA252 14 gene KO, indicating that another novel copper tolerance gene remains yet to be identified in the 11 unexamined deleted genes in MRSA252 14 gene KO.

This chapter finds that MRSA252 14 gene KO is more sensitive to copper than MRSA252 Δ *mco* and MRSA252 Δ *mco* Δ *cadAC* (Fig. 4.8), indicating that one or more of the 11 other gene deletions are responsible for the increased sensitivity to copper. To determine which gene or genes is responsible for this increased copper sensitivity, isogenic deletion mutants of each of these 11 genes could be made, and their contribution to copper tolerance could be assessed by growth in media supplemented with copper. Another approach would be the generation of a transposon mutant library of MRSA252. The generation of a transposon mutant library has been used successfully to discover novel genes involved in copper tolerance in *S. aureus* USA-300 strain LAC (Al-Tameemi *et al.*, 2020). Generation of a transposon mutant library in MRSA252 and screening of these mutants for copper tolerance could identify which gene in MRSA252 14 gene KO is responsible for copper tolerance, with the added benefit of potentially identifying other uncharacterised copper tolerance genes in MRSA252. The generation of a

transposon mutant library in MRSA252 would not only benefit copper tolerance research, but also be used for identifying novel virulence factors. Mutation of the *cydD* gene should be prioritised as it is involved in low molecular weight thiol export in *E. coli* (Poole, Cozens and Shepherd, 2019). Low molecular weight thiols such as glutathione contribute to copper tolerance in Gram-positive bacteria by buffering excess intracellular copper when copper exporting machinery are overloaded (Stewart *et al.*, 2020), it can be hypothesised that the increased copper sensitivity of MRSA252 14 gene KO was due to deletion of both *mco* and *cydD*. It is possible that *cydD* is required for export of copper loaded bacillithiol from *S. aureus*, contributing to copper tolerance in *S. aureus*. Since *cydC* and *cydD* together form a heterodimeric ABC transporter, mutation of the *cydD* gene alone may lead to a complete loss of function. Isogenic deletion of *cydD*, *cydC* and *cydCD* would allow for greater study into the function of these genes. Future experiments could include western immunoblotting of *S. aureus* supernatants of mutants without the *cydC*, *cydD* and *cydCD* genes, probing with IgG specific for *S. aureus* bacillithiol, would determine if the *cydCD* contributes to export of bacillithiol across the membrane of *S. aureus*. Furthermore, it would determine if deletion of *cydD* alone prevents export of bacillithiol. Determination of intracellular copper concentration of such mutants by ICP-MS would also determine if the *cydCD* system contributes to removal of excess intracellular copper from *S. aureus*. The copper sensitivity profile of mutants of *cydC*, *cydD* and *cydCD* could also be determined by growth analysis on copper supplemented agar plates as well as growth in nutrient rich and deficient liquid media supplemented with a spectrum of subinhibitory concentrations of copper.

Variation in growth on copper agar was observed between different batches of TSA media, where in some batches 4 mM CuCl₂ gave the clearest results, and sometimes 6 mM CuCl₂. When performing experiments analysing the growth of *S. aureus* on copper supplemented agar, *S. aureus* was always plated on a selection of different copper concentrations (2, 4, 5, 6 mM CuCl₂) in order to capture the concentration that provided the most clear results. This variation is likely due to factors such as nutrient content variations between reconstituted batches of media. Future experiments could be optimised further by carefully controlling for batch to batch media variations by making large batches of copper agar plates at once instead of multiple smaller batches.

Deletion 2 in MRSA252 14 gene KO (Fig. 4.1) was not investigated here and so the contribution of this 41 bp deletion to the copper sensitive phenotype of MRSA252 14 gene KO cannot be ruled out. No open reading frame, nor any genomic annotation or feature was associated with this 41 bp deletion in MRSA252, and was thus omitted from study in this chapter. To probe its contribution to copper tolerance, the 41 bp sequence could be restored in the 14 gene KO mutant at its original chromosomal location to determine if this leads to a restoration of copper tolerance in this mutant.

It is possible that a small regulatory RNA could be coded for within any of the three deleted regions in MRSA252 14 gene KO, and that it could be involved in copper homeostasis. So far, 248 small RNAs have been identified in MRSA252, but none of these correspond with any of the deleted regions in MRSA252 14 gene KO (Carroll *et al.*, 2016). Carroll and colleagues note that their list of annotated sRNAs is not exhaustive, and that more small RNAs are likely to be discovered as genomic technologies advance. Links of copper and metal resistance to small RNAs will likely be made as small RNAs and staphylococcal gene expression studies are continued under different growth conditions (Sorensen *et al.*, 2020). However current available studies cannot rule out the possible contribution of an unknown small regulatory RNA deletion in MRSA252 14 gene KO to copper tolerance.

This chapter's investigation suggests that the multiple transposases in this genomic locus were activated and responsible for removal of these genes, perhaps implicating these transposases in transfer of mobile genetic elements between bacteria. Frequent loss and gain of the p2-hm plasmid has been reported in MRSA bloodstream isolates (Jamrozy *et al.*, 2017). The p2-hm plasmid (p2-hm and pSCBU are different names for the same plasmid) harbours heavy metal resistance genes *copB*, *mco*, *cadA* and *arsAB*. Mobile genetic elements including bacteriophages, transposons, plasmids and pathogenicity islands represent about 15% of *S. aureus* genomes (Alibayov *et al.*, 2014), indicating the importance of mobile genetic elements for the evolution and survival of *S. aureus*. Even so, characterisation of the transposases found in this study and their target DNA sequences and activation requirements remain undetermined. Transposons often confer antimicrobial resistance to their host (Sansevere and Robinson, 2017), such as erythromycin

resistance by the *tn916* transposon family (Sansevere *et al.*, 2017), or penicillin resistance (*bla*) by Tn552 (Rowland and Dyke, 1989), or spectinomycin and macrolide-lincosamide-streptogramin B resistance in transposon Tn554 (Murphy, Huwyler and de Freire Bastos, 1985). More is known about transposases specifically such as the IS30-like DDE transposase of ICE6031 is required for excision of the integrative conjugative element ICE6031 (Sansevere *et al.*, 2017). Bacterial heavy metal resistance genes are often transferred as part of transposons along with antimicrobial resistance genes (Bruins, Kapil and Oehme, 2000). For example, cadmium resistance can be transferred in *Listeria monocytogenes* by transposon Tn5422 (Lebrun, Audurier and Cossart, 1994). The removal of the genes found in this chapter are congruent with transposon mediated removal of genes. Genes removed here included heavy metal resistance genes *cadA* and *cadC*, bacitracin resistance gene *bacA*, and two GNAT family N-acetyl-transferases, *sar0729* and *sar0731*. Some GNAT family proteins can confer resistance to aminoglycosides (Vetting *et al.*, 2005). Future experiments involving MRSA252 14 gene KO could examine resistance to antimicrobials such as bacitracin and aminoglycosides. The conditions that cause such transposon mediated movement of genes remain elusive (Everitt *et al.*, 2014; Sansevere *et al.*, 2017), but conditions in this chapter suggest that pIMAY-mediated homologous recombination near the transposases, growth in TSBd at 30°C and growth on TSA supplemented with Atc (1 µg/ml) may be involved in transposase activation and transfer of this mobile genetic element. Additional experiments investigating the effect of homologous recombination, growth temperature and antibiotic stress would improve understanding of these transposases. For example, antibiotic stress may encourage transposase activity and transfer of mobile genetic elements, which may improve understanding of how gene transfer occurs in the hospital environment, where numerous pathogens harbouring mobile genetic elements are found. Interestingly, sub-inhibitory concentrations of antibiotics and heavy metals are sufficient to sustain carriage of large mobile genetic elements even with their associated fitness cost (Gullberg *et al.*, 2014). This highlights that even low levels of antimicrobials or metals in the environment can help select for mobile genetic elements harbouring resistance to multiple antimicrobials and metals.

This chapter describes how 3 undesired DNA deletions were found during the mutagenesis process that resulted in the loss of 13 extra genes in addition to the desired gene deletion (Fig. 4.2). These off target deletions were not found through conventional screening of growth profile in TSBd and haemolysis patterns (Fig. 4.3). Previously, phenotypes wrongly attributed to deletion of the *ausA* gene in *S. aureus* were found to be due to off target mutations in the *saeS* gene (Sun, Cho, *et al.*, 2010). The *saeS* mutation was discovered by DNA sequencing of the *ausA* mutant. This chapter reinforces the importance of whole genome sequencing of newly generated mutants to identify SNPs, insertions and deletions that would otherwise be missed by targeted Sanger sequencing.

The results described here show that *mco* contributed to copper tolerance on solid medium supplemented with copper, while *cadA* did not (Fig. 4.9). However, the *cadA* deletion mutants had a slightly reduced growth in copper compared to wild type when grown in liquid media, although this difference was not statistically significant in the conditions tested (Fig. 4.8). One explanation for this small reduction in growth is that the mechanism of copper damage is influenced by the environmental conditions, and as a result, the copper detoxification mechanisms employed by bacteria may be equally diverse, with particular genes being more and less effective at detoxifying copper in certain conditions. Perhaps Mco contributes to copper tolerance more prominently when plated in solid agar conditions, while the exporting P-type ATPases such as CadA and CopB are effective at exporting excess intracellular Cu⁺ ions in liquid conditions. To support this, the toxicity of copper is changed depending on the state it is presented in. Dry metallic copper surfaces or copper containing alloys can indiscriminately kill bacteria in minutes to hours (Grass, Rensing and Solioz, 2011). Growth of *S. aureus* in copper supplemented media is changed dependent on if nutrient-rich or deficient media is used, as shown here in this thesis (Fig. 3.16 and 17) and elsewhere (Tarrant *et al.*, 2019). Furthermore, growth in anaerobic conditions also increases sensitivity to copper compared to aerobic conditions and no difference in growth was detected between MRSA252 and MRSA252 14 gene KO (Fig. 4.6), indicating that none of the deleted copper tolerance genes in MRSA252 14 gene KO help *S. aureus* resist copper toxicity in anaerobic conditions. The mechanisms of copper toxicity are multifaceted, including catalysation of hydroxyl radical formation by Haber-Weiss

and Fenton like chemistry (Ladomersky and Petris, 2015), disruption of iron-sulphur clusters (Macomber and Imlay, 2009), lipid peroxidation (Yoshida, Furuta and Niki, 1993; Chillappagari *et al.*, 2010), depletion of the buffering antioxidant GSH (Stewart *et al.*, 2020). The mechanisms of copper tolerance employed by bacteria are also likely multifaceted, with potential for certain genes to combat a certain type of copper damage, or in certain conditions. This may explain why *cadA* contributed to growth of *S. aureus* in copper supplemented TSBd (Fig. 4.8) but not on copper supplemented TSA (Fig. 4.9).

The *cadA* gene codes for a cadmium and zinc transporting P-Type ATPase (Nucifora *et al.*, 1989). The *cadC* gene codes for the cadmium, lead and zinc sensitive ArsR/SmtB family transcription regulator protein CadC (Yoon, Misra and Silver, 1991; Endo and Silver, 1995; Ye *et al.*, 2005). The *cadA* gene has been shown to confer both zinc and cadmium resistance to *S. aureus*, is under the control of its transcriptional regulator CadC (Ye *et al.*, 2005). The CadC protein forms a protein dimer and binds to the promoter region of *cadA*, preventing its transcription. Binding of cadmium, bismuth or lead to CadC will result in derepression and transcription of *cadA* (Endo and Silver, 1995). Plasmids containing *cadAC* contribute to cadmium and zinc tolerance (Zapotoczna *et al.*, 2018). However, the contribution of the *cadAC* operon to copper tolerance has yet to be investigated until now (Fig. 4.8-9). To improve understanding of the role of the P-type ATPase CadA in copper tolerance in *S. aureus*, gene expression studies should be performed, to determine if *cadA* is transcribed in response to copper. The expression of the cadmium efflux protein *cadD* was increased in group A streptococci in response to copper (Stewart *et al.*, 2020), which may suggest that the expression of the *cadA* gene in *S. aureus* is also increased in response to copper. Furthermore, ICP-MS quantification of intracellular copper concentrations of MRSA252 Δ *cadA* bacteria when exposed to copper would determine if this mutant has an increased intracellular copper load, implicating CadA in intracellular copper export, similar to *S. aureus* deficient in the copper exporting P-Type ATPase *copB* (Zapotoczna *et al.*, 2018).

4.9 Results Chapter 2 Summary

- During the pIMAY-mediated allelic exchange process, one of the putative Δmco clones likely had two transposases downstream of *mco* activated, which removed 13 extra genes from chromosome of MRSA252, generating MRSA252 14 gene KO. This highlighted the importance of whole genome sequencing every pIMAY-mediated isogenic deletion mutant to confirm the integrity of the desired mutant.
- MRSA252 14 gene KO is extremely sensitive to copper, and is unable to recover growth in 1 mM copper similar to WT or MRSA252 Δmco at ~ 8 h time point.
- The *cadAC* operon contributes to copper tolerance in MRSA252 similar to *mco* in TSBd supplemented with copper, but a copper sensitive phenotype was not detected on TSA supplemented with copper.
- The copper sensitive phenotype of MRSA252 14 gene KO was not replicated by any of the newly generated strains, including MRSA252 $\Delta mco\Delta cadAC$, indicating that a novel copper tolerance mechanism remains to be discovered in the 11 uncharacterised genes in MRSA252 14 gene KO.
- This chapter represents the initial exploratory study discovering a novel copper tolerance gene/locus in *S. aureus*, and has narrowed down this novel discovery from 14 to 11 genes with empirical data.

Chapter 5

Results Chapter 3 - Investigating the role of copper tolerance genes in resisting killing by host immune cells

5.1 Introduction

Staphylococcus aureus is a leading cause of life threatening illnesses such as bacteraemia, endocarditis, pneumonia and osteomyelitis (Turner *et al.*, 2019). Part of the reason *S. aureus* is a leading global pathogen is due to its large range of virulence factors that disrupt the host immune system (Thammavongsa *et al.*, 2015).

The discovery that murine macrophages import copper into the phagolysosome to augment killing of phagocytosed pathogens has resulted in investigations to determine if copper tolerance in microbes is a novel virulence factor to aid bacterial survival during infection (White, Lee, *et al.*, 2009). The CTR1 protein imports copper into the cytoplasm of macrophages, and the ATP7A protein imports copper into the phagolysosome of macrophages (White, Lee, *et al.*, 2009; Rowland and Niederweis, 2012). Copper resistance genes increase bacterial survival in murine macrophages and whole human blood (White, Lee, *et al.*, 2009; Purves *et al.*, 2018; Zapotoczna *et al.*, 2018). A primary mechanism of bactericidal activity of copper is the catalysation of the production of hydroxyl radicals due to Fenton and Haber-Weiss chemistry (Haber and Weiss, 1934; Liochev and Fridovich, 2002; Dupont, Grass and Rensing, 2011).

Neutrophils are the primary line of defence against *S. aureus* infection (Bogomolski-Yahalom and Matzner, 1995). Neutrophils are professional phagocytes capable of phagocytosing and killing microbes. They are essential for effective clearance of *S. aureus* from the host. Neutrophils kill *S. aureus* by internalising the bacteria within phagosomes, which fuse with lysosomes to form the pathogen killing phagolysosome. This phagolysosome utilises a number of bactericidal mechanisms to kill engulfed bacteria. One primary mechanism of phagolysosomal bacterial killing is ROS generation. Defective NADPH mediated superoxide production by granulocytes in chronic granulomatous disease patients results in an increase in *S. aureus* infection rates (Curnutte, Whitten and Babior, 2010). The production of reactive oxygen species (ROS) by human neutrophils is vital for effective killing of phagocytosed *S. aureus* (Hampton, Kettle and Winterbourn, 1996).

The toxicity of copper in aerobic conditions is due to the production of hydroxyl radicals by Fenton and Haber-Weiss reactions which cause lipid peroxidation, protein oxidation and DNA damage (Dupont, Grass and Rensing, 2011). Furthermore, ROS-mediated damage has been shown to be important for the killing of *S. aureus* in both human blood and neutrophils, and this was enhanced by disruption the *rexB* gene, which is vital for DNA repair in *S. aureus* (Ha *et al.*, 2020).

Copper tolerance genes are widespread in clinically relevant *S. aureus* strains including CA-MRSA strains across the Americas (USA-300) and in HA-MRSA strains in Europe (Purves *et al.*, 2018; Zapotoczna *et al.*, 2018). Copper tolerance improves the survival of *S. aureus* in murine macrophages *in vitro* (Zapotoczna *et al.*, 2018), and whole human blood (Purves *et al.*, 2018; Zapotoczna *et al.*, 2018). Therefore, it is postulated that bacterial copper tolerance is prevalent because it contributes to resistance to host phagocytic killing by protecting *S. aureus* from ROS-mediated toxicity of copper.

In this chapter, the role of multiple copper tolerance genes of *S. aureus* in resistance to immune killing has been investigated. This study begins by examining the role of copper tolerance in survival in murine macrophages, then whole human blood, and finally primary human neutrophils.

5.2 Survival of copper sensitive *S. aureus* in murine macrophages

Copper tolerance improves survival of phagocytosed *E. coli* in murine macrophages (White, Lee, *et al.*, 2009). The copper tolerance genes *copX*, *copL*, *copB* and *mco* contribute to intracellular survival of *S. aureus* strains JE2 and 14-2533T in murine macrophages (Purves *et al.*, 2018; Zapotoczna *et al.*, 2018). To determine if copper tolerance plays a role in enhancing intracellular survival of MRSA252, RAW264.7 murine macrophages were activated with IFN- γ and treated with CuSO₄ to induce expression of the copper transporters ATP7A and CTR1. These activated macrophages were infected with MRSA252 and MRSA252 14 gene KO (See Fig. 4.2 for detailed description of mutant) and bacterial survival after phagocytosis was assessed. In chapter 4 of this thesis, a copper sensitive mutant (MRSA252 14 gene KO) was generated that had 14 genes deleted from its chromosome, including *mco* and *cadAC* (Fig. 4.2). MRSA252 14 gene KO was chosen for this experiment as it was the most copper sensitive mutant of MRSA252 (Fig. 4.4).

At 1 hour post-infection macrophages harboured similar levels of intracellular MRSA252 and MRSA252 14 gene KO indicating that wild-type and mutant were internalised at similar levels (not shown). However, 4 hours post infection, there were more viable MRSA252 within macrophages than MRSA252 14 gene KO (Fig. 5.1). This indicates that the 14 gene KO mutant is more susceptible to killing by macrophages than wild-type MRS252. This mutant is highly susceptible to killing by copper (Fig. 4.4) raising the possibility that the results described here are due to the poor ability of the 14 gene KO to resist copper-dependent killing mechanisms owing to deletions in the *mco* gene. The possibility that other genes disrupted in 14 gene KO contribute to survival in RAW-264.7 remains.

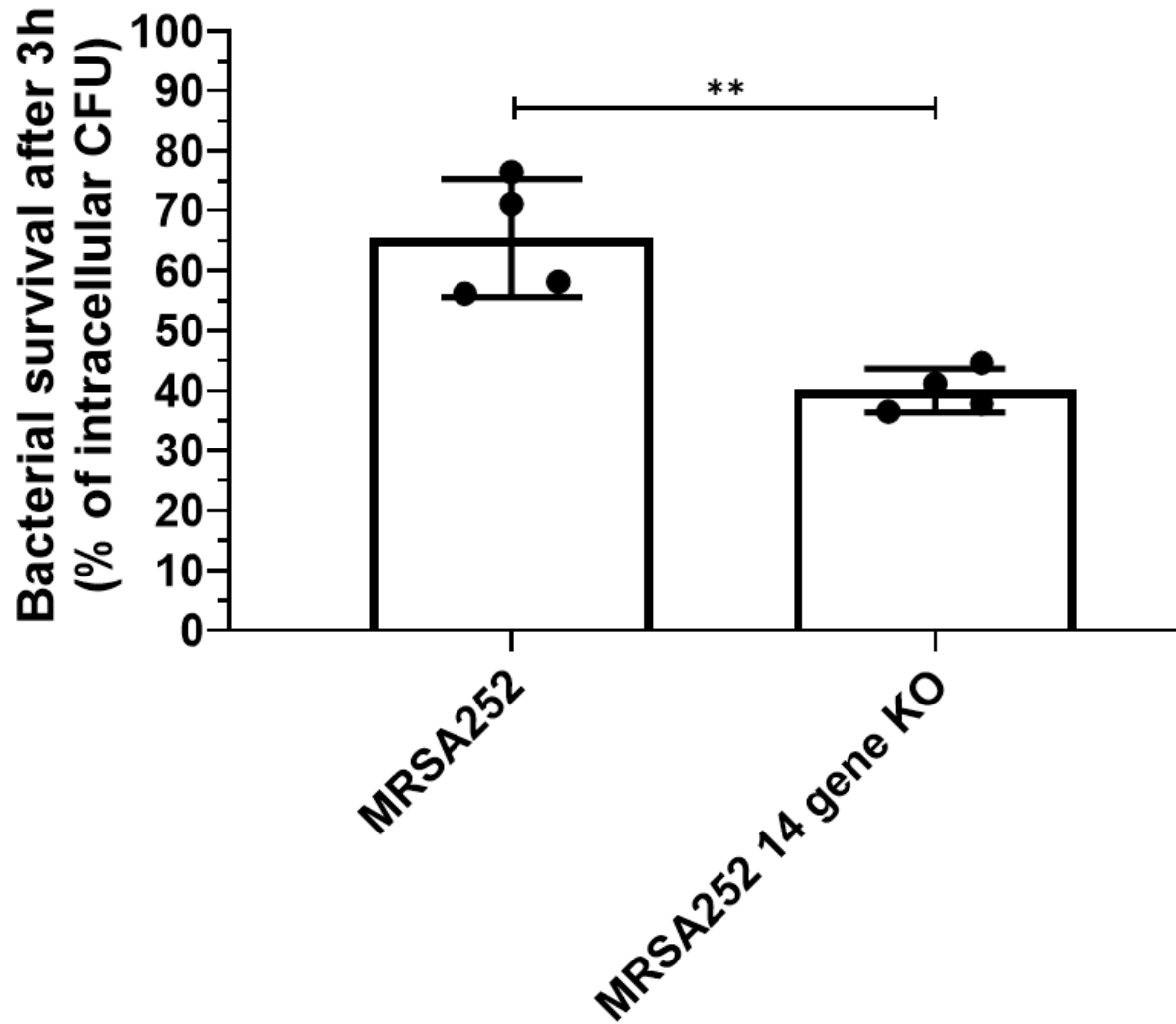


Figure 5.1 Survival of MRSA252 in murine macrophages

RAW264.7 macrophages were seeded at 2×10^5 cells per well with DMEM+10% FBS supplemented with IFN- γ (40 ng/ml) and CuSO_4 (40 μM) for 16 h prior to infection. Macrophages were infected with *S. aureus* at an MOI of 10 in DMEM allowing phagocytosis for 30 min followed by killing of extracellular bacteria with gentamicin and lysostaphin for 30 min. At 1 hour post-infection (T1) and 4 hours post-infection (T4), macrophages were lysed with ice-cold water and lysates were plated on agar to calculate CFUs/ml. The percentage survival after 3 hours was calculated as $((T4/T1) \times 100)$. Bars represent the mean from 4 independent experiments and error bars = \pm SD. Statistical significance determined by unpaired t test **, $P < 0.005$.

5.3 Survival of copper sensitive *S. aureus* in whole human blood

The *mco* gene carried on plasmid pSCBU contributes to the survival of *S. aureus* strain 14-2533T in whole human blood (Zapotoczna *et al.*, 2018). The contribution of the *mco* gene to survival of *S. aureus* in blood when located within a MGE integrated into the chromosome has not yet been examined.

To determine if the *mco* gene contributes to the survival of MRSA252 in whole human blood, MRSA252 carrying a functional chromosomal copy of *mco*, the *mco* deletion mutant MRSA252 Δ *mco*, the deletion mutant carrying the empty integrated vector pCL55 in MRSA252 Δ *mco*::pCL55, MRSA252 Δ *mco*::pCL55::UCMF, a complemented mutant where pCL55 express wild type Mco, and MRSA252 Δ *mco*::pCL55::UCMF Δ 2-53 expressing an inactive variant of Mco, were incubated with whole human blood at 37°C with orbital shaking and the percentage survival after 3 h was calculated (Fig. 5.2A).

In all experiments, fewer bacteria were recovered from blood after 3 h incubation than were present in the initial inoculum (Fig. 5.2A), while the number of bacteria recovered after incubation in plasma increased (Fig. 5.2B). This indicates that the cellular components in human blood were active and killing MRSA252. The level of killing varied greatly between blood donors with bacterial survival ranging from 10-50%. The mean percentage survival for MRSA252 and its derivatives was ~ 25% (Fig. 5.2A). No significant difference in survival was detected for the MRSA252 Δ *mco* mutant and its derivatives, suggesting that *mco* does not contribute to resistance to killing in whole human blood under the conditions tested here.

The survival of the mutants in cell-free human plasma drawn from the same donors (Fig. 5.2B) was also studied. All mutants grew in plasma (787 - 907% growth) indicating that the cellular components of blood are required for the killing of *S. aureus*. The growth and survival of the MRSA252 14 gene KO mutant in blood and plasma was also investigated. This mutant had a significantly poorer ability to proliferate in human plasma (287% growth) compared to the wild-type and *mco* mutants (Fig. 5.2B). In contrast the survival of MRSA252 14 gene KO was not impaired in human blood. This indicates that the ability of MRSA252 to grow in human plasma is impacted negatively by one or more of the mutations present in the MRSA252 14 gene KO.

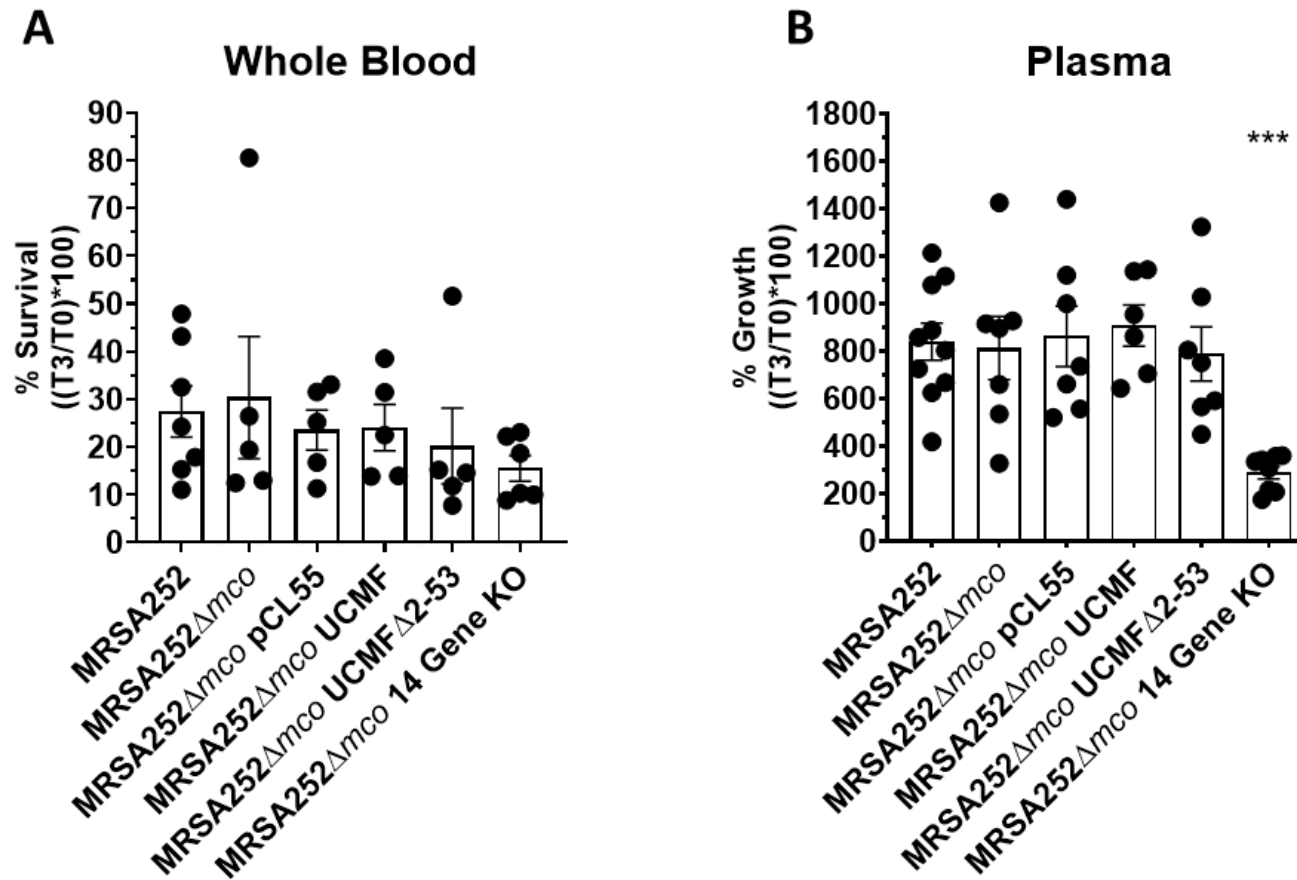


Figure 5.2 Survival of MRSA252 and its mutants in whole human blood and growth in plasma

Washed bacteria were incubated with freshly drawn whole human blood (A) or plasma (B). Percentage survival was calculate using CFU counts after 3 h growth (T3) expressed as a percentage of initial CFU counts at time point 0 (T0), N \geq 5. Error bars represent \pm SEM. Statistical significance was determined by one-way ANOVA followed by Dunnett's multiple comparison test using MRSA252 as control; ***, P \geq 0.0005. Absence of stars indicates no significant difference detected when compared to MRSA252.

5.3.1 Survival of copper sensitive mutants of MRSA252; *cadA*, *cadAC*, *mco cadA*, *mco cadAC* and *copZ*, in whole human blood

To determine if other copper tolerance genes in MRSA252 contributed to survival in whole human blood or growth in plasma, the survival of MRSA252, MRSA252 14 gene KO, MRSA252 Δ *cadA*, MRSA252 Δ *cadAC*, MRSA252 Δ *mco* Δ *cadA*, MRSA252 Δ *mco* Δ *cadAC* and MRSA252 Δ *copZ* was measured (Fig. 5.3).

Fewer bacteria from all derivatives of MRSA252 were recovered from blood after 3 h incubation than were present in the initial inoculum (Fig. 5.3A). There was no significant difference in survival of any derivative of MRSA252 compared to wild-type when incubated in blood. This indicates that none of the genes deleted in these mutants contribute to survival of *S. aureus* in whole human blood under the conditions tested here.

The number of bacteria recovered after incubation in plasma increased for all derivatives of MRSA252 (Fig. 5.3B). MRSA252 14 gene KO grew poorly in plasma compared to MRSA252 and other derivatives. While the reduction in growth is not significant ($P = 0.145$), the mean is 299% for MRSA252 14 gene KO compared to a mean of 1031-1499% for all other MRSA252 derivatives. Unlike what was observed in Fig. 5.2B, no statistical significance was achieved between MRSA252 and MRSA252 14 gene KO. This is likely due to high donor to donor variation and using only 3 biological replicates. However the trend suggests that deletion of *cadAC* and *mco* are not responsible for the growth attenuation observed in MRSA252 14 gene KO, indicating that one or more of the other 11 uncharacterised deleted genes are responsible for the poorer growth of MRSA252 14 gene KO in plasma. Repetition of this experiment is required to confirm this finding with statistical significance.

In summary, these data indicate that no difference in survival in whole human blood was detected for any of the derivatives of MRSA252 used in the conditions tested.

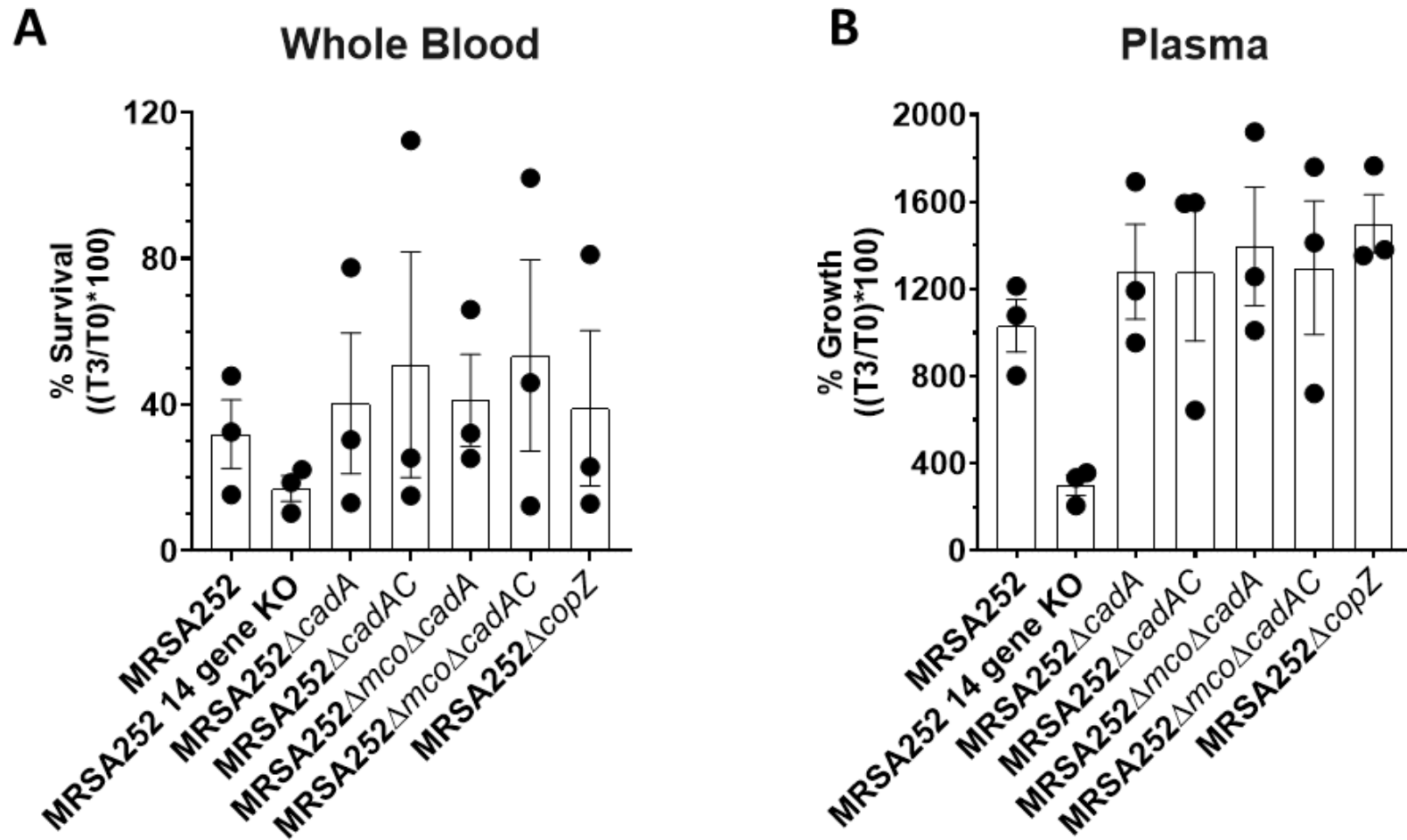


Figure 5.3 Survival of copper sensitive MRSA252 deletion mutants in whole human blood and growth in plasma
 Washed bacteria were incubated with freshly drawn whole human blood (A) or plasma (B). Percentage survival was calculate using CFU counts after 3 h growth (T3) expressed as a percentage of CFU counts at time point 0 (T0). n = 3. Error bars represent \pm SEM. No statistical significance was observed by one-way ANOVA followed by Dunnett's multiple comparison test using MRSA252 as control.

5.3.2 Survival of *S. aureus* in whole human blood using different initial inocula

The absence of a statistically significant reduction in survival by the *mco* mutant of MRSA252 was unexpected, as other copper sensitive mutants of *S. aureus* (including an *mco* mutant) were shown to have poorer survival in whole human blood compared to the parent strains (Zapotoczna *et al.*, 2018). It was postulated that the contribution of copper tolerance of MRSA252 to survival in human blood depends on the experimental conditions. Also many other virulence factors contribute to survival in human blood such as staphylococcal protein A (*spa*), the second immunoglobulin binding protein (*sbI*), chemotaxis inhibitory protein (*chp*), staphylococcal complement inhibitor (*scn*), staphylokinase (*ska*) and enterotoxin type A (*sea*) (Holden *et al.*, 2004; McCarthy, Witney and Lindsay, 2012). The blood survival experiment was carried out with different starting inocula to determine this altered the survival of *S. aureus* (Fig. 5.4).

Strains MRSA252 and MRSA252 14 gene KO were chosen for this experiment as MRSA252 14 gene KO is highly sensitive to copper (Fig. 5.4A and B), (Fig. 4.4). As a control, two strains that were previously shown to have a survival difference in blood (Zapotoczna *et al.*, 2018) were also tested (Fig. 5.4C and D). 14-2533T (pSCBU) carrying the *copBmco* operon on a multicopy plasmid is better able to survive in blood than the parental strain 14-2533T (Zapotoczna *et al.*, 2018).

The survival of both MRSA252 and MRSA252 14 gene KO in whole human blood was similar for all tested starting inocula (Fig. 5.4A). MRSA252 exhibited ~ 30% survival when 2×10^5 , 2×10^6 and 2×10^7 CFUs/ml of bacteria were added. Similarly, MRSA252 14 gene KO exhibited ~ 15% bacterial survival when 2×10^5 , 2×10^6 and 2×10^7 CFUs/ml of bacteria were added. There was no significant difference between the survival of MRSA252 and the 14 gene KO mutant regardless of the input CFU used. However, a significant difference between MRSA252 and the 14 gene KO mutant was measured when the lowest starting inoculum (2×10^5) was incubated in plasma.

The percentage growth of MRSA252 in plasma was different for each different starting inocula of bacteria. The lowest starting inocula of 2×10^5 showed the most growth of 1173%, 2×10^6 resulted in 998% growth, and 2×10^7 resulted

in the least growth of 642% (Fig. 5.4B). Growth of MRSA252 14 gene KO in plasma was 369, 464 and 434% for starting inocula of 2×10^5 , 2×10^6 and 2×10^7 respectively. suggesting that one or more of the deleted genes in MRSA252 14 gene KO is responsible. The increased growth with lowering starting inocula found in MRSA252 was not seen in MRSA252 14 gene KO, which achieved a lower percentage growth than MRSA252 at all starting inocula. The difference in percentage growth in plasma between MRSA252 and MRSA252 14 gene KO was statistically significant when a starting inoculum of 2×10^5 ($P = 0.0182$) was used, but not when 2×10^6 ($P = 0.158$) or 2×10^7 ($P = 0.8479$) was used.

The ability of 14-2533T and 14-2533T (pSCBU) to survive in blood varied depending on the initial inoculum (Fig. 5.4C). In general there was a trend towards a higher mean level of survival of 14-2533T (pSCBU) compared to 14-2533T, regardless of the number of bacteria in the starting inocula. However the differences were not significant.

The growth of 14-2533T and 14-2533T (pSCBU) in plasma was similar upon comparison between strains and different starting inocula (Fig. 5.4D). No statistically significant difference in growth in plasma between 14-2533T and 14-2533T (pSCBU) was detected.

Together these data show that across a 100-fold range of starting inocula, the 14 gene KO mutant of MRSA252 did not have a significant defect in survival in whole blood compared to wild-type MRSA252. However the failure to detect a significant difference in blood survival between 14-2533T and 14-2533T (pSCBU) under the conditions tested here suggests that further parameters should be tested in order to be able to replicate previously reported findings. Once conditions are met where previously reported findings are replicated, using these conditions will increase the robustness of investigations into the contribution of copper tolerance genes to survival of MRSA252 in blood.

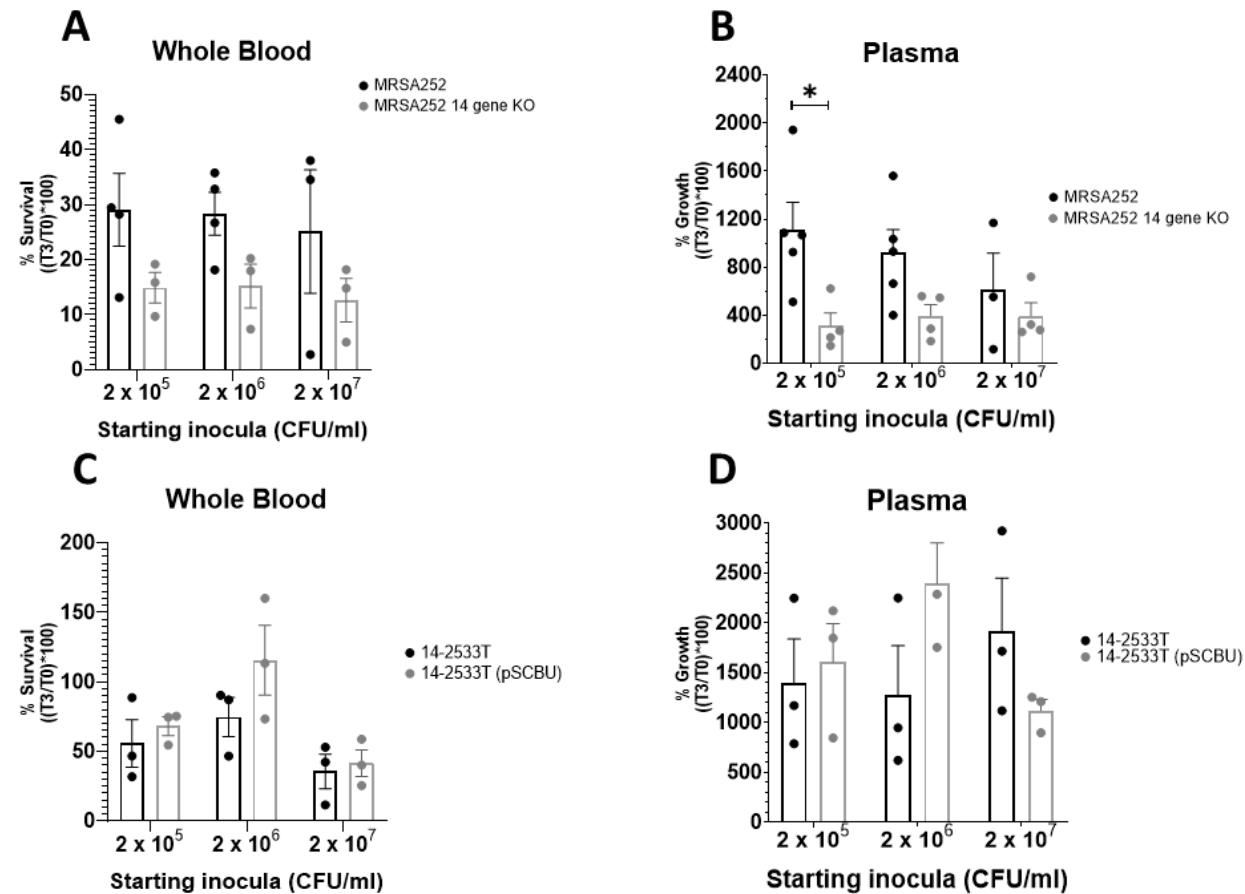


Figure 5.4 Survival of *S. aureus* in whole blood and growth in plasma when the initial inocula is changed

Washed bacteria were incubated with freshly drawn whole human blood (A+C) or plasma (B+D) with a starting inoculum of 2×10^5 , 2×10^6 or 2×10^7 . Percentage survival was calculate using CFU counts after 3 h growth (T3) expressed as a percentage of CFU counts at time point 0 (T0). $n \geq 3$. Error bars represent standard error of the mean. Statistical significance was determined by two-way ANOVA followed by Sidak's multiple comparison test. *, $P \leq 0.05$.

5.3.3 Whole blood survival of *S. aureus* grown in copper before incubation in blood and plasma

Previously, *mco* and *copB* were found to contribute to the survival of strain 14-2533T (pSCBU) in human blood (Zapotoczna *et al.*, 2018). However, the *copBmco* operon on plasmid pSCBU was not found to confer resistance to killing in whole human blood in the experiments described here (Fig. 5.4C). One possible explanation for this discrepancy is that the *copBmco* operon was not expressed sufficiently to confer a phenotype. Exposure of *S. aureus* to copper results in CsoR mediated de-repression of copper tolerance genes (Baker *et al.*, 2011). CsoR tightly represses the expression of *copBmco* in the absence of copper and the CsoR-mediated repression of *copBmco* expression is stronger for MRSA252 than 14-2533T (pSCBU) (Zapotoczna *et al.*, 2018). It was postulated that growth of *S. aureus* in copper prior to incubation in human blood would increase expression of *copB* and *mco* and increase bacterial survival.

Therefore *S. aureus* was grown in with a sub-inhibitory concentration of copper before inoculation into blood and plasma (Fig. 5.5). 3.125 μ M was used as it did not inhibit growth of MRSA252 in RPMI (Fig. 3.16A). There was no significant difference in the survival of MRSA252 in blood or growth in plasma compared to MRSA252 14 gene KO whether or not the bacteria were exposed to CuCl₂. Similarly, prior growth of 14-2533T and 14-2533T pSCBU in CuCl₂ did not alter survival in blood or growth in plasma.

In conclusion, under the experimental conditions employed in this study, growth of *S. aureus* in subinhibitory copper prior to incubation in whole blood did not enhance its survival. However these data remain inconclusive as the survival of 14-2533T was not reduced when compared to 14-2533T (pSCBU) as it is reported previously (Zapotoczna *et al.*, 2018).

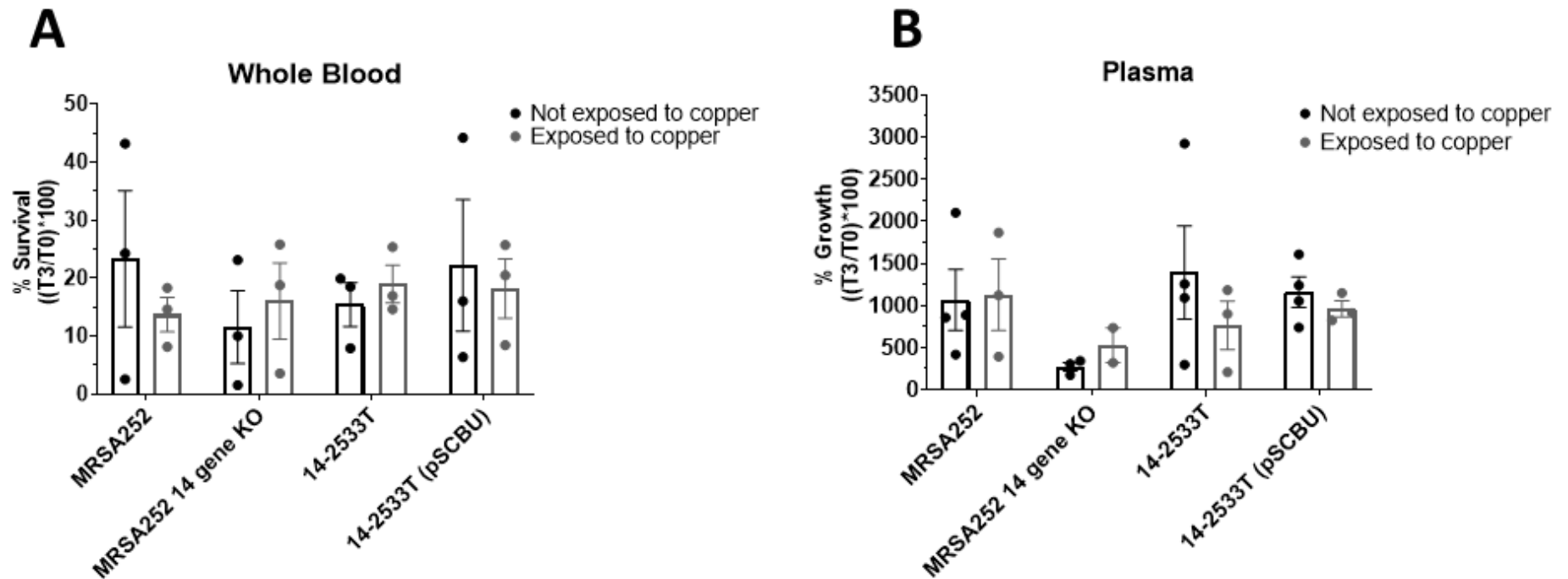


Figure 5.5 Whole blood survival and growth in plasma of *S. aureus* that had been grown in sub-inhibitory copper before incubation with whole human blood or plasma

S. aureus was grown in TSBd for 16 h, before 1:100 subculture and further growth in RPMI for 16 h with or without 3.125 μM CuCl_2 supplementation. Washed bacteria (2×10^6 CFU/ml) were incubated with freshly drawn whole human blood (A) or plasma (B). Percentage survival was calculate using CFU counts after 3 h growth (T3) expressed as a percentage of CFU counts at time point 0 (T0). $n \geq 2$. Error bars represent standard error of the mean. No statistical significance was observed by two-way ANOVA followed by Sidak's multiple comparison test.

5.4 Expression of copper importing genes in primary human neutrophils

Macrophages import copper into the phagolysosome and use it to enhance killing of phagocytosed microbes (White, Lee, *et al.*, 2009). This was demonstrated using mouse RAW 246.7 macrophage cell lines. Here, the expression of copper importing genes in primary human neutrophils was examined. It was hypothesized that human neutrophils upregulate the expression of the genes ATP7A and CTR1 when activated during inflammation. Here TNF- α was used to activate primary human neutrophils mimicking the inflammatory environment of an infected wound (Spaan *et al.*, 2013).

As a control, the expression of the human copper transporters CTR2 and ATP7B genes was also investigated. The ATP7B gene is involved in copper homeostasis associated with copper storage and use with vacuoles (Howell and Abada, 2010; Wee *et al.*, 2013). The CTR2 gene is involved in export of copper out of hepatic cells and loading copper atoms into ceruloplasmin before it is released into plasma (Chang and Hahn, 2017).

To determine if activated human neutrophils express the copper transporting genes ATP7A, ATP7B, CTR1 and CTR2, primary neutrophils purified from whole human blood were incubated with copper, TNF- α , or both for 1 h before RNA was extracted and quantitative RealTime-PCR was performed to measure the expression of these genes (Fig. 5.6).

When compared to unstimulated controls, the expression of ATP7A in neutrophils was 1.56 times higher in response to TNF- α , it was unchanged in response to copper alone, and was 2.54 times higher in response to TNF- α and copper (Fig. 5.6). This trend suggests that expression of ATP7A is greatest when both TNF- α and copper are present in the neutrophil environment. However statistical significance was not achieved in these experiments.

The expression of ATP7B in neutrophils was 3.43, 3.36 and 14.72 times higher in response to TNF- α , copper, and TNF- α + copper, respectively. This suggests that ATP7B transcription is increased in response to TNF- α or copper, and

both together further enhance expression more (Fig. 5.6). However, statistical significance was not achieved.

The expression of CTR1 was 7, 9.7 and 25.7 higher in the presence of TNF- α , copper, and TNF- α + copper, respectively (Fig. 5.6). Statistical significance was achieved when comparing TNF- α + copper to unstimulated cells, and comparing TNF- α + copper to TNF- α alone. This indicates that the human copper importing transporter is upregulated in primary human neutrophils when activated and in the presence of copper. This suggests that copper is important for human neutrophils when activated in *ex vivo* conditions.

The expression of CTR2 in neutrophils was 1.76, 3.86 and 1.13 times higher in the presence of TNF- α , copper, and TNF- α + copper, respectively (Fig. 5.6). This suggests that CTR2 is expressed in response to copper alone, and is not important in TNF-activated neutrophils as its expression is almost unchanged in comparison to unstimulated. However statistical significance was not achieved for CTR2 expression. Additional biological replicates are required.

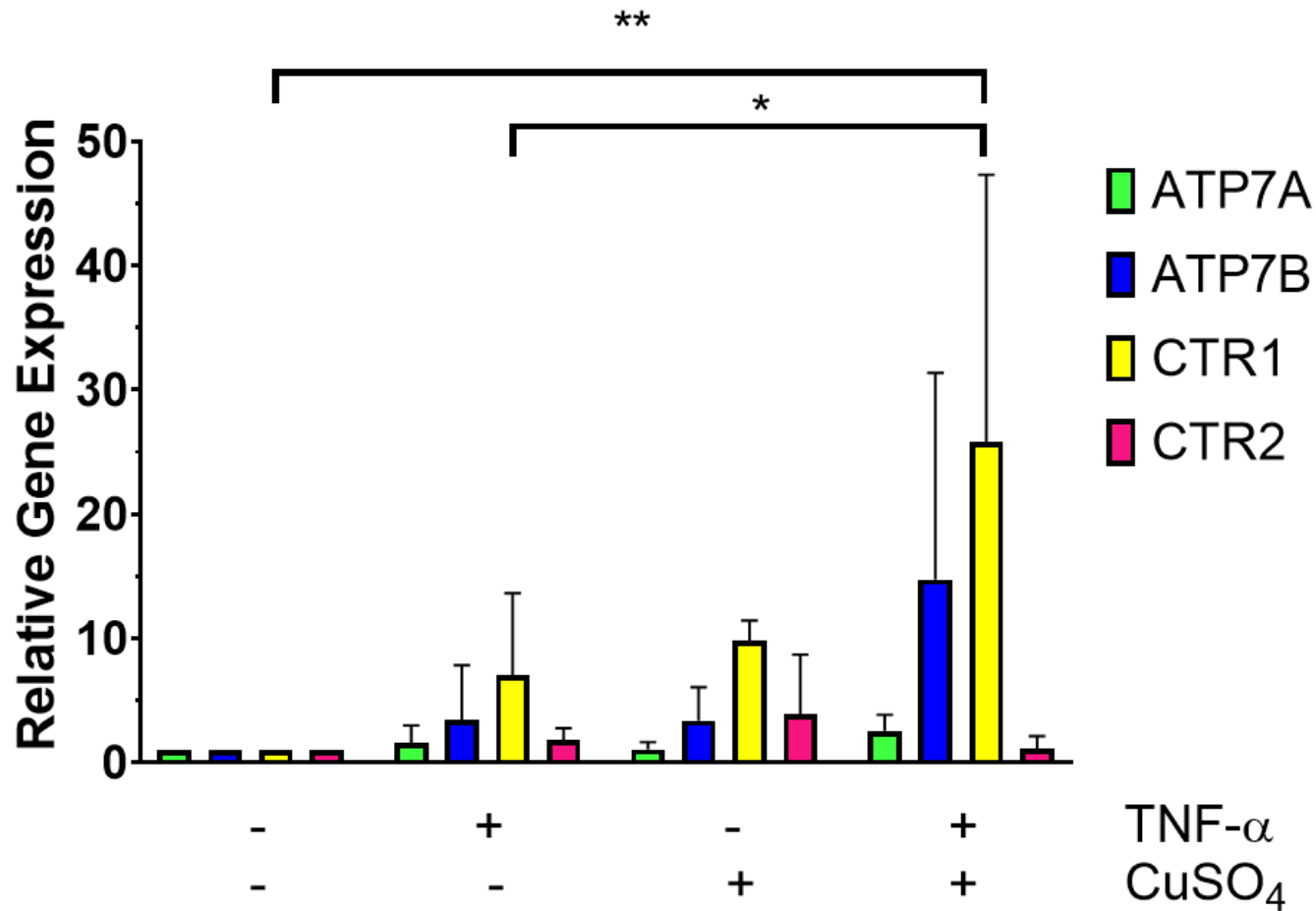


Figure 5.6. Expression of copper transporting genes in primary human neutrophils in response to copper and TNF-

α

Gene expression of the human copper transporters ATP7A, ATP7B, CTR1 and CTR2 in primary human neutrophils upon exposure to TNF- α (10 ng/ml) and copper (40 μ M CuSO₄) for 1 hour. n = 3. All gene amplifications were normalised to beta-actin and then presented as relative gene expression compared to copper transporter expression in the untreated control group. Statistical significance was determined by two-way ANOVA followed by Tukeys multiple comparisons test. *, P \geq 0.05, **, P \geq 0.01.

5.5 Survival of *S. aureus* when incubated with primary human neutrophils in RPMI

The contribution of copper tolerance to survival of *S. aureus* in human neutrophils has not been examined. Here, to determine if copper hypertolerance genes contribute to survival of MRSA252 in neutrophils, primary human neutrophils were purified from freshly drawn heparinised human blood and incubated with *S. aureus* wild type and mutants (Fig. 5.7). The bacterial numbers decreased over time throughout the experiment, indicating that neutrophils were killing the bacteria. However, no significant differences in survival were detected between the wild-type and different copper sensitive mutants of MRSA252 at any of the time points tested. Under the experimental conditions employed in this study copper hypertolerance genes do not contribute to survival of *S. aureus* in primary human neutrophils.

Neutrophils in RPMI

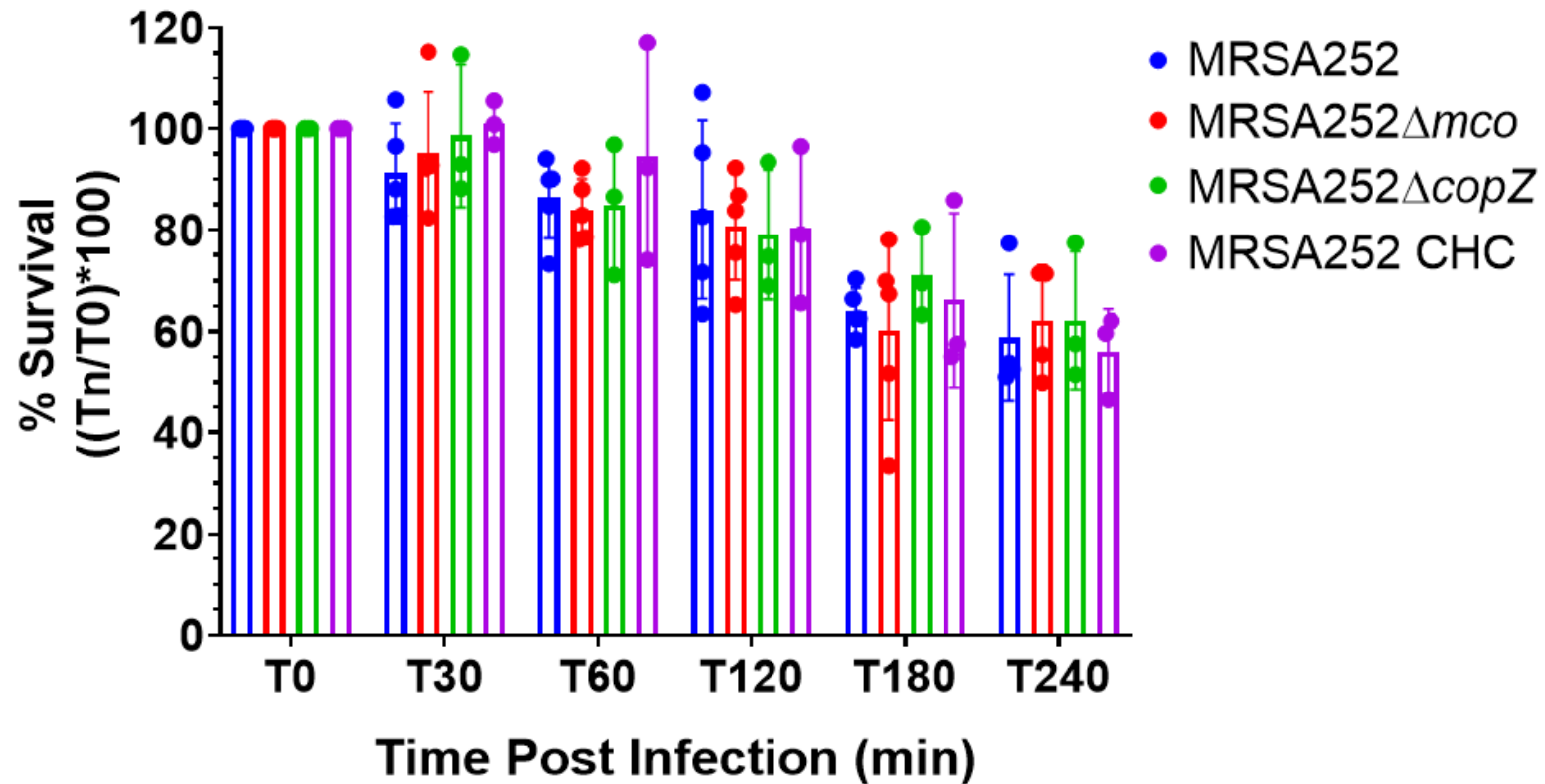


Figure 5.7 Survival of copper sensitive *S. aureus* mutants when incubated with primary human neutrophils in RPMI

Survival of copper sensitive strains of MRSA252 when incubated with primary human neutrophils at an MOI of 0.2 over the course of 4 hours, using RPMI as the primary medium for infection ($n \geq 3$). Error bars represent Standard error of the means. Statistical significance was investigated using two-way ANOVA followed by Sidak's multiple comparisons test comparing each strain to MRSA252 at each time point, no significant difference was detected for any strain at any individual time point.

5.5.1 The survival of *S. aureus* when incubated with primary human neutrophils in Hanks Balanced Salt Solution

A neutrophil infection assay was performed using slightly different conditions (Fig. 5.8). The media was changed from RPMI to Hanks Balanced Salt Solution (HBSS) as this was used previously for neutrophil infections (Ha *et al.*, 2020). The 4 h time point was replaced with a 24 h time point, and the main test strains MRSA252 and MRSA252 Δ *mco* were included. The percentage survival of *S. aureus* was calculated at 0.5, 1, 2, 3 and 24 hours post infection (Fig.5.8).

There was a general trend for all *S. aureus* strains to decrease in percentage survival over the course of the infection. The two exceptions were MRSA252 Δ *mco*::pCL55::UCMF and MRSA252 Δ *mco*::pCL55::UCMF Δ 2-53 which showed an increase in survival compared to wild-type 0.5, 1 and 2 h post infection (Fig.5.8). This was statistically significant for MRSA252 Δ *mco*::pCL55::UCMF Δ 2-53 at 1 hour post infection and for MRSA252 Δ *mco*::pCL55::UCMF at 2 hours post infection. Both of these strains carry an additional copy of *copB* and *mco* integrated into the chromosome although the Mco protein expressed by MRSA252 Δ *mco*::pCL55::UCMF Δ 2-53 is not functional (Fig. 3.12) indicating that the second copy of *copB* is likely to be important.

Although statistical significance was not achieved, at 3 hours post infection MRSA252 Δ *mco*::pCL55::UCMF survived better than all other strains including the strain expressing a truncated form of Mco (Fig.5.8). This suggests that *mco* can contribute to survival in neutrophils when expressed with an extra copy of *copB*, but after 3 hours post infection. Additional biological replicates of this experiment are required to determine if *mco* present on the UCMF insert confers a survival advantage to *S. aureus* in neutrophils.

The mean survival of the MRSA252 14 gene KO (45%) was reduced compared to wild-type (64%) at 3 h post infection (Fig. 5.8). This is not statistically significant. Once again this trend may become statistically significant with the additional replicates.

No difference in survival was detected comparing MRSA252, MRSA252 Δ *mco* and MRSA252 Δ *mco*::pCL55, suggesting that *mco* deletion alone does not contribute to survival of *S. aureus* in human neutrophils.

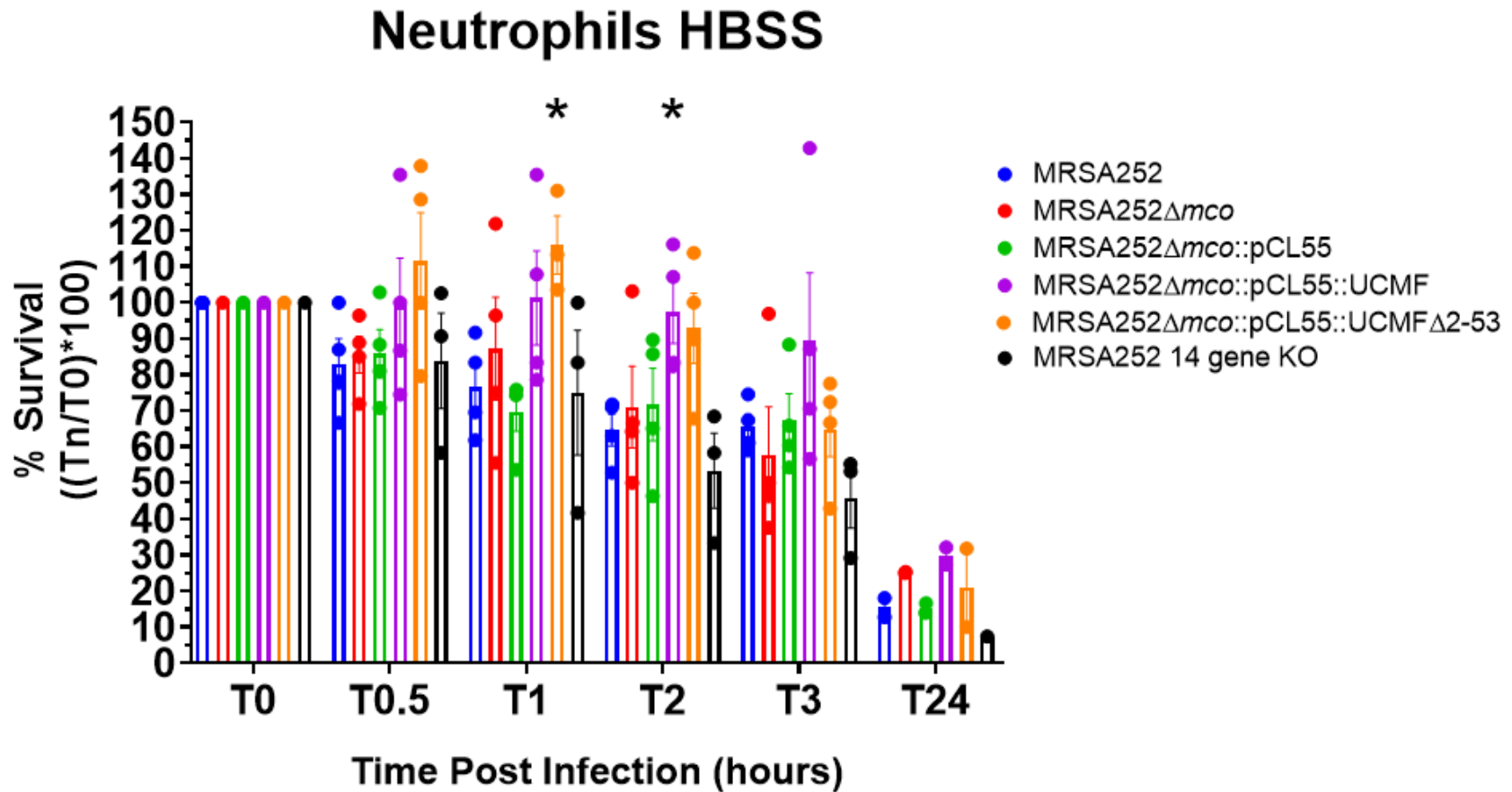


Figure 5.8. Survival of *mco* mutant derivatives of *S. aureus* when incubated with primary human neutrophils in HBSS

Survival of *mco* deletion mutants when incubated with primary human neutrophils at an MOI of 0.2 over the course of 24 hours, using HBSS as the primary medium for infection ($n \geq 3$ for time points up to T3). Error bars represent Standard error of the means. Statistical significance was investigated using two-way ANOVA followed by Sidak's multiple comparisons test comparing each strain to MRSA252 at each time point. *, $P = \leq 0.05$.

5.5.2 The survival of copper sensitive mutants of *S. aureus* in primary human neutrophils

To investigate if other copper tolerance genes contribute to survival of *S. aureus* when incubated with neutrophils, MRSA252 and a panel of copper sensitive mutants were tested. Isogenic deletion mutants of *cadA*, *cadAC*, *mco cadA*, *mco cadAC*, *copZ* and MRSA252 14 gene KO were incubated with primary human neutrophils and survival after 0.5, 1, 2, 3 and 24 hours was monitored (Fig. 5.9).

The survival of MRSA252, MRSA252 Δ *cadA*, MRSA252 Δ *cadAC*, MRSA252 Δ *mco* Δ *cadA*, MRSA252 Δ *mco* Δ *cadAC* and MRSA252 Δ *copZ* was similar at all time points during the infection, indicating that deletion of these genes does not affect survival of *S. aureus* in human neutrophils.

Neutrophils HBSS

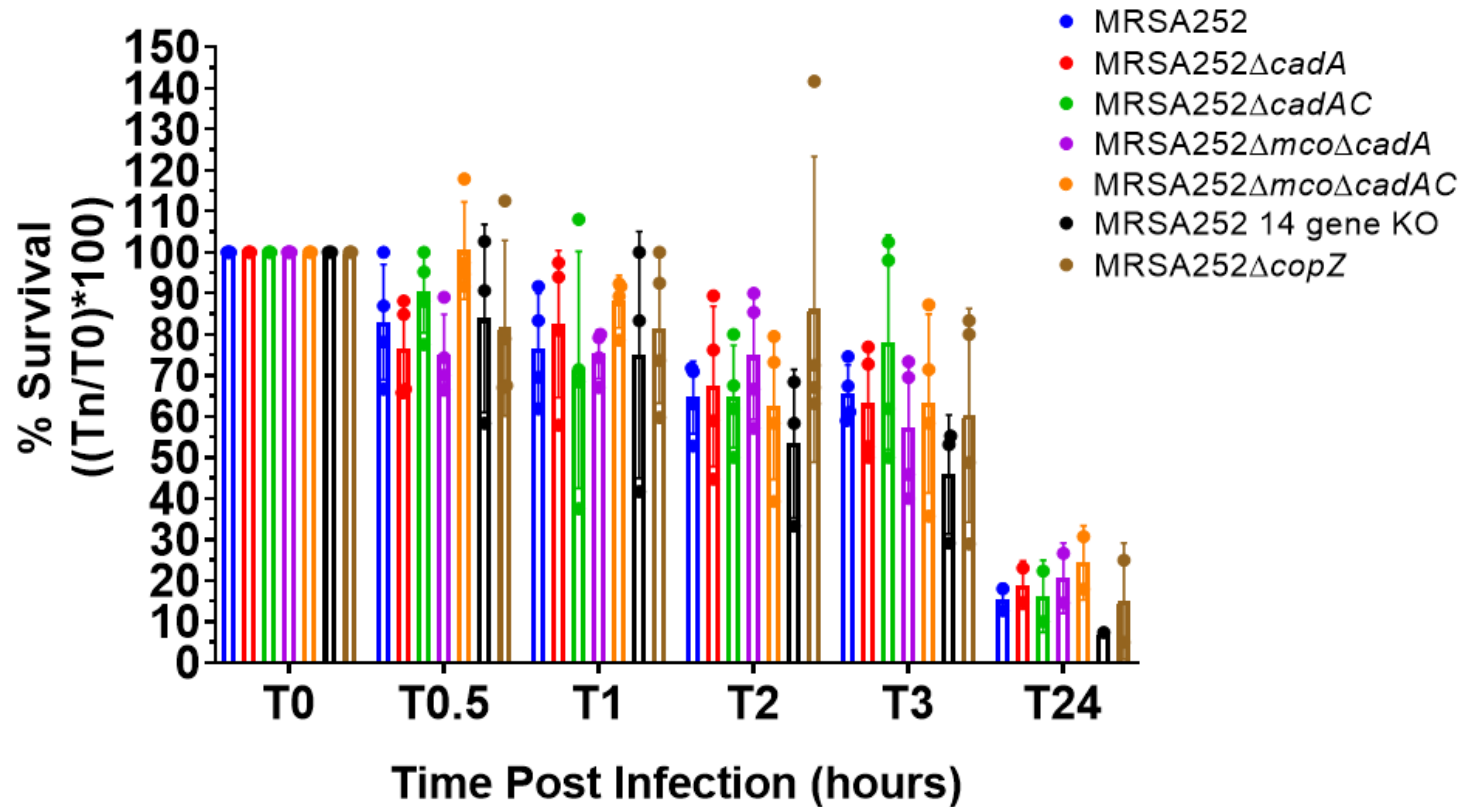


Figure 5.9 Survival of copper sensitive *S. aureus* deletion mutants when incubated with primary human neutrophils in HBSS

Survival of *cadA*, *cadAC*, 14 gene KO and *copZ* deletion mutants when incubated with primary human neutrophils at an MOI of 0.2 over the course of 24 hours, using HBSS as the primary medium for infection ($n = 4$ for time points up to T3). Error bars represent Standard error of the means. Statistical significance was investigated using two-way ANOVA followed by Sidak's multiple comparisons test comparing each strain to MRSA252 at each time point. No statistical significance was obtained.

5.6 Neutrophil survival of *S. aureus* *rexB*

Ha and colleagues reported that a *rexB*-deficient mutant of USA300 strain JE2 had a survival defect in human neutrophils compared to wild-type. The *rexB* gene contributes to DNA repair in *S. aureus*. As a control for the experimental conditions survival of JE2 and JE2 *rexB::erm* (Ha *et al.*, 2020) were compared following incubation with primary human neutrophils for 0.5, 1, 2, 3 and 24 hours (Fig. 5.10A). There was a trend towards poorer survival of the JE2 *rexB::erm* mutant when incubated with human neutrophils, compared to JE2 (Fig. 5.10A). However, there was a high degree of variation between experiments and the differences were not significant. Nevertheless the consistently reduced survival of JE2 *rexB::erm* in each individual experiment when compared to JE2 served as a reliable control to indicate that the experimental set up permitted appropriate neutrophil killing.

5.7 Neutrophil survival of an *S. aureus* 14-2533T and 14-2533T pSCBU

The contribution of the plasmid pSCBU to copper tolerance and resistance to killing in whole blood has been reported previously (Zapotoczna *et al.*, 2018). In an effort to discern if this improved survival phenotype was a result of resistance to killing by neutrophils, the survival of 14-2533T and 14-2533T pSCBU was monitored after incubation with primary human neutrophils for 0.5, 1, 2, 3 and 24 hours (Fig. 5.10B). The percentage survival of 14-2533T and 14-2533T pSCBU was similar throughout the entire experiment. These data indicate that carriage of the plasmid pSCBU does not improve survival of 14-2533T during incubation with primary human neutrophils under the conditions employed here.

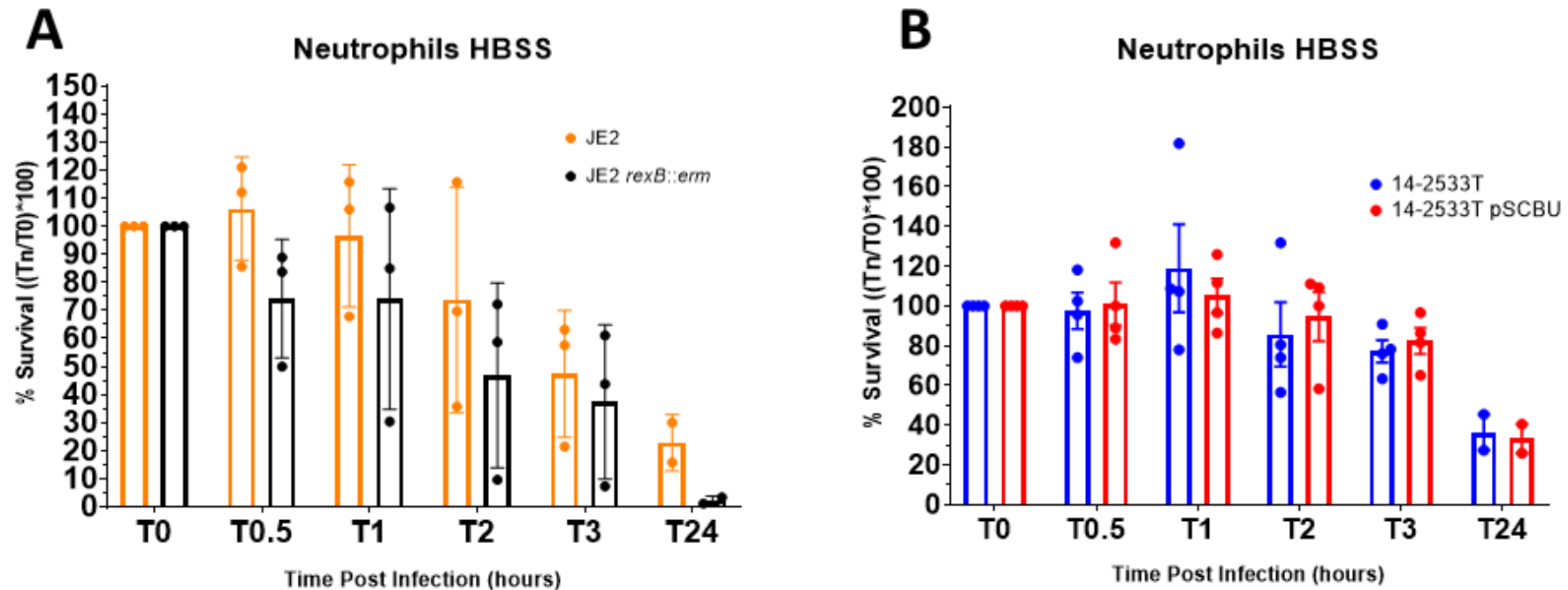


Figure 5.10 Survival of control *S. aureus* strains JE2 and 14-2533T with human neutrophils

(A) Survival of JE2 and its *rexB* disrupted mutant when incubated with primary human neutrophils at an MOI of 0.2 over the course of 24 hours, using HBSS as the primary medium for infection ($n = 3$ for time points up to T3). Error bars show the standard error of the mean. Statistical significance was investigated using two-way ANOVA followed by Sidak's multiple comparisons test comparing the *rexB* mutant to JE2 at each time point. None of the differences were significant.

(B) survival of 14-2533T and 14-2533T pSCBU when incubated with primary human neutrophils at an MOI of 0.2 over the course of 24 hours, using HBSS as the primary medium for infection ($n = 4$ for time points up to T3). Error bars represent Standard error of the means. Statistical significance was investigated using two-way ANOVA followed by Sidak's multiple comparisons test comparing 14-2533T to 14-2533T pSCBU at each time point. No statistical significance was obtained.

5.8 Discussion

This chapter aimed to investigate the contribution of copper hypertolerance genes to the survival of *S. aureus* in immune cells. The copper sensitive MRS252 14 gene KO mutant was more susceptible to killing in the murine macrophage cell line, RAW264.7 cells than wild-type MRSA252 (Fig. 5.1). This prompted investigation into whether copper tolerance genes in MRSA252 contribute to survival during incubation in whole blood and primary human neutrophils which are more relevant to human infection. However the survival of this mutant and of mutants of MRSA252 deficient in *mco*, *cadA*, *cadAC*, *mco cadA*, *mco cadAC*, and *copZ* in whole human blood was similar to the wild-type suggesting that these genes were not required for blood survival under the conditions tested here (Fig. 5.2-3). Experimental conditions were altered by varying the number of cells in the starting inocula of *S. aureus* and by prior exposure of *S. aureus* to copper in to attempt to identify conditions where copper tolerance contributes to survival in blood. However no contribution of copper tolerance genes to survival in blood was detected (Fig. 5.4-5).

Changing the input CFU did not affect the survival of MRSA252 in whole blood in contrast to 14-2533T. Prior exposure of *S. aureus* to copper did not alter survival after 3 h (Fig. 5.5). The expression of copper transporting genes in activated primary human neutrophils showed that CTR1 was upregulated by copper, TNF- α , and both copper and TNF- α combined (Fig. 5.6). This indicated that copper is trafficked into the cytoplasm when neutrophils are activated. This is the first report that human neutrophils upregulate the expression of the copper importing gene CTR1 when activated, suggesting that copper is important during human infection. Following this discovery, the survival in neutrophils of a panel of copper sensitive and resistant mutants of MRSA252 was investigated (Fig. 5.6-10). All *S. aureus* strains were killed to the same extent by neutrophils. A strain carrying an extra copy of *copB*, or *copBmco*, had improved survival compared to wild-type (Fig. 5.6). However the reduction in survival of a control strain that had previously been shown to be very sensitive to neutrophil killing was not reproduced here (Fig. 5.9A).

The precise mechanism by which copper damages *S. aureus* is not fully understood. The two main mechanisms of copper damage *ex vivo* appear to be by

the generation of the highly reactive hydroxyl radicals by Haber-Weiss and Fenton-like chemistry (Haber and Weiss, 1934) and by mis-metalation of metalloproteins (Irving and Williams, 1953). This can result in the disruption of Fe-S clusters in proteins, generate non-native disulfide bonds, cause mis-metalation of copper in metalloproteins, glutathione depletion and lipid peroxidation damage (Djoko, Achard and McEwan, 2004; White, Lee, *et al.*, 2009; Dupont, Grass and Rensing, 2011). The bactericidal effects of copper are evidently multifaceted which is likely why the host utilises the metal to boost intracellular killing of pathogens. This is also likely why bacteria have multiple mechanisms of copper resistance. A panel of copper tolerance gene mutants was used in this chapter to try to determine if any particular copper detoxification mechanism is more important for survival within host immune cells. Integrating an additional copy of the entire *copBmco* operon into the chromosome of MRSA252 Δ *mco* improved the survival of *S. aureus* in human neutrophils. This result was unanticipated and suggests that *copB* increases the ability of *S. aureus* to withstand killing by neutrophils. This effect was independent of the activity of *mco* since neutrophil survival was similar when an extra copy of *copB* was paired with a functional copy of *mco* (pCL55:UCMF) or inactive *mco* (pCL55:UCMF Δ 2-53)(Fig. 3.12). This shows that *copB* promotes survival of *S. aureus* in neutrophils when it is under the control of its native promoter on the *S. aureus* chromosome and that strains with two copies of *copB* have an advantage over strains with a single copy of the gene. This is important when it is considered that the *copBmco* operon is located on MGEs in *S. aureus*, in many cases on plasmids (Baker *et al.*, 2011). Strains with multiple copies of plasmid-borne *copB* may have an advantage over strains with a single copy. Despite the advantage conferred by an additional copy of *copB* in increasing bacterial survival within neutrophils, this did not translate into an increase in survival during incubation of bacteria in whole blood. This suggests that additional killing mechanisms are at play in whole blood and that the expression of an additional *copB* gene alone is not sufficient to overcome them. Future experiments should examine if deletion of *copB* from MRSA252 reduces its survival in human neutrophils. This would likely be completable using the strategy employed in this study using pCL55 to integrate the gene into the chromosome under the control of its native promoter.

RAW264.7 macrophages were used to attempt to generate data comparable to that published by others, and because the protocol for infecting murine macrophages is well established (White, Lee, *et al.*, 2009; Purves *et al.*, 2018; Zapotoczna *et al.*, 2018). The RAW264.7 infection experiment indicated that the copper sensitive mutant MRSA252 14 gene KO had a reduced survival in macrophages, similar to other copper sensitive mutants (Purves *et al.*, 2018; Zapotoczna *et al.*, 2018). This indicates another copper sensitive mutant had a reduced intracellular survival in macrophages. The combined *in vitro* murine macrophage data generated here and previously (Fig. 5.1), (White, Lee, *et al.*, 2009; Purves *et al.*, 2018; Zapotoczna *et al.*, 2018) provided sufficient evidence to begin investigation into the role of *S. aureus* copper tolerance genes in resisting killing by human blood and neutrophils.

Findings in this chapter inform future work for studying *S. aureus* copper tolerance and *ex vivo* primary human immune cells. There was massively reduced survival of *S. aureus* with neutrophils at 24 hours post infection (Fig. 5.8-10). This experiment should be repeated with additional time points for example 4, 6, 8, 12, 16, 24, 36 and 48 hours post infection. A thorough examination of different time points during infection may allow detection of a differences for specific mutants. This could show that different genes contribute to resistance to killing in human neutrophils at different stages of infection. For example one gene might improve survival at the beginning of infection while another might improve long term survival. The time points investigated in this chapter were outside of the scope of resolution required to discern such phenotypes.

To improve the understanding of the relationship between copper tolerance and immune resistance, a library of isogenic mutations of known copper genes in MRSA252 should be generated. This would require generation of deletions of *copA*, *copAZ*, *copB*, *copBmco*, *csaR* and any yet to be identified copper tolerance gene(s) present in MRSA252 14 gene KO. A copper sensitive mutant defective in *copAZ* and *copBL* was generated recently by Al-Tameemi and colleagues (Al-Tameemi *et al.*, 2020) which demonstrated the value of generating multiple mutations to shown the combined role of multiple copper tolerance genes. Generation of additional mutations in copper tolerance genes along with *copAZ* and *copBmco* mutations

would aid future studies of copper tolerance in MRSA252 and its survival in host immune cells. In addition, a transposon mutant library of MRSA252 could be generated and screened for copper sensitive mutants. The importance of the *mntABC* operon in copper import was discovered by generating a transposon library of their USA300 strain $LAC\Delta copAZ\Delta copBL$ (Al-Tameemi *et al.*, 2020).

One mechanism by which neutrophils kill *S. aureus* is through the generation of ROS (Hampton, Kettle and Winterbourn, 1996). If a role for copper tolerance in resisting killing by host immune cells in an *ex vivo* environment could be identified, it would be interesting to determine if this was due to increased resistance to ROS-mediated damage. The use of the NADPH inhibitor diphenyleneiodonium (DPI) as a control for ROS-mediated damage can identify any relationship between ROS-mediated damage and bacterial genes or mammalian cells including human neutrophils (Hampton and Winterbourn, 1995; Hampton, Kettle and Winterbourn, 1996; Ha *et al.*, 2020). Inhibition of ROS generation should restore survival of both WT and mutant to similar levels if the primary protection offered by copper hypertolerance genes is to ROS-mediated killing in host immune cells. DPI can be used to inhibit ROS generation in RAW 264.7 cells (Zhao *et al.*, 2010). The *in vitro* RAW264.7 macrophage survival data generated in figure 5.1 were robust and statistically significant. Repetition of this experiment using DPI to inhibit ROS mediated killing by macrophages would inform if a copper sensitive mutant was sensitive to ROS-mediated intracellular killing.

RPMI is routinely used for the culture of neutrophils and *S. aureus* grows in this medium. Two different media were used for neutrophil survival experiments, RPMI and HBSS. RPMI contains an abundance of amino acids (Moore and Hood, 1993) while HBSS lacks amino acids (Hanks, 1975). Using HBSS should have prevented *S. aureus* growth from obscuring the killing effects of neutrophils. Only in HBSS were any statistically significant differences in neutrophil survival observed between wild type and mutants of *S. aureus* (Fig. 5.8). The growth of *S. aureus* in both media could be monitored over time and compared. This could indicate if bacterial growth in infection media has an impact on neutrophil infection experiments.

Unexpectedly MRSA252 14 gene KO had a significantly reduced ability to grow in plasma compared to the wild-type (Fig. 5.2, 3 and 4). This suggests that there is a gene missing in the MRSA252 14 gene KO mutant that is required for growth of *S. aureus* in plasma, and by extension blood. It remains to be determined if this gene improves growth in plasma or if it contributes resistance to a bactericidal activity. While complement can readily kill Gram-negative bacteria via the membrane attack complex, complement is unable to kill Gram-positive bacteria including *S. aureus* (Müller-Eberhard, 1986). The reduced growth of MRSA252 14 gene KO in plasma will allow identification of a factor or factors important for growth in human plasma, and by extension human blood. Full growth analysis monitored by both changes in OD₆₀₀ readings and CFU counts over 24 hours, with MRSA252, MRSA252 14 gene KO and isogenic deletion mutants of all 14 genes (three of which were generated in this study) in freshly drawn human plasma would identify which gene is responsible for this phenotype. Competition assays between MRSA252 and MRSA252 14 gene KO co-incubated in plasma would provide additional data that measures how important the gene/genes responsible for the growth defect in plasma are to MRSA252.

The copper sensitive strain MRSA252 14 gene KO exhibited a trend of reduced survival in primary human neutrophils (Fig. 5.9), suggesting the importance of at least one of 11 uncharacterised deleted genes in that strain. This result was unanticipated and deserves further research. This experiment should be repeated further to determine if a statistically significant reduction in survival is observed. This reduction in survival of MRSA252 14 gene KO suggests that one or more of its deleted genes contributes to survival in neutrophils. The deletion of the *mco*, *cadA*, *cadAC*, or combination of *mco* and *cadAC* genes did not reduce survival of MRSA252 similar to MRSA252 14 gene KO (Fig. 5.8), suggesting that deletion of these genes alone are not responsible for the survival defect seen for MRSA252 14 gene KO. The disruption of genes in MRSA252 14 gene KO was extensive (Fig. 4.2), suggesting that a combination of mutations is responsible for the reduced survival of MRSA252 14 gene KO in neutrophils. It is also possible that one of the uncharacterised hypothetical protein gene deletions in deletion 3 is responsible for the reduced survival of MRSA252 14 gene KO in neutrophils. This highlights the importance of isolating mutations in specific targeted genes to identify that which is

causing reduced survival of MRSA252 in neutrophils. It is also possible that the behaviour of MRSA252 14 gene KO could be due to disruption of a small RNA regulatory system rather than one of the open reading frames.

Considerably donor to donor variation occurred in the whole blood experiments (Fig. 5.2A, 5.3A, 5.4A, 5.4C, 5.5A). The best way to reduce variation is to increase the number of donors/data points in the dataset. However, time and resources were a factor and careful judgement was used as to whether to perform additional whole blood survival experiments. Many biological replicates were performed in investigating the contribution of *mco* to survival in whole blood (Fig. 5.2A) to determine if increasing replicates revealed a statistically significant change in survival for MRSA252 Δ *mco*. This was not achieved, so in later whole blood experiments (Fig. 5.3A, 5.4A, 5.4C, 5.5A) only 3 - 4 replicates were performed. If a change in phenotype was not apparent with 3 - 4 replicates, alteration of experimental conditions was prioritised over further replicates. This provides a stronger foundation for future work.

No difference in survival was detected for bacteria grown in the presence of copper prior to incubation in blood, when compared to bacteria grown in the absence of copper (Fig. 5.5). This experiment could be optimised in further work. The CsoR-mediated expression of *copBmco* could be analysed by growth in different copper concentrations and quantification of RNA transcripts of *copBmco* by qRT-PCR. Furthermore, copper induced protein expression could be quantified by performing Western immunoblotting on membrane fractions of MRSA252 Δ *mco*::pCL55::UCMF grown in the presence of different copper concentrations, as in the *copBmco* expression analysis. These experiments would identify the lowest concentration of copper that increases expression of *copBmco* and the concentration of copper results in maximum expression of *copBmco*. Combining these data with growth analysis in different concentrations of copper (Fig. 3.16 and 17) would greatly improve the understanding of CsoR mediated-gene expression and function of copper tolerance genes. A concentration of copper that permits maximum expression of *copBmco* without attenuating growth of MRSA252 could be identified and then used the increase expression of *copBmco* prior to incubation in whole blood or neutrophils.

For each individual neutrophil infection experiment performed using strains JE2 and JE2 *rexB::erm*, the percentage survival of the *rexB* mutant was less than wild-type. This phenotype was expected from reports in the literature (Ha *et al.*, 2020). However no significant difference was detected between JE2 and JE2 *rexB::erm* when experiments were combined in Fig. 5.10A. This suggests that the large variation of survival of *S. aureus* between donors may have resulted in the lack of significance. To avoid this drawback in future, more donors should be used in neutrophil survival experiments to reduce variation and increase the likelihood to detect statistically significant differences.

5.9 Results Chapter 3 Summary

- MRSA252 14 gene KO is more sensitive to intracellular killing in RAW264.7 cells than MRSA252.
- No significant difference in survival in whole blood was detected for any copper sensitive strains of *S. aureus* tested.
- Primary human neutrophils express CTR1 in response to TNF- α , suggesting copper is desired by neutrophils during infection.
- The MRSA252 14 gene KO mutant has a strong, statistically significant growth attenuation in human plasma compared to wild-type.
- An Additional copy of *copB* or *copBmco* to MRSA252 Δ *mco* resulted in a statistically significant increase in survival of *S. aureus* when incubated with primary human neutrophils.
- Isogenic deletion of *mco*, *cadA*, *cadAC*, *mco cadA*, *mco cadAC*, *copZ* or inactivation of *csoR* from MRSA252 did not alter percentage survival when incubated with primary human neutrophils.

Chapter 6

Results Chapter 4 - The effect of copper on biofilm formation of biofilm positive clinical isolates of *S. aureus*

6.1 Introduction

Medical device related infections are often caused by biofilm formation on the implanted devices by pathogens such as *S. aureus* (O'Neill *et al.*, 2008). These infections are extremely difficult to treat as they are often tolerant to conventional antimicrobial therapies (Bui, Conlon and Kidd, 2017). Biofilms are difficult to treat with antimicrobials due to a number of factors. The production of an extracellular polymeric matrix protects bacteria by making it more difficult for antimicrobials to penetrate into the biofilm, and the slower growth of some cell populations in a biofilm reduces the effectiveness of many antimicrobials that require metabolic activity to destroy microorganisms (Ciofu *et al.*, 2022). Ultimately biofilm infected implants often require surgical removal of the infected implant and long-term antimicrobial therapy (Zimmerli and Moser, 2012), increasing the burden and cost on global healthcare systems significantly.

S. aureus commonly generates biofilms on biotic and abiotic surfaces within the human body (Schilcher and Horswill, 2020). The effect of copper on biofilm formation remains relatively unexplored. The effect of copper, manganese, magnesium and calcium on *S. aureus* biofilm formation in an iron-restricted environment has been investigated previously (Baker *et al.*, 2010). Copper, but not manganese, magnesium or calcium, reduced biofilm formation of *S. aureus* strain Newman when grown in the iron restricted conditions of CRPMI (Baker *et al.*, 2010). Newman has been shown to form a protein-mediated biofilm in iron restricted conditions mediated by proteins Eap and Emp (Johnson, Cockayne and Morrissey, 2008). Baker and colleagues demonstrated that copper repressed expression of *eap*, likely by repression of the positive biofilm regulators *agr* and *sae* (Baker *et al.*, 2010). The iron-regulated surface determinant C (IsdC) protein of *Staphylococcus lugdunensis* promotes biofilm formation in iron restricted conditions, indicating that staphylococci can modulate biofilm formation in response to metal ion presence (Missineo *et al.*, 2014). The copper tolerance operon *copYAZ* of *Streptococcus mutans* has been shown to contribute to the ability of *S. mutans* to form biofilm in the presence of copper (Singh *et al.*, 2015). Adequate zinc import is required for *S. mutans* to form biofilm as either zinc chelation or deletion of the zinc importing genes *adcC* and *adcB* impairs biofilm formation (Ganguly *et al.*, 2021).

In this chapter, the effect of copper on biofilm formation of *S. aureus* is examined. Strains of *S. aureus* with well characterised biofilm phenotypes were chosen for investigation. Representative strains from a diverse background of clinically relevant strains were also chosen, such as MRSA and MSSA isolates from medical device related infections, strains isolated from sputum samples of cystic fibrosis patients with chronic *S. aureus* infection, and hospital associated MRSA isolated from fatal bacteraemia.

6.2 Results

6.2.1 The effect of copper on biofilm formation of MRSA252

The ability of MRSA252 (Fig. 6.1A) and MRSA252 14 gene KO (Fig. 6.1B) to form a biofilm in the presence of different concentrations of copper was examined. MRSA252 was chosen as it forms a protein-dependent biofilm when grown in BHI supplemented with glucose (1% w/v) (Feuillie *et al.*, 2017), its genome has been sequenced (Holden *et al.*, 2004), and the copper tolerance profile of both MRSA252 (Fig. 3.12-17) and MRSA252 14 gene KO (Fig. 4.4-5) has been established previously. MRSA252 14 gene KO was included as a copper sensitive control, to determine if copper tolerance contributed to the ability of *S. aureus* to generate a biofilm in copper supplemented biofilm forming conditions.

To determine if copper affects biofilm formation of MRSA252, MRSA252 was grown in BHI+ 1% glucose supplemented with 0, 0.0625, 0.125, 0.25, 0.5 and 1 mM CuCl₂ for 24 hours, after which biofilms were gently washed with PBS to remove planktonic bacteria, stained with crystal violet, and solubilised in acetic acid before OD₅₇₀ values were measured (Fig. 6.1A). MRSA252 formed a robust biofilm in the absence of copper, but biofilm formation was reduced upon supplementation of the growth medium with copper (Fig. 6.1A). This reduction in biofilm formation was statistically significant in the presence of ≥ 0.125 mM CuCl₂ (Fig. 6.1A). Copper-mediated biofilm reduction appeared to reach a maximum at 0.25 mM CuCl₂ as the reduction in biofilm formation seen at 0.5 and 1 mM CuCl₂ is similar to 0.25 mM CuCl₂ (Fig. 6.1A).

To determine if copper tolerance genes contribute to biofilm formation of *S. aureus* when grown in biofilm forming conditions and copper, the ability of the copper sensitive mutant MRSA252 14 gene KO to form biofilm in the presence of copper was examined (Fig. 6.1B). Similar to MRSA252, MRSA252 14 gene KO formed a robust biofilm in the absence of copper, and a significant reduction in biofilm formation was observed in the presence of 0.25 mM CuCl₂ or higher (Fig. 6.1B).

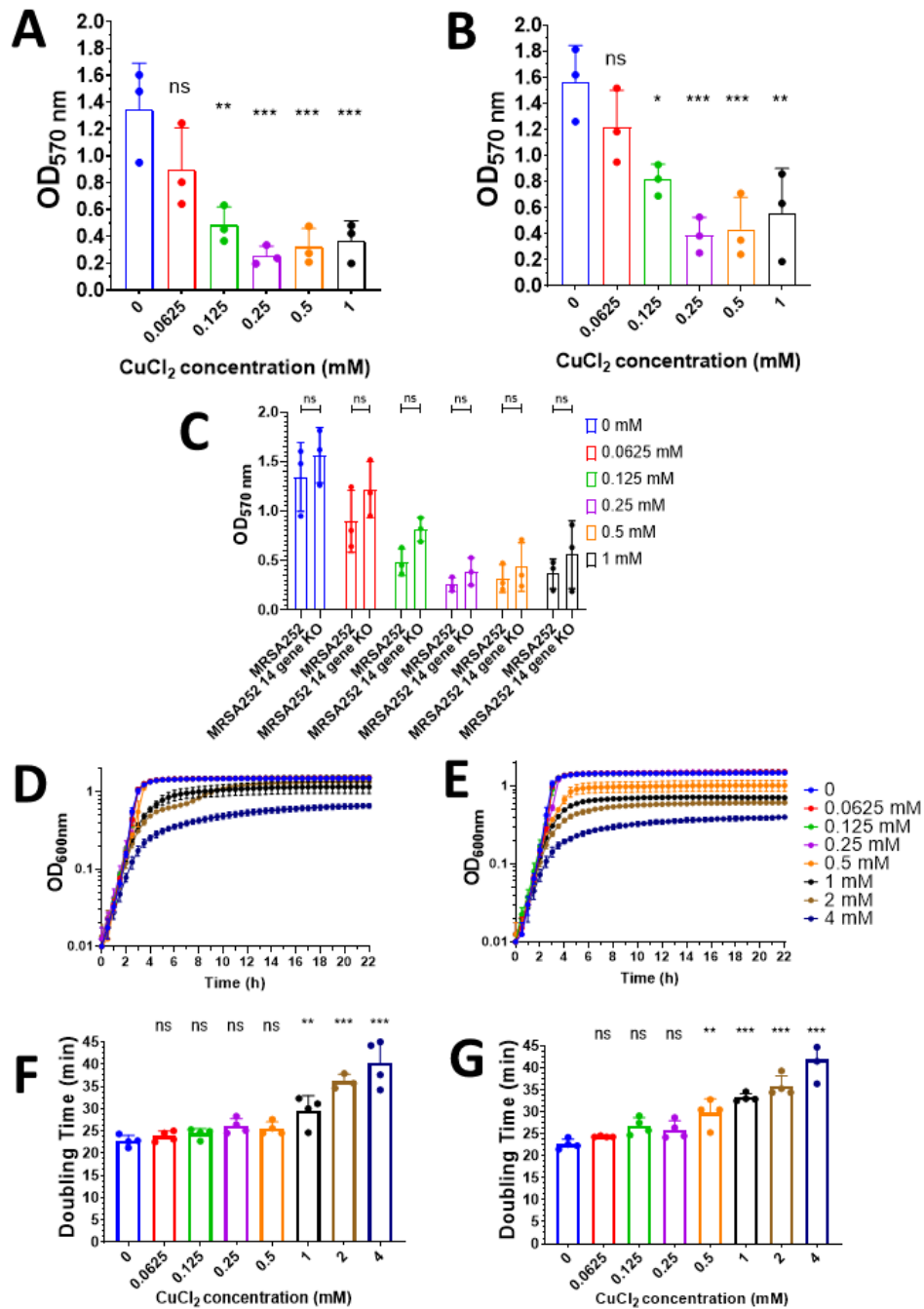


Figure 6.1 Copper reduces biofilm formation of MRSA252

Biofilm formation of MRSA252 (A) and MRSA252 14 gene KO (B) when grown in BHI + 1% glucose supplemented with copper. Comparison of biofilm formation of MRSA252 and MRSA252 14 gene KO at each concentration of copper tested (C). Growth of MRSA252 (D) and MRSA252 14 gene KO (E) in BHI + 1% glucose supplemented with copper. The doubling times of MRSA252 (F) and MRSA252 14 gene KO (G) in BHI + 1% glucose supplemented with copper were calculated using GrowthRates software. Biofilms were allowed to form for 24 h at 37°C under static conditions in microtitre plates. Biofilm was stained with crystal violet and absorbance was measured at 570nm. Graphs (A), (B), (F) and (G) were analysed by one-way ANOVA, with Dunnett's multiple comparisons test comparing each concentration of copper to 0 mM copper for each graph. Graph (C) was analysed by two-way ANOVA, with Sidak's multiple comparisons test. ns, not significant; *, $P < 0.05$; **, $P < 0.01$; ***, $P < 0.001$. Error bars represent SD.

To determine if copper tolerance contributes to biofilm formation in the presence of copper, the data in Fig. 6.1A and 6.1B were replotted to allow comparison between the two strains (Fig. 6.1C). There was no significant difference detected in biofilm formation between MRSA252 and MRSA252 14 gene KO at each concentration of copper, indicating that copper tolerance does not contribute to *S. aureus* biofilm formation in the presence of copper.

It was postulated that the reduction in biofilm formation of MRSA252 was due to copper mediated reduction in growth of *S. aureus*. To determine if supplementation of the biofilm growth media with copper reduced the growth in the planktonic phase, the copper tolerance profile of MRSA252 and MRSA252 14 gene KO was established in biofilm growth medium (BHI + 1% glucose). Growth of MRSA252 (Fig.6.1D) and MRSA252 14 gene KO (Fig.6.1E) was monitored in BHI + 1% glucose supplemented with doubling concentrations of CuCl_2 . Growth of MRSA252 remained unchanged in up to 0.5 mM CuCl_2 (Fig. 6.1D). Growth of MRSA252 14 gene KO remained unchanged in up to 0.25 mM CuCl_2 (Fig. 6.1E). This indicated that the reduction of biofilm formation seen at concentrations lower than 0.5 and 0.25 mM CuCl_2 for MRSA252 and MRSA252 14 gene KO respectively was not due to copper mediated inhibition of growth.

Next it was hypothesised that exponential growth of *S. aureus* was affected by copper supplementation, and potential copper-mediated reduction in exponential phase of growth resulted in an impaired ability to form a biofilm. In order to empirically determine if the exponential phase of growth was affected by copper supplementation, the mean doubling time of these cultures was calculated using the software GrowthRates (Hall *et al.*, 2014)(Fig. 6.1F+G). The calculation of the growth rate of a culture involves that fitting of a line of best fit to the exponential phase of a growth curve plotted on a log scale, however manual fitting of this line can lead to the introduction human bias. The software GrowthRates mathematically calculates the line of best fit to an exponential curve data set and calculates the doubling time of the culture during exponential phase, eliminating the possibility for the introduction of human bias. The mean doubling time of MRSA252 in exponential phase did not significantly increase below concentrations of 1 mM CuCl_2 (Fig. 6.1F). The mean doubling time of MRSA252 14 gene KO did not significantly increase

below concentrations of 0.5 mM CuCl₂ (Fig. 6.1G). This demonstrated that the exponential phase of growth of MRSA252 and MRSA252 14 gene KO was unaffected by copper in up to 0.5 and 0.25 mM copper respectively, and that it was unlikely that the reduced biofilm formation observed for MRSA252 and MRSA252 14 gene KO when grown in media supplemented with copper was due to reduced exponential phase growth at ≤ 0.5 and ≤ 0.25 mM copper, respectively.

6.2.2 The effect of copper on biofilm formation of ED83

Figure 6.1 shows that copper reduces biofilm formation by an MRSA clinical isolate. Next, the effect of copper on a methicillin sensitive *S. aureus* (MSSA) strain was examined (Fig. 6.2). ED83 is a clinical isolate from the lung sputum of a chronically infected cystic fibrosis patient (McAdam *et al.*, 2011). It forms a strong polysaccharide biofilm in BHI supplemented with NaCl (Turley, M.B, Geoghegan, J. A, *unpublished*). Polysaccharide biofilm formation is strongly associated with MSSA strains, and protein mediated biofilm formation is more often associated with MRSA strains (O'Neill *et al.*, 2007).

In order to determine which concentrations of copper should be used during biofilm growth experiments, the copper tolerance profile of ED83 was established. Growth of ED83 in BHI + 1% glucose supplemented with doubling concentrations of CuCl₂ was monitored for 22 h (Fig. 6.2A). In addition to this, the mean doubling time of these cultures during exponential phase was calculated using the GrowthRates software (Fig. 6.2B). The growth of ED83 in BHI + 1% glucose in up to 0.5 mM CuCl₂ was almost identical to growth of ED83 in the absence of copper (Fig. 6.2A). No significant change in doubling time of ED83 was detected with up to 1 mM CuCl₂ (Fig. 6.2B). These data informed the spectrum of copper concentrations to be used in biofilm growth experiments. Concentrations up to 1 mM CuCl₂ were chosen for biofilm formation experiments as doubling times were unaffected under these conditions, and the final optical density achieved in media up to 1 mM CuCl₂ was similar, indicating that up to 1 mM CuCl₂ did not decrease the growth of ED83, and any change in biofilm formation was not due to a decrease in growth of ED83.

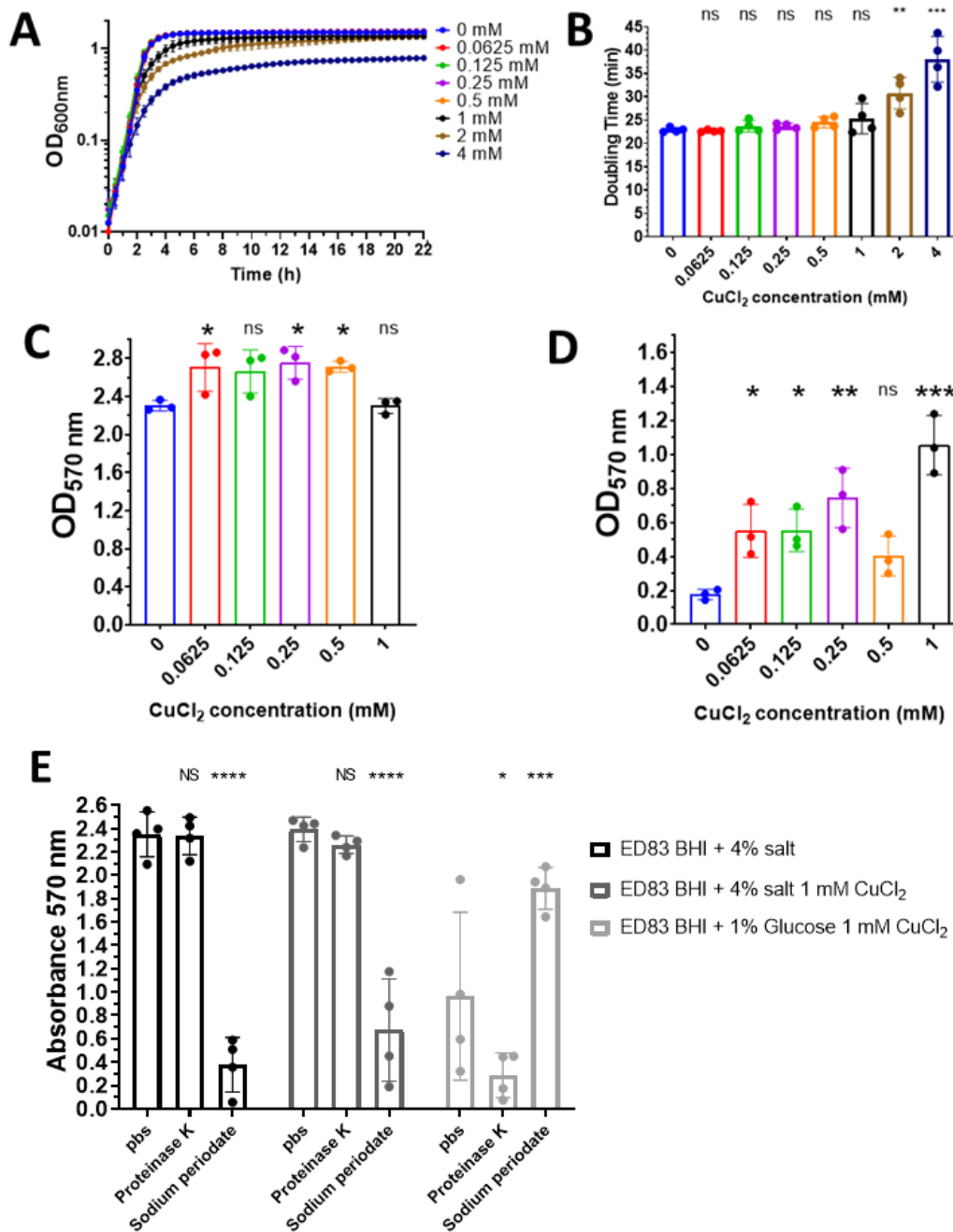


Figure 6.2 Copper induces formation of a protein-mediated biofilm in ED83

Growth of ED83 in BHI + 1% glucose supplemented with CuCl₂ (A). Doubling times of ED83 in BHI + 1% glucose were calculated using GrowthRates software (B). Biofilm formation of ED83 when grown in BHI + 4% salt supplemented with CuCl₂ (C) and in BHI + 1% glucose supplemented with copper (D). Susceptibility of ED83 biofilms to proteinase K and sodium metaperiodate treatment (E). Biofilms were allowed to form for 24 h at 37°C under static conditions in microtitre plates. Biofilm was stained with crystal violet and absorbance was measured at 570nm. Graphs (B), (C) and (D) were analysed by one-way ANOVA, with Dunnett's multiple comparisons test comparing each concentration of copper to 0 mM for each graph. Graph (E) was analysed by two-way ANOVA followed by Dunnett's multiple comparisons test comparing each condition to its pbs control. ns, not significant; *, $P < 0.05$; **, $P < 0.01$; ***, $P < 0.001$. Error bars represent SD.

To investigate if copper affects biofilm formation of ED83, ED83 was grown in BHI + 4% NaCl supplemented with 0, 0.0625, 0.125, 0.25, 0.5 and 1 mM CuCl₂ (Fig. 6.2C). A small increase in biofilm formation by ED83 was seen at 0.0625, 0.25 and 0.5 mM concentrations. To confirm that copper is responsible for this increase in biofilm formation, ED83 was also cultured in a condition that does not usually support biofilm formation, BHI supplemented with 1% glucose (Fig. 6.2D). Biofilm formation did not occur in the absence of copper. However biofilm formation was observed in BHI + 1% glucose supplemented with copper with as low as 0.0625 mM CuCl₂ (Fig. 6.2D). This increase was statistically significant for 0.0625, 0.125, 0.25 and 1 mM CuCl₂. This demonstrates clearly that copper can induce biofilm formation, even in a medium that usually does not support biofilm growth.

To determine if the copper-induced biofilm formed in glucose-supplemented broth was protein- or polysaccharide-mediated, biofilms were treated with proteinase K or sodium metaperiodate (Fig. 6.2E). A protein-mediated biofilm will be disrupted by proteinase K treatment, while a polysaccharide-mediated biofilm will be disrupted by sodium metaperiodate. 1 mM CuCl₂ was chosen as the test concentration for this experiment as 1 mM because it resulted in the highest absorbance values and most robust biofilms seen in Fig. 6.2D.

Sodium metaperiodate disrupted the biofilm formed in BHI supplemented with salt, confirming that the biofilm formed by ED83 in salt supplemented media is polysaccharide-mediated (Fig. 6.2E). Sodium metaperiodate also disrupted the biofilm formed in BHI supplemented with salt and copper, indicating that the biofilm is still a polysaccharide-mediated (Fig. 6.2E). Lastly, proteinase K disrupted the biofilm formed in BHI supplemented with glucose and copper, while sodium metaperiodate did not disrupt this biofilm (Fig. 6.2E). These data show that copper can induce the development of a protein-mediated biofilm in a strain that characteristically only produces a polysaccharide-mediated biofilm in salt conditions.

1 mM CuCl₂ was chosen as the copper concentration for all further biofilm experiments in this chapter as copper supplemented biofilm formation of MRSA252, MRSA252 14 gene KO and ED83 was most robust at this concentration. This permitted the identification of robust copper-mediated biofilm phenotypes and

reduced the number of experimental conditions employed allowing a greater number of *S. aureus* strains to be tested.

6.2.3 The effect of copper on biofilm formation of a panel of isolates of *S. aureus* from cystic fibrosis patients

In Fig. 6.1, it was shown that copper reduced biofilm formation by MRSA252. Next, it was observed that copper supplementation stimulated biofilm formation in an ordinarily biofilm negative condition, and this biofilm was mediated by proteins instead of polysaccharides (Fig. 6.2). It was unknown if this biofilm phenotype was unique to strain ED83 or if it was a phenotype representative of a wider variety of *S. aureus* strains. To investigate this the effect of copper on several *S. aureus* clinical isolates from different types of infection was performed.

The effect of copper on two *S. aureus* strains (CF10 and CF15) isolated from sputum samples from cystic fibrosis patients in Saint Vincent's Hospital Dublin were analysed (Fig. 6.3). In the absence of copper, CF10 formed a moderately strong biofilm in BHI + glucose, and a very strong biofilm in BHI + salt. In the presence of copper, the biofilm formed in BHI + glucose was reduced while the biofilm formed in BHI + salt was slightly increased (Fig. 6.3A).

In the absence of copper, CF15 formed a robust biofilm in BHI + glucose and BHI + salt. In the presence of copper, CF15 formed a robust biofilm in BHI alone as well as in BHI + glucose and BHI + salt. No biofilm was formed in BHI alone, but a strong biofilm was formed upon copper supplementation, indicating that copper induced biofilm formation for CF15 when grown in BHI (Fig. 6.3B).

The data gathered for cystic fibrosis clinical isolates (Fig. 6.2 and 6.3) indicates that there is a complex and strain dependent response to copper. In some conditions no affect is seen on biofilm formation, often in glucose conditions biofilm is reduced by copper, and in some biofilm forming conditions, copper increases biofilm formation. Interestingly, ED83 forms a protein-mediated biofilm in response to copper when grown in BHI + glucose, demonstrating a rare example of an *S. aureus* strain capable of forming both types of biofilm in response to different conditions.

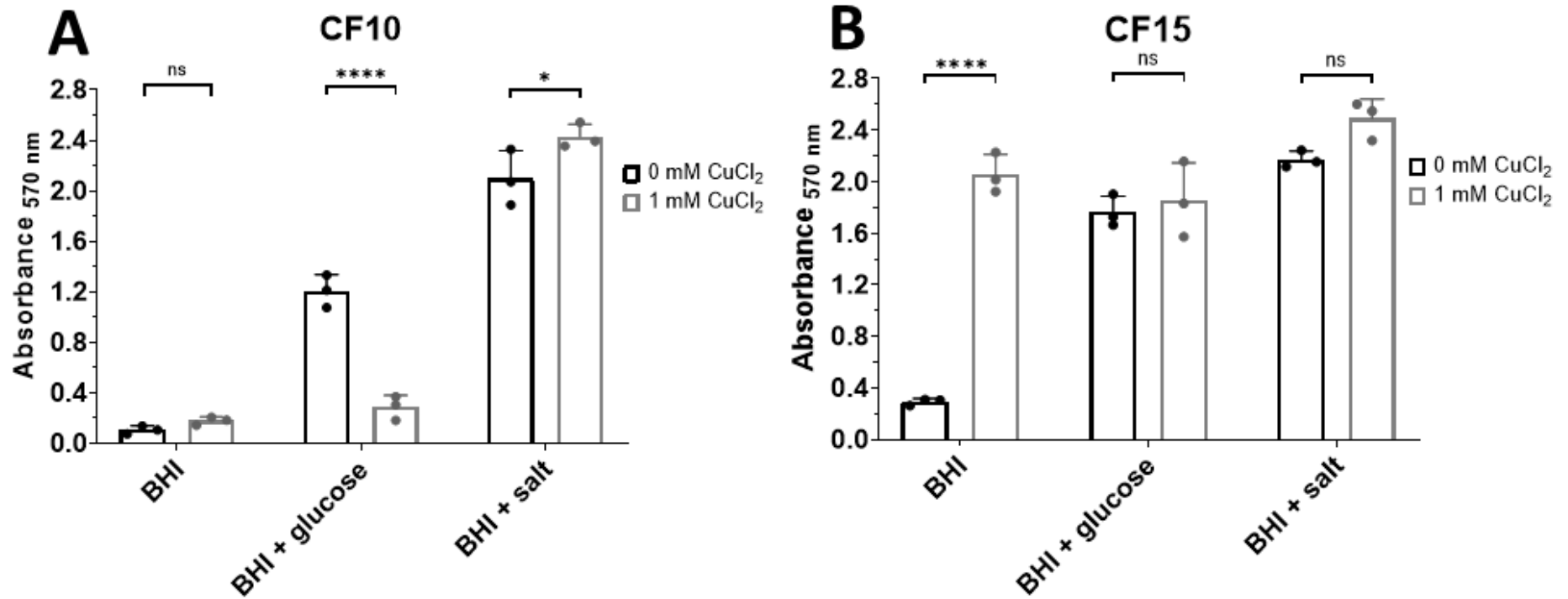


Figure 6.3 Effect of copper on biofilm formation of cystic fibrosis clinical isolates CF10 and CF15

Biofilm formation of clinical *S. aureus* strains CF10 (A) and CF15 (B) in BHI, BHI + glucose and BHI + salt with and without copper supplementation. Biofilms were allowed to form for 24 h at 37°C under static conditions in microtitre plates. Biofilm was stained with crystal violet and absorbance was measured at 570nm. Statistical significance was determined by Two-way ANOVA and Sidak's multiple comparisons test. ns, not significant; *, $P < 0.05$; ***, $P < 0.0001$. Error bars represent SD.

6.2.4 Effect of copper on biofilm formation by *S. aureus* isolates from device related infections

The effect of copper on biofilm formation by clinical isolates from device related infections from Beaumont Hospital Dublin was investigated (O'Neill *et al.*, 2007). Strains BH3, BH4, BH10, BH10(03), and BH18 are MRSA isolates, while BH48(04) is an MSSA isolate. Biofilms were allowed to grow in BHI, BHI + glucose, and BHI + salt with and without CuCl₂ supplementation (Fig. 6.4).

Strain BH3 formed a moderately strong biofilm in BHI + glucose and BHI + salt. Copper supplementation improved biofilm formation in BHI + salt two-fold, generating a robust biofilm (Fig. 6.4A). Strain BH4 formed a moderately strong biofilm only in BHI + glucose which was reduced upon supplementation with copper (Fig. 6.4B). BH10 formed a moderately strong biofilm in BHI + glucose but upon copper supplementation this was reduced. Interestingly, in BHI + salt, copper supplementation stimulated the production of a robust biofilm (Fig. 6.4C).

Strain BH10(03) formed a moderately strong biofilm in BHI and a strong biofilm in BHI + glucose. Biofilm formation in BHI + glucose was reduced slightly upon copper supplementation, but this difference was not statistically significant (Fig. 6.4D). Strain BH18 formed a biofilm only in BHI + glucose, and copper supplementation reduced this greatly (Fig. 6.4E).

Strain BH48(04) formed a robust biofilm in BHI + salt, and a very weak biofilm in BHI and BHI + glucose. Biofilm formation was increased significantly in BHI to a moderately strong biofilm when growth media was supplemented with copper (Fig. 6.4F).

Together these data suggest that the response to copper of clinical *S. aureus* strains isolated from device related infections appears to be complex. A trend is present that when biofilm is formed in BHI + glucose, copper supplementation reduces biofilm formation. On the other hand, if a strain does not form biofilm in BHI + salt, copper supplementation sometimes encourages the formation of a robust biofilm.

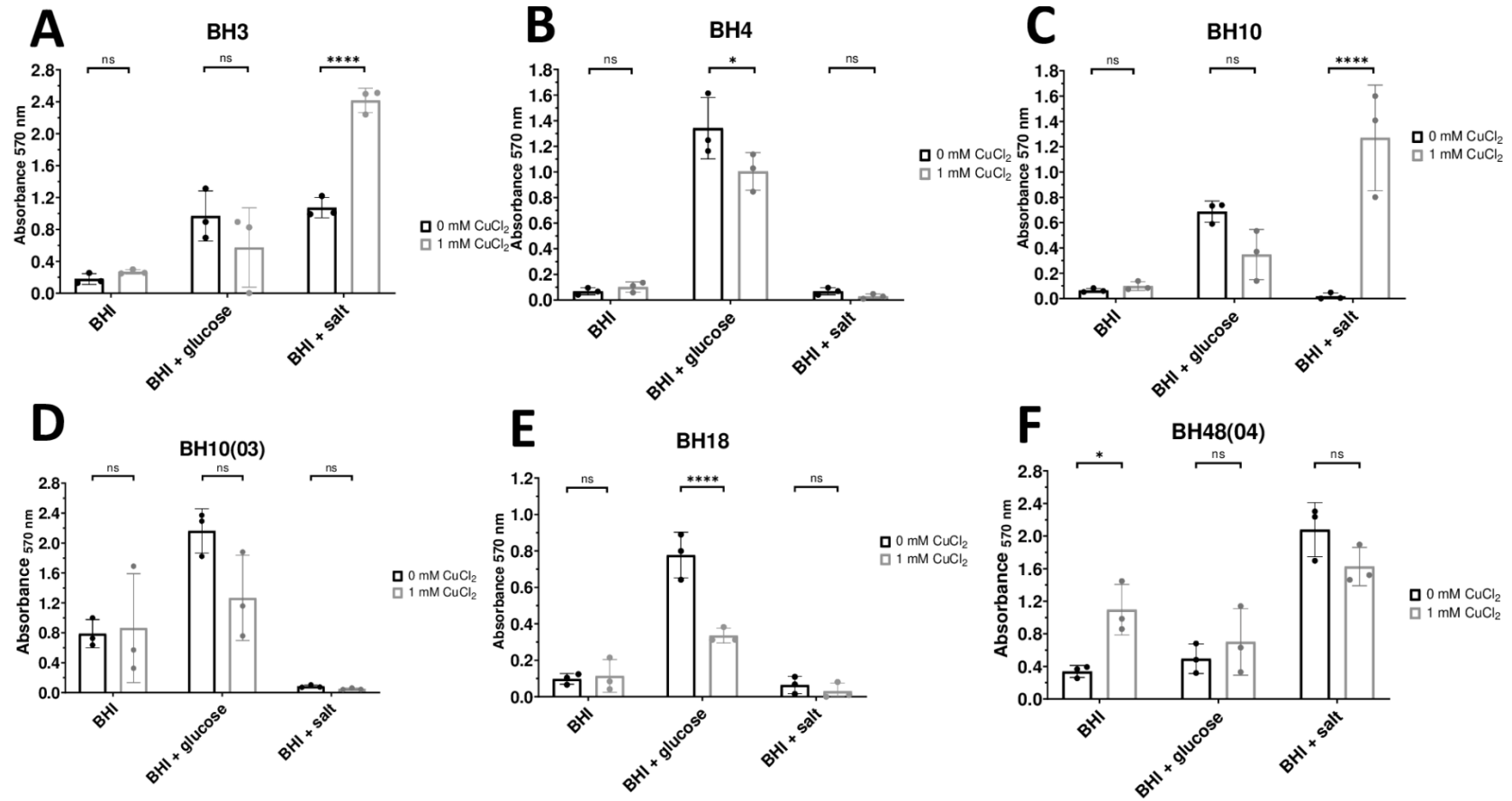


Figure 6.4 The effect of copper supplementation on biofilm formation of clinical *S. aureus* isolates from device related infections

Biofilm formation of device associated clinical *S. aureus* strains BH3 (A), BH4 (B), BH10 (C), BH10(03) (D), BH18 (E) and BH48(04) (F) in BHI, BHI + glucose and BHI + salt with and without copper supplementation. Biofilms were allowed to form for 24 h at 37°C under static conditions in microtitre plates. Biofilm was stained with crystal violet and absorbance was measured at 570nm. Statistical significance was determined by Two-way ANOVA and Sidak's multiple comparisons test. ns, not significant; *, $P < 0.05$; **, $P < 0.01$; ***, $P < 0.001$; ****, $P < 0.0001$. Error bars = SD.

6.2.5 Effect of copper on biofilm formation DAR isolates

The effect of copper on additional biofilm forming MRSA clinical isolates was examined in BHI, BHI + glucose, and BHI + salt (Fig. 6.5). DAR113, DAR217 and DAR70 are biofilm positive MRSA isolates (O'Neill *et al.*, 2008). The *fnbAB* genes were deleted from DAR70 to generate DAR70 Δ *fnbAB* to examine if fibronectin binding proteins contribute to biofilm formation (Marta Zapotoczna, Leanne Hays & Joan A. Geoghegan, *unpublished*).

DAR113 formed a robust biofilm in BHI + glucose which was greatly reduced upon supplementation with copper (Fig. 6.5A). DAR217 formed a biofilm in BHI, BHI + glucose and BHI + salt, although the biofilm formed in BHI alone was much weaker than the biofilms formed in BHI + glucose and BHI + salt. Copper supplementation appeared to increase biofilm formation in all conditions, however only the increase seen in BHI alone was statistically significant (Fig. 6.5B).

DAR70 did not form a biofilm in BHI. It formed a weak biofilm in BHI + glucose, and formed a moderately strong biofilm in BHI + salt. Copper supplementation resulted in an increase in biofilm formation for all of these conditions (Fig. 6.5C). DAR70 Δ *fnbAB* by comparison was unable to form a biofilm in BHI or BHI + glucose, and formed a weak biofilm in BHI + salt. Copper supplementation did not induce biofilm formation in BHI and BHI + glucose, and increased biofilm formation in BHI + salt (Fig. 6.5D).

Combination of data obtain in Figure 6.5C and 6.5D suggest that copper induces an FnbA and FnbB mediated biofilm in BHI and BHI + glucose by DAR70. Biofilm formation was also increased for the *fnbAB* mutant in BHI + salt, which shows that fibronectin binding proteins are not responsible for biofilm formation in this condition.

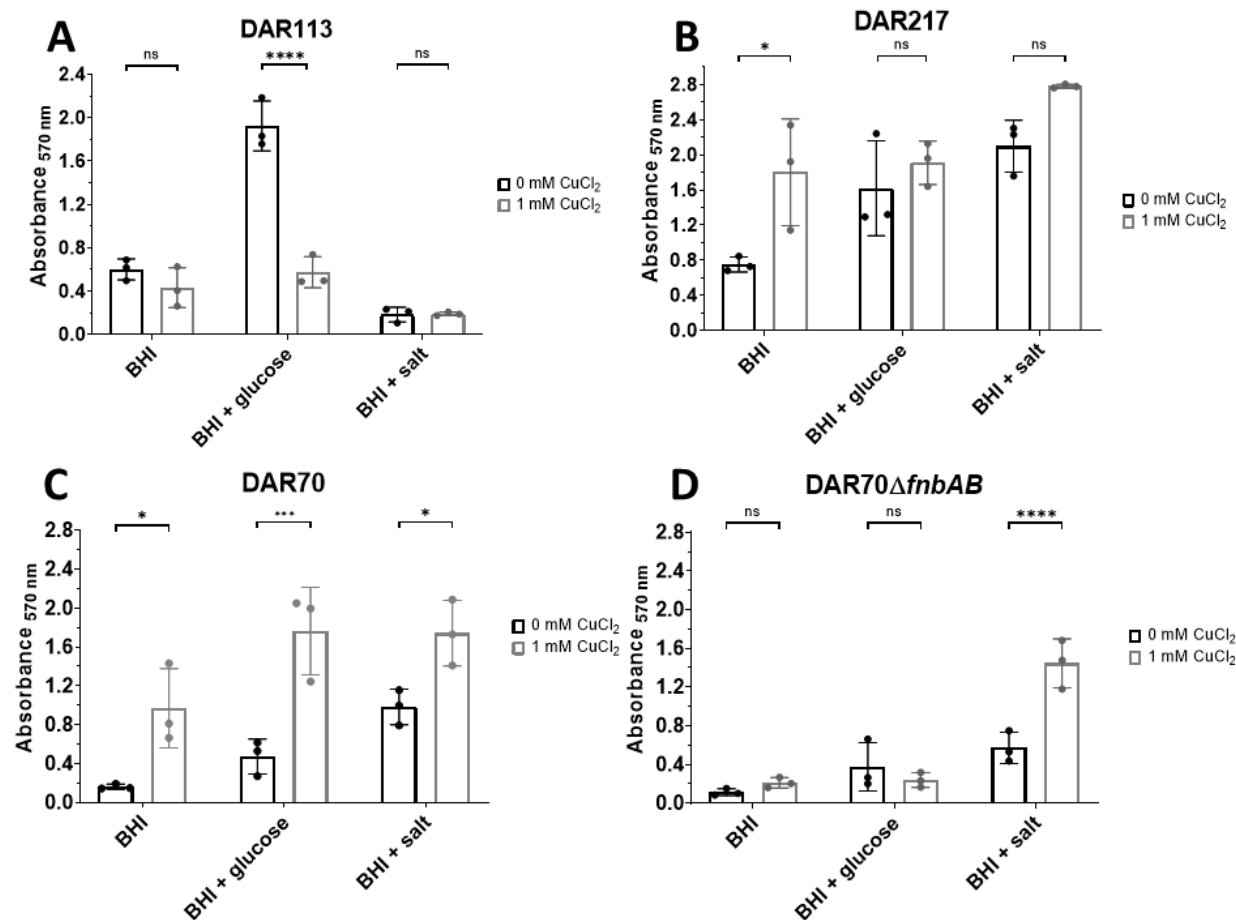


Figure 6.5 The effect of copper supplementation on biofilm formation of DAR clinical isolates

Biofilm formation of device associated clinical *S. aureus* strains DAR113 (A), DAR217 (B), DAR70 (C) and DAR70Δ*fnbAB* (D) in BHI, BHI + glucose and BHI + salt with and without copper supplementation. Biofilms were allowed to form for 24 h at 37°C under static conditions in microtitre plates. Biofilm was stained with crystal violet and absorbance was measured at 570nm. Statistical significance was determined by Two-way ANOVA and Sidak's multiple comparisons test. ns, not significant; *, $P < 0.05$; ***, $P < 0.001$; ****, $P < 0.0001$. Error bars = SD.

6.2.6 Effect of copper on BH1CC biofilm formation and its biofilm composition

BH1CC has been shown to generate a robust *fnbAB* mediated biofilm when grown in BHI + glucose (O'Neill *et al.*, 2008). Here, the effect of copper on biofilm formation by BH1CC and BH1CC Δ *fnbAB* in BHI + glucose was examined (Fig. 6.6). Biofilm formation by BH1CC was reduced significantly when grown in BHI + glucose supplemented with copper (Fig. 6.6A). BH1CC Δ *fnbAB* formed an extremely weak biofilm both with and without copper supplementation, indicating that copper did not induce biofilm formation in the absence of fibronectin binding proteins, and confirmed that they were responsible for the biofilm by BH1CC (Fig. 6.6A).

A reduced biofilm phenotype was seen when BH1CC was grown in copper supplemented BHI + glucose (Fig. 6.6A). To determine if this was due to a reduction in *fnbAB* mediated biofilm formation or if this was due to stimulation of the production of a polysaccharide-mediated biofilm, the composition of BH1CC biofilms was determined by proteinase K and sodium metaperiodate treatment (Fig. 6.6B).

The biofilm formed by BH1CC in BHI + glucose was degraded by proteinase K but not sodium metaperiodate, confirming that biofilm was protein-mediated (Fig. 6.6B). The biofilm formed by BH1CC in BHI + glucose supplemented with copper was also degraded by proteinase K but not sodium metaperiodate, demonstrating that the reduced biofilm formed in the presence of copper was still protein-mediated (Fig. 6.6B). Importantly, no biofilm was observed for BH1CC Δ *fnbAB* in PBS or untreated conditions supplemented with and without copper, indicating that *fnbAB* were responsible for the biofilm seen in BH1CC (Fig. 6.6B).

Treatment of BH1CC and BH1CC Δ *fnbAB* biofilms with sodium metaperiodate resulted in an artificial increase in optical density. This increase far exceeded the actual optical density of control PBS treated or untreated biofilms, indicating that this is an artifact of using sodium metaperiodate with these strains. As a result, statistical tests compared conditions to the PBS controls.

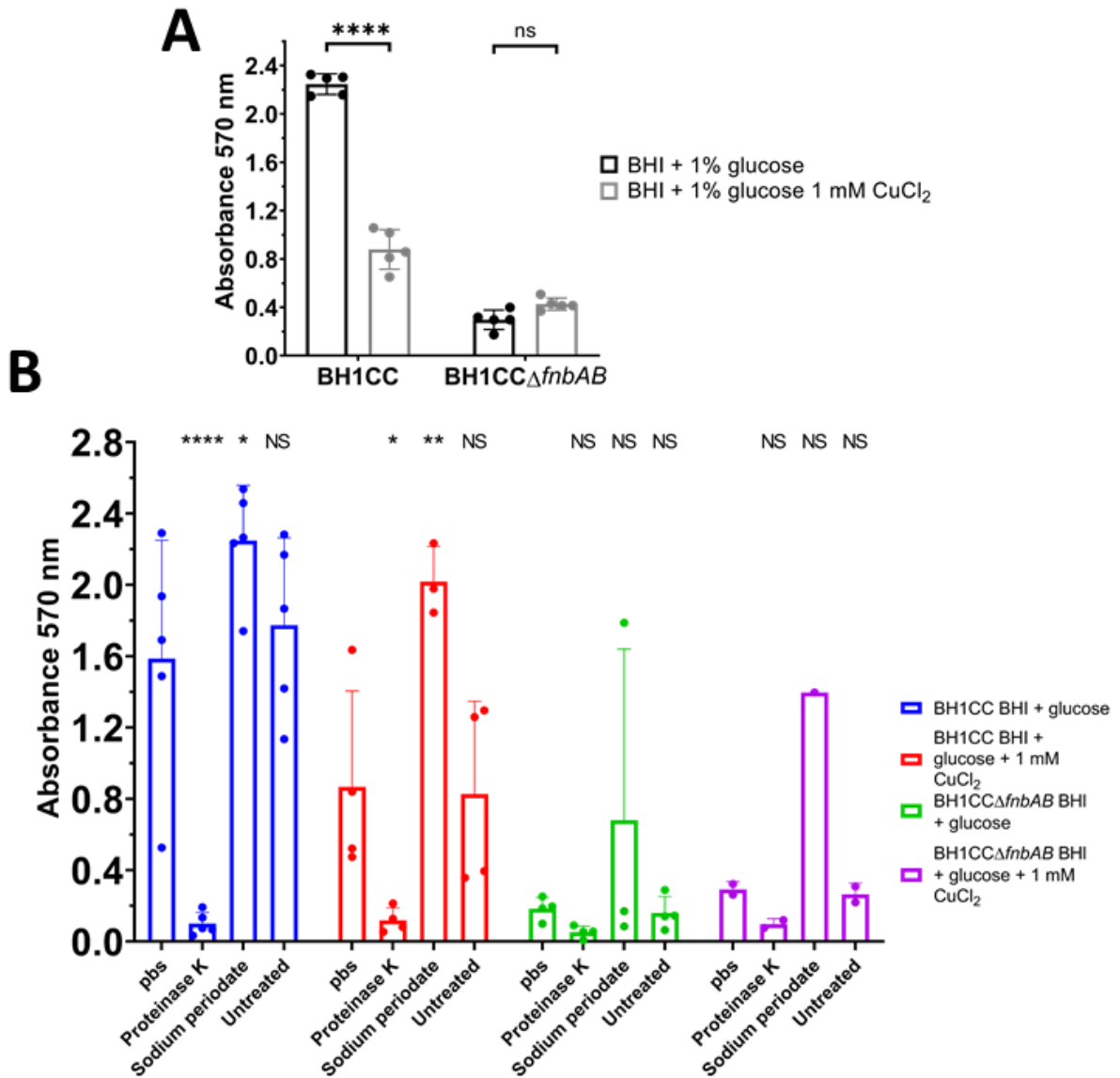


Figure 6.6 Copper reduces *fnbAB* mediated biofilm formation of BH1CC
 Biofilm formation of BH1CC and BH1CC Δ *fnbAB* in BHI and glucose supplemented with copper (A). Susceptibility of BH1CC and BH1CC Δ *fnbAB* biofilms to proteinase K and sodium metaperiodate treatment (B). Biofilms were allowed to form for 24 h at 37°C under static conditions in microtitre plates. Biofilm was stained with crystal violet and absorbance was measured at 570nm. Statistical significance was determined by Two-way ANOVA and Sidak's multiple comparisons test for graph (A), and Tukey's multiple comparison test comparing to pbs column for graph (B). NS, not significant; *, $P < 0.05$; **, $P < 0.01$; ****, $P < 0.0001$. Error bars = SD.

6.3 Discussion

This chapter provides a preliminary investigation into the effects of copper on biofilm formation of clinically relevant *S. aureus* isolates. The results generated in this chapter were unexpected and interesting. Biofilm formation of MRSA252 was decreased by copper supplementation, and copper tolerance did not improve biofilm formation in copper supplemented conditions suggesting copper tolerance does not contribute to biofilm formation (Fig. 6.1). Biofilm formation of the cystic fibrosis clinical isolate ED83 was increased by copper supplementation (Fig. 6.2C-D), which stimulated the formation of a protein-mediated biofilm, demonstrating that this strain can form both protein- and polysaccharide-mediated biofilms in different environmental conditions (Fig. 6.2E). Copper supplementation of biofilm growth media for two additional cystic fibrosis isolates generated contrasting results as it reduced biofilm formation of CF10, and increased it for CF15 (Fig. 6.3). Examination of biofilm positive clinical isolates from device related infections yielded similar results with copper increasing biofilm formation in some conditions, reducing it in some conditions, or having no effect (Fig. 6.4-5). Interestingly, copper appears to stimulate the production of an *fnbAB* mediated biofilm in DAR70, as the increase in biofilm formation was not observed in DAR70 Δ *fnbAB* (Fig. 6.5C-D). In contrast, *fnbAB*-mediated biofilm formation by BH1CC was reduced by copper supplementation (Fig. 6.6).

Together, the data gathered in this chapter provide a foundation for further examination into the effects of copper biofilm. These data have uncovered that *S. aureus* can modulate its biofilm forming phenotype in response to copper, and that this response is diverse amongst different strains as biofilm formation can increase or decrease in response to copper. Continued research elucidating the effect of copper on biofilm formation may identify a unique opportunity for copper-based anti-biofilm therapies, however care must be taken as copper increased biofilm formation in many cases here. Hence, more research is required to understand why copper increases biofilm formation of some strains, and decreases it for others.

This study shows that copper can stimulate production of a protein-dependent biofilm in cystic fibrosis clinical isolate ED83. This biofilm stimulating effect of copper has not been documented before for any bacterium. It remains

undetermined so far if this is a common trait of *S. aureus*, or a trait attributed to few *S. aureus* strains. One potential explanation for the induction of biofilm formation by copper may be that producing a biofilm in copper containing environments provides *S. aureus* with a survival advantage. Copper is present in the environment in soil (Gaetke, Chow-Johnson and Chow, 2014), water (*Copper in Drinking-water Background document for development of WHO Guidelines for Drinking-water Quality*, 2004), but also in the host in blood (bound to ceruloplasmin) (Cousins, 1985), liver and bile (Van Berge Henegouwen *et al.*, 1977), and in macrophages (Wagner *et al.*, 2005). Bile is also present in the lungs of cystic fibrosis patients (Reen *et al.*, 2014), which is where ED83 was isolated from. The presence of copper in these environments may be influencing the expression of virulence genes including those involved in biofilm formation, perhaps aiding in colonisation of a specific niche like the cystic fibrosis lung.

The genome of ED83 has been sequenced (McAdam *et al.*, 2011), but the presence of any copper tolerance genes was not investigated here. Future studies could interrogate the genome of ED83 for the presence of genes involved in copper tolerance such as *copAZ*, *csor*, *copBmco*, *copXL* and *mntABC*.

Sometimes copper reduced biofilm formation, and sometimes it increased biofilm formation, or generated a robust biofilm in conditions that were usually biofilm negative. With the data generated in this chapter, it is not possible to predict which biofilm response will occur during copper supplementation, as the responses to copper were diverse. Additional experiments with more biofilm forming strains will be required to generate enough data to begin to understand which strains will form a biofilm in response to copper, and which will result in reduced biofilm formation. Similar to work performed by O'Neill and colleagues (O'Neill *et al.*, 2007), screening of a large number of clinical isolates may identify an association between inherent traits of *S. aureus* (e.g. methicillin susceptibility, clonal complex, clinical background or location of infection) and their expected copper stimulated biofilm phenotype. To understand if the biofilm composition 'switching' phenotype of polysaccharide to protein seen for ED83 occurs in other strains, the composition of biofilms generated in response to copper should be investigated by proteinase K and sodium metaperiodate treatment. RNAseq and proteomics have been used before to

identify gene expression and proteomic changes in *S. aureus* grown in copper supplemented conditions (Baker *et al.*, 2010; Tarrant *et al.*, 2019). To identify the protein(s) mediating the protein-dependent biofilms, RNAseq or proteomics on ED83 grown in BHI + glucose with and without copper would be greatly beneficial in understanding how ED83 forms a proteinaceous biofilm in response to copper. Alternatively, qRT-PCR could be performed investigating proteins that are known to be involved such as *fnbA* and *fnbB* (O'Neill *et al.*, 2008), *sdrC* (Feuillie *et al.*, 2017), *eap* and *emp* (Johnson, Cockayne and Morrissey, 2008) and *sasG* (Geoghegan *et al.*, 2010). Likewise, qRT-PCR investigating if the expression of the operon responsible for polysaccharide production (*icaADBC*) is down regulated in these conditions would be useful. Generation of a *srtA* mutant in a strain with a protein-mediated biofilm in response to copper would allow determination if cell wall anchored proteins are involved (O'Neill *et al.*, 2008).

Streptococcus mutans is unable to form biofilm in the presence of copper, and as a result its copper resistance operon *copYAZ* is required for polysaccharide dependent biofilm formation in the oral cavity (Singh *et al.*, 2015). This indicates that some bacteria require copper hypertolerance genes to successfully form a biofilm. However, this was not the case for MRSA252, as MRSA252 14 gene KO did not have reduced biofilm formation compared to MRSA252. MRSA252 14 gene KO was more sensitive to copper and grew more slowly in copper compared to MRSA252 (Fig. 6.1A-D), but MRSA252 14 gene KO formed biofilm at similar levels to MRSA252 in the presence and absence of copper (Fig. 6.1E). These data suggest that copper tolerance does not contribute to biofilm formation of *S. aureus* in the presence or absence of copper. The similar biofilm forming ability of both strains in concentrations of copper that reduced planktonic growth of the MRSA252 14 gene KO suggests that when *S. aureus* is organised into a biofilm architecture, it has increased resistance to copper, or that non-viable cells are contributing to biofilm mass. Additional experiments to investigate this could perform CFU counts on disrupted biofilms to enumerate the number of viable bacteria in copper supplemented biofilms, and determine the number of viable bacteria present in copper sensitive and resistance derivatives of MRSA252. Live-dead staining of copper treated biofilms would also improve understanding of the effect of copper on biofilm architecture. Fluorescent microscopy could also be used to identify changes

in biofilm architecture with the added specificity for proteins of interest, such as FnBPA and FnBPB. The ability of copper to eradicate a preformed biofilm should also be investigated, and viable counts performed on these biofilms to discern if copper can kill bacteria within a biofilm, or if combining copper and antibiotics improves the eradication of biofilms.

Regulation of biofilm formation seems to be complex and strain dependent. Biofilm formation in (some strains of) *S. aureus* is affected by the major global regulators of virulence, including the Agr quorum sensing system, the SaeRS system, the Sar family of regulators, the alternative sigma factor SigB, and the transcriptional repressor CodY (Otto, 2008; Jenul and Horswill, 2018; Schilcher and Horswill, 2020). The reason for the changes to biofilm formation of ED83 and MRSA252 reported here may be due to altered regulation of global transcription regulators. Copper has been shown to inhibit SaeS function with as little as 50 μM CuCl_2 (Cho *et al.*, 2015), indicating that at least one global virulence regulator is affected by concentrations of copper even lower than those used in this study. The increase and decrease in biofilm formation seen in all strains tested in this chapter is likely a result of strain dependent differences *S. aureus* biology and gene regulation. Similar strain dependent differences were seen with iron and *S. aureus* biofilm formation, where some strains increased biofilm formation in response to iron limited conditions (Xiong *et al.*, 2000), while others showed a decrease (Johnson *et al.*, 2005). Examination of expression of *agrBDCA*, *saeRS*, *sarA*, *sigB* and *codY* by RT-qPCR will provide a clearer understanding of the changes in regulator expression occurring in response to copper. Examination of expression of *icaADBC*, *icaR*, *fnbA*, *fnbB*, *eap*, *sdrC* and *sasG* will also aid understanding of how ED83 forms biofilm in response to copper (Schilcher and Horswill, 2020).

Extracellular DNA release is an important and well established component of *S. aureus* and *S. epidermidis* biofilms (Qin *et al.*, 2007; Mann *et al.*, 2009). There is a distinct possibility that copper damages the membrane of *S. aureus* resulting in the release of intracellular DNA into the environment, increasing the supplementation of the biofilm matrix with eDNA. To investigate this, copper stimulated biofilms could be treated with DNase to determine if they are degraded, indicating that copper promotes eDNA release, augmenting biofilm formation. It is

important to note that biofilm formation was analysed in this chapter in relatively artificial *in vitro* conditions and that examination of the effect of copper on biofilm formation in *in vivo* and flow conditions is recommended to confirm these *in vitro* findings.

In conclusion, *S. aureus* exhibits a diverse biofilm response to copper supplementation of its growth media. Different biofilm responses to copper were observed for different *S. aureus* strains, indicating that there is no universal biofilm response to copper for *S. aureus*. This information can inform future therapies that targeting protein- or polysaccharide-mediated biofilm formation may be insufficient to resolve *S. aureus* infection. Furthermore, if copper is used in part to try to eradicate the biofilm, it may exacerbate the infection by stimulation of the production of a more robust biofilm. Additional research into the molecular mechanisms of how copper effects biofilm formation is required and will likely aid the generation of future anti-biofilm therapies.

6.4 Results Chapter 4 Summary

- Copper reduces biofilm formation of MRSA252 and MRSA252 14 gene KO equally, indicating copper tolerance does not contribute to biofilm formation.
- The cystic fibrosis clinical isolate ED83 forms more robust polysaccharide biofilms in response to copper when grown in BHI + salt, and generates a novel protein-mediated biofilm in response to copper in BHI + glucose.
- Biofilm positive *S. aureus* clinical isolates from Beaumont Hospital Dublin exhibit a diverse biofilm response to copper, with some strains generating a biofilm in response to copper, and some strains reducing biofilm formation in response to copper.
- Copper stimulates the formation of an *fnbAB*-mediated biofilm in DAR70, but reduces the formation of an *fnbAB*-mediated biofilm in BH1CC.

Chapter 7

Discussion

Copper tolerance genes are found in successful lineages of *S. aureus* including USA300 CA-MRSA (Planet *et al.*, 2015) and CC22 and CC30 HA-MRSA strains (Zapotoczna *et al.*, 2018). The prevalence of these genes in successful CA-MRSA and HA-MRSA strains suggests that they contribute to their success as a pathogen. Examination of the known copper tolerance genes of *S. aureus* has described roles for virulence and fitness during infection (Purves *et al.*, 2018; Zapotoczna *et al.*, 2018; Rosario-Cruz *et al.*, 2019; Saenkham-Huntsinger *et al.*, 2021). This thesis adds to this knowledge by discovering the cellular location of *S. aureus* Mco, describing a role for the *cadAC* genes in copper tolerance, examining the contribution of copper tolerance genes of MRSA252 to survival in human blood and neutrophils, and investigating the effect of copper on biofilm forming clinical isolates of *S. aureus*.

The Tat system generally transports proteins across the membrane that are fully folded and loaded with the appropriate metal cofactor, while the Sec system transports unfolded proteins, which are folded after transport (Hou and Brüser, 2011; Freudl, 2013). It is not surprising that multicopper oxidases are usually exported by the Tat system, as they require loading of at least 4 copper atoms before becoming functional. *S. aureus* Mco however is not transported by the Tat system, so it must be folded and loaded with copper extracellularly. It remains unknown how Mco does this. Stolle and colleagues demonstrated that *E. coli* CueO is transported via the Tat system in an incomplete folding state (Stolle, Hou and Brüser, 2016). They showed that copper loading occurs after transport and can contribute to copper resistance by sequestration of external copper, and that this copper binding greatly stabilised the CueO protein (Stolle, Hou and Brüser, 2016). They proposed that the Tat system may sometimes transport flexibly folded proteins in order to permit cofactor loading after transport (Stolle, Hou and Brüser, 2016). Perhaps Mco functions in a similar manner. Mco is almost certainly transported by the Sec system, and as a result, in an unfolded state. Folding of Mco after transport would allow it to bind four copper atoms in the extracellular environment and contribute to copper tolerance, and this copper binding might also stabilise the protein, rendering it functional. This proposed mechanism would be advantageous to *S. aureus* as harbouring Mco would contribute to copper tolerance in two ways, by sequestering four copper atoms extracellularly, and then detoxifying additional

copper directly or indirectly through oxidation. The ability of Mco to function as a cuprous oxidase has yet to be investigated experimentally and thus remains but one hypothesis of how it detoxifies copper. Cuprous oxidases require a T1 copper centre to be within electron transfer distance of the cuprous ion substrate binding site. For example, *E. coli* CueO possesses a methionine rich region which provides this substrate binding site within electron transfer distance of the T1 copper centre (Djoko *et al.*, 2010). Mco lacks the methionine rich region seen in CueO (Fig. 3.1). In order to determine if Mco is a cuprous oxidase, the protein should be purified and tested for cuprous oxidation using $[\text{Cu}^{\text{I}}(\text{Bca})_2]^{3-}$ as the chromophoric substrate (Djoko *et al.*, 2010). Additionally, complementation of a *cueO* mutant in *E. coli* could be attempted using constructs expressing *mco*. If Mco functionally complements a *cueO* mutant, it would suggest that it detoxifies copper similar to CueO.

Additional copper ligand binding sites would be required for Mco to oxidise copper similar to CueO. There are 10 methionines in the unique 56 residue N-terminal region of Mco (Fig. 3.1). Perhaps this methionine rich N-terminal region provides a labile N-terminal helix that can function similarly to the methionine rich helix of CueO and permit a cuprous ion oxidation site. To investigate this, the Mco and Mco2-53 truncate proteins could be purified and their crystal structures resolved, and the number of copper atoms bound to each protein estimated by absorbance at 610 nm in the presence of Gu-HCl and dithionite (Djoko *et al.*, 2010).

If Mco is not a cuprous oxidase, an alternative hypothesis as to how it detoxifies copper is required. Many multicopper oxidases are not cuprous oxidases, but laccases, ferroxidases, tyrosinases, phenol oxidases and phenoxazinone synthases instead (Solomon, Sundaram and Machonkin, 1996). Siderophores are a diverse family of small molecular weight secreted proteins that can bind oxidised metals with extremely high affinity (Koh and Henderson, 2015). They can sequester iron in iron limited conditions, or protect from metal toxicity by binding free metal ions such as copper. It has been proposed in *E. coli* that the copper binding siderophore yersiniabactin works in tandem with CueO (Koh and Henderson, 2015). Mco could be involved in oxidation of siderophores. Mco has been shown to exhibit phenol oxidase activity (Sitthisak *et al.*, 2005). Perhaps Mco can oxidise the phenolate region of a phenolate siderophore, contributing to copper detoxification

and/or acquisition by copper binding siderophores. Knowledge of *S. aureus* produced siderophores is less than *E. coli* produced siderophores and remains largely around iron binding siderophores staphyloferrin A and staphyloferrin B (Perry *et al.*, 2019). To begin investigation if Mco works in tandem with *S. aureus* produced siderophores, siderophore genes could be identified in MRSA252 and deletion mutants constructed in the backgrounds of MRSA252 and MRSA252 Δ mco and their copper tolerance profiles analysed.

It has not yet been determined how Mco is attached to the membrane. Therefore it is not clear if Mco is active at the inner or outer leaflet of the cytoplasmic membrane. If Mco functions externally, then it may be involved in external detoxification of copper. CopL is a membrane bound surface exposed copper tolerance protein that binds external copper and contributes to copper tolerance in the USA300 strain LAC (Rosario-Cruz *et al.*, 2019). CopL only confers copper tolerance when it is membrane bound. This suggests that extracellular copper can damage *S. aureus*, and that *S. aureus* has evolved mechanisms of defending against external copper. Therefore extracellular detoxification of copper confers copper tolerance to *S. aureus*. If Mco is membrane bound and surface exposed, it might contribute to copper tolerance in MRSA252 by oxidising extracellular cuprous ions into less toxic cupric ions, and by binding four copper atoms during its folding process after Sec-mediated transport. An updated model of copper tolerance in MRSA252 is provided (Fig. 7.1), indicating the cellular location of Mco in the membrane, and its proposed function in detoxifying extracellular cuprous ions.

The ability of *S. aureus* to detoxify copper is greatly affected by nutrient availability as shown here (Fig. 3.12-17) and elsewhere (Sitthisak *et al.*, 2007; Baker *et al.*, 2010; Tarrant *et al.*, 2019). This may give insight into how bacteria handle toxic copper. The more nutrient rich the environment *S. aureus* is in, the better it is able to handle copper stress. This may suggest that handling of copper stress requires a considerable metabolic investment from *S. aureus*. If this is true, it presents two unique opportunities to combat *S. aureus* infection; using copper-mediated antimicrobial strategies in nutrient deficient host niches, and combination therapy with an antimicrobial that requires high metabolic turnover to function.

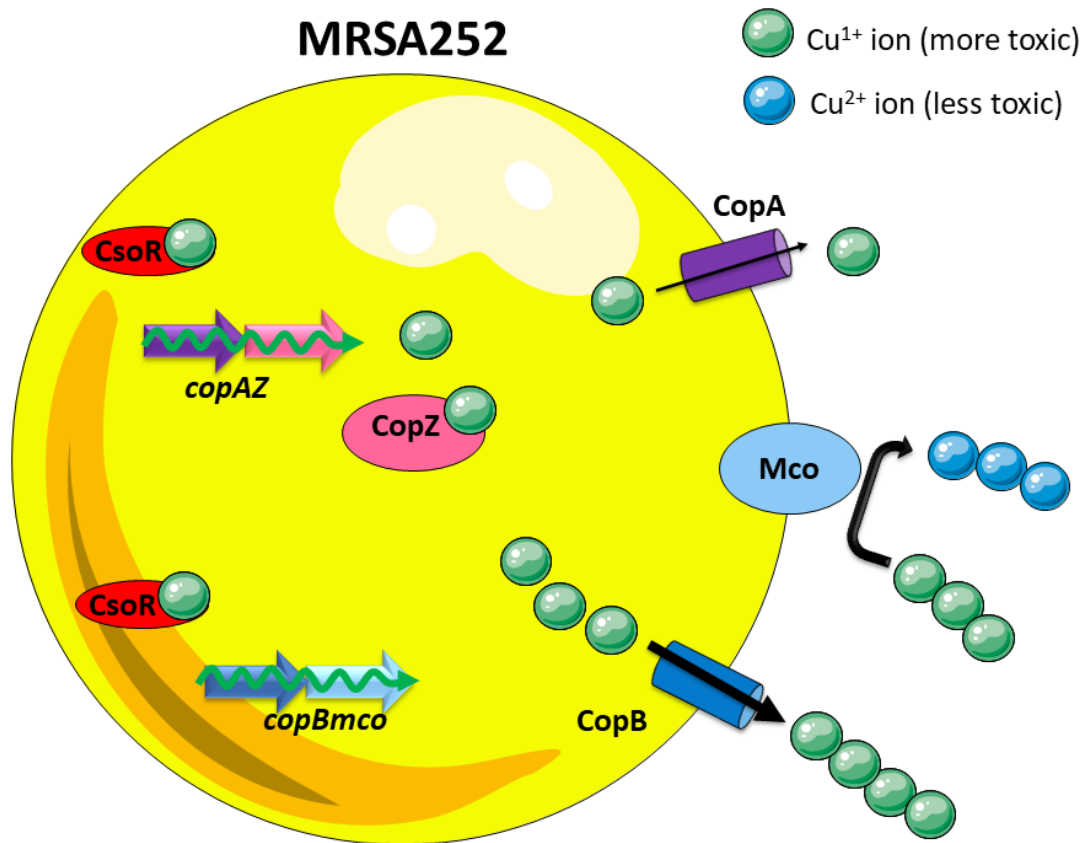


Figure 7.1 Mco is localised to the membrane of *S. aureus*

Schematic of the copper tolerance for MRSA252 (yellow sphere). Mco (light blue oval) is a multicopper oxidase that localises to the membrane of *S. aureus*, and is proposed to contribute to copper tolerance by oxidising toxic Cu¹⁺ ions (green spheres) to less toxic Cu²⁺ ions (blue spheres) in the extracellular space.

The *copBmco* operon (blue and light blue) is under the control of CsoR. CsoR derepresses transcription upon Cu¹⁺ ion binding. CopB (blue barrel) is a high efficiency P_{1B}-Type Cu¹⁺ transporting ATPase. It is depicted exporting more Cu¹⁺ ions than CopA to indicate higher efficiency.

The *copAZ* operon (purple and pink) is under the control of CsoR. CsoR (red oval) derepresses transcription upon Cu¹⁺ ion (green sphere) binding. CopA (purple barrel) is a P_{1B}-Type Cu¹⁺ transporting ATPase depicted exporting Cu¹⁺ ions out of the cell. CopZ (pink oval) is a Cu¹⁺ binding metallochaperone, binding free Cu¹⁺ in the cytoplasm.

Copper-mediated antimicrobial strategies could be well suited for use in host niches where nutrient availability for *S. aureus* is relatively poor such as the urinary tract. For example, the copper chelating drug N,N-Dimethyldithiocarbamate (DMDC) (Menghani *et al.*, 2021) might be especially effective at resolving urinary tract infections due to *S. aureus*. Copper is mobilised to urine and the urinary tract during an *in vivo* murine model of UTI (Saenkham-Huntsinger *et al.*, 2021). Copper could also be used in tandem with conventional antimicrobials that require metabolically active bacteria in order function. Metabolically dormant populations of cells such as persister cells, small colony variants and biofilms might be more effectively treated using conventional antimicrobials targeting mechanisms such as cell wall or protein synthesis in combination with copper which is more damaging to cells when they have less nutrients to metabolise. To begin to determine the effectiveness of such a therapy, this thesis investigated the effect of copper on biofilm formation of clinical MRSA strains. Copper alone resulted in a diverse biofilm response from *S. aureus*, and in many cases promoted biofilm formation. The effect of copper on preformed biofilms remains to be tested, in addition to combination with antimicrobials currently used in anti-biofilm therapy such as vancomycin, ciprofloxacin and rifampicin (Zhao and Drlica, 2002; Høiby *et al.*, 2015; Ciofu *et al.*, 2022). Alternatively, if an anaerobic metabolism response could be induced in *S. aureus* with a compound, then use of this compound in combination with copper may result in enhanced bacterial killing. Otherwise copper-mediated treatments could be used to target niches where oxygen content is already low such as biofilms and osteomyelitis (Balasubramanian *et al.*, 2017). Future bacterial copper tolerance work should look at a number of growth conditions in copper, including nutrient rich and deficient media, anaerobic and aerobic conditions, and solid and liquid media.

This thesis demonstrates for the first time that mutation of *cadA* or *cadAC* leads to a reduction in copper tolerance. Although deletion of these genes did not explain the enhanced copper sensitivity of the MRSA252 14 gene KO mutant, it did suggest that these genes contribute to copper tolerance in TSBd similar to *mco*. The *cadA* gene of *S. aureus* confers resistance to metal ions zinc and cadmium, and its expression is induced by cadmium, lead, cobalt, zinc and bismuth (Yoon, Misra and Silver, 1991) however its contribution to copper tolerance was not examined until now.

Additional experiments are required to fully understand how *cadAC* contributes to copper tolerance. Determination of intracellular copper concentration by ICP-MS would identify if *cadAC* is involved in export of intracellular copper. CadD mediated expression of the *cadD* and *cadC* genes in *Streptococcus pyogenes* was upregulated in response to copper treatment (Stewart *et al.*, 2020). It was postulated that this copper mediated expression was due to mismetallation of the metal binding sites of CadD by copper, resulting in misregulation of CadD-mediated gene expression. Alternatively, activation of CadD-mediated gene expression by copper may assist in bacterial copper tolerance if CadD regulates expression of genes that contribute to copper tolerance. (Yoon, Misra and Silver, 1991).

One hypothesis as to how copper reduced the growth of *cadA* and *cadAC* mutants is that these bacteria were suffering from zinc toxicity. CadA contributes to both cadmium and zinc resistance (Yoon, Misra and Silver, 1991; Zapotoczna *et al.*, 2018), Copper will displace zinc from metalloproteins as it lies higher than zinc on Irving-Williams series (Irving and Williams, 1953). Copper may be displacing zinc from metalloproteins and this free zinc is unable to be exported due to the lack of CadA, and thus causes zinc toxicity. To investigate this, the intracellular concentration of zinc and copper in MRSA252 and MRSA252 Δ *cadA* grown in the presence and absence of copper could be quantified by ICP-MS. If this hypothesis is correct, MRSA252 Δ *cadA* will have higher intracellular zinc concentrations than MRSA252 when grown in the presence of copper.

Mco did not contribute to survival of *S. aureus* in human blood or neutrophils in this study. These are environments most representative of bacteraemia and bloodstream infections. The *ex vivo* model of using whole human blood and purified human neutrophils for infections have a limitation in that they do not comprise of a fully functioning immune system with all of its necessary components. Other *in vivo* models may be more suitable for copper tolerance work. Perhaps copper-mediated killing of phagocytosed bacteria require other host responses not captured in the short blood infection model. Williams and colleagues demonstrated a robust contribution of multicopper oxidases PcoA and CueO to survival of *Acinetobacter baumannii* in the *in vivo* model of infection in *Galleria mellonella* (Williams *et al.*, 2020). It would be interesting to investigate the survival of *Galleria mellonella*

infected with *S. aureus* mutant derivatives of *mco* and other copper tolerance genes and determine if copper tolerance in *S. aureus* contributes to virulence in *Galleria mellonella* similar to *A. baumannii*.

Alternatively, perhaps neutrophils do not use copper to enhance phagocytic killing of *S. aureus*. A broad panel of copper sensitive strains of *S. aureus* did not have a reduced survival in purified primary human neutrophils when compared to wild-type, suggesting that neutrophils do not use on copper to enhance killing of phagocytosed *S. aureus*. Stewart and colleagues reported that copper sensitive *Streptococcus pyogenes* had no survival defect compared to wild type in primary human neutrophils or in a mouse *in vivo* model of infection (Stewart *et al.*, 2020). Taking these two findings together suggests that copper is not an antimicrobial agent used in phagolysosomes used to enhanced phagocytic killing of bacteria by neutrophils, and that other mechanisms such as myeloperoxidase- and NADPH oxidase- mediated ROS production are responsible for phagocytic killing (Guerra *et al.*, 2017). A survival defect for copper sensitive mutants was detected in mouse macrophages here and elsewhere (White, Lee, *et al.*, 2009; Purves *et al.*, 2018; Zapotoczna *et al.*, 2018). This might indicate that only macrophages employ copper to enhance phagocytic killing, and that this phenotype simply does not extrapolate to neutrophils.

Furthermore, the expression of ATP7A was not significantly increased in primary human neutrophils when stimulated with copper and/or TNF- α (Fig. 5.6), suggesting that ATP7A does not play a significant role during activation of neutrophils. This is in direct contrast to macrophages, where upon activation, ATP7A is upregulated and trafficked from the golgi apparatus to the phagolysosomal membrane where it traffics copper into the phagolysosome (White, Lee, *et al.*, 2009). Therefore it is more likely that ATP7A is utilised in neutrophils for copper homeostasis and cuproenzyme copper-loading in the golgi apparatus similar to how it functions elsewhere in the body (Lutsenko *et al.*, 2008; Xie and Collins, 2013).

Perhaps copper tolerance plays a more important role in other host niches, such as the urinary tract. Copper and ceruloplasmin are mobilised to the urine mice with USA300 MRSA urinary tract infections (Saenkham-Huntsinger *et al.*, 2021).

The copper sensitive *copL* mutant had a reduced fitness in this murine model of urinary tract infection, and dietary supplementation with additional copper reduced this fitness further (Saenkham-Huntsinger *et al.*, 2021). Future experiments investigating copper tolerance genes such as *mco*, *copB*, *copZ* and *csor* in MRSA252 could use this murine model of urinary tract infection to determine if copper tolerance contributes to fitness of MRSA252 in urinary tract infection. Furthermore, Mco is now proposed to detoxify extracellular located copper, and CopL detoxifies extracellular copper and contributes to virulence in the *in vivo* mouse model of urinary tract infection. Mco might contribute to virulence in this model similar to CopL. The potential niche dependent function of Mco and other copper tolerance genes may also explain why no significant difference in survival was found in whole human blood or purified human neutrophils in this thesis. The *mco* and *copL* genes are found together in some USA300 strains of *S. aureus* (Planet *et al.*, 2015; Purves *et al.*, 2018). These two membrane localised proteins may colocalise and function together, where CopL may sequester and bind external cuprous ions (Rosario-Cruz *et al.*, 2019), and then allow Mco to oxidise these cuprous ions and release them back into the extracellular milieu. Perhaps CopL aids in copper loading of newly transported Mco, however this is highly speculative and further experimentation is necessary. It would be interesting to investigate these hypotheses about interplay between Mco and CopL now since the work presented in this thesis has demonstrated that Mco is localised to the membrane like CopL.

A survival increase in purified primary human neutrophils was observed for two strains that harboured two functional copies of *copB*; MRSA252 Δ *mco*::PCL55::UCMF and MRSA252 Δ *mco*::PCL55::UCMF*Mco* Δ 2-53 (Fig. 5.8). This may indicate that *copB* contributes to resistance to phagocytic killing in neutrophils in the first 2-3 hours of infection. It would be valuable to generate an isogenic deletion mutant of *copB* in MRSA252, and a complemented mutant using pCL55 with *copB* including its promoter cloned into the MCS. Survival experiments in whole human blood and neutrophils with this mutant and complement combination might identify a role for CopB in resistance to killing by human neutrophils, which would complement existing data for copper transporting ATPases in enhancing survival in macrophages and blood (White, Lee, *et al.*, 2009; Purves *et al.*, 2018; Zapotoczna *et al.*, 2018).

MRSA252 14 gene KO had a significant defect in growth in plasma compared to wild-type (Fig. 5.2). One possible explanation for this not explored in this thesis is that the loss of *cydD* renders *S. aureus* more sensitive to ceruloplasmin-bound copper in serum. The *cydCD* operon is important for low molecular weight thiol export in *E. coli* (Shepherd, 2015; Poole, Cozens and Shepherd, 2019). Future experiments to investigate this would require isogenic deletion of *cydD*, growth of *S. aureus* in freshly drawn human plasma and concurrent determination of plasma ceruloplasmin and copper levels. The contribution of *cydD* to copper tolerance should also be investigated by growth in liquid media supplemented with copper, and on agar supplemented with copper. If a link is found between *cydD* and copper tolerance, it would be beneficial to generate an *S. aureus* mutant defective in bacillithiol synthesis (*bshA* deletion) and a double knockout of *bshA* and *cydD* to determine if this thiol contributes to copper tolerance mediated by CydD transport in *S. aureus*.(Gresham *et al.*, 2000; Guerra *et al.*, 2017)(White, Lee, *et al.*, 2009; Purves *et al.*, 2018; Zapotoczna *et al.*, 2018)

The cystic fibrosis *S. aureus* clinal isolate ED83 generated a protein-mediated biofilm in response to copper supplementation (Fig. 6.2). This strain forms a polysaccharide dependent biofilm in salt supplemented medium. This might suggest that *S. aureus* can adapt to host niches or environments and generate a different biofilm response. This poses the question, is there a survival advantage to this biofilm phenotype seen in ED83? Biofilms form in many different host environments such as the cystic fibrosis lung, urinary catheters, prosthetic joint implants, osteomyelitis, cardiac pacemakers, and cardiac endothelium to name but a few (Ciofu *et al.*, 2022). It can be postulated generating one biofilm matrix type over another provides a survival advantage to *S. aureus* depending on its environment. Copper is ubiquitously present in the host, especially in blood bound to ceruloplasmin (Linder *et al.*, 1998; Hellman and Gitlin, 2003). However it is also found in high levels in bile (Gupta, 2014; Wang *et al.*, 2020), and bile is a common constituent of the cystic fibrosis lung (Caparrós-Martín *et al.*, 2020). Cystic fibrosis *S. aureus* isolates might generate proteinaceous biofilm in response to copper in the cystic fibrosis lung, potentially improving its survival and persistence in this environment Future studies could examine the effect of copper on biofilm formation of additional clinical isolates of *S. aureus* from cystic fibrosis patients. Generation of

an isogenic deletion of *srtA* in ED83 would elucidate if cell wall-anchored proteins are responsible for the copper-stimulated proteinaceous biofilm. Once a mutant lacking the ability to form biofilm is generated, it could be used in a porcine cystic fibrosis model of infection to determine if generation of this proteinaceous biofilm contributes to virulence of *S. aureus* in the cystic fibrosis lung (Welsh *et al.*, 2009).

MRSA strain BH1CC forms proteinaceous biofilm mediated by FnBPA and FnBPB (O'Neill *et al.*, 2008) in media supplemented with glucose, but biofilm was reduced by copper supplementation (Fig. 6.6.). Zn²⁺ is required for *fnbAB* mediated formation of BH1CC (Geoghegan *et al.*, 2013). Perhaps copper is displacing Zn²⁺ from FnBPA and FnBPB, mismetalling them and disrupting their function in biofilm formation. This may be how copper is reducing FnBPA/FnBPB-mediated biofilm formation of BH1CC, and perhaps this mechanism is also responsible for reduction of other biofilms that require a metal cofactor containing protein to form biofilm. If this is true, copper based antimicrobials such as DMDC (Menghani *et al.*, 2021) might be an effective treatment option to eliminate proteinaceous biofilm infections by *S. aureus*.

A vaccine effective against staphylococci is required to combat staphylococcal infections (Goldstein and Proctor, 2012; Fowler and Proctor, 2014). However no successful vaccine has been generated despite numerable attempts (Daum and Spellberg, 2012). Lacey and colleagues propose that vaccines may need to be specific for different *S. aureus* diseases (Lacey, Geoghegan and McLoughlin, 2016). This principle could be applied to *S. aureus* UTIs, where a vaccine including copper tolerance proteins as antigens might elicit antibody-mediated protection by neutralising the activity of copper tolerance proteins such as CopL, CopB, CopX and Mco. Currently CopL is the only copper tolerance protein shown to contribute to virulence in UTI (Saenkham-Huntsinger *et al.*, 2021). Neutralising *S. aureus* copper tolerance proteins may improve the copper mediated clearance of *S. aureus* from the host similar to the data generated in a mouse model of UTI by Saenkham-Huntsinger and colleagues (Saenkham-Huntsinger *et al.*, 2021). Menghani and colleagues recently explored the ability of multiple copper chelating antimicrobial compounds to kill microorganisms (Menghani *et al.*, 2021). They screened 21 copper chelating compounds for their ability to kill *Streptococcus*

pneumoniae and found compounds that caused copper dependent toxicity. The most promising compound was DMDC, as it had improved *in vitro* killing of *Streptococcus pneumoniae*, *S. aureus*, *Schistosoma mansoni* and *Coccidioides posadasii* in the presence of copper, and also displayed *in vivo* bactericidal activity in mice infected with *Streptococcus pneumoniae* (Menghani *et al.*, 2021). The copper chelating antimicrobial activity is proposed to be due to external binding of copper by DMDC, which is then released into the cytosol upon uptake of DMDC by the microorganism (Menghani *et al.*, 2021). Continued research investigating the use of copper chelators as antimicrobials is required to determine if these drugs are cytotoxic to mammalian/human cells, and if microbial resistance can be easily acquired or generated upon exposure to copper chelating compounds. Novel avenues of antimicrobial therapies are required to create novel therapies to avoid the onset of untreatable superbugs.

In conclusion, the data presented here improve the current understanding of *S. aureus* Mco, the contribution of *S. aureus* copper tolerance genes to *ex vivo* models of human bacteraemic infection, and the effect of copper on biofilm formation of a diverse panel of clinical *S. aureus* strains. This thesis contributes to the understanding of copper tolerance in *S. aureus*, and may aid the generation of future treatments that harness the bactericidal properties of copper, either by reducing copper tolerance of bacteria, or by augmenting copper-mediated bactericidal killing in the host. This thesis also showed that biofilm formation is affected by copper in different manners, identifying that copper may be useful in treatment of some *S. aureus* biofilm infections, but not others.

Bibliography

Abicht, H. K. *et al.* (2013) 'Non-enzymic copper reduction by menaquinone enhances copper toxicity in *Lactococcus lactis* IL1403', *Microbiology (Reading, England)*. *Microbiology (Reading)*, 159(Pt 6), pp. 1190–1197. doi: 10.1099/MIC.0.066928-0.

Achard, M. E. S. *et al.* (2010) 'The multi-copper-ion oxidase CueO of *Salmonella enterica* serovar typhimurium is required for systemic virulence', *Infection and Immunity*. American Society for Microbiology (ASM), 78(5), pp. 2312–2319. doi: 10.1128/IAI.01208-09.

Al-Tameemi, H. *et al.* (2020) '*Staphylococcus aureus* lacking a functional MntABC manganese import system has increased resistance to copper', *Molecular Microbiology*. Wiley, p. mmi.14623. doi: 10.1111/mmi.14623.

Albers, R. W. (1967) 'Biochemical aspects of active transport', *Annu Rev Biochem*, 36, pp. 727–756. doi: 10.1146/annurev.bi.36.070167.003455.

Alexandre, G. and Zhulin, I. B. (2000) 'Laccases are widespread in bacteria', *Trends in Biotechnology*. Elsevier, pp. 41–42. doi: 10.1016/S0167-7799(99)01406-7.

Alibayov, B. *et al.* (2014) '*Staphylococcus aureus* mobile genetic elements', *Molecular biology reports*. Mol Biol Rep, 41(8), pp. 5005–5018. doi: 10.1007/S11033-014-3367-3.

Alonzo, F. *et al.* (2013) 'CCR5 is a receptor for *Staphylococcus aureus* leukotoxin ED', *Nature*. *Nature*, 493(7430), pp. 51–55. doi: 10.1038/NATURE11724.

Alonzo, F. and Torres, V. J. (2014) 'The bicomponent pore-forming leucocidins of *Staphylococcus aureus*', *Microbiology and molecular biology reviews: MMBR*. *Microbiol Mol Biol Rev*, 78(2), pp. 199–230. doi: 10.1128/MMBR.00055-13.

Altimira, F. *et al.* (2012) 'Characterization of copper-resistant bacteria and bacterial communities from copper-polluted agricultural soils of central Chile', *BMC Microbiology*. BioMed Central, 12(1), p. 193. doi: 10.1186/1471-2180-12-193.

Altschul, S. F. *et al.* (1990) 'Basic local alignment search tool', *Journal of molecular biology*. *J Mol Biol*, 215(3), pp. 403–410. doi: 10.1016/S0022-2836(05)80360-2.

Amachi, S. *et al.* (2005) 'Isolation of iodide-oxidizing bacteria from iodide-rich natural gas brines and seawaters', *Microbial ecology*. *Microb Ecol*, 49(4), pp. 547–557. doi: 10.1007/S00248-004-0056-0.

Antonanzas, F., Lozano, C. and Torres, C. (2015) 'Economic features of antibiotic resistance: the case of methicillin-resistant *Staphylococcus aureus*', *PharmacoEconomics*. *Pharmacoeconomics*, 33(4), pp. 285–325. doi: 10.1007/S40273-014-0242-Y.

Archer, N. K., Harro, J. M. and Shirtliff, M. E. (2013) 'Clearance of *Staphylococcus aureus* nasal carriage is T cell dependent and mediated through

interleukin-17A expression and neutrophil influx', *Infection and immunity*. Infect Immun, 81(6), pp. 2070–2075. doi: 10.1128/IAI.00084-13.

Babu, U. and Failla, M. L. (1990) 'Copper status and function of neutrophils are reversibly depressed in marginally and severely copper-deficient rats', *J Nutr*, 120(12), pp. 1700–1709. doi: 10.1093/jn/120.12.1700.

Baker, J. *et al.* (2010) 'Copper stress induces a global stress response in staphylococcus aureus and represses sae and agr expression and biofilm formations', *Applied and Environmental Microbiology*, 76(1), pp. 150–160. doi: 10.1128/AEM.02268-09.

Baker, J. *et al.* (2011) 'The Staphylococcus aureus CsoR regulates both chromosomal and plasmid-encoded copper resistance mechanisms', *Environ Microbiol*, 13(9), pp. 2495–2507. doi: 10.1111/j.1462-2920.2011.02522.x.

Balasubramanian, D. *et al.* (2017) 'Staphylococcus aureus pathogenesis in diverse host environments', *Pathogens and Disease*. Oxford University Press, 75(1), p. 5. doi: 10.1093/FEMSPD/FTX005.

Banbula, A. *et al.* (1998) 'Amino-acid sequence and three-dimensional structure of the Staphylococcus aureus metalloproteinase at 1.72 Å resolution', *Structure (London, England: 1993)*. Structure, 6(9), pp. 1185–1193. doi: 10.1016/S0969-2126(98)00118-X.

Barber, M. (1961) 'Methicillin-resistant staphylococci', *Journal of clinical pathology*. J Clin Pathol, 14(4), pp. 385–393. doi: 10.1136/JCP.14.4.385.

Barnett, J. P. *et al.* (2008) 'A minimal Tat system from a gram-positive organism: a bifunctional TatA subunit participates in discrete TatAC and TatA complexes', *The Journal of biological chemistry*. J Biol Chem, 283(5), pp. 2534–2542. doi: 10.1074/JBC.M708134200.

Becker, K., Skov, R. and Eiff, C. (2015) 'Staphylococcus, Micrococcus, and Other Catalase-Positive Cocci *', in *Manual of Clinical Microbiology, 10th Edition*. American Society of Microbiology, pp. 308–330. doi: 10.1128/9781555816728.ch19.

Becker, S. *et al.* (2014) 'Release of protein A from the cell wall of Staphylococcus aureus', *Proceedings of the National Academy of Sciences of the United States of America*. PNAS, 111(4), pp. 1574–1579. doi: 10.1073/pnas.1317181111.

Van Belkum, A. *et al.* (2009) 'Reclassification of Staphylococcus aureus nasal carriage types', *The Journal of infectious diseases*. J Infect Dis, 199(12), pp. 1820–1826. doi: 10.1086/599119.

van den Berg, J. M. *et al.* (2009) 'Chronic granulomatous disease: the European experience', *PloS one*. PLoS One, 4(4). doi: 10.1371/JOURNAL.PONE.0005234.

Berg, T. *et al.* (1998) 'Complete nucleotide sequence of pSK41: evolution of staphylococcal conjugative multiresistance plasmids', *Journal of bacteriology*. J Bacteriol, 180(17), pp. 4350–4359. doi: 10.1128/JB.180.17.4350-4359.1998.

Van Berge Henegouwen, G. P. *et al.* (1977) *Biliary Secretion of Copper in*

Healthy Man: Quantitation by an intestinal perfusion technique, Gastroenterology. doi: 10.1016/S0016-5085(77)80016-4.

Berks, B. C., Palmer, T. and Sargent, F. (2003) 'The Tat protein translocation pathway and its role in microbial physiology', *Advances in microbial physiology*. *Adv Microb Physiol*, 47, pp. 187–254. doi: 10.1016/S0065-2911(03)47004-5.

Berube, B. J. and Wardenburg, J. B. (2013) 'Staphylococcus aureus α -toxin: nearly a century of intrigue', *Toxins*. *Toxins (Basel)*, 5(6), pp. 1140–1166. doi: 10.3390/TOXINS5061140.

Betley, M. J. and Mekalanos, J. J. (1985) 'Staphylococcal enterotoxin a is encoded by phage', *Science*, 229(4709), pp. 185–187. doi: 10.1126/SCIENCE.3160112.

Biswas, L. *et al.* (2009) 'Role of the twin-arginine translocation pathway in *Staphylococcus*', *J Bacteriol*, 191(19), pp. 5921–5929. doi: 10.1128/JB.00642-09.

Blaudeck, N. *et al.* (2003) 'Genetic analysis of pathway specificity during posttranslational protein translocation across the *Escherichia coli* plasma membrane', *Journal of bacteriology*. *J Bacteriol*, 185(9), pp. 2811–2819. doi: 10.1128/JB.185.9.2811-2819.2003.

Bogomolski-Yahalom, V. and Matzner, Y. (1995) 'Disorders of neutrophil function', *Blood reviews*. *Blood Rev*, 9(3), pp. 183–190. doi: 10.1016/0268-960X(95)90024-1.

Bose, J. L. *et al.* (2012) 'Contribution of the *Staphylococcus aureus* Atl AM and GL murein hydrolase activities in cell division, autolysis, and biofilm formation', *PLoS one*. *PLoS One*, 7(7). doi: 10.1371/JOURNAL.PONE.0042244.

Bruins, M. R., Kapil, S. and Oehme, F. W. (2000) 'Microbial Resistance to Metals in the Environment', *Ecotoxicology and Environmental Safety*. Academic Press, 45(3), pp. 198–207. doi: 10.1006/EESA.1999.1860.

Bui, L. M. G., Conlon, B. P. and Kidd, S. P. (2017) 'Antibiotic tolerance and the alternative lifestyles of *Staphylococcus aureus*', *Essays in Biochemistry*. Portland Press, 61(1), pp. 71–79. doi: 10.1042/EBC20160061.

Bull, P. C. and Cox, D. W. (1994) 'Wilson disease and Menkes disease: new handles on heavy-metal transport', *Trends Genet*, 10(7), pp. 246–252.

Buvelot, H. *et al.* (2017) 'Staphylococcus aureus, phagocyte NADPH oxidase and chronic granulomatous disease', *FEMS microbiology reviews*. *FEMS Microbiol Rev*, 41(2), pp. 139–157. doi: 10.1093/FEMSRE/FUW042.

Caparrós-Martín, J. A. *et al.* (2020) 'The Detection of Bile Acids in the Lungs of Paediatric Cystic Fibrosis Patients Is Associated with Altered Inflammatory Patterns', *Diagnostics 2020, Vol. 10, Page 282*. Multidisciplinary Digital Publishing Institute, 10(5), p. 282. doi: 10.3390/DIAGNOSTICS10050282.

Carroll, R. K. *et al.* (2016) 'Genome-wide Annotation, Identification, and Global Transcriptomic Analysis of Regulatory or Small RNA Gene Expression in *Staphylococcus aureus*', *mBio*. *mBio*, 7(1). doi: 10.1128/MBIO.01990-15.

Cha, J. S. and Cooksey, D. A. (1991) 'Copper resistance in *Pseudomonas syringae* mediated by periplasmic and outer membrane proteins', *Proc Natl Acad*

Sci U S A, 88(20), pp. 8915–8919.

Chalker, A. F. *et al.* (2000) 'The *bacA* gene, which determines bacitracin susceptibility in *Streptococcus pneumoniae* and *Staphylococcus aureus*, is also required for virulence.', *Microbiology (Reading, England)*. Society for General Microbiology, 146 (Pt 7)(7), pp. 1547–1553. doi: 10.1099/00221287-146-7-1547.

Chambers, H. F. (2005) 'Community-associated MRSA--resistance and virulence converge', *The New England journal of medicine*. *N Engl J Med*, 352(14), pp. 1485–1487. doi: 10.1056/NEJME058023.

Chan, W. T. *et al.* (2013) 'A comparison and optimization of methods and factors affecting the transformation of *Escherichia coli*', *Bioscience Reports*, 33(6). doi: 10.1042/BSR20130098.

Chang, I. J. and Hahn, S. H. (2017) 'The genetics of Wilson disease', *Handbook of clinical neurology*. NIH Public Access, 142, p. 19. doi: 10.1016/B978-0-444-63625-6.00003-3.

Cheung, G. Y. C. *et al.* (2014) 'Phenol-soluble modulins--critical determinants of staphylococcal virulence', *FEMS microbiology reviews*. *FEMS Microbiol Rev*, 38(4), pp. 698–719. doi: 10.1111/1574-6976.12057.

Cheung, G. Y. C., Bae, J. S. and Otto, M. (2021) 'Pathogenicity and virulence of *Staphylococcus aureus*', *Virulence*. Taylor & Francis, 12(1), p. 547. doi: 10.1080/21505594.2021.1878688.

Chikramane, S. G. *et al.* (1991) 'Tn554 inserts in methicillin-resistant *Staphylococcus aureus* from Australia and England: comparison with an American methicillin-resistant group', *Journal of general microbiology*. *J Gen Microbiol*, 137(6), pp. 1303–1311. doi: 10.1099/00221287-137-6-1303.

Chillappagari, S. *et al.* (2010) 'Copper Stress Affects Iron Homeostasis by Destabilizing Iron-Sulfur Cluster Formation in *Bacillus subtilis*', *Journal of Bacteriology*. American Society for Microbiology (ASM), 192(10), p. 2512. doi: 10.1128/JB.00058-10.

Cho, H. *et al.* (2015) 'Calprotectin Increases the Activity of the SaeRS Two Component System and Murine Mortality during *Staphylococcus aureus* Infections', *PLoS Pathogens*. Public Library of Science, 11(7). doi: 10.1371/journal.ppat.1005026.

Ciofu, O. *et al.* (2022) 'Tolerance and resistance of microbial biofilms', *Nature reviews. Microbiology*. *Nat Rev Microbiol*. doi: 10.1038/S41579-022-00682-4.

Clarke, S. R. and Foster, S. J. (2006) 'Surface adhesins of *Staphylococcus aureus*', *Advances in microbial physiology*. *Adv Microb Physiol*, 51(SUPPL.), pp. 187–224. doi: 10.1016/S0065-2911(06)51004-5.

Classen, T., Pietruszka, J. and Schuback, S. M. (2013) 'A new multicopper oxidase from Gram-positive bacterium *Rhodococcus erythropolis* with activity modulating methionine rich tail', *Protein Expression and Purification*. Academic Press, 89(1), pp. 97–108. doi: 10.1016/j.pep.2013.02.003.

Conlon, B. P. *et al.* (2016) 'Persister formation in *Staphylococcus aureus* is associated with ATP depletion', *Nature Microbiology 2016 1:5*. Nature Publishing

Group, 1(5), pp. 1–7. doi: 10.1038/nmicrobiol.2016.51.

Conlon, K. M., Humphreys, H. and O’Gara, J. P. (2002) ‘icaR encodes a transcriptional repressor involved in environmental regulation of ica operon expression and biofilm formation in *Staphylococcus epidermidis*’, *Journal of bacteriology*. *J Bacteriol*, 184(16), pp. 4400–4408. doi: 10.1128/JB.184.16.4400-4408.2002.

Copper in Drinking-water Background document for development of WHO Guidelines for Drinking-water Quality (2004).

Cordano, A., Placko, R. P. and Graham, G. G. (1966) ‘Hypocupremia and Neutropenia in Copper Deficiency’, *Blood*. Content Repository Only!, 28(2), pp. 280–283. doi: 10.1182/BLOOD.V28.2.280.280.

Cormican, P. and Keane, O. M. (2018) ‘Complete Genome Sequences of Sequence Type 71 (ST71) and ST97 *Staphylococcus aureus* Isolates from Bovine Milk’, *Microbiology Resource Announcements*. American Society for Microbiology (ASM), 7(5), pp. 954–972. doi: 10.1128/MRA.00954-18.

Corrigan, R. M. and Foster, T. J. (2009) ‘An improved tetracycline-inducible expression vector for *Staphylococcus aureus*’, *Plasmid*. Academic Press, 61(2), pp. 126–129. doi: 10.1016/j.plasmid.2008.10.001.

Cortes, L., Wedd, A. G. and Xiao, Z. (2015) ‘The functional roles of the three copper sites associated with the methionine-rich insert in the multicopper oxidase CueO from *E. coli*’, *Metallomics*, 7(5), pp. 776–785. doi: 10.1039/c5mt00001g.

Cosgrove, K. *et al.* (2007) ‘Catalase (KatA) and alkyl hydroperoxide reductase (AhpC) have compensatory roles in peroxide stress resistance and are required for survival, persistence, and nasal colonization in *Staphylococcus aureus*’, *Journal of bacteriology*. *J Bacteriol*, 189(3), pp. 1025–1035. doi: 10.1128/JB.01524-06.

Cousins, R. J. (1985) ‘Absorption, transport, and hepatic metabolism of copper and zinc: Special reference to metallothionein and ceruloplasmin’, *Physiological Reviews*, pp. 238–309. doi: 10.1152/physrev.1985.65.2.238.

Cregg, K. M., Wilding, E. I. and Black, M. T. (1996) ‘Molecular cloning and expression of the *spsB* gene encoding an essential type I signal peptidase from *Staphylococcus aureus*.’, *Journal of Bacteriology*. American Society for Microbiology (ASM), 178(19), p. 5712. doi: 10.1128/JB.178.19.5712-5718.1996.

Cristóbal, S. *et al.* (1999) ‘Competition between Sec- and TAT-dependent protein translocation in *Escherichia coli*’, *The EMBO journal*. *EMBO J*, 18(11), pp. 2982–2990. doi: 10.1093/EMBOJ/18.11.2982.

Curnutte, J. T., Whitten, D. M. and Babior, B. M. (2010) ‘Defective Superoxide Production by Granulocytes from Patients with Chronic Granulomatous Disease’, <http://dx.doi.org/10.1056/NEJM197403142901104>. Massachusetts Medical Society, 290(11), pp. 593–597. doi: 10.1056/NEJM197403142901104.

Daum, R. S. and Spellberg, B. (2012) ‘Progress toward a *Staphylococcus aureus* vaccine’, *Clinical infectious diseases : an official publication of the Infectious Diseases Society of America*. *Clin Infect Dis*, 54(4), pp. 560–567. doi: 10.1093/CID/CIR828.

Diep, B. A. *et al.* (2006) 'Complete genome sequence of USA300, an epidemic clone of community-acquired methicillin-resistant *Staphylococcus aureus*', *Lancet (London, England)*. *Lancet*, 367(9512), pp. 731–739. doi: 10.1016/S0140-6736(06)68231-7.

Diep, B. A. *et al.* (2008) 'The arginine catabolic mobile element and staphylococcal chromosomal cassette *mec* linkage: convergence of virulence and resistance in the USA300 clone of methicillin-resistant *Staphylococcus aureus*', *The Journal of infectious diseases*. *J Infect Dis*, 197(11), pp. 1523–1530. doi: 10.1086/587907.

Diep, B. A. *et al.* (2010) 'Polymorphonuclear leukocytes mediate *Staphylococcus aureus* Panton-Valentine leukocidin-induced lung inflammation and injury', *Proceedings of the National Academy of Sciences of the United States of America*. *Proc Natl Acad Sci U S A*, 107(12), pp. 5587–5592. doi: 10.1073/PNAS.0912403107.

Djoko, K. Y. *et al.* (2010) 'Reaction Mechanisms of the Multicopper Oxidase CueO from *Escherichia coli* Support Its Functional Role as a Cuprous Oxidase', *Journal of the American Chemical Society*. American Chemical Society, 132(6), pp. 2005–2015. doi: 10.1021/JA9091903.

Djoko, K. Y. *et al.* (2015) 'The role of copper and zinc toxicity in innate immune defense against bacterial pathogens', *Journal of Biological Chemistry*. American Society for Biochemistry and Molecular Biology Inc., 290(31), pp. 1854–1861. doi: 10.1074/jbc.R115.647099.

Djoko, K. Y., Achard, M. E. S. and McEwan, A. G. (2004) 'Copper in Immune Cells', *Encyclopedia of Inorganic and Bioinorganic Chemistry*. American Cancer Society, pp. 1–11. doi: 10.1002/9781119951438.EIBC2145.

Djoko, K. Y., Xiao, Z. and Wedd, A. G. (2008) 'Copper Resistance in *E. coli*: The Multicopper Oxidase PcoA Catalyzes Oxidation of Copper(I) in CuI/CuII-PcoC', *ChemBioChem*. John Wiley & Sons, Ltd, 9(10), pp. 1579–1582. doi: 10.1002/CBIC.200800100.

Dollwet, H. H. A. and Sorenson, J. R. J. (1985) 'Historic uses of copper compounds in medicine', *Trace Elements in Medicine*, 2, pp. 80–87.

Dossett, J. H. *et al.* (1969) 'Antiphagocytic effects of staphylococcal protein A.', *Journal of immunology (Baltimore, Md. : 1950)*. United States, 103(6), pp. 1405–1410.

Downer, R. *et al.* (2002) 'The elastin-binding protein of *Staphylococcus aureus* (EbpS) is expressed at the cell surface as an integral membrane protein and not as a cell wall-associated protein', *Journal of Biological Chemistry*. American Society for Biochemistry and Molecular Biology, 277(1), pp. 243–250. doi: 10.1074/jbc.M107621200.

Dubin, G. (2002) 'Extracellular proteases of *Staphylococcus spp*', *Biological chemistry*. *Biol Chem*, 383(7–8), pp. 1075–1086. doi: 10.1515/BC.2002.116.

Dupont, C. L., Grass, G. and Rensing, C. (2011) 'Copper toxicity and the origin of bacterial resistance--new insights and applications', *Metallomics: integrated biometal science*. *Metallomics*, 3(11), pp. 1109–1118. doi:

10.1039/C1MT00107H.

Endo, G. and Silver, S. (1995) 'CadC, the Transcriptional Regulatory Protein of the Cadmium Resistance System of *Staphylococcus aureus* Plasmid pI258', *JOURNAL OF BACTERIOLOGY*, 177(15), pp. 4437–4441.

Espírito Santo, C. *et al.* (2008) 'Contribution of copper ion resistance to survival of *Escherichia coli* on metallic copper surfaces', *Applied and Environmental Microbiology*. American Society for Microbiology, 74(4), pp. 977–986. doi: 10.1128/AEM.01938-07.

Espírito Santo, C., Morais, P. V. and Grass, G. (2010) 'Isolation and characterization of bacteria resistant to metallic copper surfaces', *Applied and environmental microbiology*. Appl Environ Microbiol, 76(5), pp. 1341–1348. doi: 10.1128/AEM.01952-09.

Everitt, R. G. *et al.* (2014) 'Mobile elements drive recombination hotspots in the core genome of *Staphylococcus aureus*', *Nature communications*. Nat Commun, 5. doi: 10.1038/NCOMMS4956.

Feuillie, C. *et al.* (2017) 'Molecular interactions and inhibition of the staphylococcal biofilm-forming protein SdrC', *Proceedings of the National Academy of Sciences of the United States of America*. National Academy of Sciences, 114(14), pp. 3738–3743. doi: 10.1073/pnas.1616805114.

Fey, P. D. *et al.* (2013) 'A genetic resource for rapid and comprehensive phenotype screening of nonessential *Staphylococcus aureus* genes', *mBio*. American Society for Microbiology, 4(1). doi: 10.1128/MBIO.00537-12/SUPPL_FILE/MBO001131446ST03.PDF.

Flannagan, R. S., Cosío, G. and Grinstein, S. (2009) 'Antimicrobial mechanisms of phagocytes and bacterial evasion strategies', *Nature reviews. Microbiology*. Nat Rev Microbiol, 7(5), pp. 355–366. doi: 10.1038/NRMICRO2128.

Flannagan, R. S., Heit, B. and Heinrichs, D. E. (2016) 'Intracellular replication of *Staphylococcus aureus* in mature phagolysosomes in macrophages precedes host cell death, and bacterial escape and dissemination', *Cellular Microbiology*. Blackwell Publishing Ltd, 18(4), pp. 514–535. doi: 10.1111/cmi.12527.

Forsgren, A. and Sjöquist, J. (1966) "Protein A" from *Staphylococcus aureus*', *The Journal of Immunology*, 97(6), pp. 822 LP – 827.

Foster, A. W., Osman, D. and Robinson, N. J. (2014) 'Metal preferences and metallation', *Journal of Biological Chemistry*. American Society for Biochemistry and Molecular Biology Inc., 289(41), pp. 28095–28103. doi: 10.1074/JBC.R114.588145/ATTACHMENT/97529EA1-B7A7-46DC-B03D-9C94D707D0CE/MMC1.PDF.

Foster, T. J. (2019) 'The MSCRAMM Family of Cell-Wall-Anchored Surface Proteins of Gram-Positive Cocci', *Trends in Microbiology*. Elsevier, 27(11), pp. 927–941. doi: 10.1016/J.TIM.2019.06.007.

Fowler, V. G. and Proctor, R. A. (2014) 'Where does a *Staphylococcus aureus* vaccine stand?', *Clinical microbiology and infection: the official publication of the European Society of Clinical Microbiology and Infectious Diseases*. Clin Microbiol Infect, 20 Suppl 5(0 5), pp. 66–75. doi: 10.1111/1469-0691.12570.

Frain, K. M., Robinson, C. and van Dijl, J. M. (2019) 'Transport of Folded Proteins by the Tat System', *Protein Journal*. Springer New York LLC, pp. 377–388. doi: 10.1007/s10930-019-09859-y.

Freinbichler, W. *et al.* (2011) 'Highly reactive oxygen species: detection, formation, and possible functions', *Cellular and Molecular Life Sciences*. Cell Mol Life Sci, 68(12), pp. 2067–2079. doi: 10.1007/s00018-011-0682-x.

Freudl, R. (2013) 'Leaving home ain't easy: protein export systems in Gram-positive bacteria', *Research in Microbiology*. Elsevier Masson, 164(6), pp. 664–674. doi: 10.1016/J.RESMIC.2013.03.014.

Freudl, R. (2018) 'Signal peptides for recombinant protein secretion in bacterial expression systems', *Microbial Cell Factories*. BioMed Central Ltd. doi: 10.1186/s12934-018-0901-3.

Fung, D. K. C. *et al.* (2013) 'Copper efflux is induced during anaerobic amino acid limitation in Escherichia coli to protect iron-sulfur cluster enzymes and biogenesis', *Journal of bacteriology*. J Bacteriol, 195(20), pp. 4556–4568. doi: 10.1128/JB.00543-13.

Gaballa, A. *et al.* (2010) 'Biosynthesis and functions of bacillithiol, a major low-molecular-weight thiol in Bacilli', *Proceedings of the National Academy of Sciences of the United States of America*. National Academy of Sciences, 107(14), p. 6482. doi: 10.1073/PNAS.1000928107.

Gaetke, L. M., Chow-Johnson, H. S. and Chow, C. K. (2014) 'Copper: toxicological relevance and mechanisms', *Archives of Toxicology*. Springer Verlag, pp. 1929–1938. doi: 10.1007/s00204-014-1355-y.

Ganguly, T. *et al.* (2021) 'Zinc import mediated by AdcABC is critical for colonization of the dental biofilm by Streptococcus mutans in an animal model', *Molecular Oral Microbiology*. John Wiley & Sons, Ltd, 36(3), pp. 214–224. doi: 10.1111/OMI.12337.

Geoghegan, J. A. *et al.* (2010) 'Role of surface protein SasG in biofilm formation by Staphylococcus aureus', *Journal of bacteriology*. J Bacteriol, 192(21), pp. 5663–5673. doi: 10.1128/JB.00628-10.

Geoghegan, J. A. *et al.* (2013) 'Subdomains N2N3 of Fibronectin Binding Protein A Mediate Staphylococcus aureus Biofilm Formation and Adherence to Fibrinogen Using Distinct Mechanisms', *Journal of Bacteriology*. American Society for Microbiology (ASM), 195(11), p. 2675. doi: 10.1128/JB.02128-12.

Gohlke, U. *et al.* (2005) 'The TatA component of the twin-arginine protein transport system forms channel complexes of variable diameter', *Proceedings of the National Academy of Sciences of the United States of America*. National Academy of Sciences, 102(30), p. 10482. doi: 10.1073/PNAS.0503558102.

Goldstein, E. J. C. and Proctor, R. A. (2012) 'Challenges for a universal Staphylococcus aureus vaccine', *Clinical infectious diseases : an official publication of the Infectious Diseases Society of America*. Clin Infect Dis, 54(8), pp. 1179–1186. doi: 10.1093/CID/CIS033.

Golonka, E. *et al.* (2004) 'Genetic characterization of staphopain genes in Staphylococcus aureus', *Biological chemistry*. Biol Chem, 385(11), pp. 1059–1067.

doi: 10.1515/BC.2004.137.

Goodyear, C. S. and Silverman, G. J. (2003) 'Death by a B cell superantigen: In vivo VH-targeted apoptotic supraclonal B cell deletion by a Staphylococcal Toxin', *The Journal of experimental medicine*. *J Exp Med*, 197(9), pp. 1125–1139. doi: 10.1084/JEM.20020552.

Grass, G. *et al.* (2004) 'Linkage between catecholate siderophores and the multicopper oxidase CueO in *Escherichia coli*', *Journal of Bacteriology*, 186(17), pp. 5826–5833. doi: 10.1128/JB.186.17.5826-5833.2004.

Grass, G. and Rensing, C. (2001a) 'CueO is a multi-copper oxidase that confers copper tolerance in *Escherichia coli*', *Biochem Biophys Res Commun*, 286(5), pp. 902–908. doi: 10.1006/bbrc.2001.5474.

Grass, G. and Rensing, C. (2001b) 'Genes involved in copper homeostasis in *Escherichia coli*', *J Bacteriol*, 183(6), pp. 2145–2147. doi: 10.1128/JB.183.6.2145-2147.2001.

Grass, G., Rensing, C. and Solioz, M. (2011) 'Metallic copper as an antimicrobial surface', *Applied and Environmental Microbiology*, pp. 1541–1547. doi: 10.1128/AEM.02766-10.

Gresham, H. D. *et al.* (2000) 'Survival of *Staphylococcus aureus* inside neutrophils contributes to infection', *Journal of immunology (Baltimore, Md. : 1950)*. *J Immunol*, 164(7), pp. 3713–3722. doi: 10.4049/JIMMUNOL.164.7.3713.

Grosz, M. *et al.* (2014) 'Cytoplasmic replication of *Staphylococcus aureus* upon phagosomal escape triggered by phenol-soluble modulins', *Cellular Microbiology*. Blackwell Publishing Ltd, 16(4), pp. 451–465. doi: 10.1111/cmi.12233.

Guerra, F. E. *et al.* (2017) 'Epic immune battles of history: Neutrophils vs. *Staphylococcus aureus*', *Frontiers in Cellular and Infection Microbiology*. Frontiers Media S.A., p. 286. doi: 10.3389/fcimb.2017.00286.

Gullberg, E. *et al.* (2014) 'Selection of a multidrug resistance plasmid by sublethal levels of antibiotics and heavy metals', *mBio*. American Society for Microbiology, 5(5). doi: 10.1128/mBio.01918-14.

Guo, H. *et al.* (2022) 'Biofilm and Small Colony Variants-An Update on *Staphylococcus aureus* Strategies toward Drug Resistance', *International journal of molecular sciences*. *Int J Mol Sci*, 23(3). doi: 10.3390/IJMS23031241.

Gupta, S. (2014) 'Cell therapy to remove excess copper in Wilson's disease', *Annals of the New York Academy of Sciences*. *Ann N Y Acad Sci*, 1315(1), pp. 70–80. doi: 10.1111/NYAS.12450.

Ha, K. P. *et al.* (2020) 'Staphylococcal DNA Repair Is Required for Infection', *mBio*. NLM (Medline), 11(6). doi: 10.1128/mBio.02288-20.

De Haas, C. J. C. *et al.* (2004) 'Chemotaxis Inhibitory Protein of *Staphylococcus aureus*, a Bacterial Antiinflammatory Agent', *The Journal of Experimental Medicine*. The Rockefeller University Press, 199(5), p. 687. doi: 10.1084/JEM.20031636.

Haber, F. and Weiss, J. (1934) 'The catalytic decomposition of hydrogen

peroxide by iron salts', *Proceedings of the Royal Society of London. Series A - Mathematical and Physical Sciences*. The Royal Society, 147(861), pp. 332–351. doi: 10.1098/rspa.1934.0221.

van Hal, S. J. *et al.* (2012) 'Predictors of mortality in *Staphylococcus aureus* Bacteremia', *Clinical microbiology reviews*. Clin Microbiol Rev, 25(2), pp. 362–386. doi: 10.1128/CMR.05022-11.

Halfdanarson, T. R. *et al.* (2008) 'Hematological manifestations of copper deficiency: a retrospective review', *European journal of haematology*. Eur J Haematol, 80(6), pp. 523–531. doi: 10.1111/J.1600-0609.2008.01050.X.

Hall, B. G. *et al.* (2014) 'Growth rates made easy', *Molecular Biology and Evolution*. Oxford Academic, 31(1), pp. 232–238. doi: 10.1093/molbev/mst187.

Hampton, M. B., Kettle, A. J. and Winterbourn, C. C. (1996) 'Involvement of superoxide and myeloperoxidase in oxygen-dependent killing of *Staphylococcus aureus* by neutrophils', *Infection and Immunity*. American Society for Microbiology, 64(9), pp. 3512–3517. doi: 10.1128/IAI.64.9.3512-3517.1996.

Hampton, M. B. and Winterbourn, C. C. (1995) 'Modification of neutrophil oxidant production with diphenyleneiodonium and its effect on bacterial killing.', *Free Radical Biology & Medicine*, 18(4), pp. 633–639. doi: 10.1016/0891-5849(94)00181-I.

Hanks, J. H. (1975) 'Hanks' balanced salt solution and pH control', *TCA manual / Tissue Culture Association 1975 1:1*. Springer, 1(1), pp. 3–4. doi: 10.1007/BF00914425.

Haupt, K. *et al.* (2008) 'The *Staphylococcus aureus* Protein Sbi Acts as a Complement Inhibitor and Forms a Tripartite Complex with Host Complement Factor H and C3b', *PLOS Pathogens*. Public Library of Science, 4(12), p. e1000250. doi: 10.1371/JOURNAL.PPAT.1000250.

Heilmann, C. (2011) 'Adhesion mechanisms of staphylococci', *Advances in experimental medicine and biology*. Adv Exp Med Biol, 715, pp. 105–123. doi: 10.1007/978-94-007-0940-9_7.

Hellman, N. E. and Gitlin, J. D. (2003) 'CERULOPLASMIN METABOLISM AND FUNCTION', <http://dx.doi.org/10.1146/annurev.nutr.22.012502.114457>. Annual Reviews 4139 El Camino Way, P.O. Box 10139, Palo Alto, CA 94303-0139, USA , 22, pp. 439–458. doi: 10.1146/ANNUREV.NUTR.22.012502.114457.

Heresi, G. *et al.* (1985) 'Phagocytosis and immunoglobulin levels in hypocupremic infants', *Nutrition Research*. Elsevier, 5(12), pp. 1327–1334. doi: 10.1016/S0271-5317(85)80043-9.

Hingston, P. *et al.* (2019) 'Comparative analysis of *listeria monocytogenes* plasmids and expression levels of plasmid-encoded genes during growth under salt and acid stress conditions', *Toxins*. MDPI AG, 11(7). doi: 10.3390/toxins11070426.

Hoegger, P. J. *et al.* (2006) 'Phylogenetic comparison and classification of laccase and related multicopper oxidase protein sequences', *FEBS Journal*, 273(10), pp. 2308–2326. doi: 10.1111/j.1742-4658.2006.05247.x.

Høiby, N. *et al.* (2015) 'ESCMID guideline for the diagnosis and treatment of

biofilm infections 2014', *Clinical microbiology and infection : the official publication of the European Society of Clinical Microbiology and Infectious Diseases*. Clin Microbiol Infect, 21 Suppl 1(S1), pp. S1–S25. doi: 10.1016/J.CMI.2014.10.024.

Holden, M. T. G. *et al.* (2004) 'Complete genomes of two clinical *Staphylococcus aureus* strains: Evidence for the evolution of virulence and drug resistance', *Proceedings of the National Academy of Sciences of the United States of America*, 101(26), pp. 9786–9791. doi: 10.1073/pnas.0402521101.

Hou, B. and Brüser, T. (2011) 'The Tat-dependent protein translocation pathway.', *Biomolecular Concepts*. De Gruyter Mouton, 2(6), pp. 507–523. doi: 10.1515/BMC.2011.040.

Howell, S. B. and Abada, P. (2010) 'Regulation of Cisplatin Cytotoxicity by Cu Influx Transporters', *Metal-Based Drugs*. Hindawi Limited, 2010. doi: 10.1155/2010/317581.

Hussain, M. *et al.* (1997) 'A 140-kilodalton extracellular protein is essential for the accumulation of *Staphylococcus epidermidis* strains on surfaces', *Infection and Immunity*. American Society for Microbiology, 65(2), pp. 519–524. doi: 10.1128/IAI.65.2.519-524.1997.

Huston, W. M., Jennings, M. P. and McEwan, A. G. (2002) 'The multicopper oxidase of *Pseudomonas aeruginosa* is a ferroxidase with a central role in iron acquisition', *Molecular Microbiology*. John Wiley & Sons, Ltd, 45(6), pp. 1741–1750. doi: 10.1046/j.1365-2958.2002.03132.x.

I. H. Scheinberg and I. Sternlieb Philadelphia (1984) *Wilson's disease (a volume in the major problems in internal medicine series)*, *Annals of Neurology*. John Wiley & Sons, Ltd. doi: 10.1002/ANA.410160531.

Imlay, J. A. (2014) 'The mismetallation of enzymes during oxidative stress', *The Journal of biological chemistry*. J Biol Chem, 289(41), pp. 28121–28128. doi: 10.1074/JBC.R114.588814.

Inoshima, I. *et al.* (2011) 'A *Staphylococcus aureus* pore-forming toxin subverts the activity of ADAM10 to cause lethal infection in mice', *Nature medicine*. Nat Med, 17(10), pp. 1310–1314. doi: 10.1038/NM.2451.

Irving, H. and Williams, R. J. P. (1953) '637. The stability of transition-metal complexes', *Journal of the Chemical Society (Resumed)*. The Royal Society of Chemistry, 3245(0), pp. 3192–3210. doi: 10.1039/JR9530003192.

Jamrozy, D. *et al.* (2017) 'Evolution of mobile genetic element composition in an epidemic methicillin-resistant *Staphylococcus aureus*: Temporal changes correlated with frequent loss and gain events', *BMC Genomics*. BioMed Central Ltd., 18(1), pp. 1–12. doi: 10.1186/S12864-017-4065-Z/FIGURES/5.

Jenul, C. and Horswill, A. R. (2018) 'Regulation of *Staphylococcus aureus* Virulence', *Microbiology Spectrum*. American Society for Microbiology, 6(1). doi: 10.1128/microbiolspec.gpp3-0031-2018.

Jevons, M. P. (1961) "'Celbenin" - resistant *Staphylococci*', *Br Med J*. British Medical Journal Publishing Group, 1(5219), pp. 124–125. doi: 10.1136/BMJ.1.5219.124-A.

Johnson, A. P. *et al.* (2001) 'Dominance of EMRSA-15 and -16 among MRSA causing nosocomial bacteraemia in the UK: analysis of isolates from the European Antimicrobial Resistance Surveillance System (EARSS)', *The Journal of antimicrobial chemotherapy*. *J Antimicrob Chemother*, 48(1), pp. 143–144. doi: 10.1093/JAC/48.1.143.

Johnson, M. *et al.* (2005) 'Iron-responsive regulation of biofilm formation in *Staphylococcus aureus* involves Fur-dependent and Fur-independent mechanisms', *Journal of Bacteriology*. American Society for Microbiology Journals, 187(23), pp. 8211–8215. doi: 10.1128/JB.187.23.8211-8215.2005.

Johnson, M., Cockayne, A. and Morrissey, J. A. (2008) 'Iron-regulated biofilm formation in *Staphylococcus aureus* newman requires *ica* and the secreted protein Emp', *Infection and Immunity*. American Society for Microbiology (ASM), 76(4), pp. 1756–1765. doi: 10.1128/IAI.01635-07.

Josefsson, E. *et al.* (1998) 'Three new members of the serine-aspartate repeat protein multigene family of *Staphylococcus aureus*', *Microbiology*. Society for General Microbiology, 144(12), pp. 3387–3395. doi: 10.1099/00221287-144-12-3387/CITE/REFWORKS.

Kaler, S. G. *et al.* (2008) 'Neonatal Diagnosis and Treatment of Menkes Disease', *The New England journal of medicine*. NIH Public Access, 358(6), p. 605. doi: 10.1056/NEJMOA070613.

Kanehisa, M. and Goto, S. (2000) 'KEGG: kyoto encyclopedia of genes and genomes', *Nucleic acids research*. Nucleic Acids Res, 28(1), pp. 27–30. doi: 10.1093/NAR/28.1.27.

Kaneko, J. *et al.* (1998) 'Complete nucleotide sequence and molecular characterization of the temperate staphylococcal bacteriophage ϕ PVL carrying Panton-Valentine leukocidin genes', *Gene*, 215(1), pp. 57–67. doi: 10.1016/S0378-1119(98)00278-9.

Kang, M. *et al.* (2013) 'Collagen-binding microbial surface components recognizing adhesive matrix molecule (MSCRAMM) of gram-positive bacteria inhibit complement activation via the classical pathway', *Journal of Biological Chemistry*, 288(28), pp. 20520–20531. doi: 10.1074/JBC.M113.454462.

Karavolos, M. H. *et al.* (2003) 'Role and regulation of the superoxide dismutases of *Staphylococcus aureus*', *Microbiology (Reading, England)*. Microbiology (Reading), 149(Pt 10), pp. 2749–2758. doi: 10.1099/MIC.0.26353-0.

Karnachuk, O. V. *et al.* (2008) 'Precipitation of Cu-sulfides by copper-tolerant *Desulfovibrio* isolates', *Geomicrobiology Journal*. Taylor & Francis Group, 25(5), pp. 219–227. doi: 10.1080/01490450802153124.

Katayama, Y., Ito, T. and Hiramatsu, K. (2000) 'A new class of genetic element, staphylococcus cassette chromosome *mec*, encodes methicillin resistance in *Staphylococcus aureus*', *Antimicrobial Agents and Chemotherapy*, 44(6), pp. 1549–1555. doi: 10.1128/AAC.44.6.1549-1555.2000.

Kelley, L. A. *et al.* (2015) 'The Phyre2 web portal for protein modeling, prediction and analysis', *Nature Protocols*. Nature Publishing Group, 10(6), pp. 845–858. doi: 10.1038/nprot.2015.053.

Kiedrowski, M. R. *et al.* (2011) 'Nuclease modulates biofilm formation in community-associated methicillin-resistant *Staphylococcus aureus*', *PloS one*. PLoS One, 6(11). doi: 10.1371/JOURNAL.PONE.0026714.

Kirby, W. M. M. (1944) 'EXTRACTION OF A HIGHLY POTENT PENICILLIN INACTIVATOR FROM PENICILLIN RESISTANT STAPHYLOCOCCI', *Science (New York, N.Y.)*. Science, 99(2579), pp. 452–453. doi: 10.1126/SCIENCE.99.2579.452.

Koh, E. I. and Henderson, J. P. (2015) 'Microbial Copper-binding Siderophores at the Host-Pathogen Interface', *The Journal of biological chemistry*. J Biol Chem, 290(31), pp. 18967–18974. doi: 10.1074/JBC.R115.644328.

Koo, H. *et al.* (2010) 'Exopolysaccharides Produced by *Streptococcus mutans* Glucosyltransferases Modulate the Establishment of Microcolonies within Multispecies Biofilms', *Journal of Bacteriology*. American Society for Microbiology (ASM), 192(12), p. 3024. doi: 10.1128/JB.01649-09.

Kourtis, A. P. *et al.* (2019) 'Vital Signs: Epidemiology and Recent Trends in Methicillin-Resistant and in Methicillin-Susceptible *Staphylococcus aureus* Bloodstream Infections - United States', *MMWR. Morbidity and mortality weekly report*. MMWR Morb Mortal Wkly Rep, 68(9), pp. 214–219. doi: 10.15585/MMWR.MM6809E1.

Kreutzenbeck, P. *et al.* (2007) 'Escherichia coli Twin Arginine (Tat) Mutant Translocases Possessing Relaxed Signal Peptide Recognition Specificities', *Journal of Biological Chemistry*. Elsevier, 282(11), pp. 7903–7911. doi: 10.1074/JBC.M610126200.

Lacey, K. A., Geoghegan, J. A. and McLoughlin, R. M. (2016) 'The Role of *Staphylococcus aureus* Virulence Factors in Skin Infection and Their Potential as Vaccine Antigens', *Pathogens*. Multidisciplinary Digital Publishing Institute (MDPI), 5(1). doi: 10.3390/PATHOGENS5010022.

Ladomersky, E. and Petris, M. J. (2015) 'Copper tolerance and virulence in bacteria', *Metallomics*. Royal Society of Chemistry, 7(6), pp. 957–964. doi: 10.1039/c4mt00327f.

Lakhundi, S. and Zhang, K. (2018) 'Methicillin-Resistant *Staphylococcus aureus*: Molecular Characterization, Evolution, and Epidemiology', *Clinical Microbiology Reviews*. American Society for Microbiology (ASM), 31(4). doi: 10.1128/CMR.00020-18.

Langley, R. *et al.* (2005) 'The Staphylococcal Superantigen-Like Protein 7 Binds IgA and Complement C5 and Inhibits IgA-FcαRI Binding and Serum Killing of Bacteria', *The Journal of Immunology*. American Association of Immunologists, 174(5), pp. 2926–2933. doi: 10.4049/JIMMUNOL.174.5.2926.

Lausberg, F. *et al.* (2012) 'Genetic evidence for a tight cooperation of TatB and TatC during productive recognition of twin-arginine (Tat) signal peptides in *Escherichia coli*', *PloS one*. PLoS One, 7(6). doi: 10.1371/JOURNAL.PONE.0039867.

Lebrun, M., Audurier, A. and Cossart, P. (1994) 'Plasmid-borne cadmium resistance genes in *Listeria monocytogenes* are present on Tn5422, a novel

transposon closely related to Tn917.', *Journal of Bacteriology*. American Society for Microbiology (ASM), 176(10), p. 3049. doi: 10.1128/JB.176.10.3049-3061.1994.

Lee, C. Y., Buranen, S. L. and Zhi-Hai, Y. (1991) 'Construction of single-copy integration vectors for *Staphylococcus aureus*', *Gene*. Elsevier, 103(1), pp. 101–105. doi: 10.1016/0378-1119(91)90399-V.

Leonowicz, A. *et al.* (2001) 'Fungal laccase: properties and activity on lignin', *Journal of Basic Microbiology*. John Wiley & Sons, Ltd, 41(3-4), pp. 185–227. doi: 10.1002/1521-4028(200107)41:3/4<185::AID-JOBM185>3.0.CO;2-T.

Li, M. Z. and Elledge, S. J. (2007) 'Harnessing homologous recombination in vitro to generate recombinant DNA via SLIC', *Nature Methods*, 4(3), pp. 251–256. doi: 10.1038/nmeth1010.

Lim, S.-Y. *et al.* (2002) 'CuiD is a crucial gene for survival at high copper environment in *Salmonella enterica* serovar Typhimurium.', *Molecules and cells*, 14(2), pp. 177–84.

Linder, M. C. *et al.* (1998) 'Copper transport', *The American Journal of Clinical Nutrition*. Oxford Academic, 67(5), pp. 965S-971S. doi: 10.1093/AJCN/67.5.965S.

Linder, M. C. and Hazegh-Azam, M. (1996) 'Copper biochemistry and molecular biology', *The American Journal of Clinical Nutrition*, 63(5), pp. 797S-811S. doi: 10.1093/ajcn/63.5.797.

Lindsay, J. A. (2010) 'Genomic variation and evolution of *Staphylococcus aureus*', *International journal of medical microbiology: IJMM*. Int J Med Microbiol, 300(2–3), pp. 98–103. doi: 10.1016/J.IJMM.2009.08.013.

Lindsay, J. A. and Holden, M. T. G. (2004) 'Staphylococcus aureus: Superbug, super genome?', *Trends in Microbiology*, 12(8), pp. 378–385. doi: 10.1016/J.TIM.2004.06.004.

Lindsay, J. A. and Holden, M. T. G. (2006) 'Understanding the rise of the superbug: investigation of the evolution and genomic variation of *Staphylococcus aureus*', *Functional & integrative genomics*. Funct Integr Genomics, 6(3), pp. 186–201. doi: 10.1007/S10142-005-0019-7.

Liochev, S. I. and Fridovich, I. (2002) 'The Haber-Weiss cycle - 70 years later: An alternative view [1]', *Redox Report*, pp. 55–57. doi: 10.1179/135100002125000190.

Liu, G. Y. *et al.* (2005) 'Staphylococcus aureus golden pigment impairs neutrophil killing and promotes virulence through its antioxidant activity', *Journal of Experimental Medicine*. The Rockefeller University Press, 202(2), pp. 209–215. doi: 10.1084/jem.20050846.

Liu, J. *et al.* (2016) 'Staphylococcal chromosomal cassettes mec (SCCmec): A mobile genetic element in methicillin-resistant *Staphylococcus aureus*', *Microbial Pathogenesis*. Academic Press, 101, pp. 56–67. doi: 10.1016/J.MICPATH.2016.10.028.

Löfblom, J. *et al.* (2007) 'Optimization of electroporation-mediated transformation: *Staphylococcus carnosus* as model organism', *Journal of Applied*

Microbiology, 102(3), pp. 736–747. doi: 10.1111/j.1365-2672.2006.03127.x.

Lüke, I. *et al.* (2009) 'Proteolytic processing of Escherichia coli twin-arginine signal peptides by LepB', *Archives of microbiology*. Arch Microbiol, 191(12), pp. 919–925. doi: 10.1007/S00203-009-0516-5.

Lutsenko, S. *et al.* (2008) 'CELLULAR MULTITASKING: THE DUAL ROLE OF HUMAN CU-ATPASES IN COFACTOR DELIVERY AND INTRACELLULAR COPPER BALANCE', *Archives of biochemistry and biophysics*. NIH Public Access, 476(1), p. 22. doi: 10.1016/J.ABB.2008.05.005.

Lycklama a Nijeholt, J. A. and Driessen, A. J. M. (2012) 'The bacterial Sec-translocase: structure and mechanism', *Philosophical transactions of the Royal Society of London. Series B, Biological sciences*. Philos Trans R Soc Lond B Biol Sci, 367(1592), pp. 1016–1028. doi: 10.1098/RSTB.2011.0201.

Mack, D. *et al.* (1996) 'The intercellular adhesin involved in biofilm accumulation of Staphylococcus epidermidis is a linear beta-1,6-linked glucosaminoglycan: purification and structural analysis.', *Journal of Bacteriology*. American Society for Microbiology (ASM), 178(1), p. 175. doi: 10.1128/JB.178.1.175-183.1996.

Macomber, L. and Imlay, J. A. (2009) 'The iron-sulfur clusters of dehydratases are primary intracellular targets of copper toxicity', *Proceedings of the National Academy of Sciences of the United States of America*. Proc Natl Acad Sci U S A, 106(20), pp. 8344–8349. doi: 10.1073/pnas.0812808106.

Macomber, L., Rensing, C. and Imlay, J. A. (2007) 'Intracellular copper does not catalyze the formation of oxidative DNA damage in Escherichia coli', *Journal of Bacteriology*, 189(5), pp. 1616–1626. doi: 10.1128/JB.01357-06.

Mancini, S. *et al.* (2017) 'Desulfovibrio DA2_CueO is a novel multicopper oxidase with cuprous, ferrous and phenol oxidase activity', *Microbiology (United Kingdom)*. Microbiology Society, 163(8), pp. 1229–1236. doi: 10.1099/mic.0.000509.

Mann, E. E. *et al.* (2009) 'Modulation of eDNA release and degradation affects Staphylococcus aureus biofilm maturation', *PloS one*. PLoS One, 4(6). doi: 10.1371/JOURNAL.PONE.0005822.

Le Maréchal, C. *et al.* (2011) 'Genome Sequences of Two Staphylococcus aureus Ovine Strains That Induce Severe (Strain O11) and Mild (Strain O46) Mastitis', *JOURNAL OF BACTERIOLOGY*, 193(9), pp. 2353–2354. doi: 10.1128/JB.00045-11.

Mattos-Graner, R. O. *et al.* (2006) 'Functional analysis of glucan binding protein B from Streptococcus mutans', *Journal of Bacteriology*. American Society for Microbiology, 188(11), pp. 3813–3825. doi: 10.1128/JB.01845-05/ASSET/CE57F83F-3AFA-43A6-AF6C-905DC8EFAE70/ASSETS/GRAPHIC/ZJB0110657830007.JPEG.

Mazmanian, S. K. *et al.* (1999) 'Staphylococcus aureus sortase, an enzyme that anchors surface proteins to the cell wall', *Science (New York, N.Y.)*. Science, 285(5428), pp. 760–763. doi: 10.1126/SCIENCE.285.5428.760.

McAdam, P. R. *et al.* (2011) 'Adaptive evolution of Staphylococcus aureus

during chronic endobronchial infection of a cystic fibrosis patient', *PLoS ONE*. Public Library of Science, 6(9). doi: 10.1371/journal.pone.0024301.

McCarthy, A. J., Witney, A. A. and Lindsay, J. A. (2012) 'Staphylococcus aureus temperate bacteriophage: carriage and horizontal gene transfer is lineage associated.', *Frontiers in cellular and infection microbiology*. Frontiers, 2, p. 6. doi: 10.3389/FCIMB.2012.00006/BIBTEX.

McDougal, L. K. *et al.* (2003) 'Pulsed-field gel electrophoresis typing of oxacillin-resistant Staphylococcus aureus isolates from the United States: establishing a national database', *Journal of clinical microbiology*. J Clin Microbiol, 41(11), pp. 5113–5120. doi: 10.1128/JCM.41.11.5113-5120.2003.

Menghani, S. V. *et al.* (2021) ' Demonstration of N , N - Dimethyldithiocarbamate as a Copper-Dependent Antibiotic against Multiple Upper Respiratory Tract Pathogens ', *Microbiology Spectrum*. American Society for Microbiology, 9(2). doi: 10.1128/SPECTRUM.00778-21/SUPPL_FILE/SPECTRUM.00778-21-S0001.PDF.

Mercer, J. F. B. (2001) 'The molecular basis of copper-transport diseases', *Trends in Molecular Medicine*. Elsevier Current Trends, 7(2), pp. 64–69. doi: 10.1016/S1471-4914(01)01920-7.

Messerschmidt, A. and Huber, R. (1990) 'The blue oxidases, ascorbate oxidase, laccase and ceruloplasmin Modelling and structural relationships', *European Journal of Biochemistry*. John Wiley & Sons, Ltd, 187(2), pp. 341–352. doi: 10.1111/j.1432-1033.1990.tb15311.x.

Miller, L. G. *et al.* (2005) 'Necrotizing fasciitis caused by community-associated methicillin-resistant Staphylococcus aureus in Los Angeles', *The New England journal of medicine*. N Engl J Med, 352(14), pp. 1445–1453. doi: 10.1056/NEJMOA042683.

Missiakas, D. M. and Schneewind, O. (2013) 'Growth and Laboratory Maintenance of Staphylococcus aureus', *Current protocols in microbiology*. NIH Public Access, CHAPTER 9(SUPPL.28), p. Unit. doi: 10.1002/9780471729259.MC09C01S28.

Missineo, A. *et al.* (2014) 'IsdC from Staphylococcus lugdunensis Induces Biofilm Formation under Low-Iron Growth Conditions', *Infection and Immunity*. American Society for Microbiology (ASM), 82(6), p. 2448. doi: 10.1128/IAI.01542-14.

Molteni, C., Abicht, H. K. and Solioz, M. (2010) 'Killing of bacteria by copper surfaces involves dissolved copper', *Applied and Environmental Microbiology*. American Society for Microbiology, 76(12), pp. 4099–4101. doi: 10.1128/AEM.00424-10/ASSET/72384C58-A91E-43F2-A4C8-4797AFC7BFE9/ASSETS/GRAPHIC/ZAM9991010260003.JPEG.

Monk, I. R. *et al.* (2012) 'Transforming the untransformable: Application of direct transformation to manipulate genetically Staphylococcus aureus and Staphylococcus epidermidis', *mBio*, 3(2). doi: 10.1128/mBio.00277-11.

Monk, I. R. *et al.* (2015) 'Complete bypass of restriction systems for major staphylococcus aureus lineages', *mBio*. American Society for Microbiology, 6(3),

pp. 1–12. doi: 10.1128/mBio.00308-15.

Moore, G. E. and Hood, D. B. (1993) 'Modified RPMI 1640 culture medium.', *In vitro cellular & developmental biology. Animal*, 29A(4), p. 268. doi: 10.1007/bf02633952.

Mori, H. and Cline, K. (2002) 'A twin arginine signal peptide and the pH gradient trigger reversible assembly of the thylakoid Δ pH/Tat translocase', *Journal of Cell Biology*. The Rockefeller University Press, 157(2), pp. 205–210. doi: 10.1083/JCB.200202048.

Mulcahy, M. E. and McLoughlin, R. M. (2016) 'Host-Bacterial Crosstalk Determines Staphylococcus aureus Nasal Colonization', *Trends in microbiology*. Trends Microbiol, 24(11), pp. 872–886. doi: 10.1016/J.TIM.2016.06.012.

Müller-Eberhard, H. J. (1986) 'The membrane attack complex of complement', *Annual review of immunology*. Annu Rev Immunol, 4, pp. 503–528. doi: 10.1146/ANNUREV.IY.04.040186.002443.

Murphy, E., Huwyler, L. and de Freire Bastos, M. C. (1985) 'Transposon Tn554: complete nucleotide sequence and isolation of transposition-defective and antibiotic-sensitive mutants.', *The EMBO Journal*. European Molecular Biology Organization, 4(12), p. 3357. doi: 10.1002/j.1460-2075.1985.tb04089.x.

Naditz, A. L. *et al.* (2019) 'Plasmids contribute to food processing environment-associated stress survival in three *Listeria monocytogenes* ST121, ST8, and ST5 strains', *International Journal of Food Microbiology*. Elsevier B.V., 299, pp. 39–46. doi: 10.1016/j.ijfoodmicro.2019.03.016.

Nandakumar, R. *et al.* (2011) 'Quantitative proteomic profiling of the *Escherichia coli* response to metallic copper surfaces', *Biometals: an international journal on the role of metal ions in biology, biochemistry, and medicine*. Biometals, 24(3), pp. 429–444. doi: 10.1007/S10534-011-9434-5.

Nucifora, G. *et al.* (1989) 'Cadmium resistance from *Staphylococcus aureus* plasmid pI258 cadA gene results from a cadmium-efflux ATPase', *Proceedings of the National Academy of Sciences of the United States of America*. Proc Natl Acad Sci U S A, 86(10), pp. 3544–3548. doi: 10.1073/PNAS.86.10.3544.

Nygaard, T. K. *et al.* (2012) 'Alpha-toxin induces programmed cell death of human T cells, B cells, and monocytes during USA300 infection', *PloS one*. PLoS One, 7(5). doi: 10.1371/JOURNAL.PONE.0036532.

O'Gara, J. P. and Humphreys, H. (2001) 'Staphylococcus epidermidis biofilms: Importance and implications', *Journal of Medical Microbiology*. Lippincott Williams and Wilkins, 50(7), pp. 582–587. doi: 10.1099/0022-1317-50-7-582.

O'Halloran, D. P., Wynne, K. and Geoghegan, J. A. (2015) 'Protein A is released into the *Staphylococcus aureus* culture supernatant with an unprocessed sorting signal', *Infection and Immunity*. American Society for Microbiology, 83(4), pp. 1598–1609. doi: 10.1128/IAI.03122-14.

O'Neill, E. *et al.* (2007) 'Association between methicillin susceptibility and biofilm regulation in *Staphylococcus aureus* isolates from device-related infections', *Journal of Clinical Microbiology*. American Society for Microbiology Journals, 45(5), pp. 1379–1388. doi: 10.1128/JCM.02280-06.

O'Neill, E. *et al.* (2008) 'A novel *Staphylococcus aureus* biofilm phenotype mediated by the fibronectin-binding proteins, FnBPA and FnBPB', *Journal of Bacteriology*. American Society for Microbiology Journals, 190(11), pp. 3835–3850. doi: 10.1128/JB.00167-08.

O'Toole, G., Kaplan, H. B. and Kolter, R. (2000) 'Biofilm formation as microbial development', *Annual review of microbiology*. Annu Rev Microbiol, 54, pp. 49–79. doi: 10.1146/ANNUREV.MICRO.54.1.49.

Ogston, A. (1882) 'Micrococcus Poisoning.', *Journal of anatomy and physiology*. Wiley-Blackwell, 17(Pt 1), pp. 24–58.

Otto, M. (2008) 'Staphylococcal biofilms', *Current Topics in Microbiology and Immunology*. NIH Public Access, pp. 207–228. doi: 10.1007/978-3-540-75418-3_10.

Otto, M. (2013) 'Staphylococcal infections: mechanisms of biofilm maturation and detachment as critical determinants of pathogenicity', *Annual review of medicine*. Annu Rev Med, 64, pp. 175–188. doi: 10.1146/ANNUREV-MED-042711-140023.

Otto, M. (2018) 'Staphylococcal Biofilms', *Microbiology spectrum*. Microbiol Spectr, 6(4). doi: 10.1128/MICROBIOLSPEC.GPP3-0023-2018.

Outten, F. W. *et al.* (2000) 'Transcriptional activation of an *Escherichia coli* copper efflux regulon by the chromosomal MerR homologue, cueR', *J Biol Chem*, 275(40), pp. 31024–31029. doi: 10.1074/jbc.M006508200.

Outten, F. W. *et al.* (2001) 'The Independent cue and cus Systems Confer Copper Tolerance during Aerobic and Anaerobic Growth in *Escherichia coli*', *Journal of Biological Chemistry*, 276(33), pp. 30670–30677. doi: 10.1074/jbc.M104122200.

Öztürk, Y. *et al.* (2021) 'Maturation of *Rhodobacter capsulatus* Multicopper Oxidase CutO Depends on the CopA Copper Efflux Pathway and Requires the cutF Product', *Frontiers in microbiology*. Front Microbiol, 12. doi: 10.3389/FMICB.2021.720644.

Palmer, T., Sargent, F. and Berks, B. C. (2005) 'Export of complex cofactor-containing proteins by the bacterial Tat pathway', *Trends in Microbiology*. Elsevier Current Trends, 13(4), pp. 175–180. doi: 10.1016/J.TIM.2005.02.002.

Palmer, T., Sargent, F. and Berks, B. C. (2010) 'The Tat Protein Export Pathway', *EcoSal Plus*. American Society for Microbiology, 4(1). doi: 10.1128/ECOSALPLUS.4.3.2/ASSET/BCD6B067-F9ED-4320-A5E8-000B6974631D/ASSETS/GRAPHIC/4.3.2_FIG_008.GIF.

Palmgren, M. G. and Nissen, P. (2011) 'P-type ATPases', *Annual review of biophysics*. Annu Rev Biophys, 40(1), pp. 243–266. doi: 10.1146/ANNUREV.BIOPHYS.093008.131331.

Pauli, N. T. *et al.* (2014) 'Staphylococcus aureus infection induces protein A-mediated immune evasion in humans', *The Journal of Experimental Medicine*. The Rockefeller University Press, 211(12), p. 2331. doi: 10.1084/JEM.20141404.

Periasamy, S. *et al.* (2012) 'Phenol-soluble modulins in staphylococci',

<http://www.tandfonline.com/action/authorSubmission?journalCode=kcib20&page=instructions>. Taylor & Francis, 5(3), pp. 275–277. doi: 10.4161/CIB.19420.

Perl, T. M. *et al.* (2002) 'Intranasal mupirocin to prevent postoperative Staphylococcus aureus infections', *The New England journal of medicine*. N Engl J Med, 346(24), pp. 1871–1877. doi: 10.1056/NEJMOA003069.

Perry, W. J. *et al.* (2019) 'Staphylococcus aureus exhibits heterogeneous siderophore production within the vertebrate host', *Proceedings of the National Academy of Sciences of the United States of America*. Proc Natl Acad Sci U S A, 116(44), pp. 21980–21982. doi: 10.1073/PNAS.1913991116.

Petri, B. and Sanz, M. J. (2018) 'Neutrophil chemotaxis', *Cell and tissue research*. Cell Tissue Res, 371(3), pp. 425–436. doi: 10.1007/S00441-017-2776-8.

Pettersen, E. F. *et al.* (2004) 'UCSF Chimera--a visualization system for exploratory research and analysis', *Journal of computational chemistry*. J Comput Chem, 25(13), pp. 1605–1612. doi: 10.1002/JCC.20084.

Planet, P. J. *et al.* (2015) 'Parallel Epidemics of Community-Associated Methicillin-Resistant Staphylococcus aureus USA300 Infection in North and South America', *The Journal of Infectious Diseases*. Oxford Academic, 212(12), pp. 1874–1882. doi: 10.1093/INFDIS/JIV320.

Poole, R. K., Cozens, A. G. and Shepherd, M. (2019) 'The CydDC family of transporters', *Research in Microbiology*. Elsevier Masson, 170(8), pp. 407–416. doi: 10.1016/J.RESMIC.2019.06.003.

Posada, A. C. *et al.* (2014) 'Importance of bacillithiol in the oxidative stress response of Staphylococcus aureus', *Infection and immunity*. Infect Immun, 82(1), pp. 316–332. doi: 10.1128/IAI.01074-13.

Pöther, D. C. *et al.* (2013) 'Distribution and infection-related functions of bacillithiol in Staphylococcus aureus', *International Journal of Medical Microbiology*. Urban & Fischer, 303(3), pp. 114–123. doi: 10.1016/J.IJMM.2013.01.003.

Potter, A. J., Trappetti, C. and Paton, J. C. (2012) 'Streptococcus pneumoniae uses glutathione to defend against oxidative stress and metal ion toxicity', *Journal of bacteriology*. J Bacteriol, 194(22), pp. 6248–6254. doi: 10.1128/JB.01393-12.

Powers, M. E. *et al.* (2012) 'ADAM10 mediates vascular injury induced by Staphylococcus aureus α -hemolysin', *The Journal of infectious diseases*. J Infect Dis, 206(3), pp. 352–356. doi: 10.1093/INFDIS/JIS192.

Prat, C. *et al.* (2009) 'A homolog of formyl peptide receptor-like 1 (FPRL1) inhibitor from Staphylococcus aureus (FPRL1 inhibitory protein) that inhibits FPRL1 and FPR', *Journal of immunology (Baltimore, Md. : 1950)*. J Immunol, 183(10), pp. 6569–6578. doi: 10.4049/JIMMUNOL.0801523.

Pugsley, A. P. (1993) 'The complete general secretory pathway in gram-negative bacteria', *Microbiological reviews*. Microbiol Rev, 57(1), pp. 50–108. doi: 10.1128/MR.57.1.50-108.1993.

Purohit, R. *et al.* (2018) 'Cu⁺-specific CopB transporter: Revising P1B-type ATPase classification', *Proc Natl Acad Sci U S A*, 115(9), pp. 2108–2113. doi:

10.1073/pnas.1721783115.

Purves, J. *et al.* (2018) 'A horizontally gene transferred copper resistance locus confers hyper-resistance to antibacterial copper toxicity and enables survival of community acquired methicillin resistant *Staphylococcus aureus* USA300 in macrophages', *Environ Microbiol*, 20(4), pp. 1576–1589. doi: 10.1111/1462-2920.14088.

Qin, Z. *et al.* (2007) 'Role of autolysin-mediated DNA release in biofilm formation of *Staphylococcus epidermidis*', *Microbiology*. Microbiology Society, 153(7), pp. 2083–2092. doi: 10.1099/MIC.0.2007/006031-0.

Quintanar, L. *et al.* (2007) 'Shall We Dance? How A Multicopper Oxidase Chooses Its Electron Transfer Partner', *Accounts of Chemical Research*. American Chemical Society, 40(6), pp. 445–452. doi: 10.1021/AR600051A.

Rae, T. D. *et al.* (1999) 'Undetectable intracellular free copper: The requirement of a copper chaperone for superoxide dismutase', *Science*. American Association for the Advancement of Science, 284(5415), pp. 805–808. doi: 10.1126/SCIENCE.284.5415.805.

Reen, F. J. *et al.* (2014) 'Aspirated bile: a major host trigger modulating respiratory pathogen colonisation in cystic fibrosis patients', *European Journal of Clinical Microbiology & Infectious Diseases*. Springer Verlag, 33(10), pp. 1763–1771. doi: 10.1007/s10096-014-2133-8.

Rensing, C. and Grass, G. (2003) 'Escherichia coli mechanisms of copper homeostasis in a changing environment', *FEMS Microbiol Rev*, 27(2–3), pp. 197–213.

Reyes-Robles, T. *et al.* (2013) 'Staphylococcus aureus leukotoxin ED targets the chemokine receptors CXCR1 and CXCR2 to kill leukocytes and promote infection', *Cell host & microbe*. Cell Host Microbe, 14(4), pp. 453–459. doi: 10.1016/J.CHOM.2013.09.005.

Rice, K. *et al.* (2001) 'Description of staphylococcus serine protease (ssp) operon in *Staphylococcus aureus* and nonpolar inactivation of sspA-encoded serine protease', *Infection and immunity*. Infect Immun, 69(1), pp. 159–169. doi: 10.1128/IAI.69.1.159-169.2001.

Rice, L. B. (2010) 'Progress and challenges in implementing the research on ESKAPE pathogens', *Infection control and hospital epidemiology*. Infect Control Hosp Epidemiol, 31 Suppl 1(S1), pp. S7–S10. doi: 10.1086/655995.

Riva, S. (2006) 'Laccases: blue enzymes for green chemistry', *Trends in Biotechnology*. Elsevier, 24(5), pp. 219–226. doi: 10.1016/J.TIBTECH.2006.03.006.

Roberts, S. A. *et al.* (2002) 'Crystal structure and electron transfer kinetics of CueO, a multicopper oxidase required for copper homeostasis in *Escherichia coli*', *Proceedings of the National Academy of Sciences of the United States of America*. Proc Natl Acad Sci U S A, 99(5), pp. 2766–2771. doi: 10.1073/pnas.052710499.

Robinson, D. A. and Enright, M. C. (2003) 'Evolutionary models of the emergence of methicillin-resistant *Staphylococcus aureus*', *Antimicrobial agents and chemotherapy*. Antimicrob Agents Chemother, 47(12), pp. 3926–3934. doi: 10.1128/AAC.47.12.3926-3934.2003.

Roche, F. M., Meehan, M. and Foster, T. J. (2003) 'The Staphylococcus aureus surface protein SasG and its homologues promote bacterial adherence to human desquamated nasal epithelial cells', *Microbiology (Reading, England)*. Microbiology (Reading), 149(Pt 10), pp. 2759–2767. doi: 10.1099/MIC.0.26412-0.

Rodriguez-Castro, K. I., Hevia-Urrutia, F. J. and Sturniolo, G. C. (2015) 'Wilson's disease: A review of what we have learned', *World Journal of Hepatology*. Baishideng Publishing Group Inc, 7(29), p. 2859. doi: 10.4254/WJH.V7.I29.2859.

Rodríguez, E., Pickard, M. A. and Vazquez-Duhalt, R. (1999) 'Industrial Dye Decolorization by Laccases from Ligninolytic Fungi', *Current Microbiology* 1999 38:1. Springer, 38(1), pp. 27–32. doi: 10.1007/PL00006767.

Rohde, H. *et al.* (2005) 'Induction of Staphylococcus epidermidis biofilm formation via proteolytic processing of the accumulation-associated protein by staphylococcal and host proteases', *Molecular microbiology*. Mol Microbiol, 55(6), pp. 1883–1895. doi: 10.1111/J.1365-2958.2005.04515.X.

Rohde, H. *et al.* (2007) 'Polysaccharide intercellular adhesin or protein factors in biofilm accumulation of Staphylococcus epidermidis and Staphylococcus aureus isolated from prosthetic hip and knee joint infections', *Biomaterials*. Biomaterials, 28(9), pp. 1711–1720. doi: 10.1016/J.BIOMATERIALS.2006.11.046.

Rooijackers, S. H. M. *et al.* (2005) 'Immune evasion by a staphylococcal complement inhibitor that acts on C3 convertases', *Nature Immunology* 2005 6:9. Nature Publishing Group, 6(9), pp. 920–927. doi: 10.1038/ni1235.

Rosario-Cruz, Z. *et al.* (2019) 'The copBL operon protects Staphylococcus aureus from copper toxicity: CopL is an extracellular membrane-associated copper-binding protein', *Journal of Biological Chemistry*. American Society for Biochemistry and Molecular Biology Inc., 294(11), pp. 4027–4044. doi: 10.1074/jbc.RA118.004723.

Rosenbach, A. (1884) *Micro-organisms in human wound infection diseases*.

Roulling, F., Godin, A. and Feller, G. (2022) 'Function and versatile location of Met-rich inserts in blue oxidases involved in bacterial copper resistance', *Biochimie*. Elsevier. doi: 10.1016/J.BIOCHI.2021.12.015.

Rountree, P. M. and Freeman, B. M. (1955) 'INFECTIONS CAUSED BY A PARTICULAR PHAGE TYPE OF STAPHYLOCOCCUS AUREUS', *Medical Journal of Australia*. John Wiley & Sons, Ltd, 2(5), pp. 157–161. doi: 10.5694/J.1326-5377.1955.TB35001.X.

Rowland, J. L. and Niederweis, M. (2012) 'Resistance mechanisms of Mycobacterium tuberculosis against phagosomal copper overload', *Tuberculosis*. NIH Public Access, pp. 202–210. doi: 10.1016/j.tube.2011.12.006.

Rowland, J. L. and Niederweis, M. (2013) 'A multicopper oxidase is required for copper resistance in mycobacterium tuberculosis', *Journal of Bacteriology*, 195(16), pp. 3724–3733. doi: 10.1128/JB.00546-13.

Rowland, S. J. and Dyke, K. G. H. (1989) 'Characterization of the staphylococcal beta-lactamase transposon Tn552.', *The EMBO Journal*. European Molecular Biology Organization, 8(9), p. 2761. doi: 10.1002/j.1460-2075.1989.tb08418.x.

Saenkham-Huntsinger, P. *et al.* (2021) 'Copper Resistance Promotes Fitness of Methicillin-Resistant *Staphylococcus aureus* during Urinary Tract Infection', *mBio*. American Society for Microbiology 1752 N St., N.W., Washington, DC. doi: 10.1128/MBIO.02038-21.

Sakurai, T. and Kataoka, K. (2007) 'Structure and function of type I copper in multicopper oxidases', *Cellular and Molecular Life Sciences*. Springer, pp. 2642–2656. doi: 10.1007/s00018-007-7183-y.

Sansevere, E. A. *et al.* (2017) 'Transposase-Mediated Excision, Conjugative Transfer, and Diversity of ICE 6013 Elements in *Staphylococcus aureus*', *Journal of bacteriology*. J Bacteriol, 199(8). doi: 10.1128/JB.00629-16.

Sansevere, E. A. and Robinson, D. A. (2017) 'Staphylococci on ICE: Overlooked agents of horizontal gene transfer', *Mobile genetic elements*. Mob Genet Elements, 7(4), pp. 1–10. doi: 10.1080/2159256X.2017.1368433.

Schilcher, K. and Horwill, A. R. (2020) 'Staphylococcal Biofilm Development: Structure, Regulation, and Treatment Strategies', *Microbiology and Molecular Biology Reviews*. American Society for Microbiology, 84(3). doi: 10.1128/mnbr.00026-19.

Schlievert, P. M. and Davis, C. C. (2020) 'Device-Associated Menstrual Toxic Shock Syndrome', *Clinical microbiology reviews*. Clin Microbiol Rev, 33(3). doi: 10.1128/CMR.00032-19.

Schwendener, S., Cotting, K. and Perreten, V. (2017) 'Novel methicillin resistance gene *mecD* in clinical *Micrococcus caseolyticus* strains from bovine and canine sources', *Scientific reports*. Sci Rep, 7. doi: 10.1038/SREP43797.

Segal, B. H. *et al.* (2011) 'Chronic granulomatous disease: lessons from a rare disorder', *Biology of blood and marrow transplantation : journal of the American Society for Blood and Marrow Transplantation*. Biol Blood Marrow Transplant, 17(1 Suppl). doi: 10.1016/J.BBMT.2010.09.008.

Shepherd, M. (2015) 'The CydDC ABC transporter of *Escherichia coli*: New roles for a reductant efflux pump', *Biochemical Society Transactions*. Portland Press Ltd, 43, pp. 908–912. doi: 10.1042/BST20150098.

Shi, X. *et al.* (2003) 'Fre1p Cu²⁺ Reduction and Fet3p Cu¹⁺ Oxidation Modulate Copper Toxicity in *Saccharomyces cerevisiae*', *Journal of Biological Chemistry*. American Society for Biochemistry and Molecular Biology, 278(50), pp. 50309–50315. doi: 10.1074/jbc.M307019200.

Shi, X. *et al.* (2014) 'The copper-responsive RicR regulon contributes to *Mycobacterium tuberculosis* virulence', *mBio*. mBio, 5(1). doi: 10.1128/mBio.00876-13.

Shi, X. and Darwin, K. H. (2015) 'Copper homeostasis in *Mycobacterium tuberculosis*', *Metallomics*. The Royal Society of Chemistry, 7(6), pp. 929–934. doi: 10.1039/C4MT00305E.

Sibbald, M. J. J. B. *et al.* (2006) 'Mapping the pathways to staphylococcal pathogenesis by comparative secretomics', *Microbiology and molecular biology reviews: MMBR*. Microbiol Mol Biol Rev, 70(3), pp. 755–788. doi: 10.1128/MMBR.00008-06.

De Silva, D. *et al.* (1997) 'Purification and characterization of Fet3 protein, a yeast homologue of ceruloplasmin', *Journal of Biological Chemistry*, 272(22), pp. 14208–14213. doi: 10.1074/jbc.272.22.14208.

De Silva, D. M. *et al.* (1995) 'The FET3 gene product required for high affinity iron transport in yeast is a cell surface ferroxidase', *Journal of Biological Chemistry*, 270(3), pp. 1098–1101. doi: 10.1074/jbc.270.3.1098.

Singh, K. *et al.* (2015) 'The copYAZ operon functions in copper efflux, biofilm formation, genetic transformation, and stress tolerance in *Streptococcus mutans*', *Journal of Bacteriology*. American Society for Microbiology, 197(15), pp. 2545–2557. doi: 10.1128/JB.02433-14.

Singh, S. K. *et al.* (2004) 'Cuprous oxidase activity of CueO from *Escherichia coli*', *Journal of Bacteriology*. J Bacteriol, 186(22), pp. 7815–7817. doi: 10.1128/JB.186.22.7815-7817.2004.

Singh, S. K. *et al.* (2011) 'Crystal structures of multicopper oxidase CueO bound to copper(I) and silver(I): functional role of a methionine-rich sequence', *J Biol Chem*, 286(43), pp. 37849–37857. doi: 10.1074/jbc.M111.293589.

Sitthisak, S. *et al.* (2005) 'Characterization of a multicopper oxidase gene from *Staphylococcus aureus*', *Appl Environ Microbiol*, 71(9), pp. 5650–5653. doi: 10.1128/AEM.71.9.5650-5653.2005.

Sitthisak, S. *et al.* (2007) 'Molecular characterization of the copper transport system in *Staphylococcus aureus*', *Microbiology*, 153(Pt 12), pp. 4274–4283. doi: 10.1099/mic.0.2007/009860-0.

Smith, A. T., Smith, K. P. and Rosenzweig, A. C. (2014) 'Diversity of the metal-transporting P1B-type ATPases', *JBIC Journal of Biological Inorganic Chemistry*. Springer Verlag, 19(6), pp. 947–960. doi: 10.1007/s00775-014-1129-2.

Smith, E. J. *et al.* (2011) 'The Sbi protein is a multifunctional immune evasion factor of *Staphylococcus aureus*', *Infection and Immunity*. American Society for Microbiology Journals, 79(9), pp. 3801–3809. doi: 10.1128/IAI.05075-11.

Solomon, E. I., Sundaram, U. M. and Machonkin, T. E. (1996) 'Multicopper Oxidases and Oxygenases', *Chem Rev*, 96(7), pp. 2563–2606.

Song, E. K. *et al.* (2011) 'Chronic granulomatous disease: a review of the infectious and inflammatory complications', *Clinical and molecular allergy: CMA*. Clin Mol Allergy, 9(1). doi: 10.1186/1476-7961-9-10.

Sorensen, H. M. *et al.* (2020) 'Reading between the Lines: Utilizing RNA-Seq Data for Global Analysis of sRNAs in *Staphylococcus aureus*', *mSphere*. mSphere, 5(4). doi: 10.1128/MSPHERE.00439-20.

Spaan, A. N. *et al.* (2013) 'The staphylococcal toxin Panton-Valentine Leukocidin targets human C5a receptors', *Cell host & microbe*. Cell Host Microbe, 13(5), pp. 584–594. doi: 10.1016/J.CHOM.2013.04.006.

Spaan, A. N. *et al.* (2014) 'The staphylococcal toxins γ -haemolysin AB and CB differentially target phagocytes by employing specific chemokine receptors', *Nature communications*. Nat Commun, 5. doi: 10.1038/NCOMMS6438.

Spaan, A. N., Schiepers, A., *et al.* (2015) 'Differential Interaction of the

Staphylococcal Toxins Panton-Valentine Leukocidin and γ -Hemolysin CB with Human C5a Receptors', *Journal of immunology (Baltimore, Md. : 1950)*. J Immunol, 195(3), pp. 1034–1043. doi: 10.4049/JIMMUNOL.1500604.

Spaan, A. N., Reyes-Robles, T., *et al.* (2015) 'Staphylococcus aureus Targets the Duffy Antigen Receptor for Chemokines (DARC) to Lyse Erythrocytes', *Cell host & microbe*. Cell Host Microbe, 18(3), pp. 363–370. doi: 10.1016/J.CHOM.2015.08.001.

Stackebrandt, E. and Teuber, M. (1988) 'Molecular taxonomy and phylogenetic position of lactic acid bacteria', *Biochimie*. Elsevier, 70(3), pp. 317–324. doi: 10.1016/0300-9084(88)90204-0.

Stewart, L. J. *et al.* (2019) 'Handling of nutrient copper in the bacterial envelope', *Metallomics : integrated biometal science*. Metallomics, 11(1), pp. 50–63. doi: 10.1039/C8MT00218E.

Stewart, L. J. *et al.* (2020) 'Role of glutathione in buffering excess intracellular copper in streptococcus pyogenes', *mBio*. American Society for Microbiology, 11(6), pp. 1–19. doi: 10.1128/MBIO.02804-20.

Stolle, P., Hou, B. and Brüser, T. (2016) 'The Tat Substrate CueO Is Transported in an Incomplete Folding State', *Journal of Biological Chemistry*. Elsevier, 291(26), pp. 13520–13528. doi: 10.1074/JBC.M116.729103.

Stover, C. K. *et al.* (2000) 'Complete genome sequence of Pseudomonas aeruginosa PAO1, an opportunistic pathogen', *Nature*, 406(6799), pp. 959–964. doi: 10.1038/35023079.

Sun, F., Cho, H., *et al.* (2010) 'Aureusimines in Staphylococcus aureus Are Not Involved in Virulence', *PLOS ONE*. Public Library of Science, 5(12), p. e15703. doi: 10.1371/JOURNAL.PONE.0015703.

Sun, F., Li, C., *et al.* (2010) 'In the Staphylococcus aureus two-component system sae, the response regulator SaeR Binds to a direct repeat sequence and DNA binding requires phosphorylation by the sensor kinase SaeS', *Journal of Bacteriology*, 192(8), pp. 2111–2127. doi: 10.1128/JB.01524-09.

Surewaard, B. G. J. *et al.* (2012) 'Inactivation of Staphylococcal Phenol Soluble Modulins by Serum Lipoprotein Particles', *PLOS Pathogens*. Public Library of Science, 8(3), p. e1002606. doi: 10.1371/JOURNAL.PPAT.1002606.

Suzuki, M. *et al.* (2012) 'Iodide oxidation by a novel multicopper oxidase from the alphaproteobacterium strain Q-1', *Applied and Environmental Microbiology*, 78(11), pp. 3941–3949. doi: 10.1128/AEM.00084-12.

Taglialegna, A. *et al.* (2016) 'Staphylococcal Bap Proteins Build Amyloid Scaffold Biofilm Matrices in Response to Environmental Signals', *PLoS Pathogens*. Public Library of Science, 12(6), p. 1005711. doi: 10.1371/JOURNAL.PPAT.1005711.

Takahashi, N., Ortel, T. L. and Putnam, F. W. (1984) 'Single-chain structure of human ceruloplasmin: The complete amino acid sequence of the whole molecule', *Proceedings of the National Academy of Sciences of the United States of America*, 81(2 I), pp. 390–394. doi: 10.1073/pnas.81.2.390.

Tam, K. and Torres, V. J. (2019) 'Staphylococcus aureus Secreted Toxins and Extracellular Enzymes', *Microbiology spectrum*. Microbiol Spectr, 7(2). doi: 10.1128/MICROBIOLSPEC.GPP3-0039-2018.

Tan, G. *et al.* (2017) 'Anaerobic Copper Toxicity and Iron-Sulfur Cluster Biogenesis in Escherichia coli', *Applied and environmental microbiology*. Appl Environ Microbiol, 83(16). doi: 10.1128/AEM.00867-17.

Tanzi, R. E. *et al.* (1993) 'The Wilson disease gene is a copper transporting ATPase with homology to the Menkes disease gene', *Nature Genetics* 1993 5:4. Nature Publishing Group, 5(4), pp. 344–350. doi: 10.1038/ng1293-344.

Tarrant, E. *et al.* (2019) 'Copper stress in Staphylococcus aureus leads to adaptive changes in central carbon metabolism', *Metallomics*. Royal Society of Chemistry, 11(1), pp. 183–200. doi: 10.1039/c8mt00239h.

Teufel, F. *et al.* (2022) 'SignalP 6.0 predicts all five types of signal peptides using protein language models', *Nature Biotechnology* 2022. Nature Publishing Group, pp. 1–3. doi: 10.1038/s41587-021-01156-3.

Thammavongsa, V. *et al.* (2015) 'Staphylococcal manipulation of host immune responses', *Nature reviews. Microbiology*. Nat Rev Microbiol, 13(9), pp. 529–543. doi: 10.1038/NRMICRO3521.

Thorvaldsdóttir, H., Robinson, J. T. and Mesirov, J. P. (2013) 'Integrative Genomics Viewer (IGV): high-performance genomics data visualization and exploration', *Briefings in Bioinformatics*. Oxford Academic, 14(2), pp. 178–192. doi: 10.1093/BIB/BBS017.

Tillotson, L. E. *et al.* (1989) 'Characterization of a novel insertion of the macrolides-lincosamides-streptogramin B resistance transposon Tn554 in methicillin-resistant Staphylococcus aureus and Staphylococcus epidermidis', *Antimicrobial agents and chemotherapy*. Antimicrob Agents Chemother, 33(4), pp. 541–550. doi: 10.1128/AAC.33.4.541.

Traber, K. and Novick, R. (2006) 'A slipped-mispairing mutation in AgrA of laboratory strains and clinical isolates results in delayed activation of agr and failure to translate δ - and α -haemolysins', *Molecular Microbiology*, 59(5), pp. 1519–1530. doi: 10.1111/j.1365-2958.2006.04986.x.

Tsirigotaki, A. *et al.* (2017) 'Protein export through the bacterial Sec pathway', *Nature reviews. Microbiology*. Nat Rev Microbiol, 15(1), pp. 21–36. doi: 10.1038/NRMICRO.2016.161.

Tsukazaki, T. *et al.* (2011) 'Structure and function of a membrane component SecDF that enhances protein export', *Nature*. Nature, 474(7350), pp. 235–238. doi: 10.1038/NATURE09980.

Turner, N. A. *et al.* (2019) 'Methicillin-resistant Staphylococcus aureus: an overview of basic and clinical research', *Nature reviews. Microbiology*. Nat Rev Microbiol, 17(4), pp. 203–218. doi: 10.1038/S41579-018-0147-4.

Tynecka, Z., Gos, Z. and Zajac, J. (1981) 'Energy-dependent efflux of cadmium coded by a plasmid resistance determinant in Staphylococcus aureus.', *Journal of Bacteriology*. American Society for Microbiology (ASM), 147(2), p. 313. doi: 10.1128/jb.147.2.313-319.1981.

Tzagoloff, H. and Novick, R. (1977) 'Geometry of Cell Division in *Staphylococcus aureus*', *JOURNAL OF BACTERIOLOGY*, pp. 343–350.

Vandenesch, F. *et al.* (2003) 'Community-acquired methicillin-resistant *Staphylococcus aureus* carrying Panton-Valentine leukocidin genes: worldwide emergence', *Emerging infectious diseases*. *Emerg Infect Dis*, 9(8), pp. 978–984. doi: 10.3201/EID0908.030089.

Vaudaux, P. E. *et al.* (1995) 'Use of adhesion-defective mutants of *Staphylococcus aureus* to define the role of specific plasma proteins in promoting bacterial adhesion to canine arteriovenous shunts.', *Infection and Immunity*. American Society for Microbiology (ASM), 63(2), p. 585. doi: 10.1128/iai.63.2.585-590.1995.

Vetting, M. W. *et al.* (2005) 'Structure and functions of the GNAT superfamily of acetyltransferases', *Archives of Biochemistry and Biophysics*. Academic Press, 433(1), pp. 212–226. doi: 10.1016/J.ABB.2004.09.003.

Visai, L. *et al.* (2009) 'Immune evasion by *Staphylococcus aureus* conferred by iron-regulated surface determinant protein IsdH', *Microbiology*. Microbiology Society, 155(3), pp. 667–679. doi: 10.1099/MIC.0.025684-0/CITE/REFWORKS.

Vulpe, C. *et al.* (1993) 'Isolation of a candidate gene for Menkes disease and evidence that it encodes a copper-transporting ATPase', *Nature genetics*. *Nat Genet*, 3(1), pp. 7–13. doi: 10.1038/NG0193-7.

Wagner, D. *et al.* (2005) 'Elemental Analysis of *Mycobacterium avium* -, *Mycobacterium tuberculosis* -, and *Mycobacterium smegmatis* -Containing Phagosomes Indicates Pathogen-Induced Microenvironments within the Host Cell's Endosomal System', *The Journal of Immunology*. The American Association of Immunologists, 174(3), pp. 1491–1500. doi: 10.4049/jimmunol.174.3.1491.

Waldron, K. J. *et al.* (2009) 'Metalloproteins and metal sensing', *Nature*. *Nature*, 460(7257), pp. 823–830. doi: 10.1038/NATURE08300.

Waldron, K. J. and Robinson, N. J. (2009) 'How do bacterial cells ensure that metalloproteins get the correct metal?', *Nature Reviews Microbiology*. Nature Publishing Group, pp. 25–35. doi: 10.1038/nrmicro2057.

Wang, P. *et al.* (2020) 'Biological applications of copper-containing materials', *Bioactive materials*. *Bioact Mater*, 6(4), pp. 916–927. doi: 10.1016/J.BIOACTMAT.2020.09.017.

Wang, R. *et al.* (2007) 'Identification of novel cytolytic peptides as key virulence determinants for community-associated MRSA', *Nature medicine*. *Nat Med*, 13(12), pp. 1510–1514. doi: 10.1038/NM1656.

Wang, Yan *et al.* (2019) 'Genomic dissection of the most prevalent *Listeria monocytogenes* clone, sequence type ST87, in China', *BMC Genomics*. BioMed Central Ltd., 20(1), p. 1014. doi: 10.1186/s12864-019-6399-1.

Waters, E. M. *et al.* (2016) 'Convergence of *Staphylococcus aureus* Persister and Biofilm Research: Can Biofilms Be Defined as Communities of Adherent Persister Cells?', *PLOS Pathogens*. Public Library of Science, 12(12), p. e1006012. doi: 10.1371/JOURNAL.PPAT.1006012.

Wee, N. K. Y. *et al.* (2013) 'The mammalian copper transporters CTR1 and CTR2 and their roles in development and disease', *The international journal of biochemistry & cell biology*. Int J Biochem Cell Biol, 45(5), pp. 960–963. doi: 10.1016/J.BIOCEL.2013.01.018.

Weinstein, M. P. *et al.* (2020) *M100 Performance Standards for Antimicrobial Susceptibility Testing A CLSI supplement for global application. Performance Standards for Antimicrobial Susceptibility Testing Performance Standards for Antimicrobial Susceptibility Testing*.

Welsh, M. J. *et al.* (2009) 'Development of a Porcine Model of Cystic Fibrosis', *Transactions of the American Clinical and Climatological Association*. American Clinical and Climatological Association, 120, p. 149.

Whitby, M., McLaws, M. L. and Berry, G. (2001) 'Risk of death from methicillin-resistant *Staphylococcus aureus* bacteraemia: a meta-analysis', *The Medical journal of Australia*. Med J Aust, 175(5), pp. 264–267. doi: 10.5694/J.1326-5377.2001.TB143562.X.

Whitchurch, C. B. *et al.* (2002) 'Extracellular DNA required for bacterial biofilm formation', *Science (New York, N.Y.)*. Science, 295(5559), p. 1487. doi: 10.1126/SCIENCE.295.5559.1487.

White, C., Lee, J., *et al.* (2009) 'A role for the ATP7A copper-transporting ATPase in macrophage bactericidal activity', *Journal of Biological Chemistry*, 284(49), pp. 33949–33956. doi: 10.1074/jbc.M109.070201.

White, C., Kambe, T., *et al.* (2009) 'Copper transport into the secretory pathway is regulated by oxygen in macrophages', *Journal of Cell Science*, 122(9), pp. 1315–1321. doi: 10.1242/jcs.043216.

Widdick, D. A. *et al.* (2006) 'The twin-arginine translocation pathway is a major route of protein export in *Streptomyces coelicolor*', *Proceedings of the National Academy of Sciences of the United States of America*. Proc Natl Acad Sci U S A, 103(47), pp. 17927–17932. doi: 10.1073/PNAS.0607025103.

Wiethaus, J., Wildner, G. F. and Masepohl, B. (2006) 'The multicopper oxidase CutO confers copper tolerance to *Rhodobacter capsulatus*', *FEMS Microbiology Letters*. John Wiley & Sons, Ltd, 256(1), pp. 67–74. doi: 10.1111/j.1574-6968.2005.00094.x.

Wilke, G. A. and Wardenburg, J. B. (2010) 'Role of a disintegrin and metalloprotease 10 in *Staphylococcus aureus* alpha-hemolysin-mediated cellular injury', *Proceedings of the National Academy of Sciences of the United States of America*. Proc Natl Acad Sci U S A, 107(30), pp. 13473–13478. doi: 10.1073/PNAS.1001815107.

Williams, C. L. *et al.* (2020) 'Characterization of *Acinetobacter baumannii* Copper Resistance Reveals a Role in Virulence', *Frontiers in Microbiology*. Frontiers Media S.A., 11, p. 16. doi: 10.3389/fmicb.2020.00016.

Woehl, J. L. *et al.* (2014) 'The extracellular adherence protein from *Staphylococcus aureus* inhibits the classical and lectin pathways of complement by blocking formation of the C3 proconvertase.', *Journal of Immunology (Baltimore, Md. : 1950)*. The American Association of Immunologists, 193(12), pp. 6161–6171.

doi: 10.4049/JIMMUNOL.1401600.

Wolschendorf, F. *et al.* (2011) 'Copper resistance is essential for virulence of *Mycobacterium tuberculosis*', *Proceedings of the National Academy of Sciences of the United States of America*. Proc Natl Acad Sci U S A, 108(4), pp. 1621–1626. doi: 10.1073/pnas.1009261108.

Wong, M. D., Fan, B. and Rosen, B. P. (2005) 'Bacterial Transport ATPases for Monovalent, Divalent and Trivalent Soft Metal Ions', *Handbook of ATPases: Biochemistry, Cell Biology, Pathophysiology*. John Wiley & Sons, Ltd, pp. 159–177. doi: 10.1002/3527606122.CH6.

Xie, L. and Collins, J. F. (2013) 'Copper stabilizes the Menkes copper-transporting ATPase (Atp7a) protein expressed in rat intestinal epithelial cells', *American Journal of Physiology - Cell Physiology*. American Physiological Society, 304(3), p. C257. doi: 10.1152/AJPCELL.00336.2012.

Xin, Z. *et al.* (1991) 'Effects of Copper Status on Neutrophil Function, Superoxide Dismutase, and Copper Distribution in Steers', *Journal of Dairy Science*. Elsevier, 74(9), pp. 3078–3085. doi: 10.3168/JDS.S0022-0302(91)78493-2.

Xiong, A. *et al.* (2000) 'Molecular characterization of the ferric-uptake regulator. Fur, from *Staphylococcus aureus*', *Microbiology*. Society for General Microbiology, 146(3), pp. 659–668. doi: 10.1099/00221287-146-3-659.

Ye, J. *et al.* (2005) 'Crystal structure of the *Staphylococcus aureus* pl258 CadC Cd(II)/Pb(II)/Zn(II)-responsive repressor', *Journal of Bacteriology*. American Society for Microbiology, 187(12), pp. 4214–4221. doi: 10.1128/JB.187.12.4214-4221.2005/ASSET/909D69F3-5EF7-4100-802C-528CE8061341/ASSETS/GRAPHIC/ZJB0120547940006.JPEG.

Yoon, K. P., Misra, T. K. and Silver, S. (1991) 'Regulation of the cadA cadmium resistance determinant of *Staphylococcus aureus* plasmid pl258', *Journal of Bacteriology*. American Society for Microbiology (ASM), 173(23), pp. 7643–7649. doi: 10.1128/jb.173.23.7643-7649.1991.

Yoshida, Y., Furuta, S. and Niki, E. (1993) 'Effects of metal chelating agents on the oxidation of lipids induced by copper and iron.', *Biochimica et biophysica acta*, 1210(1), pp. 81–8. doi: 10.1016/0005-2760(93)90052-b.

Yuliana, T. *et al.* (2015) 'A novel enzyme-based antimicrobial system comprising iodide and a multicopper oxidase isolated from Alphaproteobacterium strain Q-1', *Applied Microbiology and Biotechnology*. Springer Verlag, 99(23), pp. 10011–10018. doi: 10.1007/s00253-015-6862-0.

Zapotoczna, M. *et al.* (2018) 'Mobile-genetic-element-encoded hypertolerance to copper protects *Staphylococcus aureus* from killing by host phagocytes', *mBio*, 9(5). doi: 10.1128/mBio.00550-18.

Zhang, Y. *et al.* (2017) '*Staphylococcus aureus* SdrE captures complement factor H's C-terminus via a novel "close, dock, lock and latch" mechanism for complement evasion.', *The Biochemical Journal*. Portland Press Ltd, 474(10), pp. 1619–1631. doi: 10.1042/BCJ20170085.

Zhao, K. *et al.* (2010) 'Induction of inducible nitric oxide synthase increases

the production of reactive oxygen species in RAW264.7 macrophages', *Bioscience reports*. Biosci Rep, 30(4), pp. 233–241. doi: 10.1042/BSR20090048.

Zhao, X. and Drlica, K. (2002) 'Restricting the Selection of Antibiotic-Resistant Mutant Bacteria: Measurement and Potential Use of the Mutant Selection Window', *The Journal of Infectious Diseases*. Oxford Academic, 185(4), pp. 561–565. doi: 10.1086/338571.

Zimmerli, W. and Moser, C. (2012) 'Pathogenesis and treatment concepts of orthopaedic biofilm infections', *FEMS Immunology & Medical Microbiology*. Oxford Academic, 65(2), pp. 158–168. doi: 10.1111/J.1574-695X.2012.00938.X.

Zimmerli, W., Trampuz, A. and Ochsner, P. E. (2009) 'Prosthetic-Joint Infections', <http://dx.doi.org/10.1056/NEJMra040181>. Massachusetts Medical Society, 351(16). doi: 10.1056/NEJMRA040181.